Study of the Impact of Anthropic Pressure on Coastal Landscape and its Influence upon the Coastal Vulnerability due to Climate Change along the Coastal Tracts of South Goa District, West Coast of India

A Thesis submitted in partial fulfillment for the Degree of

DOCTOR OF PHILOSOPHY

in

Earth Science

School of Earth, Ocean, and Atmospheric Sciences,

Goa University

By

Ritwik Nigam

School of Earth, Ocean and Atmospheric Sciences,

Goa University

March-2024

DECLARATION

I, **Ritwik Nigam** hereby declare that the thesis represents work which has been carried out by me and it has not been submitted, either in part or full, to any other University or Institution for the award of any research degree.

Place: Taleigao Plateau

Date:

Ritwik Nigam
Senior Research Fellow
School of Earth Ocean and
Atmospheric Sciences, Goa University

CERTIFICATE

I, hereby certify that the work was carried out under my supervision and may be placed for the evaluation.

Prof Kotha Mahender
Professor (Superannuated)
School of Earth, Ocean and Atmospheric Sciences,
Goa University

Acknowledgement

The culmination of this Ph.D. thesis signifies not only the fulfillment of an academic pursuit but also the realization of a profound journey enriched by the invaluable contributions of numerous individuals and institutions. These acknowledgments are more than words; they are a tribute to the collective effort and support that have profoundly influenced my life and scholarly development.

I want to say a big thank for all the help and guidance my Ph.D. research guide, Dr. Kotha Mahender and co-guide, Dr. Alvarinho J. Luis have given me during my Ph.D. journey, not only related to the thesis but also in the areas which are out of their research interests. Their unwavering dedication to my intellectual development has been a beacon of inspiration. The countless hours spent in deep discussions on interdisciplinary issues, their wise advice, and support have played a transformative role in shaping not only the content of this thesis but my perspective on scholarship and life itself. It's meant more to me than they may realize. Their belief in me and their encouragement have been a huge source of motivation. Their support has been a game-changer for my academic journey. Their willingness to collaborate and help me understand unfamiliar areas has been crucial. They've guided me through the complex parts of my research, and their patient approach has made a world of difference. They didn't let the barrier of inter-disciplines hold back our collaborative research endeavors, and that's something I deeply appreciate. Their open-mindedness and dedication to helping me, even in uncharted territory, have been a foundation for my success and with their unconditional support, we became the first research group ever from Goa University to publish a research paper in the prestigious Nature journal and many more in other reputed journals and I can't thank them enough.

I'm excited to continue on this academic journey, and I'm committed to making them proud not only in the academic field related to my Ph.D. thesis but also in the field of Climatology, Anthropo-geomorphology, Environmental science, Disaster management, Hydrodynamics and Polar studies in which I got to tried my hands all because of their support. I wouldn't be in all these disciplines where I am today without their exceptional mentorship. Thank you from the bottom of my heart.

I extend my deepest gratitude to the members of my Doctoral Research Committee, Dr V. J. Loveson and Dr. Anthony Viegas. Their wisdom, diverse perspectives, and comprehensive feedbacks have significantly enriched this work. Their expert advice, meticulous scrutiny, challenging questions, and thoughtful critique have deepened my understanding of the subject matter and elevated the quality of the research. Their guidance has been essential to the development of this thesis.

The academic environment at Goa University has been an ideal breeding ground for intellectual growth and research. The School of Earth, Ocean and Atmospheric Sciences deserves special recognition for fostering a culture that celebrates curiosity, innovation, and collaboration. The institutional resources, ranging from research facilities to extensive library archives, have been indispensable in conducting comprehensive research. The unwavering support of the administrative staff especially, Mrs. Sangeeta Tilwe, Mrs. Tulsi Gaonkar, Mrs. Heena Mulla and Mr. Gyaneshwar has created a nurturing backdrop for this scholarly endeavor.

Within the dynamic and intellectually stimulating community of several important persons Dr. Pankaj Prasad, Dr. Karthik Nagarajan, Dr. Ramanand Yadav, Mr. Sachit Kuttikar, Dr. Ashwini Panandikar, Dr. Raghav Gadgil, Dr. Poornima Dhawaskar, Dr. Purushottam Verlekar, I have found inspiration and camaraderie. The exchange of ideas among my friends and colleagues, the strong bond we have formed, and our mutual passion for research have played a crucial role in my growth as an academic. It is not only the achievements we have attained through collaboration, but also the relationships we have nurtured that have made this journey truly satisfying.

My heartfelt gratitude to my coauthors, Miss Kanvi Pandya, Dr. Eric Vaz, Dr. Bruno Damasio, Dr. Raja Sengupta, Dr. Rahul Dey, Mr. Ruturaj Daphale, Mr. Mit Kotecha, Mr. Pratik Santra, Dr. Lino Yovan, Mr. Vikas Ghadamode, Ms. Tannu Priya for their invaluable contributions to the fifteen research publications which I have been able to complete during this tenure. Their diverse expertise enhanced the depth and breadth of our findings. Those publications would not have been possible without their dedication, expertise, and collaboration.

My heartfelt gratitude to the mentors, Dr. N. R. Dash and Prof Rolee Kanchan, I had during my time at The Maharaja Sayajirao University of Baroda. Their guidance, support, and expertise were invaluable in shaping my academic and personal growth. I am deeply thankful for their commitment to my education. Their guidance went beyond the classroom. Their willingness to provide advice, encouragement, and insight into my career aspirations was instrumental in my development. I appreciate the time they invested in helping me discover my strengths and supporting my ambitions. Also, my appreciation to all the faculty and staff at The Maharaja Sayajirao University of Baroda who contributed to my educational journey. Their collective efforts in fostering a conducive learning environment played a significant role in my success.

The sacrifices and enduring support of my family, especially my parents and my sister (Ritika), deserve special mention. Their support, both emotional and financial, have been the bedrock of my academic pursuits. Their unwavering belief in my potential has been a driving force for me, and I am profoundly grateful for their enduring faith in my abilities. I want to take a moment to express my deepest gratitude for their support and encouragement in allowing me to pursue my passion for geography. Their trust and the freedom they gave me to choose this field over other in-fashion disciplines have been invaluable, and I can't thank them enough for that. I am well aware that not everyone is as fortunate as I am to have parents who not only provide emotional support but also give their children the freedom to make choices that align with their passions. Their unwavering support is a gift that I will forever cherish, and it has played a pivotal role in shaping my life and my career.

I promise to continue working hard, pursuing excellence in my chosen field, and making them proud. Thank you, Mom and Dad, for believing in me, for supporting my dreams, and for giving me the freedom to choose my path. Their love and encouragement mean the world to me.

This success would not have been possible without the contribution of numerous individuals and organizations; District Disaster Management Authority, South Goa, Goa Pollution Control Board, Drishti Lifeguard, TERI (Goa), NCPOR, NCSCM, NIO, INCOIS, NIOT and the all the news reporters and their respective organizations based all over the country, who generously shared their data, and insights. To each of them, I extend my heartfelt thanks for their valuable contributions.

Financial support from the University Grant Commission has played an integral role in the realization of this research. I extend my heartfelt appreciation for their recognition of the significance of this work and their investment in the advancement of knowledge.

I also extend my appreciation to the unknown persons who assisted during the field survey. Their willingness to offer support and insights, often behind the scenes, was instrumental in the collection of data and the progress of this research. Their contribution, though anonymous, is deeply appreciated.

Last, but most definitely not least, I want to express my appreciation to Miss Kanvi Pandya, Dr. Pankaj Prasad and Dr. Ramanand Yadav whose support, understanding, and camaraderie have been indispensable. They have provided not only emotional sustenance but also moments of levity during challenging times. Their presence in my life has been invaluable, and I am grateful for their support.

With heartfelt appreciation,

Ritwik Nigam,

School of Earth, Ocean and Atmospheric Sciences, Goa University,

March, 2024.

QUOTES

1. *"The greatest threat to our planet is the belief that someone else will save it."*— **Robert Swan**

2. *"Twenty-five years ago people could be excused for not knowing much, or doing much, about climate change. Today we have no excuse."* - **Desmond Tutu**

3. *"We are the first generation to feel the impact of climate change and the last generation that can do something about it."*— **Barack Obama**

4. *"By polluting the oceans, not mitigating CO_2 emissions and destroying our biodiversity, we are killing our planet. Let us face it, there is no planet B."* - **Emmanuel Macron**

5. *"Climate change knows no borders. It will not stop before the Pacific Islands and the whole of the international community here has to shoulder a responsibility to bring about sustainable development."* - **Angela Merkel**

6. *"To leave the world better than you found it, sometimes you have to pick up other people's trash."* —**Bill Nye**

7. *"A vibrant, fair, and regenerative future is possible — not when thousands of people do climate justice activism perfectly but when millions of people do the best they can."*— **Xiye Bastida**

8. *"We do not inherit the earth from our ancestors, we borrow it from our children."*- **Native American Proverb**

9. *"What you do makes a difference, and you have to decide what kind of difference you want to make."* –**Jane Goodall**

10. *"Look after the land and the land will look after you, destroy the land and it will destroy you."* —**Aboriginal Proverb**

My Inspiration,

<u>The Road Not Taken</u>

Two roads diverged in a yellow wood,
And sorry I could not travel both
And be one traveler, long I stood
And looked down one as far as I could
To where it bent in the undergrowth;

Then took the other, as just as fair,
And having perhaps the better claim,
Because it was grassy and wanted wear;
Though as for that the passing there
Had worn them really about the same,

And both that morning equally lay
In leaves no step had trodden black.
Oh, I kept the first for another day!
Yet knowing how way leads on to way,
I doubted if I should ever come back.

I shall be telling this with a sigh
Somewhere ages and ages hence:
Two roads diverged in a wood, and I-
I took the one less traveled by,
And that has made all the difference.

– By Robert Frost, 1915 AD

Content

List of Figures

List of Tables

Glossary

Af	Tropical Wet (Koppen Classification)
AGI@E	Anthropogeomorphic Impact At Ecumene
AGP	Anthropogeomorphic Process
AGP	Anthropogeomorphic Pressure
AHP	Analytical Hierarchy Process
ALOS	Advanced Land Observing Satellite
Am	Tropical Monsoon (Koppen Classification)
ANOVA	Analysis of Variance
AQ	Air Quality
AR5	Fifth Annual Report
AR6	Sixth Annual Report
As	Tropical (Savanna, dry summer) (Koppen Classification)
ASTER	Advanced Spaceborne Thermal Emission and Reflection Radiometer
Aw	Tropical (Savanna, dry winter) (Koppen Classification)
BHM	Bayesian Hierarchical Model
BM	Bathtub Modelling
BMTPC	Building Materials And Technology Promotion Council
BPL	Below Poverty Line
BRI	Belt And Road Initiative
BS	Semi arid, Steppe (Koppen Classification)
BTM	Bathtub Modeling
BW	Arid desert (Koppen Classification)
CAD	Computer Aided Designing and Drafting
CF	Temperate, no dry season (Koppen Classification)
CFC	Chloro Flouro Carbon
CH_4	Methane
CH3D-SSMS	Curvilinear-grid Hydrodynamics 3D – Storm Surge Modeling System
CHI	Composite Hazard Index
CHIRPS	Climate Hazards Group InfraRed Precipitation with Station data
cm	Centimetre
CO	Carbon Monoxide
CO_2	Carbon Dioxide
COVID-19	Coronavirus Disease
CPCB	Central Pollution Control Board
CPCB	Central Pollution Control Broad
CPI	Consumer Price Index
CRI	Computed Integrated Coastal Risk Index
CRUTEM3 and HadSST2	Land-Surface Air Temperature Dataset And Sea-Surface Temperature Datasets
CRZ	Coastal Regulation Zone

CS	Temperate, dry summer (Koppen Classification)
CVI	Coastal Vulnerability Index
CW	Temperate, dry winter (Koppen Classification)
CWC	Central Water Commission
˚C	Degree Celsius
DEA	Data Envelopment Analysis
Def.	Definition
DEM	Digital Elevation Model
DF	Continental, no dry season (Koppen Classification)
DS	Continental, dry summer (Koppen Classification)
DTR	Diurnal Temperature Range
DW	Continental, dry winter (Koppen Classification)
eBTM	Enhanced Bathtub Modelling
EF	Exceedance Factor
EF	Exceedance Factor
ESRI	Environmental Systems Research Institute
EVI	Environmental Vulnerability Index
FTIR spectroscopy	Fourier transform infrared spectroscopy
FVCOM	Finite Volume Community Ocean Model
g	Gram
g/m^2	Gram Per Square Metre
GAM	Generalised Additive Models
GCPs	Ground Control Points
GDP	Gross Development Product
GHG	Green House Gases
GIS	Geographic Information Systems
GLM	Generalised Linear Models
GMSL	Global Mean Sea Level
GPS	Global Positioning System
GRACE)	Gravity Recovery And Climate Experiment
GRD	Ground Range Detected
GSPCB	Goa State Pollution Control Board
GVMC	Greater Visakhapatnam Municipal Corporation
H_2So_4	Sulphuric Acid
HC	Hydrological Connectivity
HHWS	Higher High Water At Spring
HPI	Hazard Potential Index
Ht.	Hectare
HTL	High Tide Line
ICMAM	Integrated Coastal And Marine Area Management
ICZM	Integrated Coastal Zone Management
IEA	International Energy Agency
IITM	Indian Institute Of Technology And Management
IMD	Indian Meteorological Department
INCOIS	Indian National Centre For Ocean Information Services
INR	Indian National Rupee

NGO	Non Governmental Organization
NH	National Highway
NIO	National Institute Of Oceanography
NIO	North Indian Ocean
NNW-SSE	North North West – South South East
NO_x	Oxides Of Nitrogen
NOx	Nitrous Oxide
NRSC	National Remote Sensing Centre
NSDP	National State Domestic Product
NW-SE	North West – South East
OSPAR	Oslo and Paris Conventions
pH	potential of hydrogen
PM	Particulate Matters
$PM_{2.5}$	Particulate Matter 2.5 micrometers or less in diameter
PM_{10}	Particulate Matter 10 micrometers or less in diameter
PVI	Physical Vulnerability Index
RCP	Representative Common Pathways
RMSE	Root Mean Square Error
S	South
SAPCC	State Action Plan For Climate Change
SIDS	Small Island Developing States
SLOSH	Sea, Lake and Overland Surges from Hurricanes
SLR	Sea Level Rise
SO2	Sulphur Di Oxide
SoVI	Social Vulnerability Index
SPLASH	3D Splash Model
Sq. km.	Square Kilometre
(Sq. m)	Square Metre
SRES	Special Report On Emission Scenarios
SRTM	Shuttle Radar Topography Mission
SS	Storm Surge
SSP	Shared Socioeconomic Pathways
SST	Sea Surface Temperature
SUHI	Surface Urban Heat Island
Supp.	Supplementary
SVI	Social Vulnerability Index
t	Ton
TAR	Third Annual Report
TCH4	Total Column Integrated Methane
TCO	Total Column Integrated Carbon Monoxide
TERI	The Energy And Research Institute
T_{mean}	Temperature Mean
T_{min}	Temperature Minimum
TPI	Tourist Pressure Index
TVI	Total Vulnerability Index
UAV	Unmanned Aerial Vehicle

IPCC	Intergovernmental Panel On Climate Change
IRS P6 LISS 3	ResourceSat-1
IUCN	International Union for Conservation of Nature
IW	Interferometric Wide Swath
JTWC	Joint Typhoon Water Center
Kg/head	Kilogram Per Head
km	Kilometre
LAC	Latin America And The Caribbean
Landsat ETM+	Landsat Enhanced Thematic Mapper Plus
Landsat OLI-TIRS	Landsat Operational Land Imager and Thermal Infrared Sensor
Landsat TM	Landsat Thematic Mapper
LDM	Litter Distribution Model
LHII	Landscape Human Interference Index
LiDAR	Light Detection and Ranging
LST	Land Surface Temperature
LST	Land Surface Temperature
LULC	Land Use Land Cover
LVI	Landscape Vulnerability Index
m	Metre
m/yr	Metre Per Year
MACR	Mission Arkansas Coastal Region
MAE	Mean Absolute Error
MARS	Multivariate Adaptive Regression Splines
MCI	Mitigation Capacity Index
MCGM	Municipal Corporation Of Greater Mumbai
MHHW	Mean Higher High Water
MLC	Maximum Likelihood Classifier
mm	Millimetre
mm/yr	Millimetre Per Year
MoEF	Ministry Of Environment And Forests
MoES	Ministry Of Earth Science
MoHUA	Ministry Of H
MOOC	Massive Open Online Courses
MPT	Marmugao Port Trust
MSI	Multispectral Instrument
MSL	Mean Sea Level
MSW	Maximum Sustained Wind
N	North
NA	Not Applicable
NAMP	National Air Quality Monitoring Program
NASA	National Aeronautics and Space Administration
NASA POWER	National Aeronautics and Space Administration - Prediction of Worldwide Energy Resources
NCCR	National Centre for Coastal Research
NCSCM	National Centre Of Shoreline And Coastal Management
NDMA	National Disaster Management Authority

UHI	Urban Heat Island
UN	United Nations
UNDP	United Nation Development Programme
UNEP	United Nations Environment Programme
UNFCCC	United Nations Framework Convention on Climate Change
USA	United States Of America
USD	United States Dollar
USGS	United States Geological Survey
VGR	Vulnerability Growth Rate
Vs.	Versus
w.r.t.	With Respect To
WWF	World Wide Fund for Nature
Yr.	Year
$\mu g/m^3$	Microgram per cubic metre

Abstract

In the context of the United Nations' declaration of the UN Decade on Ecosystem Restoration (2021-2030), this doctoral work has rigorously explored the imperative of restoring coastal ecosystems and enhancing the resilience of coastal communities in the face of mounting challenges arising due to coastal hazards. A primary emphasis is given to coastal vulnerability, with a strong focus on the outcomes of combining coastal hazards, and their complex interaction with the utilization of land and land surface changes (LULC) dynamics. The coastal tracts of South Goa have witnessed a profound economic transformation, primarily influenced by the tourism and mining sectors. This rapid growth has led to urbanization, leading to adverse environmental impacts. The State Action Plan for Climate Change (SAPCC) of Goa stresses about the shifting environmental landscape in the region, revealing temperature increases, alterations in rainfall patterns, and the impending sea-level rise.

In addition to coastal vulnerability, the research assesses climate trends over the four decades. The trends and their effects on the coast are analyzed in relation to the broader issue of coastal flooding. LULC assessment is a fundamental component of this study as it helped unravel the complex interplay between human activities, environmental and geomorphological changes, and the vulnerability of South Goa's coastal tracts. To gauge the anthropogenic influence deeply, a novel and holistic model, Nigam-Kotha model of Anthropogeomorphic Impact at Ecumene (AGI@E), is introduced to evaluate human influence on the geomorphology. The assessment showed remarkable impact on geomorphology in taluka(s) which have witnessed high development and thus, indicates the applicability of this model in globally measuring anthropogenic geomorphic pressure in any ecumene. This doctoral work further encompasses a sea-level rise vulnerability assessment, using land-use and elevation data to project inundation risks under diverse plausible sea level rise scenarios. The findings show relationship between land-use changes, and sea-level rise vulnerability, advocating the need for strategic interventions in low lying coastal areas to mitigate coastal vulnerability. Later, it delves deeply into coastal vulnerability, by introducing a robust Coastal Vulnerability Index (CVI), combining 21 physical and socio-economic variables to offer a nuanced understanding of coastal vulnerability at village level.

Additionally, beach litter and air quality are introduced as essential indicators to gauge human footprints in previously uninhabited regions of the study area. Overall, before 2000 A.D., the region exhibited a balance between natural land covers and human activities, with significant vegetation and minimal urbanization in all the taluka (s). However, post 2000 A.D., the coastal landscape has witnessed rapid urbanization, industrial growth, and tourism-related developments. This transformation resulted in the encroachment of natural land covers, habitat loss, deforestation, and increasing vulnerability to climate change-induced coastal hazards. This doctoral work offers a holistic methodology to examine the multifaceted relative coastal vulnerability within South Goa's coastal tracts, which has never been attempted before. In a nutshell, this research and

research framework could significantly inform policy development and disaster management strategies in developing countries and ultimately contribute to the sustainable development and resilience of the region.

Chapter-1

Introduction

1.1 Research Background

1.1.1 The Changing Climate

Climate change encompasses alterations in temperature and various meteorological patterns resulting from a combination of natural and human-driven factors. While natural elements, like solar cycle phases, predominantly influence climate dynamics, it is widely acknowledged that contemporary alterations in Earth's weather are primarily driven by human activities, as established by Haigh (1999), Howe et al. (2013), and Prakash (2021). It's crucial to emphasize that global warming refers to the long-term increase in the Earth's average surface temperature, primarily caused by the accumulation of greenhouse gases in the atmosphere, such as carbon dioxide (CO_2) and methane (CH_4) and denotes the sustained rise in the Earth's average surface temperature that has been observed since the pre-industrial era (from 1850 A.D to 1900 A.D).This phenomenon is a significant aspect of climate change, leading to various environmental and climatic impacts. This warming is generally because of the build-up of greenhouse gases such as carbon dioxide, methane among the others, due to human activities such as land-use changes. These gases trap gets warmth from the sun in the atmosphere, making a blanket around the earth and eventually leads to a stronger greenhouse impact and higher temperatures. It is crucial to understand that international warming is just one thing of climate change, and the term encompasses broader adjustments in weather patterns past just temperature increases. It consists of shifts in precipitation styles, sea level upward push, melting glaciers and ice caps, and modifications in the frequency and depth of intense weather occasions like hurricanes, droughts, and heatwaves (NASA, 2022).

It is a well-established reality that greenhouse gases and aerosols can substantially have an effect on weather via changing incoming solar radiation and outgoing infrared (thermal) radiation, which can be a part of Earth's energy balance. Changing the atmospheric concentrations of those gases and particles can cause a warming or cooling of the climate system (IPCC, 2007). Since the begin of the industrial era, the overall effect of human activities on weather has been a warming affect (Betts et al., 2007; Steffen et al., 2007; IPCC, 2007). It is critical to understand that the human effect on climate at some point of this era significantly exceeds recognized caused due to solar adjustments and volcanic eruptions (Karl and Trenberth, 2003).

1.1.2 The Concept of Hazard Vulnerability

The examination of the vulnerability of human and natural systems to changes and fluctuations in climate, along with their ability to conform to climate-related hazards, brings together professionals from diverse fields such as climate science, development studies, disaster management, health, social science, policy development, economics, and others (Brooks, 2003). the definitions provided below assist to clarify the concepts pertaining to multi-disciplinary terms.

Table-1.1 Definitions of vulnerability and allied terms commonly used in the vulnerability studies.

i.	Vulnerability (IPCC Def.-1)	The IPCC Third Assessment Report (TAR) describes vulnerability as *"The degree to which a system is susceptible to, or unable to cope with, adverse effects of climate change, including climate variability and extremes. Vulnerability is a function of the character, magnitude, and rate of climate variation to which a system is exposed, its sensitivity, and its adaptive capacity."* (IPCC, 2001, p. 995)
ii.	Vulnerability (IPCC Def.-2)	Moreover, The IPCC Third Assessment Report (TAR) also describes vulnerability as Smit et al. (1999), the "*degree to which a system is susceptible to injury, damage, or harm (one part - the problematic or detrimental part - of sensitivity)"* (IPCC Def. 2) and Sensitivity is in turn described as the *"Degree to which a system is affected by or responsive to climate stimuli"* (IPCC, 2001, p. 894).
iii.	Risk	Risk is *"Expected losses (of lives, persons injured, property damaged, and economic activity disrupted) due to a particular hazard for a given area and reference period. Based on mathematical calculations, risk is the product of hazard and vulnerability."* UN DHA, 1992. A file from the International Strategy for Disaster Reduction which separates *"hazard factors"* into two additives: *"threat (determines geographical place, depth and chance)"* and *"vulnerability/capacities (determines susceptibilities and capacities)"* (UN, 2002, sixty six).
iv.	Exposure	The exposure is defined in the same report as *"The nature and degree to which a system is exposed to significant climatic variations."* (Brooks, 2003; IPCC, 2007)
v.	Sensitivity	The sensitivity is *"the degree to which a system is affected, either adversely or beneficially, by climate-related stimuli (IPCC, 2001, p. 894). The effect may be direct or indirect (e.g., damages caused by an increase in the frequency of coastal flooding due to sea level rise)."*
vi.	Adaptive capacity	Adaptive capacity is *"The ability of a system to adjust to climate change (including climate variability and extremes) to moderate potential damages, to take advantage of opportunities, or to cope with the consequences."* (Brooks, 2003; IPCC, 2007)

vii.	Climate hazards	Climate hazards may be defined in terms of absolute values or departures from the mean of variables such as rainfall, temperature, wind speed, or water level, perhaps combined with factors such as speed of onset, duration and spatial extent. Hazards are also referred to as climate events (Brooks, 2003; IPCC, 2007). (Note: The term hazard is used throughout in this doctoral work to refer specifically to physical manifestations of climatic variability or change, such as coastal floods, storms and Sea level rise).
viii.	Disaster	A disaster, as measured in human terms (lives lost, people affected, economic losses) is therefore the outcome of a hazard, mediated by the properties of the human system that is exposed to and affected by the hazard (Brooks, 2003; IPCC, 2007).
ix.	Climate-resilient infrastructure	The infrastructure which is "planned, designed, built and operated in a way that anticipates, prepares for, and adapts to changing climate conditions. It can also withstand, respond to, and recover rapidly from disruptions caused by 34 these climate conditions" (Brooks, 2003; IPCC, 2007).

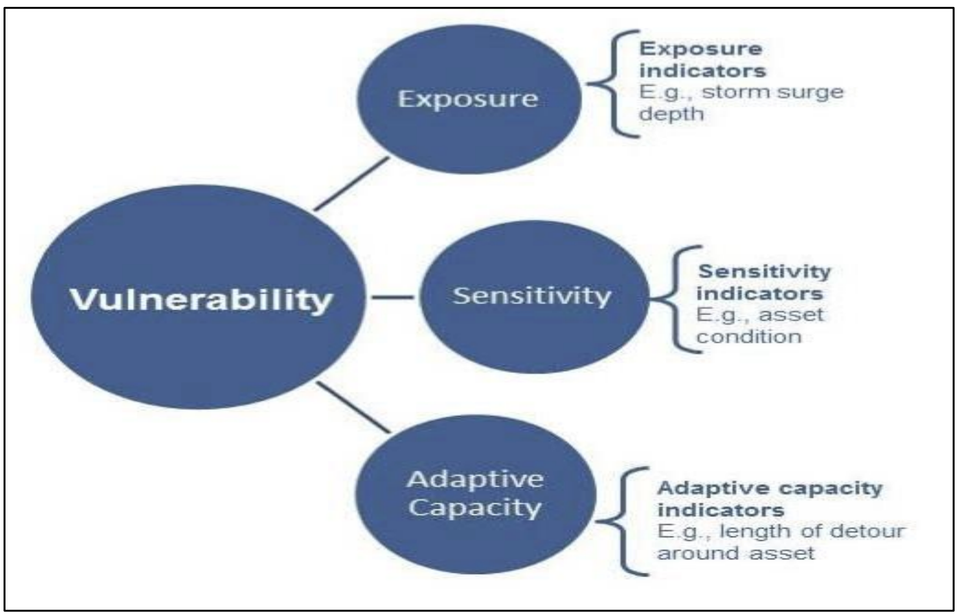

Fig - 1.1 Components of Vulnerability (Source: US Climate Toolkit, 2015)

1.1.2.1 Physical vulnerability vs. Social vulnerability

There are basically two types of vulnerability, physical and social vulnerability. Physical vulnerability is determined by the frequency and severity, or likelihood of occurrence, of a particular type of hazard, whereas social vulnerability, which is inherent vulnerability is not determined by physical factors (Brooks, 2003). The absence of damages from a hazard in an unpopulated area or an area with well-adapted human systems could be retrospectively considered as "invulnerable" to that hazard. However, studies on the impacts of climate change have generally examined factors such as the demography at risk of flooding due to projections of sea level rise (Nicholls et al., 1999), and therefore focused on human exposure to hazards (social vulnerability).

1.1.2.2 Components of Coastal Physical Vulnerability

The first point of contact between the landmass and a coastal hazard is the coastline. In addition to process-based factors, physical variables controlled by topography, such as the type of coastline and coastal slope gradient and elevation, are major contributors to coastal physical vulnerability.

Hence, an emergent shoreline can be defined as a coastal region that has undergone a decrease in sea level due to either global or local factors resulting in the exposure of otherwise drowned coastal landforms above the high tide mark such as raised beaches. In contrast, a submergent coastline is one where the sea level has risen due to a global sea-level change, local subsidence, or isostatic rebound, with submerged or "drowned" landforms such as rias (drowned valleys) and fjords (Davidson-Arnott et al., 2019).

According to the second principle of coastline classification, a concordant coastline is where bands of different rock types run parallel to the shore, forming distinctive landforms such as coves. Discordant coastlines, on the other hand, feature distinctive landforms because the rocks are eroded by the ocean waves. The less resistant rocks erode faster, creating inlets or bays, while the more resistant rocks erode more slowly, remaining as headlands (Jackson et al., 2005).

The gradient of coastal slope plays a crucial role in determining the likelihood of flooding in coastal regions. Gentle slope is more prone to flooding than the locations having steeper slope as gentle slopes retreat faster than steeper slope and wave energy can penetrate more inside the gentle slope (Nigam et al., 2020). Coastlines can be categorized as a cliffed coast or abrasion coast based on their coastal slopes, where marine action has resulted in steep declivities known as cliffs (high slope). In contrast, a flat coast is one where the land gradually descends into the sea (moderate slope), and a graded coast is one where wind and water action has produced a flat and straight coastline (low slope) (Whittow, 1984).

Coastal regional elevation is another critical factor that influences coastal vulnerability and refers to the common mean elevation of the coastal vicinity above mean sea level (MSL). It is an essential parameter in the analysis of coastal vulnerability, as it provides an estimate of the extent of land under threat by projected sea level rise (SLR) (Kumar and Kunte, 2012; Kumar et al., 2010), as well as the sensitivity of the coast to flooding during a storm surge (SS) (Diez et al., 2007) or tsunami. Hence, areas with high coastal elevation are generally considered less vulnerable, and vice versa (Gornitz et al., 1994).

1.1.2.3 Components of Coastal Social Vulnerability

Coastal flooding poses a massive challenge in regions with human activities, leading to risk of lives and assets. The world is presently going through a growing danger of coastal flood failures, which can be attributed to the growing coastal population and the rise in sea level (Rosendahl, 2013; Rosendahl, 2016). The increment in human population can be both temporary and permanent, because of seasonal migration and different factors (Cook, P.J. 1996).

The IPCC AR6 report of 2019, explicitly states with a very high confidence that unsustainable land-use and land cover modifications, deforestation, pollution, and their interactions adversely affect the capability of ecosystems and groups to conform to climate change. Non-climatic human-triggered elements increase the vulnerability of ecosystems to climate change. The coastal regions are closely pressured because of the tremendous population increment, which is discussed above, which has precipitated everlasting destruction of habitats and fragmentation of habitats. Furthermore, engineering measures have additionally contributed to this destruction (Bulleri and Chapman, 2010).

Reclamation of salt marshes and mangroves has taken areas in estuaries, intertidal bays, and inlets globally (Gibson et al., 2007). Industrial development has altered and destroyed coastal ecosystems, inclusive of rich coastal habitats. Globally, several major industrial centers are situated on estuaries and in the area of urban areas and ports. As an end result, the primary impacts on marine ecosystems has been the destabilization of shallow banks and accelerated erosion. Beach erosion is a severe problem shared by many countries (Luijendijk et al., 2018).

Moreover, IPCC, 2019 highlighted with high confidence that the areas with large development constraints encountering illiteracy, poverty, and low quality of life of the populations have an excessive vulnerability to climatic hazards. Between 2010 and 2020, human mortality from floods, droughts and storms have been 15 times higher in exceptionally prone regions compared to regions with low vulnerability.

1.1.2.4 Risk vs Vulnerability

The community focused on natural hazards, which stresses on risk, and the community focused on climate change, which stresses on vulnerability, are essentially examining the same processes. However, this may not have always been immediately obvious, owing to differences in terminology (Brooks, 2003; IPCC, 2007) but both are ultimately interested in the physical hazards that endanger human systems.

According to the IPCC Def.-1 (Table-1.1), the vulnerability of a system is viewed as a function of its sensitivity, while Def.-2 (Table-1.1) views vulnerability as a subset of sensitivity. IPCC Def. 1 clearly refers to biophysical vulnerability, where "sensitivity" plays an equivalent role to social vulnerability in the context of human systems, while IPCC Def.-2 refers solely to social or inherent vulnerability.

The division of vulnerability into social and biophysical vulnerability enables us to appreciate the compatibility of the risk-based and vulnerability-based approaches (Brooks, 2003; IPCC, 2007). The concept of biophysical vulnerability addresses the same issues as the concept of risk, or, adopting the more precise terminology of Sarewitz et al. (2003), outcome risk. Therefore, if we view IPCC Def. 1 as a definition of biophysical vulnerability and IPCC Def.-2 as a definition of social vulnerability, the vagueness is cleared.

In other words, the threat posed to a coastal area by sea level rise depends on the rate at which it occurs. The existing vulnerability of the system or region depends on the state of socio-economic variables in question (IPCC def.-2). Hence, evaluating the existing (social) vulnerability is crucial, as it constitutes the "baseline" from which any reduction of vulnerability to "acceptable" levels through adaptation could take place (Nicholls et al., 1999; Parry et al., 2001).

1.1.3 Indian Coastal Region and Coastal Hazards

India is ranked as the third worst-affected country in the world due to climate-induced natural disasters. The coastal regions, mainly, are surprisingly prone to these disasters due to the rapid urbanization, high population densities, and related economics activities. The 7,517-km-lengthy coastline is home to 260 million of population, that's equal to one-third of India's population. These people live in low-lying areas within 50 km of the sea coast and are perennially exposed to climate variability and extreme weather events (Roy, 2019).

India's shoreline has already been affected by the sea level rise (SLR) that has been recorded at a rate of 2-5 mm according to 12 months since 1950s. This situation has led to a projected rise in sea level along India's coast by 2050, ranging from 15 to 38 cm. This rise is likely to affect 5,763 sq. km combined area of the coastal states. The result will be the submergence of coastal areas, flooding, and an increase in tropical cyclones and storm surges, thereby threatening infrastructure events (Roy, 2019).

In recent years, India's coastal regions have become more vulnerable to multiple risks related to climate change. Intense and more frequent cyclones such as the recent Fani, Gaja, and Hudhud, as well as severe floods, have caused massive devastation to the country's coastal states (Business Today, June 7, 2019; Roy, 2019).

This situation has made it highly challenging for most of the coastal states to rebuild the critical infrastructure and to recover from the consequent disruptions caused by disasters. For example, the August 2018 floods in Kerala destroyed 280,000 homes, 140,000 hectares of status vegetation, and approximately 70,000 km of transport network. The total recovery needs of the State were estimated at INR 310 billion, according to the Post Disaster Needs Assessment conducted by the UN Agencies (UNDP, 2018; Vijayan, May 15, 2019). Similarly, the April 2019 cyclone Fani damaged 500,000 houses, 6,700 hospitals, and 100,880 lakh ha. of agricultural land. Electricity infrastructure was also damaged, bringing the total losses to INR 500 billion. Studies and the damage assessment report indicate that it will take the coastal states about five to 10 years to rebuild and recover (Business Today, June 7, 2019).

The grass-root reasons behind the high vulnerability due to coastal extremes are severe degradation of sand dunes (Cabral et al., 2017) and mangroves ecosystem (Amosu et al., 2012) along the coastal regions. These factors, among others, such as risks related to climate change and its impact on infrastructure, are yet to be integrated into the urban development planning paradigm in coastal India. In addition, most of the infrastructure planning in coastal states such as water, sewage, telecommunication, and roads lie with various government departments that have no integration point for multi-sectoral development (Roy, 2019). These factors cumulatively increase the coastal vulnerability.

1.1.3.1 Increasing Coastal Hazards Vulnerability along the West Coast of India

India is presently considered to be at an excessive risk of experiencing severe cyclones because of the thermal expansion of sea water due to warming oceans (Rao et al., 2020). This phenomenon leads to a significant increment in the frequency of storm surges and cyclones in coastal areas (Weisse et al., 2012; Lin et al., 2013). Between 1877 and 2005, India's coastal regions experienced a total of 283 cyclones, with 106 of them being severe and taking place at the east coast, while 35 have been much less severe at the west coast (Roy, 2019).

A latest research study by the scientists of the Indian Institute of Tropical Meteorology (IITM) underneath the Ministry of Earth Sciences (MoEF) has proven a decline in the frequency of cyclones in the Bay of Bengal as compared to the Arabian Sea. Over 19-year period between 1982 and 2002, there has been an 8% decrease in the frequency of cyclones over the Bay of Bengal. However, throughout the identical duration, there was a 52% upsurge in the frequency of cyclones over the Arabian Sea (Deshpande et al., 2021).

One of the reasons for this increase in the frequency of cyclones over the Arabian Sea is global warming. The surface temperatures of the Arabian Sea have has increased gradually all through the past century, and the temperature now is 1.2–1.4 °C higher than the temperature witnessed 4 decades ago. These warmer temperatures support active convection, heavy rainfall, and intense cyclones (Singh and Roxy, 2022). The rising temperature is eventually enabling the Arabian Sea to supply ample energy for the intensification of cyclones (Deshpande et al., 2021).

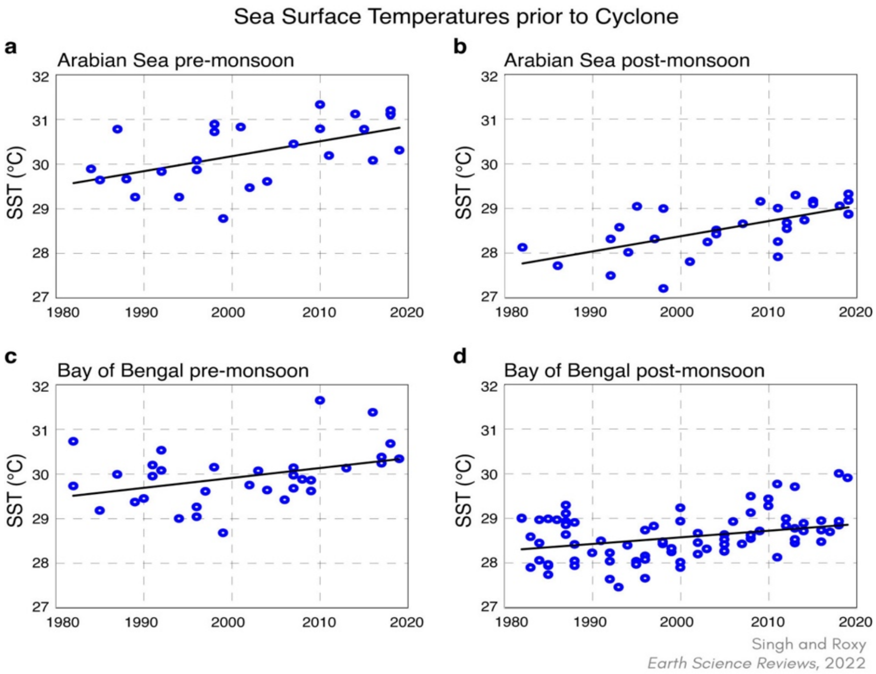

Fig-1.2 Sea Surface Temperature (SST) prior to Cyclogenesis—for (a) Arabian Sea pre-monsoon, (b) Arabian Sea post-monsoon, (c) Bay of Bengal pre-monsoon and (d) Bay of Bengal post-monsoon. (Adopted from: Singh and Roxy, 2022).

According to Singh and Roxy, 2022, the total SST change over the Arabian Sea during 1982–2019 is 1.4°C in the pre-monsoon and 1.2°C in the post-monsoon season. While over the Bay of Bengal, the observed change in SST is 0.8°C in the pre-monsoon and 0.5°C in the post-monsoon (Fig.-1.2). In addition, Tiwari et al., 2022, found that the proportion of Arabian Sea cyclones was initially 1:4 compared to the Bay of Bengal, but the study found that it has become 2:4 from 2001-2020. For example, in 2019, out of a total of eight cyclones in the North Indian Ocean, five were formed in the Arabian Sea. The total figure was seven for 2018, including three over the Arabian Sea. Not just the frequency, even the intensity of the cyclones over the Arabian Sea also are changing.

Moreover, as compared to earlier period, during 1980-2019, the intensity of the Arabian Sea cyclones during the pre-monsoon season (April–May) has increased by 40% and by 20% during the post-monsoon season (October–December). Resultantly, the accumulated cyclone energy has also shown increment in the Arabian sea cyclonic episodes which are not highly significant in the Bay of Bengal during the similar period.

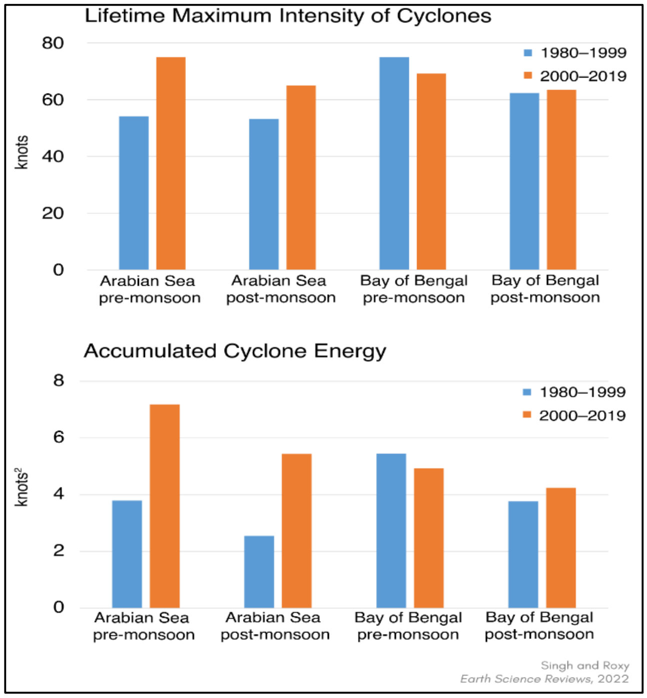

Fig-1.3 Lifetime Maximum Intensity of Cyclones and Accumulated Cyclone Energy during pre-monsoon and post-monsoon period between 1990-2019 in the Arabian sea and Bay of Bengal (Adopted from Singh and Roxy, 2022).

This trend clearly suggests that the India's west coast needs to get prepared for more frequent and stronger storms (Fig.-1.3). The Arabian Sea is supplying ample energy for the intensification of cyclones, and the increasing temperature is enabling it to do so. The warmer temperatures are supporting active convection, heavy rainfall, and intense cyclones, which are all contributing to the increase in frequency of cyclones over the Arabian Sea (Deshpande et al., 2021).

Table- 1.2 Characteristics of the coastline along the west coast of India (values in percentage).

West Coast State	Sandy Beach	Rocky Coast	Mudflats	Marshland
Gujarat	28	21	29	22
Maharashtra	17	37	46	-
Goa	44	21	35	-
Karnataka	75	11	14	-
Kerala	80	5	15	-

Source: Rishi and Mudaliar, 2014

1.1.3.2 Current Threats along the Coastal Tracts of South Goa

South Goa is situated on the west coast of India and facing the Arabian sea. Over the past few decades, the district has experienced an unprecedented economic boom due to tourism and mining, resulting in a significant increase in floating population (Noronha et al., 2002, Sawkar et al., 1998; (Desousa, 1999).

In addition to the above facts, heavy immigration from other states has further contributed to the population increase and has led to a rise in demand for city housing, all over the Goa state. According to the Census of India, 2011, Goa's housing has tripled in relation to its decadal population growth rate of 8.2 percent. The higher demand for city housing in Goa has led to more construction and increased supply. Unfortunately, the rapid urbanization along the coast has resulted in several negative consequences, such as deforestation, significant LULC conversion to built-up, destruction of ancestral properties to build high rise infrastructure etc. Consequently, it has prompted irreversible harm to the coastal landscape, along with the destruction of dune vegetation, permanent elimination of several wetlands and coastal sand dunes, and localized seashore erosion (Business Goa, November 1, 2018).

Despite the harmful impact of urbanization on natural landscape, coastal South Goa stays a popular tourist vacation spot and a hub of financial interest, attracting both home and global visitors. Therefore, it's very important for the authorities and stakeholders to cope with the challenges of urban sprawl and enforce sustainable measures to maintain the natural landscape and promote responsible improvement. More importantly, Goa's success as a model state in India depends on how well it balances economic growth with environmental conservation and social welfare, ensuring a brighter future for generations to come (Business Goa, November 1, 2018).

1.1.4 Need of the study

The United Nations has already declared the decade of 2021-2030 as the UN Decade on Ecosystem Restoration, in pursuit to repair the coastal ecosystems (Fischer et al., 2021; Eger et al., 2022) because the coastal communities across the globe need to brace themselves for a great deal more challenging futures than what's presently predicted. It is vital to conduct researches on possible coastal flooding impacts, to limit the human losses resulting from such threats (IPCC, 2019). The IPCC AR6 has stated (with high confidence) that human vulnerability in the future will keep to concentrate in regions in which capacities to offer infrastructures and fundamental offerings are least, and that coastal vulnerability can also be concentrated in rapidly growing casual settlements. Additionally, rural regions' vulnerability could be increased because of diverse compounding factors which include high emigration charge, sanitation, water, health, shipping, communications, and energy.

Furthermore, policy planners at the national and subnational levels in coastal regions would require a definite risk assessment that includes probability, occurrence, and the degree of potential hazard to different infrastructure (Roy, 2019).

According to the State Action Plan for Climate Change (SAPCC) prepared in 2020 by the Government of Goa, the state's mean annual temperature has increased by over 1°C since the beginning of the 20th century till 2018 (1901-2018), much of it during 1990-2018 period. The average yearly rainfall in Goa has grown by 68% between 1901 and 2015. Inter-annual rainfall variability in the state has grown with rising rainfall, particularly since the 1970s. Moderate to light rainfall days (IMD category I) have decreased between 1901 and 2015, and extremely heavy and very high rainfall events (IMD category III) in the state have increased by more than 100%.

The SAPCC, 2020 report has also revealed that 14.73% of the land in Goa is under 15m elevation, majority of it in the coastal zones which are severely vulnerable to coastal flooding. It is also estimated that a one-meter sea level rise, would affect 7 percent of Goa's population and cause damage worth Rs. 8,100 crores. In terms of coastal vulnerability, Salcete is the most vulnerable taluka.

In addition, elsewhere as well, communities living in low lying areas, informal settlements and whose livelihood is dependent mainly on low lying ecosystems including riverine ecosystems are in particular the most vulnerable groups. Also, Marmugao, and Salcete, house more than 80% of the population and are hubs of economic activity as well as, increasing popularity of Canacona beaches attracts a huge amount of floating population.

Thus, it is imperative to determine the impact of anthropogenic influence in the coastal tracts of South Goa, to pave the way forward on resilience to coastal vulnerability, which has been also argued by Vaz (2017). This thesis work has adopted a robust and holistic methodology which incorporates multi-disciplinary assessments to bring out the fact about the role of human interaction in increasing the coastal vulnerability arising due to climate change induced coastal hazards.

1.2 Study Area

1.2.1 Location

The study area is situated within the administrative boundaries of the coastal taluka(s) in South Goa district, namely Marmugao, Salcete, Quepem, and Canacona, spanning between latitudes 15˚ 29' 32" N and 14˚ 53' 57" N and longitudes 73˚ 46'21" E and 74˚ 20'11"E. Bounded by the Arabian Sea to the west, North Goa district to the north, Uttar Kannada district of Karnataka to the south and southeast, and Sanguem taluka of South Goa district to the east, the study area covers a total geographical area of 1072.36 Sq. km (Fig.-1.4). It fully or partially encompasses five topographical sheets 48E/16, 48I/3, 48I/4, 48J/1, 48J/5) of the Survey of India.

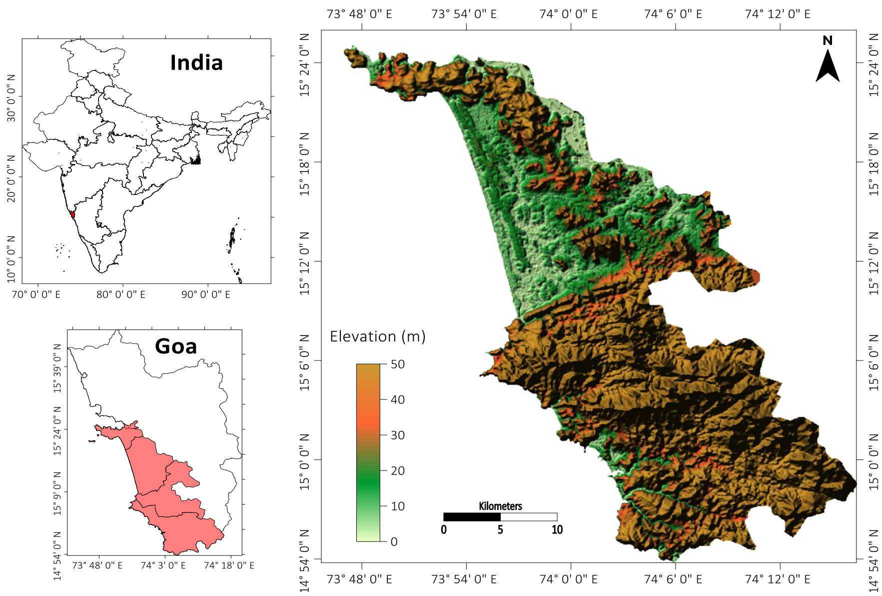

Fig-1.4 Location and physiographic map of the study area.

Table-1.3 Total geographical area under the study.

Taluka	Area (Sq. km)
Marmugao	109.13
Salcete	292.94
Quepem	318.25
Canacona	352.04
Total area under study	1072.36

1.2.2 Physiography

Goa can be physiographically classified into the coastal tract, sub-ghat region, and high ranges of the Western Ghats (Dessai, 2023), and the same holds true for coastal South Goa coastal taluka(s). The study area has three natural divisions, namely, the coastal tracts, the plateaus, and the mountain region.

1.2.2.1 Coastal Tracts (Low Lands)

Coastal South Goa is part of the Konkan area, with the low land area mainly consisting of coastlines (Pombo, 2019). The western belt constitutes the coastal plains. While the central land masses in this portion of Goa seem to have emerged from the sea, as is evident at Margao and Canacona (Vaz and others, 2017). The formation of the major river systems, Zuari, resulted from faults during the uplift of landmasses which flows in a westerly direction (Sharma and others, 2022). The coastal plains include beaches, mudflats, swamps, and fluvio-littoral plains. This area is fertile and dominated by tourism activities, hence thickly populated (Vaz et al., 2017).

1.2.2.2 Plateau Lands

The plateau region is located between the Western Ghats (Sahyadri) in the southeast and the coastal plains in the west, as well as the Marmugao headland. Plateau land height ranges from 30 meters to 100 meters (Nayak. 1999), predominantly located in Marmugao and Quepem. The eastern parts of Quepem are occupied by undulating uplands with gentle to moderate slopes, intercepted by concave depressions comprising valleys mainly under paddy cultivation. The slope gradients range from 5 to 20%, occasionally going up to 30% (Singh et al., 2018). This region has a good amount of minerals such as iron-ore, resulting in extensive mining in this belt. Moreover, plenty of lateritic stones are found, which are used for building purposes (Naik, 2017).

1.2.2.3 Mountainous Area

The Western Ghats are to the south and south-east of the research area. These mountains cover around 33% of Goa's entire land area. The main hills range in elevation from 1022 m MSL (Darsinga) to 251 m in Cape de Rama, where the Sahyadri protrudes into the Arabian Sea to the west. This section is densely forested. Some of the mountains in this area are quite steep. This area is home to several streams and rivers.

1.2.3 Topography

The study area boasts undulating topography with slope ranging from plain (slope <1%) to very gentle, predominantly found in the coastal areas, and very steep (slope >35%) along the southeastern boundary. However, gentle to moderate slope types are relatively evenly distributed throughout coastal South Goa taluka(s) (Kamat, 1990; Dessai, 2023).

1.2.4 Geology

The study area's geology is primarily composed of the Goa Group formation, which belongs to the Dharwad Super Group of the Archaean to Proterozoic age (Dessai, 2023). The metamorphic rocks of green schist facies comprise this group, which are arranged in a general NW-SE direction and indicate three folding cycles. The west coast's straight coastline suggests a significant fault, along with several weak planes that have developed. A prominent fault zone is represented by the Western Ghats, which extends in the N-S to NNW-SSE direction (Fernandes, 2018).

The Goa Group is intruded by granite gneiss, feldspathic gneiss, hornblende gneiss, and porphyritic granite, followed by basic intrusive (Li et al., 2020). Additionally, metabasalts are extensively exposed in Canacona and Marmugao taluka(s), along with small outcrops in Salcete Taluka (Dessai, 2011). Greywacke with conglomerate exposures are found to occur in Quepem and Canacona taluka(s) (Fernandes, 2018), while granite gneiss is found in a large portion of Salcete taluka and limited exposures are in Quepem and Canacona (Dessai, 2023). Small outcrops of granite are found in Canacona taluka, while laterite occurs extensively, covering almost all formations in coastal South Goa (Widdowson, 2009). Coastal alluvium is present as a thin strip along the western part of Salcete taluka's coastal plains, consisting of fine to coarse sands with the mixture of sandy loam, silt, and clay (Dessai, 2023).

1.2.5 Soil

The study area is characterized by a variety of soil types derived from three geological formations, namely Basalt/Metabasalt, Granite/Granite gneiss, and Quartzite. Additionally, the soils are associated with rock outcrops and laterite crusts.

The study area can be classified into four major types of soil, namely Laterite, Saline, Marshy, and Alluvial soil. The Lateritic soil is the dominant soil type in the study area. Saline soil occurs in flood plains of Zuari, Sal, Saleri, Talpona, and Galjibagh rivers in all of Salcete, Marmugao, Quepem, and Canacona taluka(s). Marshy soil occurs in low-lying waterlogged and tidal affected areas of Salcete, Marmugao, and Canacona taluka(s) and Alluvial soil occurs as very thin strip along the coastline towards the western part of Salcete taluka and a limited exposure occurs in Canacona taluka. It is well-drained, acidic with low pH, and organic content.

1.2.6 Coastal Geomorphology

Table 1.4 Coastal sand dunes area within 200m from the High Tide Line (HTL) in the study area.

Taluka	Village	Area of Sand Dunes Within 200m (in sq. m)
Marmugao	Pale-Velsao	31727
	Cansaulim-Arossim	86217
Salcete	Betalbatim	208409
	Colva	196776
	Cana-Benaulim	123149
	Varca	363438
	Cavelosim	613175
Canacona	Poinguinim	559886

Source: Goa State Diversity Board, 2020

1.2.6.1 Vasco - Bogmalo

This stretch of the coastline is composed of rocky headlands, sparsely wooded, hosting only two primary beaches. The Baina beach is severely degraded and polluted (Nigam et al., 2021) while the Bogmalo beach, lined by dense coconut trees, is more natural. This area comprises low sand dunes, but some of them are obliterated. Towards the south, the coast is predominantly rocky (Chicolna, Dabolim), with some pocket beaches and secluded coves such as the one at Hollant.

1.2.6.2 Pale - Colva

The coastline from starting from Pale and up to the Mobor peninsula is a linear stretch characterized by sand dunes which make up the most exquisite dune belt of the entire coastal zone of Goa (Mascarenhas, 1998).

Velsao to Betalbatim coastal zone section consists of very prominent vegetated sand dunes. However, at several places in this stretch, sand dunes have been flattened and obliterated (Mascarenhas, 1998). At Velsao, the coastal area is defined by thick coconut plantations, with low sand dunes (Wagle, 1995). Most of the shoreline is under threat of erosive processes, as evidenced by eroded berms and uprooted trees (Fig-1.5 (a)).

At Colva, dune vegetation and coconut plantations, are still visible on either side of the main beach point, which has turned into a crowded area (Fig-1.5 (b & c)).

1.2.6.3 Sernabatim - Cavelossim - Mobor

This coast is protected by sand dunes, varying in elevation, with associated vegetation, including luxuriant casuarina plantations, as in Varca (Fig-1.5 (d)).Here also, several dunes have been flattened and even removed and Several new coast perpendicular roads have been built during the last few years. The Cavelossim - Mobor coastal strip is a unique sandy peninsula about 250 m wide found between the ocean and the river Sal, is experiencing an exceedingly fast rate of buildup (Mascarenhas, 1998).

Fig-1.5 Drone imageries showing the linear sandy coast of Marmugao and Salcete; (a) Bogmalo-Velsao stretch, (b) Colva beach, (c) Colva beach parking area and, (d) Varca - Sernabatim beach stretch.

1.2.6.4 Cola-Agonda-Palolem

This stretch starts at Cola where there are numerous small sandy pockets and beach fronts located within promontories consisting of hill slopes that extend into the Arabian sea. The Agonda area comprises a kilometer-long secluded beach between two wooded headlands, and is backed by low sand dunes in the southern part only. The complete shoreline is prone to erosive forces, especially in the northern part which is more evident due to monsoon inundation and severe erosion as seen from a large number of uprooted trees lying on the beach (Mascarenhas, 1998).

Palolem is another popular beach between two thinly forested headlands, with the entire coastal area dotted with coconut plantations. Low sand dunes are seen in the southern part, being less prominent in the north (pic). Further south, Colamb beach between two promontories, and the pristine Rajbag beach backed by dunes and with a lagoon at one end, are the two sandy areas, where the dunes have been razed for a resort development.

1.2.6.5 Talpona - Galgibaga

This stretch comprises a linear beach with a minor wooded headland in between, characterized by sand dunes, some as high as 6 - 8 m. At some places close to the existing parallel road, high dunes have been razed and obliterated

Except for the mangrove dominant Maxem backwaters, the entire shore up to the southern border is rocky but with vegetated slopes. Along this stretch, pocket beaches and sandy patches are found, the most prominent being the secluded Xendrem beach with a rocky shore, and Polem beach, which is less than a kilometer long and well protected with promontories and still mostly out of reach from the human influence.

1.2.7 Climate

The study area has a tropical climate, and it receives rainfall from South-West monsoon winds during June-September (Sachin and Rasheed, 2020). The mountain region receives more rainfall than the coastal region (Nandargi and Mulye, 2014). The months of October-January have a cool climate, whereas from February, the temperature starts rising and remains until May. May is the hottest month whereas January is the coolest with a mean daily temperature of 30˚C, and 23˚C respectively. The temperature is highest (around 33˚C) in pre-monsoon months of April and May and again in November. The humidity annually, is more than 60%, with a range from 80 to 90% during the monsoon period (IMD, 2019).

As a result of orographic influence, the rainfall increases towards the Western Ghats (Venkastesh et al., 2021), with an average annual rainfall of 2875 mm (in Salcete taluka) & 2466 mm (Marmugao taluka) respectively to 3825 mm (in Sanguem taluka). The annual rainfall predominantly occurs during the monsoon months of June to September (more than 90%, and about 32% of the annual rainfall is received during July (IMD, 2019).

1.2.8 Drainage Pattern

The drainage pattern in the study area have rivers which are navigable all year round, have their source in the Sahyadri ranges and flow towards the west into the Arabian Sea, which is approximately 60 kilometers away. Additionally, there are a number of streams and rivulets in the study area and flow in a westerly direction, finally draining into the Arabian Sea, which also helps the surface drainage (Wagle, 1982).

The rivers are both tidal and rain-fed, making them perennial, with the exception of Talpona, which is partially perennial (Morakar and Kishan, 2021. Goa's surface water system is linked to eco-development since it provides irrigation facilities for agriculture, produces biotic and mineral resources, transports ore from the mining areas to the port, and ferries people and goods to different parts of the state (Kamat, 1990). The principal rivers that flow through the study area are Zuari, Sal, Galjibaga and Talpona. Zuari is the longest river in the state of Goa, and its second-largest basin extends from Netravali (Sanguem taluka, South Goa district) to Marmugao.

In the area, the underlying rocks primarily govern the drainage system. The drainage pattern is generally of the dendritic type. The river valley is "V" shaped in the western high hill ranges but broadens in central midlands and becomes "U" shaped in the lowlands and coastal plains (Wagle, 1982).

Wetlands encompass a variety of habitats including marshes, floodplains and tidal marshes (Bassi and others, 2014). Loutalim, Verna, Raia, and Curtorim villages in Salcete taluka are the most prominent wetlands in the study area. The eco-sensitive low-lying areas known as Khazan lands are influenced by tidal action and play a vital role in protecting the agricultural lands and surrounding villages in the study area from tidal ingress through the use of complex bunds (Ansari and others, 2012). The total Khazan land area within the study area is 9.26 sq. km.

1.2.9 Forest

According to the Department of Forest, the recorded forest cover in coastal South Goa is approximately 300.71 sq. km (Table-1.5). The study area's vegetation cover comprises dense forests of deciduous to moist deciduous type. The forests offer diversity due to variations in altitude, aspect, soil characters, slope, etc. The major species found include Teak, Eucalyptus, Bamboo, Cashew, Casuarina etc.

Only high hills mainly in Canacona have evergreen forests, which are further divided into Semi-evergreen forests. This occurs through intermingling between tropical evergreen and moist deciduous forest, mostly above 500 MSL. The northern, southern, and eastern parts of Canacona have dense forests. Moderately dense forests are found between high ranges of Western Ghats and the gently sloping lands ranging between 150 m and 300 m. Laterite outcrops that are hard and indurated have scrub forests with scanty vegetation. Commonly, luxuriant growth of grasses is found (Bourgeon, 1989; Naithani and others, 1997).

The coastal tracts with marine alluvium are mainly covered with palms. The shoreline and the west coast has a thick palm fringe with a small area covered by mangroves. While the estuarine vegetation consisting of Mangroves also occurs along swampy riverbanks in isolated patches, of Zuari, Tiracol and Galgibag rivers. The mangroves are found mainly at Durbhat and Cortalim in the South Goa district. This vegetation occurs from sea level to an altitude of 100m (Singh and others, 2004).

Table 1.5 Area under the forest in the study area.

Taluka	Area (sq. km.)
Marmugao	Nil
Salcete	Nil
Quepem	114.91
Canacona	185.82
Total	300.73

Source: Department of Forests, Goa & Zoning Atlas Report

1.2.10 Demography

The Census of India for the year 2021 has not been conducted due to the Covid-19 pandemic in 2020-2021. Thus, this doctoral thesis has considered the demographic data of the 2011 census. According to 2011 Census of India, the demographic statistics of the study area is provided below:

Table 1.6 Demography of the study area

Taluka	Total Population	Population Density/ Sq. Km	Percentage of Rural Population	Percentage Of Urban Population	Percentage to State Population
Mormugao	154561	1416	14.38	85.62	10.60
Salcete	294464	1005	27.85	72.15	20.19
Quepem	81193	255	44.63	55.37	5.57
Canacona	45172	128	72.47	27.53	3.10

Source: Census of India, 2011

Table 1.7 Distribution of households and slum population in the study area

Taluka	No. of Households	Average Family size	No. of Slum Households	Slum Population	Percentage to total slum population (in Goa)
Mormugao	35702	4.33	4974	23625	90.01
Salcete	71717	4.11	265	1641	6.25
Quepem	19119	4.25	0	0	0
Canacona	10239	4.41	0	0	0

Source: Census of India, 2011

Table 1.8 Distribution of working population (Total workers) by Industrial category.

Taluka	Total Workers	Cultivators	Agricultural Laborers	Household Industries	Other Workers
Mormugao	62,162	1,332	732	877	59,221
Salcete	1,08,209	3,269	2,169	2,926	99,845
Quepem	32,890	3,684	4,289	708	24,209
Canacona	19,048	5,009	1,920	767	11,352

Source: Census of India, 2011

1.2.11 Socio-economic

Transportation in the study area is facilitated by two National highways, NH 17 and NH 4A (Dessai, 2023), as well as the Konkan Railway and South-Central Railway lines (Ranade, 2009). Additionally, there is a major cargo handling Port at Mormugao and the Dabolim airport provides connectivity to major cities within India and abroad. Margao city is considered as the commercial capital in the study area (D'Mello, 2015).

Mining has been a significant contributor to the economic history of modern Goa, with the land away from the coast being rich in minerals and ores such as iron ore, ferro manganese, and bauxite (Dessai, 2023; Jakati, 2021). However, mining has been stalled in the region since the Honorable Supreme Court cancelled 88 mining leases order in the state on February 7, 2018 (The Economic Times, Feb 7, 2018) due to environmental concerns raised by open-cast mining which severely affects the environment and the land use pattern.

The industrial landscape of the study area has diversified since liberation in 1961, with tourism, electronics, automobile accessories, pharmaceuticals, and agro chemicals being some of the prominent industries. The region has emerged as a manufacturing base for several leading companies, with pharma industries being mostly located in Verna industrial area in Marmugao taluka (Govt. of Goa, 2018).

The services sector is dominated by tourism, which is the largest segment. The study area is famous for its natural and cultural landscapes. Colva beach, Agonda beach, and Palolem beach are some of the major beaches in South Goa district. Additionally, relics of rich Portuguese architectural legacy can be seen throughout the study area (Govt. of Goa, 2018).

Tourism activities in the study area is thriving. However, specific tourist arrival data for the study area is not available. Nonetheless, Goa state has seen a significant influx of tourists in recent years which indirectly indicates towards the tourism impact in the study area.

Table 1.9 Number of tourists (in million) arrivals, domestic & international between 2012 and 2020 in Goa state.

Year	Domestic Tourists	International Tourists
2012	2.34	0.45
2013	2.63	0.49
2014	3.54	0.51
2015	4.76	0.54
2016	5.65	0.68
2017	6.90	0.89
2018	7.08	0.93
2019	7.12	0.93
2020	3.26	0.3

Source: Department of tourism, Govt. of Goa

1.3 Aim & Objectives of the study

- **Aim**

To determine the role of anthropic pressure on natural landscape thereby influencing coastal hazard vulnerability arising due to anticipated climate change.

- **Objectives**

- To conduct multi-temporal climate trend analysis, to find out climatic variations in the study area.
- To determine the anthropogenic impact (human footprints) on local environment and geomorphology by quantifying multi-temporal LULC changes, Anthropo-Geomorphic Process (AGP), beach litter, air quality assessments in the study area.
- To determine the coastal flood vulnerability induced by compounding effects of coastal flood drivers. To identify future hazard zones in the study area.

- To create a Comprehensive Coastal Vulnerability Index (CCVI) comprising of different parameters from interdisciplinary domains.

1.4 Scope of the study

1.4.1 Spatial Coverage

The study focuses on the coastal tracts of South Goa district, specifically the regions of Marmugao, Salcete, Quepem, and Canacona talukas. This geographical area covering a total area of approximately 1072.36 sq. km.

1.4.2 Temporal Coverage

The study employs various temporal windows for different assessments:

- Climate Trend Analysis (1981-2020): This is a long-term analysis spanning 40 years, from 1981 to 2020. It aims to identify trends and patterns in weather conditions.
- Multi-temporal Assessments (2000-2020): These assessments cover the past two decades, from 2000 to 2020. They include Land Use/Land Cover (LULC), Anthropogenic Geomorphic Processes (AGP), and Sea-Level Rise (SLR) assessments. This allows for the evaluation of how human activities have impacted the landscape and coastal processes during this time frame.
- Air Quality Assessment (Seven-Years): Due to data availability constraints, the study assesses air quality over a seven-year period. This analysis aims to understand variations in air pollution levels in the region.
- Beach Litter and CCVI Assessment (Present Time): The assessments for beach litter and CCVI are conducted for the present time, offering a snapshot of the current state of these factors in the coastal area.

1.4.3 Research Population

The research considers not only the permanent population residing in the studied talukas but also includes the floating population who have a significant impact on the coastal environment.

1.4.4 Theory

The core theory underlying the research is the recognition that anthropogeomorphic processes, which result from human activities, are currently the most dynamic forces shaping the geomorphology (physical landscape) of the coastal area. These processes not only alter the landforms but also significantly heighten the region's vulnerability to various coastal hazards, particularly those induced by climate change.

1.4.5 Purpose

The primary purpose of this research is prove the dominant influence of human activities in increasing coastal vulnerability and to provide a holistic and robust methodology to explore how human activities and geomorphological processes interact in the coastal region and eventually exaggerate coastal vulnerability. Specifically, it aims to quantify various key variables, including the impact of Anthropogenic Geomorphic Processes (AGP), the potential impact of coastal hazards, and the overall vulnerability of the area. It seeks to unearth the role of human activities in increasing coastal hazards, which is critical in the context of climate change assessment. This doctoral work has created a novel methodological framework, by combining different interdisciplinary assessments that can comprehensively quantify the spatial coverage of coastal hazards and elucidate the role of human activities in increasing vulnerability.

1.4.6 Constraints in conducting Research

The current research does not have resources to acquire costly high resolution Data Elevation Model and satellite imageries and advance hydrological modelling software.

1.4.7 Field Study

To gather empirical data, the research includes various field activities.

- Collected beach litter covering the study area's coastline, to assess litter presence during usual peak tourist period and the period of total tourism absence.
- Collected Ground Control Points (GCPs) for supervised LULC assessment using geospatial techniques.
- Conducted extensive photographic surveys to collect the visual evidence of the impact of Anthropogenic Geomorphic Processes (AGP) in the coastal landscape.
- Photographic survey.

1.4.8 Potential Assistance in Policy-Making

This doctoral work holds the potential to inform policy-making in several ways:

- By providing a novel and robust methodological framework for quantifying the spatial coverage of coastal hazards and vulnerability.
- By shedding light on how anthropogenic activities contribute to increased vulnerability.
- By offering insights into the coastal management strategies needed to address these challenges and enhance resilience to environmental hazards.

1.5 Limitation of the study

- **Index Based vs. Modelling Based Approach**

An index-based approach involves the development of an index or a set of indicators to assess a particular aspect or vulnerability of a region. It relies on collecting data for these indicators and then combining them into a single numerical value or index score. The resulting index provides a relative measure of vulnerability, allowing for comparisons between different regions or over time. Index-based approaches are often more straightforward, cost-effective, and accessible. They are particularly useful when comprehensive data and computational resources are limited.

On the other hand, Modeling-based approaches involve the use of sophisticated computer models to simulate complex processes within a region. These models can provide detailed and quantitative insights into the absolute vulnerability of a region, considering various factors and scenarios. They are well-suited for regions where advanced data and modeling capabilities are available and necessary.

This doctoral work acknowledges the limitations of using an index-based approach, which primarily provides relative vulnerability assessments. However, it highlights the need for baseline data on coastal vulnerability, especially at the local level, which is often lacking in most of the developing countries especially, South Asian countries. To address this data gap, this doctoral work has deliberately incorporated and modified the index-based approach to provide a consolidated quantitative value for coastal vulnerability. The modification includes a holistic assessment that considers relevant physical and social geographical variables, making the assessment more comprehensive.

The aim is to create a robust, practical and holistic CVI framework for determining relative coastal vulnerability in regions where sophisticated assessments may not be feasible due to cost constraints.

The study acknowledges that it can only provide relative vulnerability assessments, but it emphasizes the value of this approach in collecting baseline data, which can be invaluable for disaster management and regional planning authorities, especially in economically disadvantaged coastal regions.

- **Medium Spatial Resolution of SRTM DEM**

High to very high resolution Digital Elevation Models such as LiIDAR and other L-band data elevation products are not free available for the study, therefore, due to the absence of any choice, this doctoral work has incorporated most suitable freely available, medium resolution SRTM 30 m DEM product downloaded from the USGS Earth Explorer. However, the use of medium-resolution data does come with limitations and in comparison LiDAR data, for example, offers much higher spatial resolution and accuracy.

Keeping the limitation in mind, this doctoral work has employed techniques like resampling to improve the spatial resolution of SRTM 30 m DEM Additionally, the SRTM DEM has been combined with the ground-truth data, to assist in enhancing its utility and accuracy for LULC mapping.

- **Gridded Meteorological Dataset in Place of Point Based Meteorological Dataset**

Due to the unavailability of the 'point based more accurate' IMD meteorological data, the present doctoral work has incorporated the 'gridded' NASA POWER dataset. However, the utilization of the NASA POWER datasets is a pragmatic and justifiable choice. Here's an exploration of the rationale behind this decision:

The NASA POWER datasets are global, gridded meteorological datasets that provide climate and weather information at high spatial and temporal resolutions. They are widely recognized and accepted in regions around the world, especially when point-based meteorological data is not readily accessible. The use of NASA POWER datasets is a common practice in climate studies. These datasets offer a variety of climatic variables spanning nearly four decades, which is essential for conducting comprehensive climate trend analyses. It's essential to acknowledge the potential limitations of using gridded datasets, as they may not capture localized variations as accurately as point-based data. Validation and cross-referencing can help ensure the reliability of the results derived from gridded datasets.

Keeping the limitation in mind, this doctoral work also conducted a robustness assessment (correlation analysis0 of the NASA POWER datasets with the point-based IMD datasets, to validate their suitability for climate trend analysis in your study area.

- **Limited Period of Air Quality Data**

The air pollutants data was acquired from Goa State Pollution Control Board (GPCB) website, which has made the air pollution data public only recently in 2021. However, the oldest data available on the website is of 2014. Hence, data unavailability has led to only seven years of air pollution analysis in the study area.

The doctoral work acknowledges that the long-term data is ideal for detecting trends and patterns, however, short-term data can be sufficient to identify immediate concerns, seasonal fluctuations, and responses to specific events or interventions. However, the seven years of air pollution data has successfully assisted in showing human influence proxy in the study area.

- **Bathtub Hydrological Modelling**

This doctoral work has used a modified bathtub approach with local DEM to delineate future SLR inundation areas. The decision to use the modified Bathtub inundation model can be attributed to the two constraints:

- Lack of access to more sophisticated hydrological models like MIKE-21 or others.
- Cost considerations, as advanced hydrological models often require substantial resources, including licensing fees and computational power.

Keeping the limitation in mind, this doctoral work has adopted a modified bathtub inundation modelling. In contrast to the old "bathtub" model, which assumes that land elevations below expected sea levels would be flooded, the updated model takes into consideration hydrological connection (HC), which exclude inundation areas that are separated from open water (sea water).

There are two kinds of HC rules: "four-sided" rules and "eight-sided" rules. The "four-sided" rule posits that a grid cell in the DEM is hydrologically linked if any of its cardinal directions connect to a flooded cell, whereas the "eight-sided" rule implies connectedness on both cardinal and diagonal directions. The former rule has the ability to underestimate SLR consequences, whereas the latter has the capacity to overstate them. The "eight-sided" rule was chosen for the study merely because overestimation is typically more acceptable for planning reasons.

However, the study employs a comprehensive bottom-to-top approach, from the village to taluka levels, to mitigate these limitations and provide as accurate an assessment as possible.

1.6 Outline of the thesis

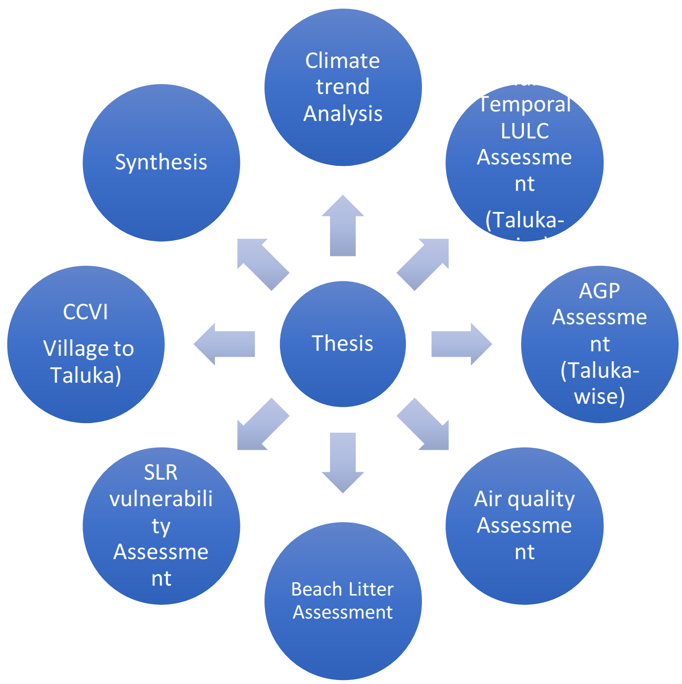

Fig - 1.6 Components of the Thesis.

The current study has determined how the increment in anthropogeomorphic process swells up coastal vulnerability, which is rapidly increasing due to climate change.

The current doctoral work is study interdisciplinary which consists of a total of seven quantitative analyses and assessments of physical and human geographic variables. It has predominantly followed quantitative approach to determine the results. The qualitative variables have been transformed into quantitative variables by deploying novel index based approaches (AGP and CVI quantification). The nature of the study is primarily inductive, which has assessed various geographic phenomena from different realms of earth sciences (physical and human geography, coastal and applied geomorphology, climatology, environmental science and remote sensing techniques) as the separate building blocks, which have been combined together to get the results as a single quantitative values.

This doctoral work is divided into nine different chapters. The overview of the objectives is as follow:

- **Objective 1** - Climate Trends Analysis: This objective focuses on analyzing how the weather patterns has been trending in the study area over a 40-year period, from 1981 to 2020. The goal is to understand if there have been significant changes in the weather patterns of the study area such as; rainfall, temperature, land surface temperature etc., which can be crucial for assessing potential climate-related risks.

- **Objective 2** - Anthropogenic Impact Assessment: This objective aims to quantify the impact of human activities on the local environment and the shape of the land (geomorphology) in the coastal tracts. It involves assessing how human induced land-use change activities have altered the natural landscape. The goal is to determine the extent to which human actions have modified the coastal environment between 2000 and 2020 periods.

- **Objective 3** – Multi Hazard Inundation Mapping and Assessment: This objective is concerned with evaluating the potential impact of coastal hazards on the study area. It examines the associated with events like storm surges, sea-level rise and how they might affect the study area. The aim is to understand the magnitude of these hazards consequences, in terms of future inundation zones in the study area.

- **Objective 4** - Coastal Vulnerability Assessment: This objective seeks to quantify how vulnerable the coastal area has become due to human activities in the last 20 years (2000 to 2020) in different talukas (sub-districts) within the study area. It aims to identify which specific areas are more susceptible to coastal hazards and where vulnerabilities are most pronounced. The goal is to provide a localized assessment of risk within the study region.
  In summary, these objectives collectively provide a comprehensive view of the environmental changes, climate trends, human impact, and vulnerability to coastal hazards in the study area. The research aims to contribute valuable data and insights that can inform policy-making and management strategies for the coastal region, ultimately enhancing its resilience to environmental challenges.

The overview of the chapters is as follow:

- **Chapter -1**

The chapter discusses about the background of the research, the study area, aim, objectives, scope of the study and limitations.

- **Chapter-2**

The chapter discusses about the extensive literature survey pertaining to the thesis objectives.

- **Chapter-3**

The chapter discusses about the different methodology employed in the assessments conducted to accomplish the objectives of the thesis.

- **Chapter-4**

The chapter discusses the meteorology in the study area by analyzing the multi-temporal (1982-2020) trends of six climatic variables namely; precipitation, minimum temperature, maximum temperature, temperature range, earth skin temperature and cloud amount using Mann-Kendall method and Pearson correlation coefficient to claim that local climatic trends are becoming more or less conductive for the increment in coastal hazard vulnerability.

- **Chapter-5**

The chapter discusses about the regional development by assessing the decadal land use and land cover changes, carried out for the period of 30 years (1990, 2000, 2010 and 2020). The assessment has provided the status of changes land use during the last three decades. The assessment has used Landsat-5,7 & 8 imageries processed in ArcGIS software to create LULC maps at 1:25000. The LULC maps have been created using 'level-1' classification given by the National Remote Sensing Centre, India. This level classifies the land use under five categories; agriculture, built-up, forest, water body and others which comes under. Although 'level-1' classification has low spatial resolution as compared to 'level-2' classification however, this was the actual requirement for the current study because these results have also been used as the input in the anthropogeomorphic process assessment as well as it also assisted in determining the increment in human foot prints in the study area.

- **Chapter-6**

This chapter discusses about the importance of traditionally neglected and recently emerging subject of 'Anthropo-geomorphology' in influencing hazard vulnerability in a given area. A novel methodology has been used to quantify the impact of anthropogenic activities upon geomorphic processes and landforms. The equation is data intensive which requires data from various sources such as; remote sensing (data elevation model), geology (rock type), geomorphometry (slope and aspect) and socio-economics (census data). Using this novel equation, the resultant value gets quantified into an index. Higher the value, higher the anthropic stress on geomorphology. This assessment has been found to be very effective especially for the hazard vulnerability assessments as it could quantify the anthropogeomorphic impact by combining physical and human aspects.

- **Chapter-7**

Air quality analysis: This chapter discusses the atmospheric phenomenon by analyzing the current status of air quality to describe anthropogenic pressure on the atmosphere in the urban centres and mining belt of the study area. Seven-year available pollutant (PM_{10}, $PM_{2.5}$, SO_2 and NO_2) data (2014-2020) was divided into two different periods (monsoon and non-monsoon) to determine air quality. Later, the Exceedance Factor (EF) method given by the Central Pollution Control Board (CPCB) was applied to determine the status these air pollutants in comparison to prescribed standard values.

- **Chapter-8**

This chapter discusses about the coastal environmental pollution. The significance of litter as one of the most potent agent of land as well as an important proxy to determine human footprints in an area. Spatio-temporal beach litter collection surveys were carried out to collect litter from 4 of the south goa popular beaches; Baina (Marmugao), Velsao (Marmugao), Colva (Salcete) and Palolem (Canacona) during two different periods. Covid-19 lockdown phase was specifically chosen along with January (peak tourist period in Goa) to compare and contrast the litter concentrations during both the periods. Covid-19 induced lockdown provided a rare window when all the outside activities were banned was compared to peak tourist period. This chapter discusses crucial findings about the anthropogenic footprints in the study area.

- **Chapter-9**

This chapter discusses about the coastal hazard. It is about the risk and vulnerability arising due to anticipated coastal flooding. It is becoming evident around the world that the increment in sea level would most likely inundate the wetlands due to which the high tide line would shift inland and habitable coastal land area would shrink. More alarming is the higher amount of sea level due to which 'new hazard zones' would emerge. Hence, this chapter deals with coastal flood inundation modelling and mapping of the study area. Scenario based approach was implemented using bathtub modelling technique. Three different sea level rise scenarios have been created and each of them has been overlaid upon the data elevation model (DEM). This assisted in quantifying total area under the risk of inundation (in sq. km) in each taluka as well as the LULC map was also overlaid upon the inundation maps which determined inundated area under each of the land use type. Coastal flood inundation modelling assisted in determining plausible 'new hazard zones' which may emerge by 2100 AD in the study area, as well as, it provided inundation zone maps and statistics which have been used as the input data as 'hazard variable' in the CCVI (Chapter-8).

- **Chapter-10**

This chapter sums-up all the above factors along with other physical, geological and socio-economical vulnerability factors to determine a singular quantified score of coastal vulnerability for each of the taluka(s), first by evaluating the CCVI at village and then adding them up to determine the coastal vulnerability at taluka level. A robust index based approach has been used which consists of 21 variables are considered to compute the index scores. 10 physical variables: coastal slope, coastal regional elevation, percentage of sandy coast, sand dune density, vegetation behind the beach, rate of relative sea-level change, shoreline change (erosion or accretion) rate, mean tidal range, significant wave height, plausible storm surge height and 11 Social variables. This chapter also highlights the CCVI itself because most of the CVI studies previously conducted in India or abroad has focused on district or state level scale and generally considered two to three socioeconomic variables to calculate the CCVI. However, this detailed study conducted at the village level included 11 social variables to reveal the smallest of differences among the population under the scope of the study to estimate the vulnerability index.

- **Chapter-11**

The chapter discusses about the synthesis between all the above analyses and assessments. This is the first study which has tried to incorporate all these analyses and assessments together to determine a singular hazard vulnerability score thus, this chapter discusses the interrelationship among all these assessments as well as their individual significance as how they contribute as the building blocks influencing coastal vulnerability, which together made an index based coastal hazard vulnerability score more robust than ever.

- **Chapter-12**

The final chapter discusses about the conclusion, research novelty of the present doctoral work, and the recommendations.

Chapter-2

Literature Review

2.1 Changing Climate Trends and Global Warming in the Coastal Areas

According to the IPCC's, the Sixth Assessment Report (AR6) has unequivocally concluded that the significant increment in the amount of CO_2, methane, and nitrous oxide inside the atmosphere is the product of human activities. The report further asserts that anthropogenic activities are the primary driver of many modifications found across the surroundings, ocean, cryosphere, and biosphere. Therefore, it's far high time that we take decisive motion to mitigate the effect of climate change.

According to the IPCC's, the Fifth Assessment Report (AR5), it is an undeniable truth that human activities have been the most dominant primary driving force behind the drastic climate change that has emerged through the years. This can be majorly attributed to the burning of fossil fuels like coal, oil and gas, which has led to the emission of copious amounts of greenhouse gases, thereby causing almost 100 % of the warming that has been witnessed since 1950. The evidence that supports these findings is compelling and leaves no room for doubt (Forsters et al., 2007).

A multitude of factors come into play while measuring the numerous elements that affect the quantity of energy that reaches and stays within the Earth's weather. These elements, known as "radiative forcing". It contains greenhouse gases that inhibit outgoing warmth, aerosols emanating from each human activities and volcanic eruptions that reflecting incoming daylight and have an impact on cloud formation, changes in sun output, modifications within Earth's albedo due to land use changes etc.

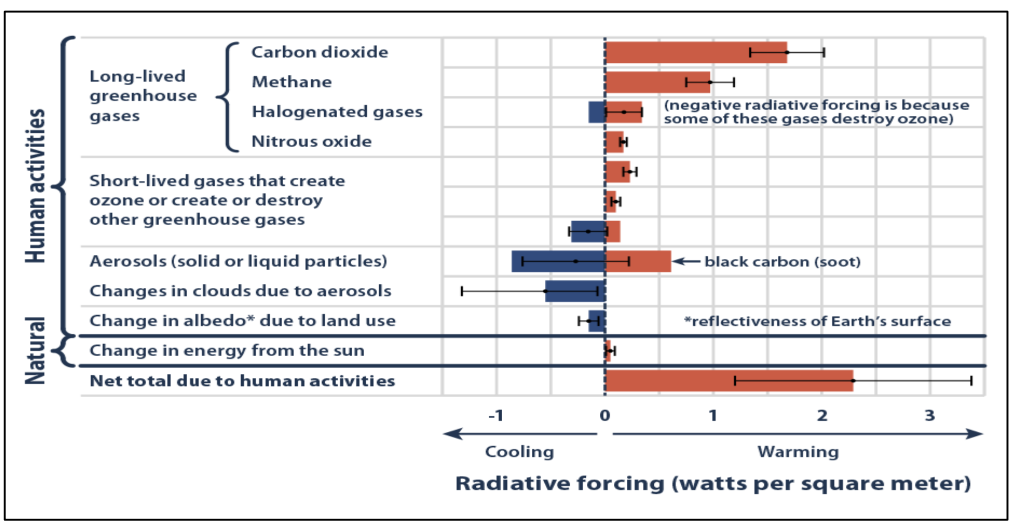

Fig 2.1 Radiative Forcing Caused by Human Activities Since 1750. This figure shows the total amount of radiative forcing caused by human activities—including indirect effects—between 1750 and 2011. Radiative forcing is calculated in watts per square meter, which represents the size of the energy imbalance in the atmosphere. Each colored bar represents best estimate, while the thin black bars indicate the likely range of possibilities. The natural change in the energy received from the sun over this time period is provided for reference. Source: (IPCC, 2013).

Although the amount of sun energy that earth receives has passed through minor fluctuations following the Sun's 11-year cycle, without net growth since 1950s, but the global temperature has marked an upward rise during the same temporal period. Hence, it's extraordinarily unlikely that the Sun could have been liable for the observed global temperature warming trend over the past half-century, thus indicating anthropogenic influence.

Moreover, since 1750 A.D, the average amount of the incoming solar energy has either remained constant or grew slightly. In the event that more active sun had caused the warming, scientists would have expected hotter temperatures in all layers of the environment. However, as opposed to the temperature increment in all the atmospheric layers, they have noticed a cooling within the top surroundings and a warming at the bottom and lower layers of the atmosphere. This is because greenhouse gases are gradually and uniformly slowing heat loss from the lower atmosphere, leading to warming in these layers and at the earth surface.

The combustion of fossil fuels offers upward thrust to greenhouse fuel emissions that act like a warm layer covering the earth, trapping the sun's energy and elevating temperatures to unparalleled stages. The culprits in this weather alternate conundrum consist of carbon dioxide and methane, among different gases (IPCC, 2007; Wuebble and Jain, 2001; Soeder and Soeder, 2021).

- Carbon dioxide (CO_2) is a major warming gas that stems from numerous sources like combustion of fossil fuels, wildfires, and volcanic eruptions. During this economically dominated era, human activities have amplified the atmospheric CO_2 by 50%, which is a dazzling 150% increment since the 1750 A.D. This growth is higher than what occurred naturally since the last ice age, 20,000 years ago IPCC (2007).
- Methane concentrations have surged because of agriculture, fuel distribution, and landfills. Wetlands also are an instance of natural sources that release methane IPCC (2007).
- Anthropogenic activities like fertilizer usage and fossil fuel combustion are also responsible for the emission of nitrous oxide. The oceans and soils additionally release NO_2 IPCC (2007).
- Halocarbon gasoline concentrations have skyrocketed in particular due to human activities, with chlorofluorocarbons including CFC-11 and CFC-12 being the primary culprits. These

gases are widely used in refrigeration, which has led to the depletion of the stratospheric ozone layer IPCC (2007).

- Ozone is an indispensable greenhouse fuel that undergoes a continuous cycle of production and destruction via chemical reactions inside the surroundings. Anthropogenic activities have depleted ozone in the troposphere via the release of gases which includes carbon monoxide, hydrocarbons, and nitrogen oxide, which chemically react to form ozone IPCC (2007).
- Water vapor is the most dominant and enormous greenhouse gas inside the atmosphere, albeit human activities have a minor direct have an effect on its amount. However, human beings have the capacity to significantly change to the amount of atmospheric water vapor circuitously by means of altering the weather (IPCC, 2007; Wuebble et al., 2017).
- Aerosols are minute particles found in the environment that come in varying sizes, concentrations, and chemical compositions. The burning of fossil fuels and biomass has boosted aerosols containing sulfur compounds, natural compounds, and black carbon (soot). Human activities which include surface mining and commercial approaches have accelerated the amount of dust in the surroundings. Natural aerosols encompass mineral dust, sea salt aerosols, and dirt aerosols from volcanic eruptions, amongst others (IPCC, 2007; Myhre et al. 2013).

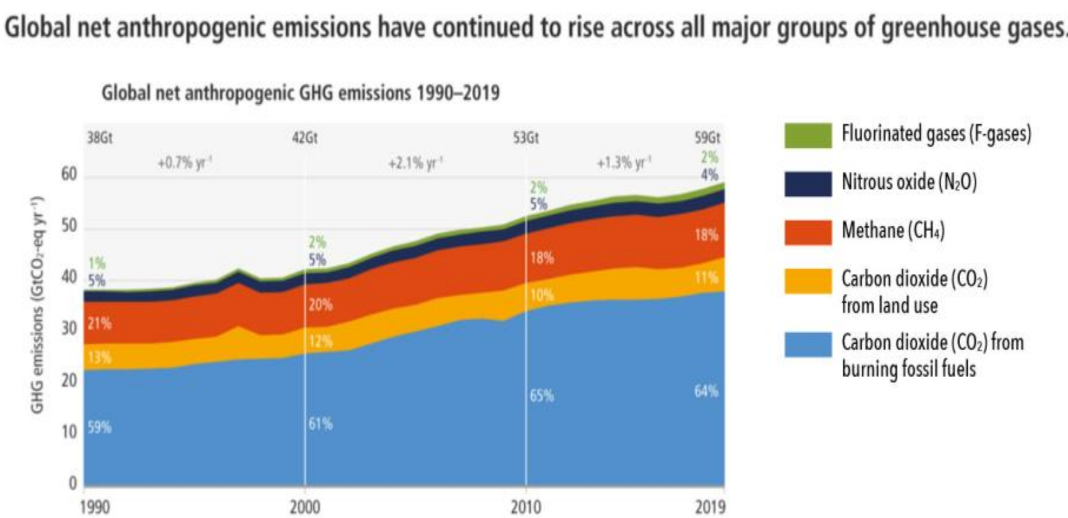

Fig-2.2 Total annual anthropogenic greenhouse gas (GHG) emissions (Giga tonne of CO_2-equivalent per year, $GtCO_2$-eq/yr) for the period 1970 to 2010, by gases. (Source: IPCC Working Group III, 2013).

Therefore, for the reason that pre-industrial period, human activities have appreciably contributed to growing the global average temperature of about 1 degree Celsius, an amount that is currently growing more than 0.2 stages Celsius per decade (Allen et al., 2018). Consequently, the Earth is now approximately 1.1°C hotter than it in late 1800s. It is noteworthy that the last decade (2011-2020) has been the warmest on record (NASA, 2022).

Climate change does not only refer to warmer temperatures as it is much more than that. The Earth functions as a system where everything is interconnected, and changes in one area can significantly affect changes in all others (Ferdig, 2007).

The ocean is experiencing 90 percent of the total global warming, causing a considerable increase in the water's internal heat since modern record-keeping began in 1955 (NASA, 2022). Also, there is a significant growth in the amount of heat stored in the ocean since the 1950s, as highlighted with the aid of the International Energy Agency, IEA in 2020.

According to IPCC (2022), Climate change has extensively affected the Earth's snow- and ice-protected regions because of the upward push in global temperature. Such changes have a long way-attaining implications worldwide, as snow and ice play a critical role in influencing sea level, ocean currents, and storms. For example, the Arctic sea ice, which used to reach its minimal extent each September, is now shrinking at a rate of 12.6% each decade, in comparison to its average extent during the period 1981 to 2010.

Moreover, sea level increment is basically due to the two major factors related to global warming. The added water from the melting ice sheets and glaciers and the expansion of seawater as it warms (IPCC, 2001). During the last four decades, 75 percent of the sea level upward push can be attributed to glacier mass loss and ocean thermal growth, according to Garcia-Soto et al. (2021).

2.1.1 Ramifications of the Changing Climate in the Coastal Areas

Table-2.1 The global scenario of the coastal regions (Adopted from the United Nations, 2017).

1	**Geography**	The ocean encompasses 363 million square kilometers, which is approximately equivalent to 72 percent of the Earth's surface.
		Less than 10 meters above sea level, coastal regions are home to more than six hundred million people, which contributes for around 10 percentage of the global population.
		Approximately 40 percent of the coastal populace, or 2.4 billion people, live within a hundred kilometers (60 miles) of the coast.
		As of 2017, coastal communities make up 37 percent of the global population.
		Most of the employees in secondary marine-related activities such as fish processing and marketing are women, and roughly 97 percent of the world's fishermen reside in developing countries.

2	**Economy**	The ocean economy is estimated to be between US$3-6 trillion/year.
		Fisheries and aquaculture contribute US$100 billion per year and around 260 million jobs to the global economy.
		Coastal areas attract around 50 percent of all international tourists.
		Every year, oil tankers transport approximately 2,900 million tonnes of crude oil and oil products worldwide via sea.
3	**Marine Debris**	Every year, more than 8 million tonnes of plastic are dumped into the oceans, which is equivalent to a garbage dump.
		Land-based activities are responsible for 80 percent of all pollution in seas and oceans.
		In addition to large tanker incidents, small oil spills occur daily, resulting in the deaths of birds, marine mammals, algae, fish, and shellfish. Oil spills continue to be a concern.
		Over the past 200 years, oceans have absorbed as much as half of of all anthropogenic carbon emissions. Blue carbon ecosystems, inclusive of mangroves, seagrass beds, tidal marshes and so forth. Are some of the most good sized carbon sinks on earth.

According to the Intergovernmental Panel on Climate Change (IPCC) report of AR5 and AR6, stated with high confidence, that the impacts of human-caused climate change on the nature and other stockholders have been observed especially since the AR5. Moreover, the upward thrust in climate and weather extremes has brought about a many irreversible influences on natural and human systems which are now way beyond their potential to adapt. Furthermore, the negative impacts from tropical cyclones have considerably increased because of sea level rise and the increase in heavy precipitation. Additionally, ocean acidification is another factor that has contributed to such adverse impacts, stated with medium confidence, by the IPCC AR6. Additionally, ocean acidification is another factor that has contributed to such adverse impacts, stated with medium confidence.

The AR6 report also concludes with high confidence that the observed global mean sea-level rise since at least 1970 is very likely anthropogenic forcing. These climate extremes have hindered the efforts to meet Sustainable Development Goals. Furthermore, as multiple climate and non-climate hazards, also known as cascading hazards, impact cities and settlements, damages are magnified.

Again, stated with high confidence by the IPCC AR6 report, (Oppenheimer, 2019) that, human (socio-economic) and ecosystem vulnerability are interdependent. The current unsustainable development patterns have escalated the exposure of ecosystems and people to climate hazards, with high confidence. Consequently, climate change has contributed to humanitarian crises where climate hazards interact with high vulnerability. Hence, Climate and weather extremes are increasingly driving displacement in all regions. All these adverse impacts are primarily due to the extent and magnitude of climate change, which are larger than estimated in previous assessments, with high confidence.

2.2 Climate Trend Analysis in the Coastal Area

Climate trend analysis is the process of identifying trends and understanding how the climate changes over time by evaluating long-term patterns and changes in climate-related variables (Duc et al., 2019). The main objective of climate trend analysis is to identify and measure changes in the climate system that go beyond natural variability and may be related to human activities, such as burning fossil fuels and deforestation, which release greenhouse gases into the atmosphere and cause global warming (Fussel et al., 2006). Coastal climate trends are especially concerning since they are particularly vulnerable to the effects of climate change, such as sea-level rise, more frequent and powerful storms, coastal erosion, and flooding (Nicholls et al., 2007). To better understand the ongoing changes and their implications for coastal regions, it is critical to monitor and analyses these climate patterns. Its comprehension can aid in coastal zone management, the construction of resilient infrastructure, and the reduction of greenhouse gas emissions in order to reduce the worst effects of climate change in coastal areas (Zhang et al., 2011).

French and Burningham (2013) has examined the difficulties in establishing empirical links between climate factors and coastal morphological development in terms of data availability and variability. They found that landform reactions to climate change are regionally and locally mediated and Geomorphologists are critical in comprehending the coastal effects of climate change. While Nicholls and others (2008) argued that coastal vulnerability assessments are primarily concerned with sea-level rise, with significantly less attention paid to other aspects of climate change such as meteorology. This study examined climate and non-climate change drivers of change in coastal areas, as well as the importance of integrated evaluations. It focuses on non-climate drivers and illustrates them using widely used SRES scenarios, as well as the significance of including non-climate drivers in coastal risk assessments.

However, a paradigm shifts towards understanding the climate trends in coastal areas has been observed to determine its subtle but prominent impact in influencing coastal vulnerability. Ayyam and others (2019) has proposed that integrated approaches are necessary at many levels to control the impact of climate change on coastal regions, such as integrating physical and socioeconomic characteristics of coastal population to identify holistic solutions. In this regards, Leal-Filho (2018) had summarized the main development and trends related to climate change in coastal areas. While Ali and others (2020) examined the effects of climate change on coastal communities, describing natural values, coastal landforms, and infrastructure types which are most likely to be affected by climate change and provided information for assessing inundation, erosion, and recession risks for a chosen location, and they recommended incorporating climate change impact and risk assessment into long-term national development strategies.

On the other hand, Curtis (2019) conducted a study which spanned 80 years and discovered that global climate models do not accurately capture coastal zone precipitation because there is an increasing trend in precipitation in the coastal zone, with the interior increasing faster than the coastline, and the discrepancy is most significant during the austral summer season. As well as, Watkinson (2009) discussed the effects of climate change on coastal areas. It investigated how to downscale the global analysis to the local level within the framework of a coastal simulator, which provides information on possible future states of the coast through the 21st century under a variety of climate and socioeconomic futures, as well as shoreline management options. It was discovered that there are significant increases in the global heat content of the oceans, causing sea level rise, and that the impact of climate change on coasts will be worsened by human-induced pressures.

Recently, many studies have come up across the world to understand the implications of climate trend variability in coastal areas. Dailidiene and others (2012) examined long-term climate trends such as wind, air, water temperatures and the winter North Atlantic Oscillation (NAO) index in Lithuanian coastal areas of the Baltic Sea based on monitoring data from 1961 to 2005 and discovered clear trends in hydro-meteorological parameters such as increasing air and surface temperatures and sea level rise. Ngare and others (2020) used basic regression analysis to evaluate climatic variability changes in Mombasa County, Kenya between 1989 and 2019, finding an increase in temperature with a maximum temperature of t=-5.000 and a minimum temperature of t=-5.4°C. and a decrease in rainfall during the previous 30 years.

Kabanda (2018) used Mann-Kendall test to discover long-term trends, while Sen's slope estimator test used to determine the magnitude of change over time along the Tanzanian coast. The outcomes revealed rainfall varied by month at different stations, with July showing a considerable decrease in rainfall and a link between July rainfall and horizontal winds. High-quality daily climatic parameters were developed by Abbasnia and Toras (2020) to examine long-term variations in weather extremes from 1961 to 2016. The study discovered that warm temperature extremes in 71 sites along Turkey's coast exhibited more significant trends than cold extremes, and there was a decline in the number and volume of precipitation. Wang and Wang (2017) discovered a small rising trend in extreme precipitation events in the southern coastal area and a downward trend in the northern coastal area of China based on a daily precipitation dataset of 156 station records from 1961 to 2014. Trend analysis, wavelet analysis, Mann-Kendall test, accumulative anomaly analysis, and Pettitt test are among the approaches used. Wickramaarachchi and Samita (2020) found out positive rainfall patterns in the majority of the North-Western coastal line and four sites along Sri Lanka's Eastern coastal line. It emphasized climate mitigation activities to mitigate the effects of changes in rainfall trends.

Additionally, temperature is an essential factor in coastal climate patterns. Temperature changes have a substantial impact on the climate, weather patterns, and environmental conditions in coastal areas (Harley et al., 2006).

Efthymiadis and Jones (2010) found that coastal land warmed by 0.02° C per decade compared to sea surface temperature by comparing the rate of temperature change between land and marine temperatures for the same grid squares using 5° by 5° latitude/longitude grid-boxes utilizing CRUTEM3 and HadSST2 datasets. Elhacham and Alpert (2021) found that the average coastal surface temperature in Dubai has increased by 0.1° C/year as the temperature gradient between land and water has shrunk and the coastline has urban heat island characteristics as a result of extensive urbanisation. Ladochy and Alzert (2007) examined air temperature patterns in California from 1950 to 2000 using continuous data from 331 weather stations and discovered that places with dense urbanization had the most positive increases and that minimum temperatures grew more than maximum temperatures. While Lakhraj-Govender and Grab (2019), using the modified Mann-Kendall test investigated the temperature trend in coastal areas of KwaZulu-Natal, South Africa from 1930 to 2015 which indicates a significant increasing trend in annual maximum temperature but not in annual minimum temperature. It concluded that higher-lying interior regions are warming quicker than coastal locations and oceanic moderating effects may be reducing coastal warming.

In India, Jamir and Kumar (2015) investigated changes in cyclones and depressions, floods and droughts, thunderstorms and hailstorms, fog and low visibility days in India's Northeast and West Coast regions. The study employed linear regression, correlation coefficients and Student t-test to determine significant levels (0.05 and 0.01%). The study found mixed trend in extreme occurrences, such as declining tendencies in cold waves and heat waves, as well as cyclones and depressions that were not consistent with global warming. While Jaswal (2010) evaluated the annual and seasonal trends in total cloud cover, diurnal temperature range, and rainy days for 1961-2007, based on 172 well-distributed surface meteorological stations across India. It discovered an overall decline in total cloud cover throughout the majority of India, as well as a negative relationship between monsoon cloud cover and sea surface temperature. Jindal and Mitra (2019) also analyzed the changes in trend of temperature, water vapour, and ozone profiles at different atmospheric layers, total column integrated methane (TCH4), and total column integrated carbon-monoxide (TCO) over the Indian region. It discovered that the temperature in eastern and southern India has risen, whereas water vapour has risen in western and southern India.

However, Radhakrishnan and Adhikari (2017) analyzed the climate trend in India which showed a declining rainfall and rapid warming, especially in the last 30 years over the period of 1901–2014. Rao (2013) analyzed climate variability and its effects on coastal ecosystems in India, with an emphasis on the Sundarbans and Tamil Nadu. It highlighted the importance of climate variability in transforming natural resource ecology, confronting conventional knowledge systems with new research concepts, improving coastal communities' coping capacity, and the need for incorporating climate adaptation practices into development planning. Also in southern India, Ashwin and Vinay (2021) examined the climate trend in the coastal region of Karnataka from 1984 to 2017, utilizing the Mann-Kendall trend and Sen's slope estimator test, and found an increase in the trend of rainfall in particular grid sites. In the western Ghats and coastal Karnataka, using the Mann-Kendall test and the Theil-Sen estimator, Chandrashekhar and Shetty (2018) found statistically significant positive trends in annual total rainfall, yearly 1-day maximum rainfall and in the frequency of very heavy rainfall in the coastal region. As well as contrasts in extreme rainfall indices in low and high land regions of coastal Karnataka.

2.3 Anthropogemorphic Impact

Anthropogeomorphology can have a major and wide-ranging impact on both human society and the environment (Bhunia et al., 2022). Essentially, the impacts of anthropogeomorphology can increase coastal vulnerability in a number of ways. When human activities affect coastal geomorphological processes, the natural dynamics of the coast are altered, making it more susceptible to dangers (Aguilar et al., 2020).

Mackay and others (2003) examined several archives of environmental change utilizing radiocarbon dating, Dendrochronology, and sediment studies of corals, lake sediments, glaciers, and ice cores. It found that the Holocene epoch has seen significant global environmental change, with human impacts hastening the rate of change. According to Jefferson and others (2013), anthropogenic geomorphology studies the direct and indirect consequences of human activity on the Earth's surface using empirical data collection and numerical modeling. Szabo, 2010 opined that the impact of anthropogenic geomorphology is significant and surpasses the efficiency of exogenetic natural processes in shaping surface landforms. Goudie (2020) discussed, the human impact on geomorphology has a long history.

Since 1969, a number of developments have occurred that have led to an increasing realization of its importance, including technological developments that alter geomorphological processes, demographic trends, and the proliferation of techniques for the study of landform and process change. The study discovered that land-use change can have a major impact on geomorphology, modifying erosion and sedimentation rates as well as affecting landform and process change.

Meadows and Lin (2016) reviewed various systemic and cumulative drivers of geomorphic change before delving into the time-transgressive impacts of humans on virtually all environments on the planet, emphasizing the critical role of geomorphology in understanding humanity's expanding footprint on earth systems. According to the study, the society-geomorphology nexus is important but complex, although anthropogenic geomorphology provides critical insights. Brown and others, (2017) addressed the impact of human activities on geomorphological processes and landform evolution, and it was discovered that the applicability of the Anthropocene concept differs across geomorphology branches, with human impact being more visible in fluvial and coastal geomorphology. Meadows, 2016 briefly reviews different systemic and cumulative sources of geomorphic change before delving into the time-transgressive influence of people on nearly all of the earth's habitats.

In terms of land use changes impact on geomorphology, James (2022) has examined agricultural development and potential geomorphic changes on broad time and space scales, concluding that agriculture and deforestation have had significant impacts on geomorphic systems throughout history, and societies before the 15th century had much lower geomorphic potential than European colonists. Migon and Latocha (2018) discussed the direct and indirect geomorphic effects of human activities such as agriculture, ore and coal mining, quarrying, forestry, and tourism on the geomorphic system in the Sudetes, Central Europe, and discovered that mining and agriculture areas are the most altered. most of others have covered often a specific type of anthropogenically impacted landform but in detailed manner, as for coastal and estuarine areas (Pye and Blott 2014; Ferrer-Valero et al. 2017), mining landforms (Harnischmacher and Zepp 2014; Byizigiro 2015; Dullas 2016), catchment areas (Slabá et al., 2015), and agriculture (Martinez-Casasnovas 2003; Houben et al., 2006; Chartin et al., 2013) in addition the impact quantification of transportation upon landforms has also been studied (Sofia and others 2016).

Mapping of anthropogenically impacted landforms has also been carried out using a holistic approach that incorporates the underlying notion of earth movement. Hooke (1994) made a pioneering attempt in this area, calculating and mapping the amount of earth movement per year in the United States. while Pirkhoffer (2009) mapped anthropically impacted landforms in Hungary based on different land use categories.

According to Rozsa (2007), Nir's 'index of potential anthropic geomorphology', published in 1983, is a highly recognized model for quantifying human impact on geomorphology due to its simplicity and widespread data availability. However, some Nir's index notions are debatable, such as the generalization of topographic and climatic factors for a greater area, equal weightage to climate and terrain, and consideration of solely the urban population (Rozsa, 2007), insufficiency in quantifying the AGP at micro level due to generalized parameters (Nigam et al., 2023) etc. Because these parameters are dynamic which change at different spatio-temporal scales.

Recently, Tarolli (2014) and also Tarolli and others (2017) have made pioneering attempts to use geospatial technology to determine human impact on landforms using landscape metrics and the extent of anthropogenic modification.

2.4 Land Use Land Cover Assessment

2.4.1 Land Use Land Cover Assessment in the Coastal Areas

Land use alterations in coastal areas can be influenced by a variety of reasons, including population increase, economic development, urbanisation, industrialization, agricultural expansion, tourism, and the effects of climate change (Dale, 1997). Resultantly, the repercussions of land use changes in coastal areas can be large and far-reaching, affecting biodiversity, water quality, coastal erosion and sedimentation, floods and storm surge threats, and the general resilience of coastal ecosystems to climate change impacts. Sustainable and deliberate land use planning is essential for balancing human growth with the preservation and protection of coastal habitats (Li et al., 2010).

Numerous studies have come up in this context across the world, primarily concerned about the negative effects of human influence in coastal areas and almost all have advocated for the reduction in human influence and raise in sustainability. McEvoy (2015) has predicted a nine-fold rise in flood risk in coastal communities by 2050 as a result of climate change, which might result in huge socioeconomic losses. Current defenses and policies are severely insufficient, and without adjustments in the coastal land-use patterns, worldwide flood losses might exceed $1 trillion.

According to Anderies and Barreteau (2019) coastal locations have many sensitive borders and thresholds, such as the land-water interface, the intersection of salty and freshwater habitats, and limited space for specific land use patterns, hence the concentration of environmental consequences in coastal areas is a concern caused by land use change. According to Newton and others, 2012, coastal zone "Hotspots" are locations with severe difficulties, such as river mouth systems, urbanized and low-lying coasts vulnerable to flooding and sea-level rise. To address difficulties caused by land use change in coastal areas, a variety of societal responses and suitable governance frameworks, as well as effective communication are required. Schultz (2018) had also explored the effects of man-made changes in coastal land use and concluded that careful selection of areas and design criteria are critical for effective development. Improvements to drainage and flood protection provisions are also required.

Even Blackburn and others (2019) found that coastal megacities encounter a variety of risks as a result of demographic, infrastructure, environmental, social, and economic changes. Changes in land use in coastal areas enhance flood danger and air pollution from industrial activity. They believe that innovation, inclusive knowledge capture, and responsive social institutions are critical for coastal megacities' resilience and transformation. Also, Shin (2019) observed that heavy urbanisation and agricultural intensification in valleys and coastal locations, such as industrial complexes and harbour facilities, are causing erosion and land depletion.

Magarotto and other (2017) compared two case studies, Boa Viagem Beach in Recife, Brazil, and Rocha Beach in Portimo, Portugal, and concluded that green environments in urban areas contribute to well-being and urban green areas are important for sustainable development, but urban growth in coastal cities has resulted in a decrease in large green areas, affecting landscape design and planning. Dzurik (1984) examined issues between development and the coastal environment, such as construction on coastal wetlands and the protection of beaches and barrier islands. It argued for the importance of addressing environmental issues related with coastal engineering projects by balancing project requirements with environmental protection. Macintosh (2013) explored Victoria, Australia's coastal climate hazard planning framework to demonstrate how poorly conceived or implemented urban planning strategies can raise costs and vulnerability in coastal locations. It emphasizes the need of urban development in reacting to coastal climate hazards. While Ozyurt and Ergin (2012) determined that changes in land use in coastal areas damage coastal ecosystems, increase erosion, and modify sediment transport, ultimately affecting geomorphologic processes. The explanation of geomorphological changes in coastal areas is necessary for restoring the balance of coastal landforms because integrated coastal zone management is critical for sustainability, and geomorphology provides the foundation for ICZM plans by integrating spatial and temporal scales in the model.

2.4.2 Multi-Temporal Land Use Land Cover Assessment

The assessment of multi-temporal LULC in coastal areas is critical for understanding the dynamics of land use changes and their consequences for the sustainable coastal environment, socioeconomic development (Munthali et al., 2019) and geomorphology (Nigam and Kotha, 2024, under review).

Holland and others (2011) examined changes in land use and land cover patterns in the surrounding basin of a coastal lagoon in Mexico between 1985 and 2000 using satellite photos (Landsat TM and Landsat ETM+) and image processing with Idrisi32 software. The analysis found that urban and tourist land rose by 43%, Mangroves fell by 39% and became fragmented. Similarly, Guneralp and others (2013) investigated land use changes in the Mission-Aransas coastal region of Texas from 1990 to 2010, as well as their consequences for coastal vulnerability and protected areas. The study found that MACR has witnessed considerable LULC changes, increasing the vulnerability of urban populations, infrastructure, and biodiversity to coastal hazards. De Andres and Barragan (2015) examined the key implications of coastal development on coastal and marine ecosystems in over 400 coastal cities in Latin America and the Caribbean (LAC) in this research. The study discovered that coastal areas are experiencing substantial population expansion.

In Europe, Iglesias and others (2015) argued that there is mounting evidence of serious environmental degradation along Europe's coasts. Because coastal areas encounter challenges in population expansion and physical development, shorelines, transitional waters, and near-shore marine areas are under significant environmental stress and are highly vulnerable. The report recommended for sectorial policies to address environmental deterioration, as well as the awareness of policy synergies. While Kostoni and others (2017) analyzed the lack of spatial planning in Georgioupoli's coastal zone, Greece, and provides a framework for planning sustainable development in coastal regions.

In Asia, Lubis and Nakagoshi (2011) determined LULC variations in the Bodri watershed, Indonesia, over the last two decades (1991-2001 and 2001-2009) using ERDAS Imagine 8.7 - GIS analysis using ArcGIS 9.3.1. They detected an increase in built-up area while decreasing agricultural land area. Rizvi and others, 2020 analyzed Karachi's surface urban heat island (SUHI) based on an investigation of rapid Land Use Land Cover (LULC) changes on average temperature warming. The study used satellite photos to extract land-use statistics and create land surface temperature (LST) maps for 2009 and 2017, as well as regression analysis to determine the association between UHI and LULC. According to the study, built-up areas rose by 40%, while UHI intensity increased by 0.04 °C. Khan and others (2015) used satellite image analysis and regression analysis to investigate the combined effects of land-use changes and natural disasters in Bangladesh's southwest coastal area, and observed that cyclones and storm surges had significant effects on income, agricultural production, and migration. While in South Africa, Palmer and van der Elst (2012) analyzed land cover and development in KwaZulu-Natal coastal zone. According to the study, a large percentage of the study area is already highly developed, with much of it unevenly distributed.

2.4.3 Different Approaches in Land Use Land Cover Assessments

In addition, various studies have found interesting results by applying different approaches to determine land use impacts upon coastal areas such as, Helderop and Grubesic (2019) used a holistic approach that included meteorological, sociological, and geomorphic elements to calculate coastal vulnerability in a USA coastal city. The report proposed several solutions for mitigating the impact of sea level rise, such as zoning and land use management, erosion and flood control, water management, reinforcing of existing coastal facilities, and waste management. Haruvama (2016) analyzed disaster vulnerability, specific liquefaction designated upon the maps of risk levels, landform, land use, and vulnerability of the lower Tone River floodplain and found that Geomorphology as a core subject for disaster mitigation. Because landform modification and sedimentation contribute to natural disasters and rapid land use change increases vulnerability level. Salgado and Martinez (2017) used anecdotal observations, experimental tests, mathematical analyses, models and forecasts, economic assessments, and field observations to investigate the evidence that supports the usefulness of natural ecosystems for flood and erosion protection. It stated that, in addition to improving coastal protection techniques, it is critical to lessen human pressure by mobilizing communities inland to relieve coastal pressure.

Ara and others (2021) examined the relationship between the tourist pressure index (TPI) and land use land cover change (LULC) from 2005 to 2019 and found that tourism activities have resulted in changes in land use and land cover, which affects the coastal environment. This phenomenon is also supported by an increase in land surface temperature in the area. It pushes for stricter law enforcement in order to reduce environmental effect. Zhou and Zhu (2020) found that land use changes in Jiangsu Province, China, had a large and diversified impact on landscape vulnerability, as measured by the landscape vulnerability index (LVI) and the landscape human interference index (LHII), implying that they can increase coastal hazards risk.

Halls and Magolan (2019) used Matrix change analysis, computing adjacency statistics to design a methodology and found a significant association between residential development and wetland loss. Increased flood risk and wetland loss are caused by urbanisation and land cover change, showing a greater vulnerability to coastal hazards. The combination of methodologies used here has resulted in data that local government planners are assessing and incorporating into the County's new long-term plan, which will incorporate smart growth and risk detection. Su and others (2021) developed a research framework to evaluate the impact of land use changes on disasters, in which land use changes, disaster losses, and an environmental variable (runoff increment) were integrated into a three-stage data envelopment analysis (DEA) assessment model to dynamically evaluate the impact of land-use changes on disasters, which can assist agencies in ranking various types of land development, determining the acceptable risk level, and incorporating dislocation.

2.4.4 Land Use Land Cover Assessment in the Coastal Areas in India

India's coastal regions support a diverse range of ecosystems, including mangroves, salt marshes, estuaries, beaches, and coastal wetlands. Rapid urbanisation is underway in India's coastal cities and towns, resulting in the spread of urban areas along the coastline (Pavri, 2010). Furthermore, tourism development leads to the construction of resorts, hotels, and recreational facilities, all of which contribute to changes in land use patterns (Lakshmi and Shaji, 2016).

Kaliraj and others (2017) assessed the decadal variations of land use and land cover (LULC) features under the Level II category of the USGS-LULC classification system over the period 2000-2011 using Landsat ETM+ and TM data and the Maximum Likelihood Classifier (MLC) algorithm. The study discovered that the LULC features along the Kanyakumari coast have evolved dramatically during the last decade and the expansion of built-up territories and towns threatens coastal resources. While Bama and Rajakumari (2020) conducted shoreline analysis and vulnerability assessment in Tamil Nadu to analyze the influence of LULC on the historical shoreline between 1978 and 2017. According to the report, 6 km of the shore are extremely vulnerable, and 45 km are highly vulnerable. It came to the conclusion that croplands and coastal dunes conversion increased the coast's vulnerability to episodic natural catastrophes. Muthusamy and others (2010) used multi-temporal Landsat satellite data (1977, 1991, and 2006) to conduct exploratory assessments of land use/cover changes along India's Southeast coast.

Between 1977 and 2006, there was a substantial expansion in built-up land, as well as an increase in settlement within plantations due to population growth and building. Anil and others, 2012 investigated the changes in LULC in the Greater Visakhapatnam Municipal Corporation (GVMC) and neighbouring areas. The study also looked at illegal construction on hill slopes and found a spike in built-up, industrial, and plantation areas, as well as a decrease in forest area, although the harbour area remained unaltered. Das and Angadi (2020) examined the link between LULC and Land Surface Temperature in the Barrackpore Subdivision of West Bengal, India. The researchers employed multi-spectral satellite data to map LULC alterations. The study discovered that unplanned urban growth has resulted in LULC alterations and an increase in Land Surface Temperature (LST).

Prasad and Ramesh (2019) remote sensing and GIS to examine changes in land use and land cover in Alappuzha District, Kerala. The study discovered the relationship between the extent of built-up land and population growth. Basanna and Wodeyar (2013) showed in ERDAS, supervised classification involves employing the maximum likelihood estimator to derive statistical connections between input and ground truth habitats to build a habitat signature. The case study of Belgaum, Karnataka revealed that urban growth in the recent decade has resulted in a rapid loss of vegetated land and wasteland. Kumar and others (2021) looked at variations in LULC in coastal Karnataka between 1990 and 2019. Using satellite data, the K-means method is used for unsupervised categorization. Significant alterations have been found in barren land and scrub forest. During this time, water bodies occupied 40% of the studied area, and considerable barren land was replaced by scrub forest. These studies highlight the importance of considering land use changes in assessing and managing coastal hazards vulnerability.

Considering the land use changes into account when assessing and managing coastal hazards risk is critical for comprehending the complicated relationship between development and natural coastal processes. It permits the formulation of effective policies for reducing hazards, increasing resilience, and ensuring the long-term use of coastal resources (Dolan and Walker, 2006).

2.5 Beach Litter as Proxy of Human Influence

Beach litter accumulation is an excellent indicator of human impact on coastal habitats. It is impacted by biotic, abiotic, and anthropogenic causes, among others (de Febrarro et al, 2021). According to studies, the amount of human pressure on beaches contributes to beach deterioration and decreased water quality (Pervez and others, 2020). Litter abundance and composition along beaches can provide important information on the sources and forms of marine pollution (Ribiero and others, 2021). Furthermore, beach litter can be used to assess the general cleanliness and health of coastal environments, with excessive levels of litter suggesting pollution and degradation (Theil and colleagues, 2011). Understanding and eliminating beach litter is therefore critical for the conservation and management of coastal ecosystems. In this regard, numerous studies across the world have come up to quantify the amount of litter (Bergmann et al., 2015).

Santos and others (2005) interviewed beach users and assessed tourism-related litter output to conclude that beach litter input is higher in places visited by persons with lower yearly income and literacy degree, showing the influence of educational level on environmental awareness and behaviour. They believe that beach litter is an important indicator of human influence on coastal ecosystems, with tourism being the primary source of marine debris. Theil and others (2011) found that the composition of litter found on the beach indicates that the majority of it is from anthropogenic causes, which is common on beaches in the southeast Pacific region. considering that it reflects the type and volume of anthropogenic waste in the southeast Pacific, beach litter is an important proxy for human influence. Ribeiro and others (2021) in Southeast Brazil found that plastics and cigarette butts were the most common types of litter collected on the beach. It was established that beach litter can be used as a proxy for human influence because the number of beach users and local hydrodynamics influenced the density of marine litter. Krelling and others (2017) found that perception and reaction to beach litter did not vary between tourist groups on different beaches. Although stranded litter can potentially reduce local tourism income by 39.1%. Pervez and others (2020) found that plastic is the most common and abundant sort of litter in Qingdao, China, and that human recreational activities are the primary cause of trash. It believes that beach litter is a proxy for human influence on coastal regions, and that assessing it can assist inspire effective litter management programs.

Aydin and others (2016) in the Cilician basin, Turkey, conducted using Multivariate Adaptive Regression Splines (MARS) - Generalised Linear Models (GLM) and Generalised Additive Models (GAM), revealed a lack of local awareness of coastal litter and highlights the need for educational programmes to help reduce coastal litter. It also believes that beach litter can be used as a proxy for human influence on coastal regions and that educational programmes can help minimise litter. Di Febbraro and others (2021) investigated the applicability of a Litter Distribution Model (LDM) to map litter buildup in coastal sand dunes. The results revealed that LDMs had fair-to-good prediction performance. It comes to the conclusion that beach trash can be used as a proxy for human influence on coastal habitats.

2.5.1 Does Beach Litter Indicate the Human Presence?

Beach litter is indeed an indicator of human presence. Studies have shown that the abundance and composition of litter on beaches are primarily caused by anthropogenic activities such as tourism, fisheries, and recreational activities (Parvez and Lai, 2022)

Lo and others (2020) suggested using an aerial drone for beach litter assessment, which is faster and more efficient than visual surveys. Camedda and others (2021) quantified and discovered beach litter in Sardinia, Italy, in addition to indirect input sources such as waves, wind, rivers, and currents, direct input sources such as beach users also found. According to the study, beach litter may indicate human presence. Corbau and others (2022) also found the presence of beach litter at North Sardinia island, Italy, particularly land-based litter and suggested human activities are responsible for the same. Vincent and Hoellein (2017) investigated litter accumulation at Pratt Beach in Chicago, USA, by demarcating five 60-meter transects parallel to the shoreline and collecting litter within 1 metre of each transect twice a week. The study concluded that direct littering by beachgoers and the preservation of wind- and wave-blown anthropogenic litter at the wall dominated litter inputs at the pier.

Silc and others (2018) in the southern Adriatic Sea found a definite increase in litter cover along the sea-inland gradient, with fore dunes and pine woods having the highest litter cover, and humid dune slacks having essentially no litter. It came to the conclusion that beach litter implies human presence, with shorelines and recreational activities being the primary sources of beach litter. Poeta and others (2016) used a random sampling approach and a generalized linear mixed-effect model to assess the impact of three major possible land sources on litter occurrence: urban areas, rivers, and beach users in central Italy. The study discovered that metropolitan areas are the primary causes of marine litter, implying that the prevalence of such litter on Lazio beaches may be reduced by improving waste management and sewage treatment in urban areas.

Some of the studies on the litter monitoring assessments conducted along the various parts of Indian coastline reveals that inefficient waste management, mainly in the coastal areas, along with population behavior towards waste disposal, is one of the root causes for marine litter. Behera (2020) conducted a survey on the types of plastic litters and their quantification from January to March 2020 along Mandvi beach in Gujarat, with a total of 10 quadrates along the shoreline considered for quantification of the plastic materials based on density, colour, and weight. Plastic trash sampling was done with 10x10m quadrates. Manickavasagam (2020) developed an entrapment device, which was erected at the downstream end of Juhu Creek in Mumbai, India, to characterise and quantify marine debris going to the sea through a water channel. Again, Manickavasagam (2021) designed a new sampling device for the assessment of micro-plastics in the floating plastic debris of the water channel flowing from the creek towards the sea and Carried out six samplings in the water channel.

Mugilasaran (2021) studied the spatiotemporal distribution, composition and beach quality of marine litter pollution, 17 beaches along the Hooghly estuary, a part of the Gangetic delta was studied. - Marine litter collected from 17 beaches using OSPAR monitoring standard applied to litter items. It found that marine litter pollution is a severe concern in northeast beaches of India and management practices should include source reduction and environmental education. Sulochanan (2019), revealed changes in total beach litter at Panambur Beach, Monthly litter samples collected from three major beaches. Fishing litter found to be the most abundant type of litter on the beaches. Moreover, plastic items on the beaches are influenced by rainy days, rainfall, and river discharge thus appropriate incentive-based management options for the resident fishermen could result in collection and elimination of litter.

Vidyasagar and others (2018) determined the abundance of white-colored and irregular-shaped plastic debris in this study area. Polypropylene was identified as a dominant polymer variety, followed by polyethylene, polystyrene, nylon, and polyvinyl chloride using Visual examination and FTIR spectroscopy methods. Tourist activities, fishing practices and Aeolian process were found to be the dominant sources. Kaladharan and others (2017) highlighted that coastal tourism played a pivotal role in beach litter. Goa, one of the most popular tourist destinations globally, has the highest amount of beach litter along with the highest quantity of plastic among all the Indian coastal states.

2.6 Air Pollution as the Proxy of Increasing Human Influence

In certain ways, air pollution can be considered as a proxy for urbanisation, although it is not an exact metric or indicator of urbanisation. Instead, one of the several environmental effects of urbanisation is air pollution but a definite indicator of human footprints (Sahoo and Sethi, 2022).

Urbanisation and air pollution are closely related. Air pollution and urbanisation have been the subject of several research (Deng and Mendelsohn, 2021; Wang and Zhou, 2021). The results imply that urbanisation can increase air pollution. Depending on variables including economic development, technological advancement, and population growth, urbanisation has different effects on pollutant emissions (Liang and Gong, 2020).

Goossens and others (2021) has found that air pollution is a proxy of urbanization as it has become a major problem since the industrial revolution. Salahodiaev (2014) evaluated the influence of urbanisation on various metrics of air pollution in a broad sample of industrialized and developing countries and discovered that over-urbanization increases per capita greenhouse gas emissions, as assessed by CO2, NOx, and SO2 emissions. Sarzynski (2012) used a spatially explicit global dataset of emissions and cross-sectional regression analysis to investigate the pressures placed on the environment by cities in terms of urban air pollution and discovered that urban pollution is associated primarily, but not exclusively, with demographics, implying a link between air pollution and urbanisation.

Deng and Mendelsohn (2021) observed that the global shift of population from rural to urban areas has dramatically increased the marginal damage of air pollution emissions in urban areas; thus, air pollution can be considered a proxy for urbanisation because the increase in urban population has led to an increase in air pollution damage. McDonald (2012) stated that individuals have a tremendous amount of control over the emissions generated in metropolitan areas, and that approximately 80% of the emissions caused by fuel combustion have the potential to be directly influenced by consumer choices such as transportation, personal and residential choices, and industrial or commercial activities. Lazaridis and Lazaridis (2011) investigated human exposure and health risks from air pollutants by skin absorption and inhalation and developed dose-response functions, including estimations of particle deposition and clearance in the human respiratory tract via inhalation. It came to the conclusion that air pollution is a proxy for human activities since humans contribute to the discharge and accumulation of air pollutants. Wang and Zhou (2021) used panel data analysis and a spatial econometric model to empirically test the influence of urbanisation on pollutant emissions from both direct impacts and spatial spillover effects perspectives. They discovered a U-shaped relationship between urbanisation and pollutant emissions, indicating that air pollution can be used as a proxy for urbanisation.

Liang and Gong (2020) found the primary causes of decadal-long fine particulate matter ($PM_{2.5}$) trends in all 626 Chinese cities by categorizing city groups based on development level, geographical autocorrelation, and population size. It also used panel data models for hypothesis testing and determining determinants. It found that urbanisation has an impact on air pollution, but the mechanisms determining pollution levels differ depending on the stage of urban growth. Wei and others (2021) investigated the spatial-temporal fluctuations in $PM_{2.5}$ in the Belt and Road Initiative (BRI) region, which is undergoing fast urbanisation and is the key field of future urbanisation. The study discovered "typical regions" where urbanisation increases PM2.5 accumulations using spatial autocorrelation of urbanisation and $PM_{2.5}$ concentrations and concluded that air pollution is a proxy for urbanisation in the BRI area. Within a Bayesian Hierarchical Model (BHM), Shaddick and Vienneau (2011) explored multiple scales of variation in pollution concentrations in Europe, ranging from large scale trans-boundary effects to more localized effects that are directly tied to human activities. According to the report, human activities in metropolitan areas are connected with considerable increases in nitrogen dioxide concentrations across Europe.

2.7 Coastal Flooding

The rise in sea level leads to a multitude of adverse consequences. These include but are not limited to coastal erosion, inundations, storm floods, tidal waters encroachment into estuaries (Kennish, 2002), contamination of freshwater reserves, displacement of coastal lowlands and wetlands (IPCC, 2019; Neelamani, 2021). It is vital to notice that sea level rise has the ability to reshape cities, economies, coastlines and complete international areas (Vitousek et al, 2017). Shockingly, over the last 200 years, it's estimated that about a million humans have been killed in flood related activities especially in South Asia (IPCC, 2019).

Kulp and Strauss in 2019 suggested that, the choices we make today will likely determine whether our planet's coastlines will even be recognizable by the middle of the twenty first century. Currently, over 100 million people are living below high tide levels. By 2050, coastal areas that are presently home to 300 million people will be extremely vulnerable to flooding, irrespective of how seriously humanity controls carbon emissions, according to Climate Central. Moreover, Antarctica alone has the potential to contribute more than a metre of sea level rise by 2100 and more than 15 metres by 2500 (DeConto and Pollard, 2016)

The situation is even more dire for Small Island Developing States (SIDS). It is estimated that minimum 11to 15% of the SIDS population lives on land with an elevation of five meters or lower (McGranahan et al., 2007). If the ocean level rises only by half a meter, 1.2 million people could be displaced, and this range could nearly double if the ocean level rises by 2 metres (IPCC, 2019). Furthermore, almost two-thirds of the world's urban areas with populations of over 5 million are placed in the coastal regions vulnerable to sea level rise, and over two -third of the population is at risk in China, Bangladesh, India, Vietnam, Indonesia and Thailand (McGranahan et al., 2007; Strauss et al., 2021) The high tide lines could permanently rise above land occupied by some 150 million people, mostly in Asia, by 2050 (Kulp and Strauss, 2019).

IPCC AR6, 2019, has stated with high confidence that, the adverse impacts from climate hazards and resulting risks are cascading across sectors and regions. Multiple climate hazards will occur simultaneously, and multiple climatic (risks) and non-climatic (vulnerability) will interact, resulting in compounding overall risk and vulnerability across sectors and regions. Future sea level rise combined with storm surge and heavy rainfall will increase compound flood risks.

It is no surprise that an IPCC AR6 report found that major storms that until recently occurred once a century will, by 2050, happen on average once a year in many places, especially in the tropics. Annual coastal flood damages are projected to increase 100 to 1,000-fold by 2100 (IPCC, 2019). Shockingly, it has been reported that an annual average of 21.5 million people has been forcibly internally displaced by sudden weather-related hazards since 2008 (Rajeev, 2016; Marcus et al., 2023).

2.8 Multi-Hazard Vulnerability Assessment

Multi-hazard vulnerability assessment is a dynamic and iterative process that aids in enhancing disaster preparedness, guiding informed decision-making, and fostering resilience in India's diverse and hazard-prone geography (Islam and others, 2016).

The Energy and Research Institute (TERI), 2014 prepared a report about the present information and knowledge bases available in 6 Indian States on climate change risks and vulnerabilities including Maharashtra and Kerala. The report identified in terms of coastal vulnerability that State-level assessments of climate change risks and vulnerabilities and future projections of climate parameters are found to be largely inadequate at present. there remains a huge void in all the States, in terms of present knowledge on sectorial impacts of climate change. The study called for establishing an appropriate system of adaptation and mitigation project data base. The Indian National Centre for Ocean Information Services (INCOIS) in 2016, prepared a training manual to conduct Multi Hazard Vulnerability Mapping (MHVM), It stated that The Multi-Hazard Map is a "composite, synthesized and overlay of multiple hazards" using remote sensing and GIS. It included a case study of Andaman coral bleaching which were severely impacted during 2004 tsunami.

Mahendra and others (2010) prepared maps of coastal multi hazard vulnerability of Nellore, Tamil Nadu. They used the parameters such as historical storm surge heights, future sea level, future shoreline and high resolution coastal topography. It resulted that an area of 1708.36 sq. km. is found to fall under the multi-hazard zone. The study also revealed that creek systems act as the corridors for the oceanic hazards causing the inundation. The sea level change rate calculated using the monthly mean tide gauge data during 1952-2005 for the Chennai station depicted the net sea level rise of 0.0852 m/yr. Again, Mahendra and others (2011) assessed multi-hazard vulnerability along Cuddalore, Villupuram coast in Tamil Nadu. They assessed Probability of maximum storm surge height during the return period, future sea level rise, coastal erosion and high resolution coastal topography. The study consisted of multi hazard parameters which provided comprehensive assessment for the coastal area.

Vivek and others (2017) conducted multi-hazard mapping of Vishakhapatnam by using 5 parameters as inputs i.e. the probability of Coastal erosion, Coastal slope, Coastal elevation, Sea level change rate and Tsunami arrival height. The study revealed that study area experienced erosion at 5.8 m/yr during 1973-2015. The sea level rise trend was about 0.75mm/yr for a recorded slope of 0.2° indicating the high vulnerability of the area to storm surges and SLR and the maximum extent of the hazard zone was found to be 20 km inland from the current coastline of the Visakhapatnam district with a total area of 150 km^2 for the delineated hazard zone.

Karuppusamy and others (2021) measured coastal vulnerability at micro-administrative units. Tamil Nadu, India, with 5235 villages/wards, is highly inhabited (2000 inhabitants/km^2). The assessment found that the study area is very sensitive to multi-hazard occurrences due to its socioeconomic fragility. Mondal and other (2021) assessed the multi-hazard risk in coastal West

Bengal, India, using analytical hierarchical processing, GIS, and secondary dataset from the government. The study discovered that coastal West Bengal is very vulnerable to a wide range of hazards. Also, using the Coastal Hazard Wheel methodology, Paul and Das (2021) determined the coastal vulnerability of 185 km of coastline in West Bengal, India. It discovered a high sensitivity to a variety of hazards, including gradual inundation, saltwater intrusion, erosion, and coastal flooding. The study found that the entire coast is extremely vulnerable to these coastal hazards.

2.9 Coastal Flooding Assessment – Sea Level Rise

Small Island Developing States (SIDS) are at risk from sea level rise, so it's important to address the effects and dangers of this trend (Horton et al., 2021). The range of anticipated sea level rise has changed over time, with upper forecasts from individual research typically larger than those from the Intergovernmental Panel on Climate Change (IPCC) Though many studies have examined sea level rise estimates, there is still a great deal of vagueness in the sea level increase that will occur in the future (Garner et al., 2018).

Meo (1991) first addressed the necessity for accurate projections and assessments of the effects of sea level rise in order to design successful policies such as a coastal protection master plan and an inter-distributary basin model land use plan. Later, Martyr-Kollar and others (2021) has conducted a literature review on key topics in sea level rise, including the lasting effects of near-term mitigation on long-term sea-level rise; new global coastal vertical elevation data and their impact on existing sea-layer rise projections; and the interaction of sea-water rise with other hazards such as salinization, tropical cyclones, and extreme precipitation. Also, Horton and others (2014) conducted a thorough examination of ninety recent studies by experts on the topic of sea level gave a probabilistic evaluation of sea-level rise by AD 2100 and AD 2300 under two opposing temperature scenarios. The study found that sea-level rise estimates are highly unreliable, and that climate mitigation actions can restrict future sea-level increase.

Garner and others (2018) analyzed the past and present state of sea-level rise projections using a comprehensive database of global mean sea-level rise (SLR) projections for the twenty-first century. Along with the categorization of emission scenarios used in IPCC reports, eight methodological categories were employed. According to the study, projection approaches have evolved throughout time. Despite more than 70 research, the future of SLR remains highly unknown.

Hauer and others (2021) evaluated how the spatial zone selection influences population exposure to sea-level rise by using a Spatio-temporal flood-modeling approach that integrates across different spatial zones to quantify the annual probability of population exposure to floods from sea-level rise. It has proposed a more thorough evaluation method that can analyze coastal flooding exposure holistically. Grinsted and others (2015) constructed regional forecasts of 21st century sea level rise in northern Europe and investigate the uncertainties beyond the IPCC's expected range, such as the danger and potential rate of polar ice sheet disintegration. This study has found that regional predictions with a median projection of 0.8m between London and Hamburg and a

95th percentile estimate is an additional 0.9m sea level rise by simulating individual major sea level components and estimating sea level budget evolution for regional projections. While Abou-Mahmoud (2021) assessed the sensitivity of the Alexandria coastal zone, Egypt, to sea-level rise has been assessed in this research by comparing land elevation datasets with analytical methods under a 1m sea-level rise scenario.

Also Kekeh and others (2020) identified that in many countries, local drainage infrastructures were not designed to account for the mean of sea level rise observed in the last few years, and as a result, outlet pipes are frequently inundated and covered at high tide, reducing drainage efficiency in the event of heavy rain. As a result, sea level rise and inadequate waste management can have a severe detrimental impact on coastal fishing communities' livelihoods, hurting their general well-being.

Through the economic point of view, Chinowsky and Helman (2021) investigated 36 different sea level rise and storm surge scenarios across 5.7 million geographic locations and three time periods in the United States and discovered that sea level rise and minimal storm surge pose a USD 400 billion threat to the lower 48 United States' coastline by 2040, necessitating the construction of at least 80,000 km of protective barriers.

2.9.1 Sea Level Rise Assessment using Bathtub Hydrological Method

The bathtub method of measuring sea level rise involves determining the areas that could flood from seawater inundation. This method makes the assumption that the water table and sea level rise uniformly across a coastal research area (Maliya & Maliya, 2021). The modeling approach and the level of accuracy of the topographic data used both affect how accurate the assessment is. To determine the degree of inundation and uncertainty, high-resolution digital elevation models are employed (Yunus et al., 2015). Potential impacts of flooding in particular areas are calculated using plausible sea level rise scenarios (Kim and Cho, 2013). Moreover, a comprehensive vulnerability grade assessment system may be built by taking into account a variety of influence factors to quantitatively evaluate the vulnerability of coastal areas to sea level rise (Wu, 2002).

However, this method ignores significant hydrodynamic effects that are critical in estuarine settings, such as tidal wave amplification, dampening, and reflection (Khojasteh et al., 2021). Furthermore, because it neglects to take flow and sediment distribution into account realistically, the bathtub approach may lead to inaccurate predictions of wetland resistance to sea level rise (Breda et al., 2021).

According to the review conducted by Khojasteh and others (2021), static (Bathtub) approaches in assessing SLR consequences in estuaries should be avoided because they fail to account for significant hydrodynamic phenomena such as tidal wave amplification, damping, and reflection. While Breda and others (2021) used a computational framework that covers all essential hydrodynamic and sediment transport mechanisms to study how vertical accretion and migration processes affect wetland response to future SLR. The results reveal that sophisticated simulations show greater wetland vulnerability to sea-level rise compared to basic models, and changes in elevation owing to accretion are 10-50% of those predicted by simple models.

However, researchers have created improved versions of the bathtub model that take into account extra elements including beach slope, surface roughness, and hydrological connection to overcome these constraints (Williams and Luck-Vagel, 2020). It has been demonstrated that these improved models yield more conservative inundation estimates and give a clearer picture of the risk of infrastructure flooding along the coast (Hebel et al., 2020).

In addition, despite its shortcomings, the bathtub technique can also be used as a basis for early planning and the identification of priority areas for additional research and adaption strategies (Ramm et al., 2018). Conducting national or regional SLR vulnerability evaluations is made more straightforward by the bathtub approach's simplicity, which enables consistent and comparable assessments across many regions. (Yunus et al., 2015). It can serve as a beginning point for inquiries and decision-making about coastal planning, adaptation, and resilience measures (Vollstedt et al., 2021). Bathtub approach can be a cost-effective solution for developing countries that have restricted financial resources because it doesn't necessitate complex modelling and costly data collection (Albert et al., 2013).

Various studies across the world has employed bathtub technique with modifications to make it more robust. Yunus and others (2015) analyzed the possible sea level rise flooding for London boroughs by employing tidally-adjusted bathtub modelling (Evaluation of inundation extents using digital elevation models (DEMs). The study presented a broad-scale estimate of the potential repercussions of SLR and uncertainties in the DEM-based bathtub type flood inundation modelling for London boroughs, indicating that 3% to 8% of Greater London might be inundated by 2100, with Newham, Southwark, and Greenwich being the most vulnerable. While Maliya and Maliya (2021), by using a hydrostatic or "bathtub" approach proposed that sea level rise will contribute to salinization of coastal aquifers by increasing the frequency and extent of overwash events and saline water intrusion, with the latter evaluated using density-dependent numerical groundwater modelling. It came to the conclusion that sea level rise is a direct hazard due to permanent inundation and transient flooding from heavy storms and king tide.

Kim and Cho (2013) predicted sea level rise inundation under various scenarios. A semi-empirical technique, Bathtub Modelling (BM) was applied, and each scenario needed a rise in air temperature. According to the findings, sea-level has been progressively rising in all scenarios, with the highest difference in sea-level rise reaching more than 1.2m in 2120. Williams and Luck-Vogel (?? developed a GIS-based enhanced Bathtub Modelling (eBTM) that incorporates beach slope, surface roughness, and instills hydrological connection to make it more suited and relevant for event scale coastal flooding. The study found that the eBTM offers more conservative inundation estimates, which can be used to quantify coastal flooding risk to infrastructure. Habel and others (2020) analyzed the application of a bathtub method version to estimate sea level rise flooding from other sources such as groundwater inundation and storm-drain backflow. The method determines flooding extents and infrastructure vulnerabilities that are expected to occur as a result of alternate flood sources, and it is applied to Honolulu's core urban centre and current tidal flooding difficulties. The study found that high-resolution raster datasets are necessary for flood simulation, and different flood sources necessitate distinct engineering strategies.

2.9.2 Sea Level Rise Assessments in India

Due to its heavily populated coastal regions and low-lying islands, sea level rise poses an enormous risk to India. According to Kumar and Sardana (2021), the North Indian Ocean (NIO) experiences significant fluctuations in sea surface temperature that affect the sea level along the Indian coastline. Projections show probable sea level increases ranging from 7.1 cm to 77.88 cm by 2100. Sea level rise could have a negative socioeconomic impact on coastal areas in India, particularly Mumbai (Pednekar and Siva-Raju, 2020).

Pednekar and Siva-Raju (2020) have found that Sea Level Rise (SLR) is a by-product of climate change on a global scale and in India, Mumbai is particularly vulnerable to the impacts of sea level rise. Krishnamurthy and others (2014) emphasized on accurate sea level predictions which could be vital for planning coastal development. Empirical and semi–empirical and process based modelling have been undertaken to reduce uncertainties in the future projections. Deepa and Gnanaseelan (2021) looked at long-term tide gauge records, sea level pressure, rainfall, and winds and discovered a link between sea level fluctuation in the Indian Ocean and global climate models like the Pacific Decadal Oscillation and the Atlantic Multi-Decadal Oscillation.

According to Kumar and Sardana (2021), sea level rise along the Indian coastline is growing due to enormous variations in Sea Surface Temperature (SST) in the North Indian Ocean (NIO). Rising sea levels pose a threat to highly populated places along the Indian coastline and low-lying islands, with Vishakhapatnam, Mangalore, Mumbai, and Chennai being the most vulnerable cities. Space Application Centre (2012) prepared a comprehensive report on Coastal zones of India. Status of Mangroves, Coral reefs, Marine protected area was provided, as well as Impact of sea level rise vulnerability along the Indian coast covering 25 km inland area from HTL was also assessed. Amarnath and others (2017) authored a report on Mapping multiple climate-related hazards in South Asia. A synthetic overview of south Asia has been provided about flood, Drought, Sea level rise to name a few and a Composite Hazard Index (CHI). Kumar and Jayappa (2018) studied Makran subduction zone on India's west coast to assess tsunami threat and modelled earthquake source scenarios using the community Model Interface for Tsunami. The modelling findings reveal that in the worst-case scenario, all seven coastal areas are minimally inundated, with maximum water levels in the range of 100-200 cm.

On the east coast, Natesan and Parthasarathy (2010) revealed that about 13 sq. km of the land area would be inundated permanently due to SLR along Kanyakumari coast. Khan and others (2012) carried out sea level rise simulation study using SimCLIM model to determine the impact of Sea level rise for the coasts of Tamil Nadu. Also Khan and others (2020) evaluated the impact of sea level rise on tide, which is the biggest source of variability in sea level along the Bengal delta's macro-tidal shoreline. The study discovered that sea level rise will raise the risk of tidal flooding and decrease tidal amplitude in the middle region of the Bengal delta.

Pramanik and others (2015) using Sea level and tidal gauge data and advanced geo spatial technologies studied climate change induced present sea level rise along the eastern coast of India. The study used SRTM 90m DEM to derive the coastal elevation, inundation risk zones. Sea level rise scenario had been explained by using a 5th order polynomial curve which also interpolates and extrapolate the gaps within the available data of four tidal gauge stations. The study showed that northern portion (Ganga-Brahmaputra delta region) coast, mostly affected by the sea level rise (4.7 mm/yr.). Also Visakhapatnam and Bhubaneswar have a higher rate of sea level rise respectively 0.73 mm and 0.43 mm which increase the erosional activity and probable inundation level.

Praveen and others (2018) constructed local sea level scenarios for assessing possible impact to Indian coast. A climate simulator model based sea level rise data based on the IPCC-Special Report on Emission Scenarios (SRES) has been used to project the sea level rise at local level under different scenarios. The results revealed that sea level for Visakhapatnam, Chennai, Cochin and Mumbai may increase by 1.16 m, 1.19 m, 1.34 m, 1.24 m, respectively, by 2100 under RCP 8.5 of IPCC AR5, as well as the sea level of west coast tends to rise slightly more than the east coastal areas of India.

While on the west coast, Kumar (2006) studied the potential vulnerability of Cochin coast due to Sea level rise coupled with probable storm surge. It incorporated numerically modeled storm surge value along with sea level rise scenarios to determine coastal inundation extent. The study revealed that mean beach slope and the relief of the study area play a controlling factor in determining the amount of land that will be lost to sea level rise.

UNFCCC conducted a case study to assess vulnerability of Cochin, Kerala to sea level rise using SRTM 30m DEM for elevation & slope data and IRS P6 LISS 3 images to extract land use land cover of the study area. The study revealed that due to sea level rise ocean front and inland properties would get temporarily or permanently inundated and increase in these water levels would alter the coastal drainage gradients as well. Reduction in these gradients would increase flooding to rainstorms which could promote saltwater intrusion into coastal aquifers and force water tables to rise. This was one of the few comprehensive study in India which did not only show the coastal vulnerability but it presented inland flooding extent and also the cascading effects of Sea level rise. Patel and others, 2013 prepared the 3-D visualizations of Okha coast, Gujarat. They used Tsunami N2 model and GIS/CAD based models for simulation. The aim was to understand effect of plausible Tsunami at Okha coast due to its proximity to Makran coast, which is highly vulnerable to earthquakes.

In Goa, Morner (2017) studied coastal morphology and sea level changes in Goa during last the 500 years. Coastal morphology, stratigraphy, radiocarbon dating, archaeological remains, historical documentation, and tide gauge records were analyzed to determine sea level changes. It revealed a low level in the early 16th century, a þ50-cm high level in the 17th century, a level below present sea level in the 18th century, a þ20-cm high level in the 19th and early 20th centuries, a 20-cm fall in 1955–1962, and a virtually stable level over the last 50 years.

Likewise, numerous studies have come up in Maharashtra, also on the west coast and particularly concerning Mumbai. Patankar and others (2010) conducted a case study of Mumbai for Climate Change Vulnerability Assessment and Urban Development Planning. It overviewed the climate risks for Mumbai and identified the physical, economic, social vulnerabilities and responsibilities of all the stakeholders. Studies indicate that Mumbai is likely to be highly vulnerable to climate change with majority of its population living on the flood prone and reclaimed land. Chowdhary and Behera (2015) studied regional sea level variations along Kandla, Mumbai, Cochin and Hiren Point coast. Master station approach to study variation in sea level was used. the study revealed that, on macro level the average rise in AMSL in Bay of Bengal based on available tide gauge data was 1.92 mm/yr. and in Arabian Sea was 1.72 mm/yr. (which were well within the global estimate of 1-2 mm/year) (IPCC). In terms of Satellite data estimation, the trend in sea level rise, in Bay of Bengal was 3.05 mm/yr. and in Arabian Sea was 2.15 mm/yr., whereas, the IPCC reported a global rise of 3.2 mm/yr. for 1993-2012. Black and others (2017) had prepared the shoreline management plan of Maharashtra. For the first time in India, rather than considering larger regions only, every beach in Maharashtra was visited and documented. The report mainly identified most sustainable ways to manage coastal resources and risks, including those due to climate change, for next 100 years and support the planning system CRZ to minimize inappropriate developments in the long term.

Singh and Kambekar (2017) assessed impact of Sea level rise along Mumbai coastline to determine the possible extent of inundation by sea water. The study used single-value water surface method in ArcGIS 10.1 to estimate the probable flooding. Comparative study for vulnerability intensity for every ward coming under Municipal Corporation of Greater Mumbai (MCGM) was prepared. It resulted that loss of land due to coastal inundation might reach 3.84 %, 8.79 %, and 14.16 % for probable sea level rise of 1 m, 2 m, and 3 m. Patwardhan and others (2010) studied the impacts of climate change on coastal zones in 2003. the study reviewed then state of knowledge about the Vulnerability of coastal zones of India due to climate change and different assessment methodologies. According to the review, Mumbai and Ratnagiri were found to be most and least vulnerable to 1m sea level rise in Maharashtra. Dhiman and others (2019) reviewed an article quantification, management and climate change impacts of flood risks in Surat, Mumbai, Chennai and Kolkata, which are the most populated coastal cities in India.

2.10 Coastal Flooding Assessment - Storm Surge

An essential component of India's disaster readiness and coastal resilience is assessing the effects of storm surges, especially considering the country's susceptibility to tropical cyclones and other extreme weather conditions (Sahoo and Bhaskaran, 2018).

Dube and others (1984) constructed a coastal zone numerical model of storm surge in the Arabian sea by simulating the surge generated by the devastating 1975 Porbandar cyclone. The result of the calculation was in good agreement with the actual values reported from Porbandar coast. They emphasized that this model could be used for simulating the surge generated by the cyclone of any speed or intensity. Despite, Lodhia (2012) studied coastal Gujarat to assess the risk due to climate induced disasters in coastal regions. The study identified the need of stakeholder approach in the current planning strategies which have failed to deal with coastal issues and problems, an integrated regional framework for coastal development is required which encompasses trade-off among various sectors. Kalsi and Gupta (2003) studied Gujarat Cyclone of June, 1998 and revealed that the two-stage alert and warning were given to the state Authorities well in time, but the cyclone warnings did not reach the community level, which caused havoc and took a toll of about 3000 people, damaged 200000 houses, and resulted in losses worth over 700 million dollars.

Evan and Camargo (2010) studied the climatology of Arabian sea cyclones. They used JTWC and IMD dataset. The study emphasized that over the last 30 years (1979-2008) several intense Arabian storms formed and made landfall with large impacts. The study also revealed that November cyclones primarily form during periods when the Bay of Bengal experiences a broad region of high sea level pressure, which means November storms form in either the Arabian Sea or the Bay of Bengal but not in both during the same year. While Rao and others (1997) attempted to simulate storm surges along the Andhra coast occurred due to severe cyclones between 1891-1996, and the computed results were validated with the available observations using empirical formula. Gayathri and others (2017) reviewed the critical factors that contribute to coastal inundation. Various models were reviewed like ADCIRC, SWAN, drying and wetting algorithms, coupled models ADCIRC, SPLASH, FVCOM and CH3D-SSMS etc. This article provided a detailed evaluation of the progress made in storm inundation research as well as, this work also focused on the status of storm-surge research in the Indian subcontinent. They stated that sea-level rise, coastal erosion, geomorphologic alterations and anthropogenic activities are responsible for permanent flooding and retreat of the coast.

Dube and others (2010) reviewed storm surge modelling and their applications in the coastal area. Numerical models, SLOSH, ADCIRC and Remote sensing techniques and their applicability were reviewed. As well as case study of Andhra Pradesh vulnerability to storm surge by using synthetic surge models was incorporated. Chhitibabu developed the storm surge prediction models for the Bay of Bengal and the Arabian sea. a description of a fine resolution numerical for the prediction of storm surges along the Gujarat coast was described. Experiments were performed using wind stress forcing data representative of the 1982 Veraval cyclone, 1996 Diu cyclone and 1998 Kandla cyclone. The surge values computed by the fine resolution model was compared with those of the coarse resolution for the Gujarat coast. Shukla (2015) published a book on vulnerability and risk measurement of climate change induced disasters in Gujarat. It has assessed the pattern of climate induced disaster in Gujarat. It has argued that development and disaster are positively correlated.

Mahapatra and other (2016) studied the coastal vulnerability of Saurashtra coast, Gujarat related to storm surge events. The study calculated Vulnerability of exposure index, Sensitivity index and adaptive capacity index separately and Total Vulnerability Index (TVI) by integrating all above. It showed that areas with coastal cliffs, higher elevations, small coastal length are less vulnerable among all. Mathur (2018) studied coastal flooding, storm surges and the vulnerability of India states and Gujarat specifically. It was determined that in Gujarat, South Gujarat coast is most vulnerable along with Porbandar district. Kumar and other (2021) addressed the effects of the Amphan cyclone on LULC such built-up areas, agriculture, brick-kiln industries, and vegetation cover in nine coastal districts of West Bengal, India. Sentinel-1A and B images, Interferometric Wide swath (IW), Ground Range Detected (GRD), VV polarisation images, and Sentinel-2B Multispectral Instrument (MSI) images were used in this study.

2.11 Coastal Vulnerability Index

The Coastal Vulnerability Index (CVI) is a technique for assessing and quantifying coastal areas' vulnerability to the effects of coastal disasters (Kumar and others, 2010. It assists in identifying areas that are more vulnerable to coastal erosion, inundation, and other negative effects due to their physical characteristics and susceptibility to these hazards (Torresan et al., 2012).

The coastal vulnerability index approach has been found to be iterative in nature in India. Numerous studies have come up revealing different CVI variables which have immensely assisted to robust the CVI technique. Hegde and Reju (2007) was the first study to apply the Coastal Vulnerability Index (CVI) methodology in India applied at Mangalore coast. Using technique given by (Gornitz et al., 1994; Gornitz et al., 1997) to assess coastal vulnerability to SLR. The index comprises physical and geological indicators and, on occasion, socio-economic indicators comprised of shoreline change, coastal slope, geomorphology and population density. Nonetheless, they recommended the use of additional parameters, such as sea-level change, tidal range, significant wave height, and the probability of storm surges, and which were later included in more recent studies in coastal areas of India. Mani Murali and others (2013) incorporated population density and tourist density, While Jana and Bhattacharya (2013), Sankari and others (2015) and Mahapatra and others (2015) included LULC change as CVI parameters.

Moreover, Kumar and others (2010), Kumar and Kunte (2012), Mani Murali and others (2013), and the Indian National Centre for Ocean Information Services (INCOIS) (2012) further added coastal regional elevation to their CVI for their assessment conducted in Orissa State, Chennai, Puducherry, and the entire coast of India. Kumar and Kunte (2012) included storm surge as a CVI parameter and Nayak and Bhaskaran (2014) tsunami run-up and the frequency of cyclones making landfall. Later, Parthasarathy and Natesan (2015) further included beach width in their CVI of the

Tuticorin coast on the Gulf of Mannar, a parameter that had not previously been used in other studies in India.

The vulnerability of the coast to SLR or any other coastal hazard is not only a function of its susceptibility to geological parameters (i.e., rate of shoreline change, coastal regional elevation, coastal slope, geomorphology, and beach width), physical processes (i.e., rate of sea-level change, tidal range and significant wave height) and its exposure to short-term hazards such as storm surges and tsunamis, but also contextual or social vulnerability, as this influences the capacity for adaptation. Social vulnerability refers to the socio-economic and demographic factors affecting the resilience of communities (Flanagan et al., 2011).

2.11.1 Coastal Vulnerability Index in India

In this regard, there have been numerous studies assessing the vulnerability of different sections of the coast of India to SLR following the methodology developed or by incorporating more coastal vulnerability variables.

Along the east coast of India, Ahsan and Warner (2014) also computed a socio-economic index comprising 60 indicators that they obtained from household surveys to assess the vulnerability a region of southwestern Bangladesh to climate change. In addition to population density and the rate of population growth, other variables influencing the capacity for adaptation, i.e., percentage of dependent population, percentage of households living below poverty line, illiteracy rate, to name a few, were included. Kumar and others (2010) assessed the coastal vulnerability of Orissa coast. the study considered shoreline change rate, sea level change rate, coastal slope, significant wave height, tidal range, regional elevation, coastal geomorphology and tsunami arrival height. in earlier studies, tidal range was assumed to include both permanent and episodic inundation hazards. However, the mean of the long-term tidal records tends to dampen the effect of episodic inundation hazards such as tsunamis due to which, tsunami run-up was considered. it concluded that, it proves the usefulness of remote sensing data, in situ observations, numerical modeling, and GIS analysis tools for coastal vulnerability studies. Chandrasekar and Joevivek (2011) studied coastal geomorphological vulnerability of the coastline between Kallar and Vembar lies in the Gulf of Mannar. They studied different parameters like LULC, shoreline changes, sediment transport during pre-monsoon, monsoon, post-monsoon seasons and opined that, Beach morphological changes are influenced by intensive sand mining along the coast and coral mining in the barrier coral islands. Ahammed and Pandey (2019), focusing on the vulnerability of the coast of Andhra Pradesh to cyclones, used only five social variables; population growth and density, number of people living in a household, cyclone shelter house and transportation accessibility to compute their SoVI. Yadav and Barve (2017) assessed the socio-economic vulnerability of coastal communities affecting by cyclones in the State of Odisha using 29 socio-economic variables, which population density, the rate of population growth, percentage of rural population, distance to cyclone shelter, unemployment rate, and the frequency and impacts of floods, and lack of logistical support during a cyclone as the most influential.

Mujabar and others (2013) assessed the coastal vulnerability index for erosion of the coast between Kanyakumari and Tutikorin, Tamil Nadu. they considered parameters like: Geomorphology, shoreline change rate, coastal slope, sea level change, mean wave height, mean tidal range for the assessment and it was resulted that physical and human intervention processes are major causes of erosion in the study area. Poompavai and Ramalingam (2013) studied Coastal risk of Kattivakkam to Kovalam, Tamil Nadu. The study used different parameters from other vulnerability assessments. They used Environmental Vulnerability Index (EVI), Social Vulnerability Index (SVI), Hazard Potential Index (HPI), Mitigation Capacity Index (MCI). Computed integrated coastal risk index (CRI). It is a multi-scale approach in which Cyclones are used as the indicator of coastal risk. Likewise, the Coast between Rasulpur and Subarnarekha (Odisha) was assessed by Jana and Bhattacharya (2013). They took Shore line change rate, land use and human activities, population density. They studied social parameters also to assess coastal vulnerability.

Chandrasekhar (2014) assessed the vulnerability of Orissa coast at district level to cyclones and floods by focusing on the biophysical components. An 'integrated approach' was adopted to assess vulnerability which is viewed as a function of exposure, sensitivity and adaptive capacity. Pearson's correlation was calculated between determinants and major components of vulnerability which revealed that Balasore, Bhadrak, Jajpur, Kendrapada, Malkangiri, Nabarangpur, Nuapada and Rayagada were highly vulnerable and Angul, Jharsuguda, Khurda, Sambalpur and Sundargarh least vulnerable, rest found to be moderate.

Kantamaneni and others (2019) conducted an extensive literature review of coastal vulnerability assessments and an assessment of Andhra Pradesh coastline which tried to understand hazard factors and threat risk levels, they emphasized that despite substantial vulnerabilities, the risk to the coastline of Andhra Pradesh has not been rigorously evaluated. Anticipated SLR is likely to result in the loss of land, increase in salinity and the decline of water quality, especially in agricultural fields, with predominantly negative impacts on the economy and population of coastal Andhra Pradesh.

Along the west coast of India, Mohan and Jairaj (2013) assessed the coastal vulnerability of Kerala coast by taking Physical vulnerability and Social vulnerability variables into account by deploying Analytical Heirarchy Process (AHP) and Remote sensing techniques. They also studied shoreline change rate of Kerala coast. The study revealed that about 65% of the Kerala coastline is eroding, 21% is under accretion and about 14% is under stable status. Coastal vulnerability is high at Poovar, Punathura, Poonthura to Veli, Kadinamkulam, Kollam to Chavara regions and Punnapura in South zone, in Central zone include Fort Kochi to Vypin, Cochin Harbour to Azhikode, Chavakkad and Ponnani. And in the north the highly vulnerable areas include Kasargod Harbour, Azhikal to Mappila fishing harbor, Kizhunn to Dharmadam, Kozhikode beach to Kuttichira and Beypore.

Dwarakish and others (2008) used the CVI methodology to assess the vulnerability of Udupi coast, Karnataka. Their study used information on past sea-level change, tidal range and significant wave height, in addition to the physical and geological parameters but without considering population density and any socio-economic variable. Hegde and Reju (2007) assessed Mangalore coast, from Talapady to Surathkal. Index method was used and Physical and Social parameters were taken, geomorphology, regional coastal slope, shoreline change rates and population but they opined that additional physical parameters like wave height, tidal range, probability of storm, etc. can enhance the quality of the CVI. Kantamaneni (2016) referred a modified vulnerability assessment model in addition to Geomorphology and physical parameters dominant assessment methods. The referred methodology was applied in Aberystwyth coast which estimated the vulnerability of the coastal infrastructure (comprising population, commercial and residential properties).

de Sherbinin and Bardy (2015) assessed the social vulnerability of two cities to flooding, i.e., Hurricane Sandy, which affected New York City in 2012, and the Mumbai flash floods of 2005, by developing an index incorporating 20 social variables for New York City and 12 variables for Mumbai, including population density and variables representing the characteristics of the population impacting on its capacity for adaptation such as the percentage of the population that is female and under six years of age, and the rates of literacy and unemployment. Mahapatra and others (2015) conducted a study to assess the vulnerability of Gujarat coast due to predicted Sea level rise, by using remote sensing techniques, numerical simulations and field work. The study computed CVI and revealed that, 45.67% coast is under high to very high risk category and 54.33% coast in under moderate to low risk category., and concluded that this approach can be used effectively by coastal management authorities.

2.11.2 Coastal Vulnerability Studies in Goa

Goa is highly susceptible to tropical cyclones and monsoon-related severe rainfall, which can create storm surges and coastal floods. This endangers coastal communities, livelihoods, and infrastructure in the region.

In this regards, Mascarenhas (1999) studied Coastal regulation zone of Goa from different perspectives of Oceanographic, environmental and Societal perspectives. The study found that, sectoral practices, partisan policies, unbalanced tourism, and absence of political have contributed to the violation of CRZ legislation, also an unplanned developmental activities made Baga–Sinquerim the most severely degraded strip of the Goan coast. Again, Mascarenhas (2000) also studied the status of coastal environment of Goa. As the degrading environment may lead to higher costal vulnerability of the region, He observed various factors which are degrading coastal areas, as well as he opined that predicted sea level rise effect may be less severe on the sandy beaches of Goa as most of them have an appreciable gradient. But minor increase in levels will significantly influence inland water bodies and particularly the low-lying "khazan lands" of Goa as these lowlands are at or even below the present sea level.

The INCOIS and the Integrated Coastal and Marine Area Management (ICMAM) carried out mapping multi-hazard coastal vulnerability for the states. The general trend was demarcated in to four classes (very high, high, medium and low), at macro-synoptic scales for all the coastal states.

They emphasized that, coastal vulnerability aspects at micro level are to be accounted with additional parameters such as cyclone, storm surge and coastal flooding. INCOIS also studied and mapped the Coastal Vulnerability of Goa on 1:100000 scale.

Central Water Commission (CWC) (2016), prepared the status report on coastal protection and development in India. The scope of the report covered general geography, causes of coastal erosion, coastal protection measures and shoreline change rate. The shoreline change rate atlas was prepared for all the coastal states and the study presented that in 2016, Goa had 27.06 sq. km as eroding, 46.98 sq. km as accreting and 81.38 sq. km as stable shoreline. Similarly, Reddy and others (2013) had presented a comprehensive account of soil erosion in Goa. Universal soil loss equation method was deployed to determine erosion rate. The study revealed that Sanguem (83682) ha/yr., Canacona (35204) ha/yr. and Quepem (31825) ha/yr. respectively, topped the chart of highest soil erosion in all 11 talukas. Ponda Salcete, Pernem, Bardez, Bicholim, and Tiswadi were among moderate and Marmugao had the lowest with (10913 ha/yr). According to the study higher beach erosion rate was found in Sinquerim, Candolim, Dona Paula.

Before, Chachadi and Ferraira, 2002 had assessed aquifer vulnerability to sea-water intrusion using GALDIT method. According to the study Goa falls under high to very high risk of salt water intrusion, the surface inundation due to sea level rise is maximum along the Baga creek, Anjuna area, Chapora creek and Nerul creek, whereas along the main coast it is minimum due to typical topography. The eustatic SLR can inflict irreversible damages on the coastal freshwater aquifers in the form of seawater intrusion. This could jeopardize the water availability and supply in the heavily urbanized coastal belts.

In terms of wind and storm related vulnerability, National Disaster management authority (NDMA) prepared the report of vulnerability profile of India. Goa lies under moderate damage risk zone of Wind and Cyclone hazard, on the scale of low to very high damage risk. Also, the Building Materials and Technology Promotion Council (BMTPC) (2019) has produced the vulnerability atlas of India. The maps showed that, Goa fall under moderate category 48-63 MSW (Maximum. Sustained Wind, in knots) speed. However, it is higher than north Karnataka. It has also predicted storm surge height of 4.5 m for Goa. As well as, it has demarcated coastal south goa as landslide prone area.

Human induced impacts on coastal areas have always been found to be dangerous for the coastal ecosystem. Sawakar and others (1998) studied the issues of concern due to tourism in the coastal part of Goa. They pointed out that there was a large amount of demerits also present due to uncontrolled growth of tourism also it damaged coastal aquifers, sand dune system, and mangrove vegetation. Panandikar (2016) studied vulnerabilities of Goa due to climate change. She observed that Coastal erosion, Impact of infrastructure, Coral bleaching, adverse effect on fresh water and salt water intrusion would be accelerated due to anthropogenic activities in the coastal belt. Likewise, Nayak (2010) prepared a report for the National Centre for Sustainable Coastal Management (NCSCM) about Goa coast Vulnerabilities. Climate change and associated sea level rise can be disastrous to Goa. It is realized that uncontrolled activities either on the waterfront or beyond or on the land-based side could cause irreversible damage. The study emphasized that, to maintain coastal regions of Goa, a detailed coastal zone resource information system is a prerequisite. The issues found were erosion at Anjuna and Kerim beaches, seasonal erosion during monsoon in several parts of the coastal stretch including headlands.

Chapter-3

Methodology

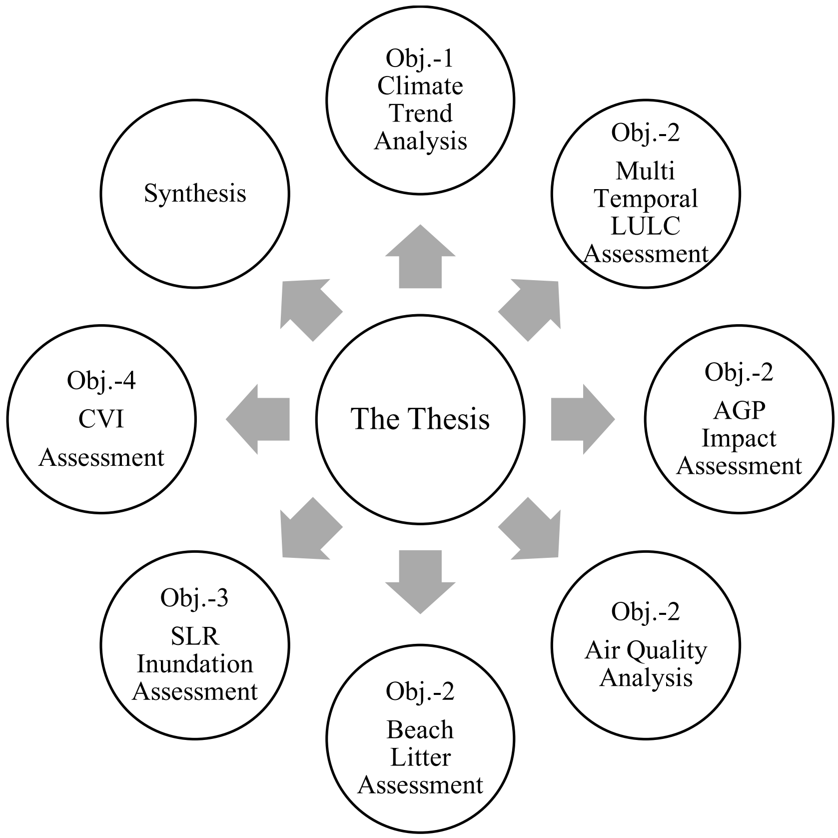

Fig 3.1 Flowchart of Research Methodology Presented in this Doctoral Work (Obj. Refers to Thesis Objectives).

3.1 Multi-Temporal Climate Trend Analysis

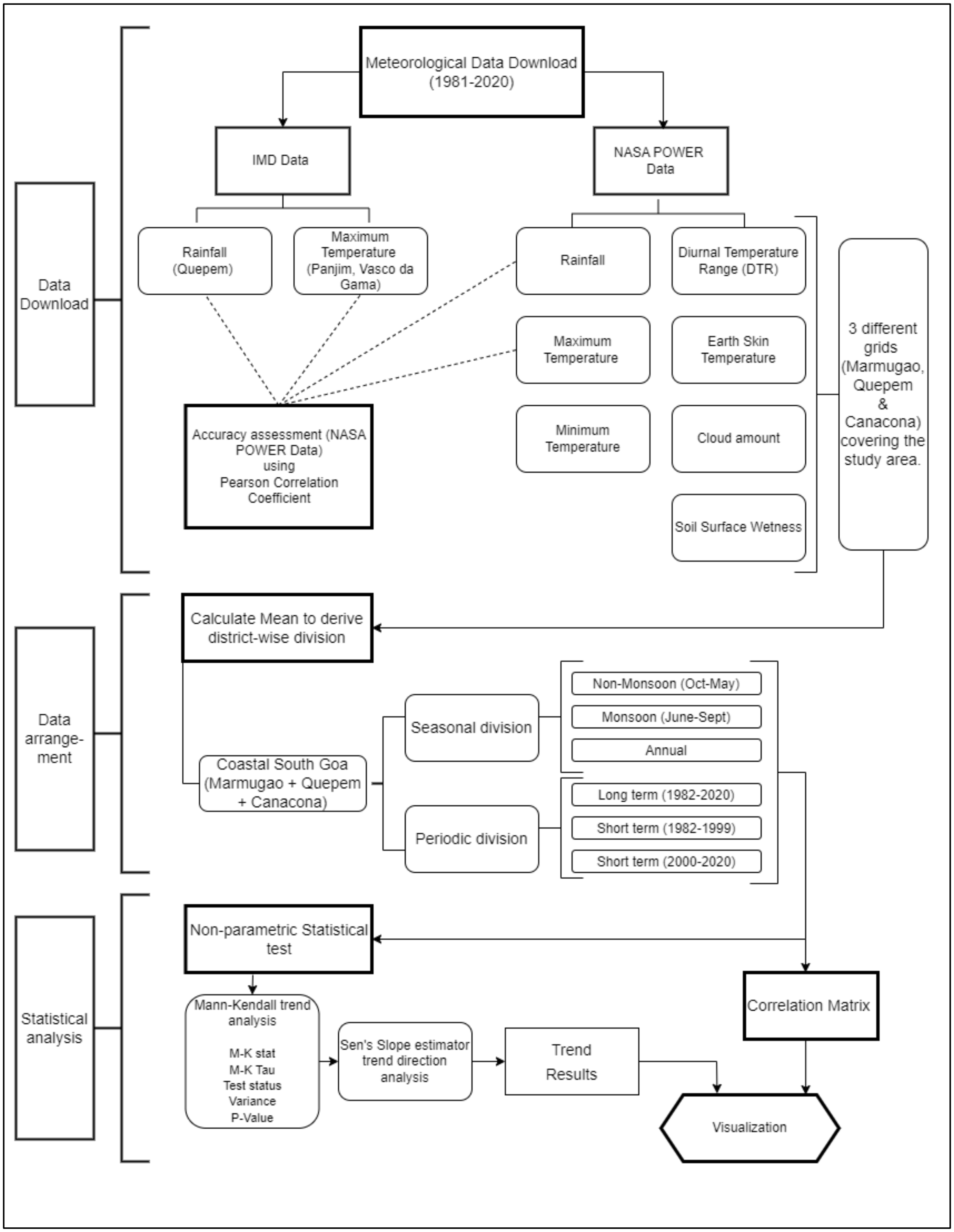

Fig 3.2 Flowchart of methodology of the Multi-Temporal Climate Trend Analysis.

The assessment has the spatial extent upon the coastal tracts of south goa and comprises of 40 years of meteorological datasets downloaded from the NASA POWER project. The data has been divided into three different temporal periods to determine the climatic trends during different eras (based on generally different socio-economic situations). Therefore, firstly, the long term trend (1981-2020) has been analyzed and then, two short term trends (1981-1999, late twentieth century phase) and (2000-2020, recent phase) have been analyzed to compare and contrast the impact of changing socio-economic and demographic scenarios upon different climatic parameters.

In addition, the annual data has been divided each year into three periods (non-monsoon, monsoon and annual) to investigate the annual and seasonal trends for both the long term and the recent term periods (Table 3.1).

Table 3.1: Temporal Division of the Datasets for Climate Trend Analysis

Long Term
(1981-2020)

- Annual (Jan-Dec)
- Non-monsoon (Oct-May)
- Monsoon (June-Sep)

Late Twentieth century
(1981-1999)

- Annual (Jan-Dec)
- Non-monsoon (Oct-May)
- Monsoon (June-Sep)

Recent
(2000-2020)

- Annual (Jan-Dec)
- Non-monsoon (Oct-May)
- Monsoon (June-Sep)

Mann-Kendall test method is used to investigate all the seven climatic variables (Rainfall, Minimum Temperature, Maximum Temperature, Diurnal Temperature Range, Land Surface Temperature, Cloud amount and Soil Wetness) for each time period. To find out the magnitude of the changes Sen's slope test is applied to compare and understand the variables trend in different periods and phases, to find out if there are any dramatic changes in the trends during past forty years (1981-2020).

3.1.1 Pearson's Correlation Coefficient

The correlation between two data points X and Y is the measure of the linear relationship between the attributes X and Y. Pearson correlation takes a value from −1 (perfect negative correlation) to +1 (perfect positive correlation) with the value of zero being no correlation between X and Y.

Pearson correlation between two data points *X* and *Y* is given by:

$$\text{Correlation (X,Y)} = \frac{Sxy}{Sx \times Sy}$$

where s_{xy} is the covariance of *X* and *Y*, which is calculated as:

$$s_{xy} = \frac{1}{n-1} \sum_{i=1}^{n} (xi - x)(yi - y) \quad (1)$$

and s_x and s_y are the standard deviation of *X* and *Y*, respectively.

The Pearson correlation method is the most common method for numerical variables; it assigns a value between − 1 and 1, where 0 is no correlation, 1 is total positive correlation, and − 1 is total negative correlation (Kotu & Deshpande, 2019).

3.1.2 Mann – Kendall Test

As a tool for estimating the significance of trends in meteorological time series, the Mann-Kendall statistical test has been frequently used (Tabari & Marofi, 2010, Subash et al., 2011, da Silva et al., 2013). Mann-Kendall test statistics (Mann, 1945; Kendall, 1948) are calculated as follows:

$$S = \sum_{i=1}^{n-1} \sum_{j=i+1}^{n} Sign(T_j - T_i) \quad (2)$$

where n is the number of data points, T_i and T_j are the data values in the time series i and j (j > i), respectively, and Sign ($T_j - T_i$) is the sign function as:

$$Sign(T_j - T_i) = \begin{cases} 1 & if\ T_j - T_i > 0 \\ 0 & if\ T_j - T_i = 0 \\ -1 & if\ T_j - T_i < 0 \end{cases} \quad (3)$$

Variance is calculated as follows:

$$Var(S) = \frac{n(n-1)(2n+5) - \sum_{i=1}^{P} t_i(t_i-1)(2t_i+5)}{18} \quad (4)$$

where n is the number of data points, P is the number of tied groups, the summary sign (∑) indicates the summation over all tied groups, and t_i is the number of data values in the P^{th} group. This summary process may be ignored when there are no tied groups (Kisi & Ay, 2014). In the case of samples with a sample size n > 30, the standard normal test statistic Z_S is calculated using Eq. (5):

$$Z_S = \begin{cases} \frac{S-1}{\sqrt{Var(S)}}, & if\ S > 0 \\ 0, & if\ S = 0 \\ \frac{S+1}{\sqrt{Var(S)}}, & if\ S < 0 \end{cases} \quad (5)$$

In general, positive values indicate an increasing trend, while negative values indicate a decreasing trends. The significance level is determined when testing the trends. When $|Z_S| > Z_{1-\alpha/2}$, the null hypothesis is rejected, and a significant trend exists in the time series. $Z_{1-\alpha/2}$ is obtained from the standard normal distribution table.

3.1.3 Sen's Slope Estimator

The slope of the trend in n pairs of data can be estimated using a nonparametric procedure developed by (Sen, 1968). Based on Sen's method, the slope of the trend is estimated using a linear model, and the variance of the residuals is calculated as follows:

$$Q_i = \frac{X_j - X_k}{j - K} \quad for\ I = 1, \ldots, n \tag{6}$$

where X_j and X_k are the data values at times j and k (j > k), respectively. There is only one datum

$Qi=Xj-Xkj-K \quad for\ I=1,\ldots,n$ (6)

in each time period, so $N = \frac{n(n-1)}{2}$, where n is the number of time periods. If there are multiple observations in one or more time periods, then $N < \frac{n(n-1)}{2}$. Based on the n values of Q_i, the median slope or Sen's slope estimator is calculated as:

$$Q_{med} = \begin{cases} Q_{(n+1)/2}, & if\ n\ is\ odd \\ \frac{Q_{n/2}+Q_{(n+2)/2}}{2}, & if\ n\ is\ even \end{cases} \tag{7}$$

Data trends are reflected in the Q_{med} sign, whereas the value indicates the steepness of these trends. A confidence interval of Q_{med} at a specific probability can be obtained to determine whether the median slope is statistically different from zero. According to Gilbert (1987), a confidence interval can be calculated for the time slope as follows:

$Qmed= \quad Q(n+1)/2,Qn/2+Q(n+2)/22, \quad if\ n\ is\ oddif\ n\ is\ even$ (7)

$$C_\alpha = Z_{1-\alpha/2}\sqrt{Var(S)} \tag{8}$$

$C\alpha=Z1-\alpha/2Var(S)$ (8)

where Var(S) is defined in Eq. (4) and is derived from the standard normal distribution table. Following this, M1 = (n−Cα)/2 and M2 = (n + Cα)/2 are computed. Q_{min} and Q_{max} are the lower and upper limits of the confidence interval, respectively. They are the lowest and largest n-ordered slope estimates (Gilbert, 1987). If the slopes of the two limits (Q_{min} and Q_{max}) have a similar sign, the slope Q_{med} is statistically different from zero. Since there is no requirement for data to conform to a particular distribution and no restrictions on missing values, Sen's slope estimator has been widely used in meteorological time series (Yue and others, 2002, ElNesr, 2010). These advantages to this method has made it useful for analysing atmospheric chemistry and climatological data.

3.2 Multi-Temporal Land Use Land Cover Assessment

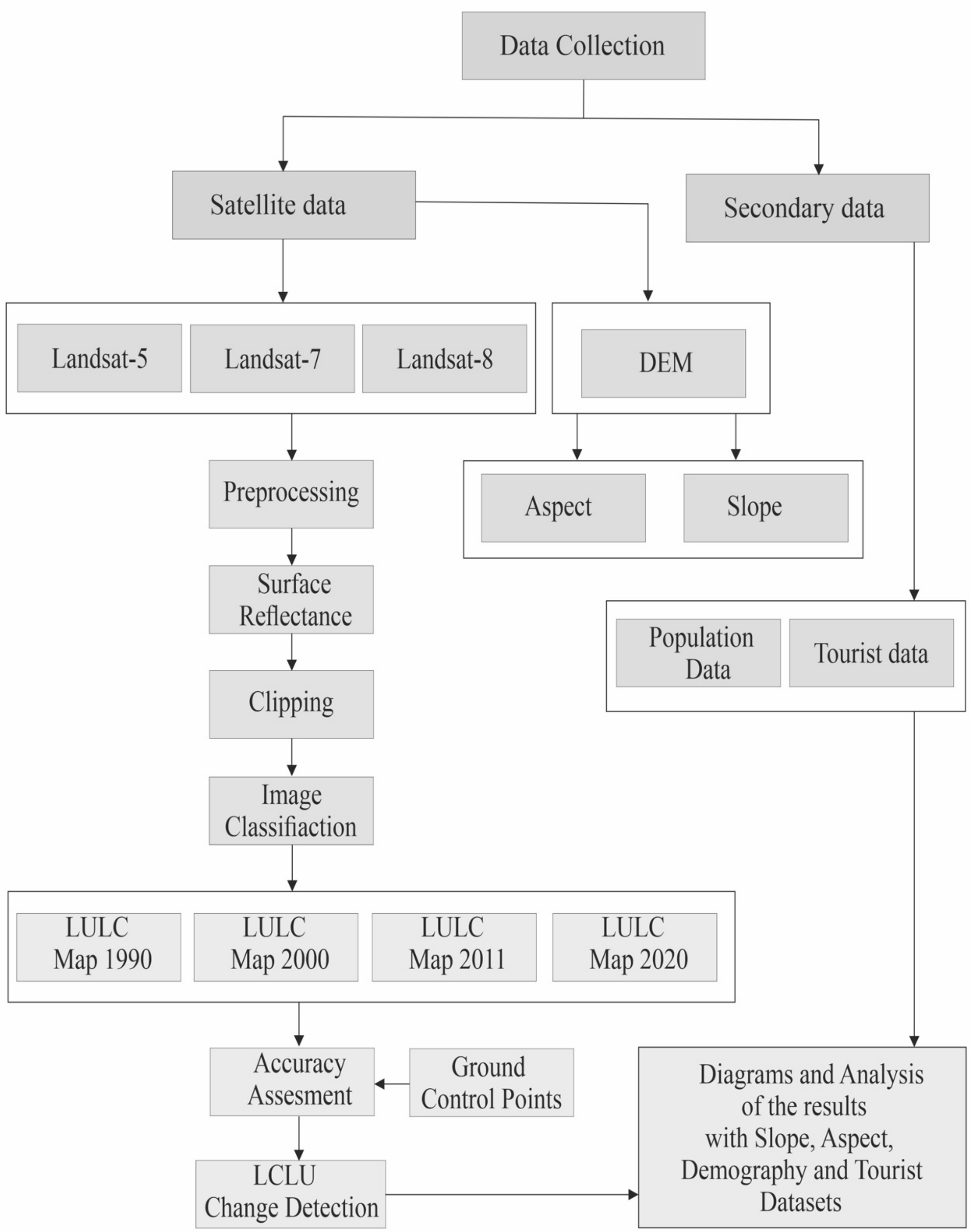

Fig 3.3 Flowchart of Methodology of the Multi-Temporal LULC Assessment.

3.2.1 Datasets

In the present study, multi-temporal Landsat TM, ETM, OLI-TIRS have been utilized for a comprehensive land use land cover study. These Landsat datasets have been acquired from the USGS Earth Explorer platform (https://earthexplorer.usgs.gov/), and specific details regarding each dataset are provided in Table 3.2. To ensure precision and consistency, the multi-temporal images were selected from the same season. All images shared a consistent spatial resolution of 30 meters. For the land use and land cover analysis, the visible and infrared bands (excluding the thermal infrared) have been integrated. The topographical maps of the study region have been collected from the Survey of India (https://www.surveyofindia.gov.in/) (Refer to Section-1.2 for toposheet numbers) A total of 120 ground control points have been gathered for the training of the classification. The meticulous selection of Landsat and IRS LISS-3 data, incorporation of relevant spectral bands, integration of topographical information collectively contribute to the robustness and accuracy of the land use and land cover analysis conducted in this study (In the coastal areas, Mean Absolute Error (MAE), Root Mean Square Error (RMSE), LE90 error of the SRTM 30m DEM compared to the GPS measurements, are 2.83m, 3.82m, 5.85m respectively (Zhang et al., 2019)).

Table 3.2 Data Acquisition Details for the Multi-Temporal LULC Assessment.

Dataset	Resolution	Month & Year	Source
Landsat 5 TM	30 m	23-Feb-1990 & 19-Feb-2000	USGS Earth Explorer
IRS - LISS 3	23.5 m	13- Nov 2011	Bhuvan NRSC
Landsat 8 OLI	30m	March-2020	USGS Earth Explorer

3.2.2 Image Pre-processing

Image preprocessing is a vital step in remote sensing before applying land use land cover classification analysis (Jianya et al., 2007). This essential phase involves a series of techniques designed to enhance image quality, reduce noise, correct geometric and radiometric distortions, and prepare the data for subsequent analysis. The goal of image preprocessing is to ensure that the data is in a suitable format for accurate and meaningful interpretation. The level 2 data of the Landsat images have been acquired in this study which was already geometrically and radiometrically corrected (Prasad et al., 2022). Image enhancement and noise removal have been performed in the ERDAS Imagine software.

3.2.3 Image Classification

The mapping of land cover classes typically derives from digital remotely sensed data, facilitated by the process of digital image classification (Kiefer et al., 1994; Shalaby and Tateishi, 2007). The overarching objective of image classification is to automatically categorize all pixels within an image into distinct land cover classes or themes (Kiefer et al., 1994). There are different land use land cover classification methods available in the literature. Among them, the supervised classification method is most popular and robust in comparison to the other methods. Therefore, in the current research, supervised method has been employed. Supervised land use classification serves as a technique employed in remote sensing and geographic information systems to categorize and map diverse land use types within a defined geographical area. This methodology hinges upon the utilization of labelled training data to instruct a classification algorithm, subsequently employed to categorically assign and map the entirety of the study area. This process involves the incorporation of ground checkpoints and topographic data from the study region. The study area has been divided into Six principal classes, encompassing Agriculture, Barren land, Built-up land, Vegetation, Water bodies and Wetlands.

3.2.4 Accuracy Assessment

In the realm of land use land cover mapping, three pivotal metrics—user accuracy, producer accuracy, and the kappa coefficient play a fundamental role in evaluating the precision and dependability of the classification or mapping process (Hassan et al., 2016; Prasad et al., 2022). These metrics yield invaluable insights into the caliber of classification outcomes and the degree of concordance between the classified map and the reference data.

3.2.4.1 User Accuracy

User accuracy, commonly referred to as user's accuracy or commission error, gauges the proportion of correctly classified pixels within a specific class on the classified map, relative to the reference data. Generally, the user accuracy for a class "i" is calculated as follows:

$$User\ Accuracy\ (Class\ i) = \frac{Number\ of\ Correctly\ Classified\ Pixels\ of\ Class}{Total\ Number\ of\ Pixels\ Classified\ as\ Class} * 100\% \qquad (1)$$

Elevated user accuracy signifies that the classification algorithm adeptly identifies the authentic class of pixels, thereby minimizing the misclassification of pixels into that particular class.

3.2.4.2 Producer Accuracy

Producer accuracy, also known as producer's accuracy or omission error, quantifies the proportion of correctly classified pixels within a specific class on the classified map with respect to the reference data. Essentially, it reflects the accuracy of the classification algorithm in effectively detecting and mapping genuine occurrences of a class. The producer accuracy for a class "i" is calculated as follows:

$$Producer\ Accuracy\ (Class\ i) = \frac{Number\ of\ Correctly\ Classified\ Pixels\ of\ Class}{Total\ Number\ of\ Actual\ Pixels\ of\ Class} * 100\% \qquad (2)$$

High producer accuracy indicates that the classification algorithm is effectively capturing and mapping the true occurrences of the class on the map.

3.2.4.3 Kappa Coefficient

The kappa coefficient, frequently referred to as Cohen's kappa, represents an additional statistical measure of concordance between the classified map and reference data, accounting for the expected agreement arising solely by chance. It furnishes a more robust assessment of accuracy compared to individual user and producer accuracies, particularly when dealing with imbalanced classes or a substantial number of classes. The formula for computing the kappa coefficient is as follows:

$$K = \frac{Pi - Pq}{1 - Pq} \quad (3)$$

Where Pi denotes observed agreement between the classified map and the reference data (the ratio of correctly classified pixels to the total number of pixels) and Pq illustrates the expected agreement due to chance. The kappa coefficient ranges from -1 to +1, where +1 indicates perfect agreement, 0 suggests agreement no better than random chance, and -1 indicates complete disagreement.

The application of user accuracy, producer accuracy, and the kappa coefficient in land use land cover mapping holds paramount significance in evaluating the overall credibility of classification outcomes. Moreover, these metrics aid in identifying potential error sources and steering the enhancement of classification algorithms and methodologies. Collectively, these metrics empower researchers and practitioners to make informed judgments about the caliber of land cover maps, thereby augmenting the accuracy of ensuing analyses and applications.

3.3 Multi-temporal Anthropogeomorphic Impact Assessment

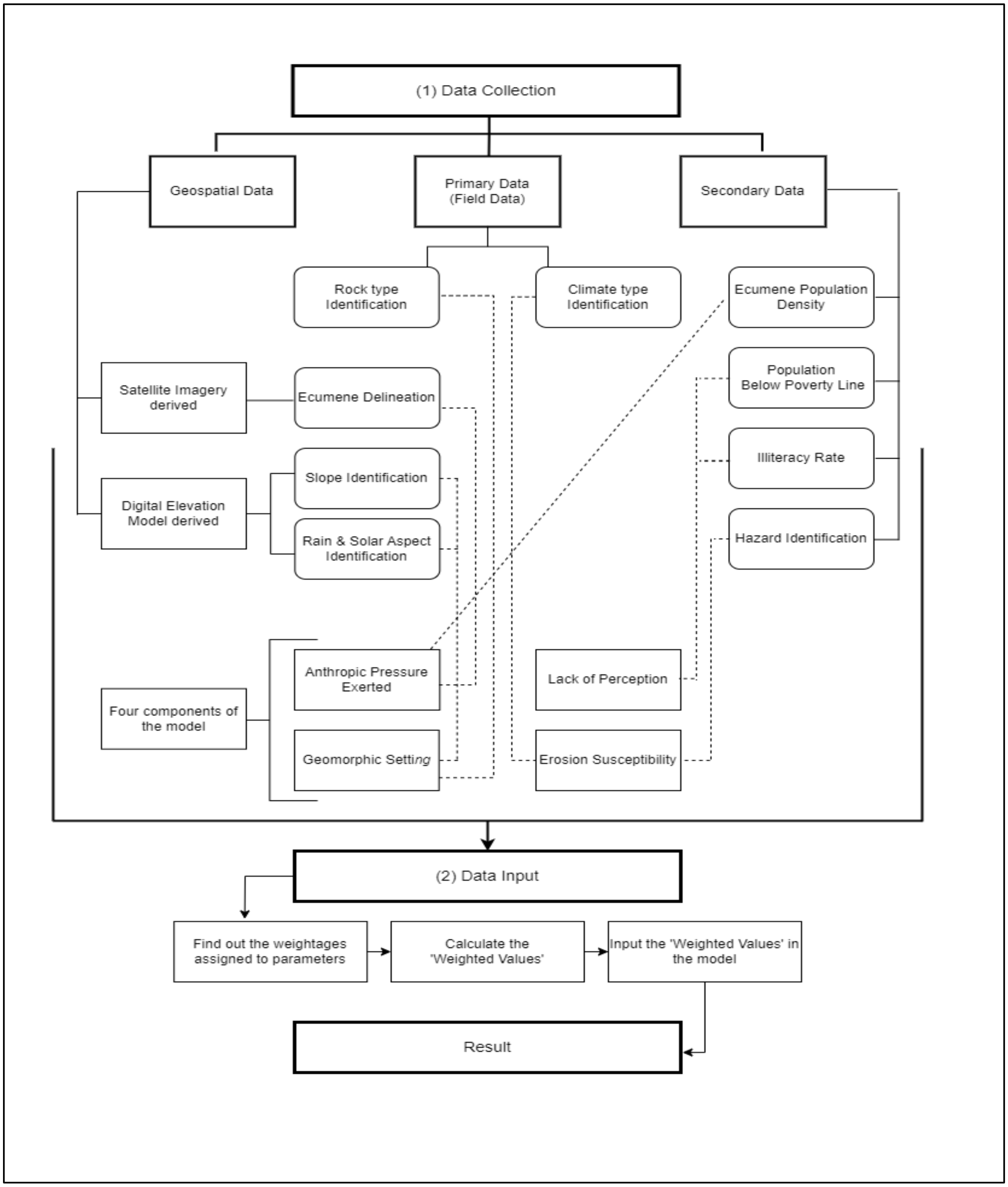

Fig-3.4 Flow Chart showing the Methodology of Multi-Temporal Anthropogeomorphic Impact Assessment Conducted using the Newly Postulated Model – Nigam-Kotha Model of Anthropogeomorphic Impact At Ecumene (AGI@E).

According to the newly postulated model "Nigam-Kotha model of Anthropogeomorphic Impact at Ecumene", also known as "AGI@E" - To quantify the impact of the Anthropogeomorphic Process (AGP), "The pressure of anthropogenic activities upon the geomorphic system is the product of the square roots of anthropic stress and the geomorphic susceptibility of the region".

3.3.1 Nigam-Kotha model of Anthropogeomorphic Impact at Ecumene (AGI@E) - Mathematical expression

Mathematically, AGI@E can be expressed as,

$$\text{AGI@E} = \sqrt{\frac{(2(a+b)+c+d)}{4}}\sqrt{\frac{(2(e+f+g+h)+i+j)}{6}} \qquad (1)$$

Which can further be divided into,

Amount of Anthropic Stress (AS) $= \sqrt{\frac{(2(a+b)+c+d)}{4}}$ (2)

Where,

Anthropic pressure (a & b) exerted is twice the intensity compared to the Lack of perception (c & d) in a given area and,

Amount of Erosive Susceptibility (ES) $= \sqrt{\frac{(2(e+f+g+h)+i+j)}{6}}$ (3)

Where,

Geomorphic Setting (e, f, g & h) in a given area is twice the resistance against Erosive driver (i & j).

Where,

a = Ecumene

b = Population Density

c = Illiteracy

d = Population below poverty line

e = Rock type

f = Slope

g = Aspect (Rain)

h = Aspect (Solar)

i = Climate

j = Hazard

Table-3.3 Data Sources of the Ten Parameters used in the Model AGI@E.

Parameter	**Category**	**Source**
Ecumene Area (a)	Anthropic pressure	Satellite Imagery
Population Density (b)	Anthropic pressure	Population Census
Illiteracy (in %) (c)	Lack of perception	Population Census
Population Below Poverty Line (In %) (d)	Lack of perception	Population Census
Rock Erodibility (e)	Geomorphic setting	Field Data
Slope (f)	Geomorphic setting	DEM & Field Survey
Rain Aspect (g)	Geomorphic setting	DEM & Field Survey
Solar Aspect (h)	Geomorphic setting	DEM & Field Survey
Climate (i)	Erosive Driver	Field Survey And Koppen Climatic Classification
Hazard (j)	Erosive Driver	Field Data & Hazard Inventory

Table-3.4 AGI@E Score Classification with Color Coding, According The Level of Impact

Degree of Anthropic Pressure & Degree of Erosive Susceptibility	
Score	**Level of Impact**
Below 5	Low Impact
5-10	Moderate Impact
10-20	High Impact
Above 20	Severe Impact
Anthropogeomorphic Impact at Ecumene (AGI@E)	
Score	**Level of Impact**
Below 50	Low Impact
50-100	Moderate Impact
100-200	High Impact
Above 200	Severe Impact

3.3.2 Analytical Hierarchy Process

The weightages of different parameters incorporated in the model AGI@E have been calculated by using the Analytical Hierarchy Process (AHP).

A multi-attribute evaluation method: AHP uses ‘pair-wise comparisons’ and matrix algebra to weigh criteria. The decision is made by using the derived weights of the evaluative criteria (Saaty, 1980). After the hierarchy of the problem is constructed, the matrices of pair-wise comparisons (Eq. (4)) are obtained. In this matrix, the element aij ¼ 1/aij and thus, when i ¼ j, aij ¼ 1. The value of wi may vary from 1 to 9, and 1/1 indicates equal importance while 9/1 indicates extreme or absolute importance (Saaty, 1980).

$$\begin{bmatrix} 1 & w1/w2 & \cdots & w1/n \\ w2/w1 & 1 & \cdots & w2/n \\ wn/w1 & wn/w2 & \cdots & 1 \end{bmatrix} \tag{4}$$

In the comparisons, some inconsistencies can be expected and accepted. When A contains inconsistencies, the estimated priorities can be obtained by using the matrix (Eq. (4)) as the input using the eigenvalue technique (Eq. (5)) (Saaty, 1980).

$$(A - \lambda maxI)q = 0 \tag{5}$$

where λmax is the largest eigenfactor of matrix A of size n; q, is its correct eigenfactor; and I is the identity matrix of size n. The correct eigenfactor, q, constitutes the estimation of relative priorities. Each eigenfactor is scaled to sum up to one to obtain the priorities. Saaty (1977) demonstrated that λmax ¼ n is a necessary and sufficient condition for consistency. Inconsistency may arise when λmax deviates from n due to inconsistent responses in pair-wise comparisons. Therefore, the matrix A should be tested for consistency using index, CI, has been constructed (Eq. (6)).

$$CI = (\lambda max - \mathrm{n}) \, (n - 1) \tag{6}$$

CI estimates the level of consistency with respect to a comparison matrix. Then, because CI is dependent on n, a consistency ratio CR is calculated, which is dependent of n (Eq. (7)) (Saaty, 1980).

$$CR = CI/RI \tag{7}$$

where CI is the consistency Index; RI is Random Index (RI) generated for a random matrix of order n, and CR is consistency ratio (Saaty, 1993). The general rule is that CR 0.1 should be maintained for the matrix to be consistent. Otherwise, all or some of the comparisons must be repeated in order to resolve the inconsistencies of the pair-wise comparisons.

3.3.3 AGI@E parameter weightages

- **Ecumene area (a)**

  - Steps to determine the amount of an ecumene area are as follow;

i. Carry out LULC classification of the study area.

ii. Demarcate the agriculture, built-up and mining regions (ecumene) in the study area.
iii. Find out the area (in sq. km) under these land use out of the total study area.
iv. Convert the values to percentage of the total study area to get the input value.

- **Population density of the study area (b)**

  - Population density of the city/village/state $= \frac{Total\ population}{Total\ area}$ (8)

- **Illiteracy (c)**

  - Illiteracy (in percentage) $= \frac{\text{Number of illiterates}}{\text{Total population}} \times 100$ (9)

- **Population below poverty line (d)**

  - BPL (in percentage) $= \frac{\text{Population below poverty line}}{\text{Total population}} \times 100$ (10)

- **Rock type (e)**

  - Steps to determine rock type weightage are as follow;

i. Determine the rock type present in the study area.
ii. Select the weightage according the rock present in the study area (Ecumene).
iii. If more than one rock type is present, then calculate the mean weightage of the available rock types to get the input value.

Table-3.5 Rock Erodibility Weightage.

Type of Rock	Level of Erodibility	Weightage
Acidic Plutonic, Metamorphic, Carbonate Sedimentary	Low	8.893
Acidic Volcanic	Low	9.493
Mixed Sedimentary	Low	9.681
Basic Plutonic, Siliciclastic Of All Grain Sizes	Medium	17.986
Basic Volcanic Rocks	Medium	18.786
All Unconsolidated Sediments	High	35.161

- **Slope (f)**
  - Steps to determine Slope input value:

i. Create a slope map of the ecumene area.
ii. Overlay the LULC map upon the slope map to determine the amount of different land use (only the built-up, agriculture and mining are considered to form an ecumene) (in sq. km) located in different slope range (Table-3.6).
iii. Convert the land use areas from sq. km to percentage under each of the slope range. For instance; 23% of ecumene located in the slope range of 1˚-5˚ and so forth.
iv. Multiply the area of ecumene (in percentage) under each slope range with the respective slope weightage. From the above example; 23% of ecumene located in the slope range of 1˚-5˚ will be 23 multiply by 5.806 and so forth.
v. Lastly, add the product values of all the slope range to determine the final slope value.

Table-3.6 Slope Range Weightage.

Slope Weightage	**Slope Range (in Degrees)**	**Slope Type**
5.680	<1	Level Slope
5.806	1-5	Gentle Slope
11.360	5-10	Moderate Slope
11.949	10-20	Steep Slope
22.720	20-40	Very Steep Slope
42.485	>40	Extremely Steep Slope

- **Aspect Rain (g) and Solar (h)**

  - Steps to determine Rain and Solar Aspect input value are as follow:

i. Create an aspect map of the ecumene area.
ii. Find out which aspect direction having maximum of ecumene of the study area.
iii. Determine the windward and leeward sides of the ecumene with respect to rain and sunlight.
iv. Determine where the 'aspect direction having maximum amount of ecumene' is located, windward side or leeward side.
v. Select one of the types of rain aspect (from table-4) where the majority of ecumene is located.
vi. Repeat (Step-v) for the solar aspect as well.
vii. Put the selected aspect values of rain and solar into the AGI@E equation.

For instance: a case study (see chapter-5, results), Southwest direction has the maximum ecumene amount. Additionally, southwest is also the windward side in the study area. Therefore, the predominantly windward side category's weightage (25.954) is chosen for rain aspect. Similarly, weightage (25.954) is selected as solar weightage because coastal south goa lies in northern hemisphere, facing south (Table-3.7).

Table-3.7 Rain and Solar Aspect weightages

Rain Aspect Weightage	**W.R.T Rainfall (Chemical Weathering)**	**Solar Aspect Weightage**	**W.R.T. Sunlight (High/Low Sun) (Exfoliation Weathering)**
5.933	Predominantly Leeward Side, If >80% Facing	5.933	North Facing(In N. Hemisphere) South Facing (In S. Hemisphere)
6.192	Partially Leeward Side, If >50% Facing	6.192	Partially North Facing (In N. Hemisphere) Partially South Facing (In S. Hemisphere)
12.384	Partially Windward Side, If >50% Facing	12.384	Partially South Facing (In N. Hemisphere) Partially North Facing (In S. Hemisphere)
25.954	Predominantly Windward Side, If >80% Facing	25.954	South Facing (In N. Hemisphere) North Facing (In S. Hemisphere)
49.537	Negligible Slope = No Aspect = Maximum Exposure	49.537	Negligible Slope = No Aspect = Maximum Exposure

- **Climate (i)**

  - Steps to determine climate weightage:

i. Determine the climatic type (Koppen climate classification, see Acronyms for more details) of the study area.
ii. Select the weightage of the suitable climatic type from (Table-3.8).
iii. Put the weightage value in the model AGI@E equation.

Table-3.8 Climate weightages.

(Note- Consider the mean of the climatic weightages, if more than one climate type is present in the study area).

Climate Type	Weightage	Sub-Category	Weightage
Tropical	52.086	Aw Or As	7.440
		Am	14.880
		Af	29.760
Dry	5.928	BW	1.187
		BS	4.743
Temperate	24.290	CS	3.471
		CW	6.939
		CF	13.879
Continental	11.625	DS	1.660
		DW	3.319
		DF	6.669
Polar	6.072	EF	2.023
		ET	4.046

- **Hazard (j)** ***(According to their severity)***
  - Steps to determine hazard weightage are as follow;

i. If more than one type of geomorphic hazard is present/suspected in the study area, Calculate the sum of the hazards from (Table-3.9) and put the weightage into the model AGI@E equation.

ii. If only one type of geomorphic hazard is present, then select a single hazard weightage from the (Table-3.9).

Table-3.9 Geomorphic hazard weightages

Hazard Type	Weightage	Sub-category	Weightage
Wildfire	2.10	NA	NA
Drought	2.13	NA	NA
Thunderstorm	2.24	NA	NA
Blizzard	2.31	NA	NA
Avalanche	2.74	NA	NA
Cyclone	3.50	NA	NA
Sink Hole	5.65	NA	NA
Land Subsidence	6.05	NA	NA
Landslide	6.05	NA	NA

Flood	6.74	NA	NA
Sea Level Rise	7.44	NA	NA
GLOF	9.69	NA	NA
Tsunami	10.14	NA	NA
Earthquake		<MSK-VI (1),	1.108
		MSK-VII (3)	2.215
		MSK-VIII (4)	4.432
		>MSK-IX (8)	8.863
Volcanic Eruption	16.90	NA	NA

3.3.4 Ground Trothing – Soil Erosion Assessment using Revised Universal Soil Erosion Equation (RUSLE) Model.

- Data Input

- The required geospatial datasets such as precipitation, soil, land cover, topography, and slope were imported into Google Earth Engine. These datasets were acquired from reputable sources and were preprocessed to ensure compatibility with the Earth Engine platform.
- The imported datasets were organized into Earth Engine Image Collections. This step involved structuring the data to create a foundation for subsequent calculations.

- Calculation of RUSLE Factors

- Rainfall Factor (R): It is a critical component of the RUSLE model, was calculated by employing long-term precipitation data obtained from the Earth Engine dataset collection. This involved utilizing methods like the Fournier Index or the Modified Fournier Index to accurately estimate patterns of rainfall erosivity in the study area.
- Soil Erodibility Factor (K): This was determined by analysing soil properties such as texture, organic matter content, permeability, and other soil characteristics. High-resolution soil datasets were accessed within Google Earth Engine repository to derive these parameters.
- Slope Length and Gradient (LS): Accurate calculations of the slope length and gradient factor (LS) are crucial. Utilizing SRTM 30m digital elevation models (DEMs) available in Earth Engine, slope and flow accumulation were computed. This allowed for the derivation of LS values, considering both the length and steepness of slopes.
- Cover Management Factor (C): The cover and management factor (C) was assessed by integrating land cover classification datasets available in Google Earth Engine. These

datasets captured information on various land cover types, vegetation density, and land management practices, which significantly influence soil erosion rates.

- Support Practices Factor (P): The support practices factor (P), encompassing conservation practices such as terracing, contour farming, and other soil conservation measures, was examined. This involved incorporating additional datasets or field-based information to quantify the influence of support practices on soil loss.

Table- 3.10 Data used in the soil erosion assessment in the study area.

Period Jan-1-2001 to Dec-31-2001 Jan-1-2020 to Dec-31-2020	 Landsat-5 MSS, L-2, Collection-2, Tier-2 Sentinel-2, Multi-Spectral Instrument, L-2
Datasets Rainfall Soil DEM	 CHIRPS Open Land Map SRTM 30m
Classification	Priority Scale for Classification

- RUSLE Calculation

With the computed values of R, K, LS, C, and P in place, the Revised Universal Soil Loss Equation (RUSLE) was applied to estimate soil erosion rates at each spatial location within the study area. The RUSLE equation used for this estimation was as follows:

$$\text{Erosion } (A) = R * K * LS * C * P \tag{11}$$

- Soil Erosion Mapping

The results of the RUSLE calculations were visually using Google Earth Engine. Maps and statistics are created to describe and validate the spatial distribution of estimated soil erosion rates. These visualizations enabled a clear understanding of the erosion risk in the study area.

- Validation and Accuracy Assessment

Validation of the model was a critical step. To evaluate the accuracy of the RUSLE-derived erosion rates, a thorough comparison was made with ground truth data and other reliable sources of erosion information. Statistical measures, including the Root Mean Square Error (RMSE) was computed to assess the model's performance and provide insights into its reliability.

3.4 Multi-Temporal Beach Litter Assessment

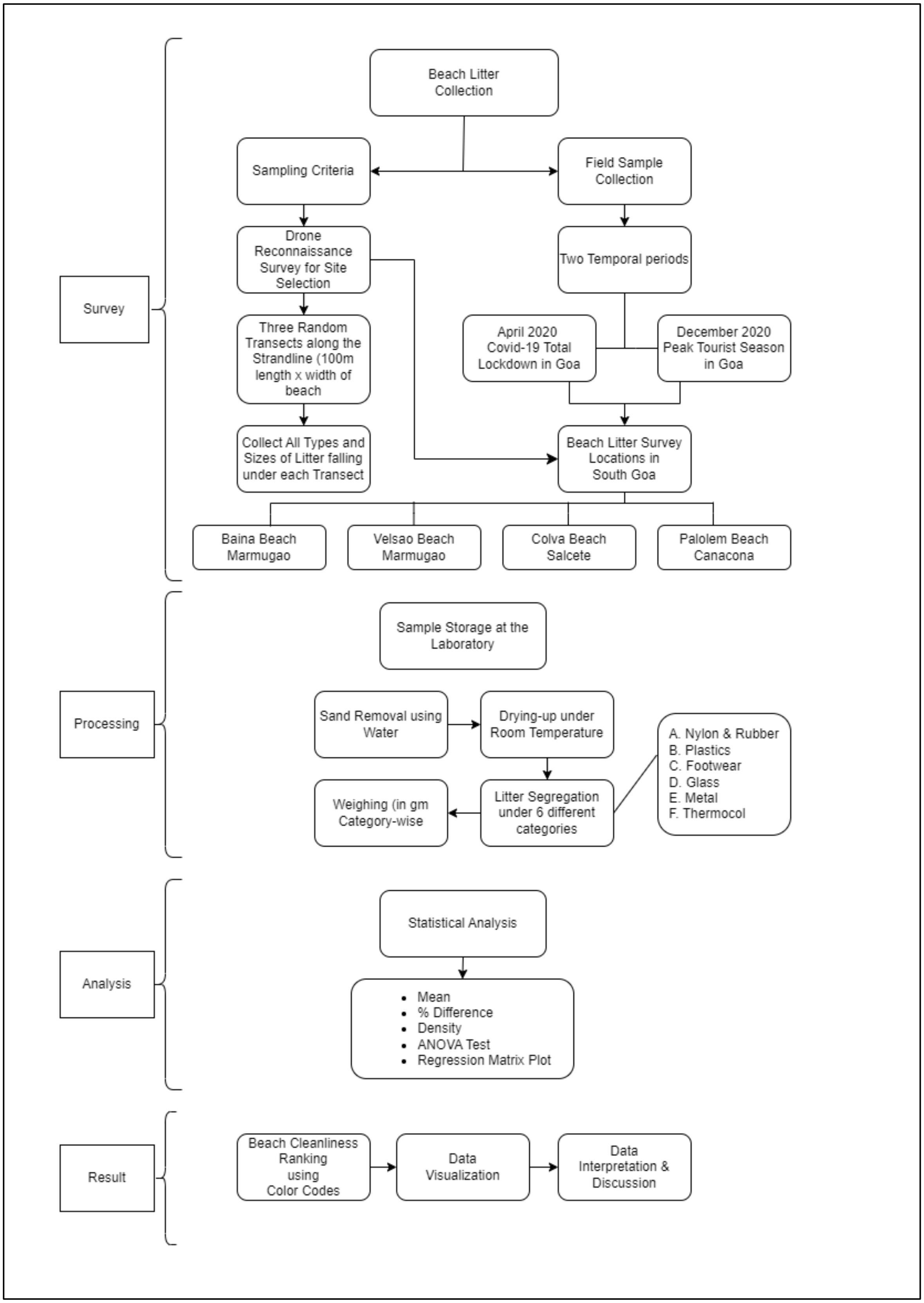

Fig-3.5 Flowchart of the methodology of Multi-Temporal Beach Litter Assessment.

There are several methods to collect beach litter samples for its status and composition assessments; however, the present study has adopted the Oslo and Paris Commission (OSPAR) methodology. The OSPAR Commission has a standardized methodology implemented in the North-east Atlantic region by the member countries, which was also adopted by researchers worldwide. The OSPAR led conditions were largely followed in the present beach litter surveys that include that all the four selected beaches are composed of fine sand and exposed to the open sea, more than 1 km in length, easily accessible for surveying year around; and are easily accessible to remove/collect beach litter. However, the two conditions (free of buildings, no litter collection by any agency) of OSPAR methodology could not be applied in the present study area, as the coastline is dotted with several beachfront resorts and seasonal beach shacks (which are generally considered as the prime factor of beach littering hence, collection agencies are active).

For the categorization and assignment of separate IDs for each litter particle type, slightly deviated method is followed as adopted in Kaladharan et al. (2017), that has enabled the present study to compare the results with a previous study conducted by Kaladharan et al. (2017). The initial aerial surveys using UAV for reconnaissance of study area helped us to select the suitable beaches and sites data collection during lockdown phase, as the entry to the beaches was restricted due to COVID-19 lockdown restrictions.

Each sampling transect was demarcated by creating a transect quadrant by taking a length of 100 m (parallel to the sea, at the low tide line) from the permanent reference point and the beach width (perpendicularly between the low tide line and the first plants behind the beach). Permanent reference points were marked using permanent building structures (such as; resort boundaries, electric poles, etc.) and GPS coordinates to ensure the next survey visit should collect the samples from a similar site. As each of the selected beaches is more than 1 km long, three different sampling transects were demarcated at each of the four beaches to collect the samples (in total, 12 transects). All the three transects on each beach had more than 100 m distance between them. Arrangements were made with the beach cleaning agency to provide their cleaning schedule, so surveying was carried out before the cleaning schedule. The litter samples were transported to the collection site, and the details of samples which could not be transported in their quantity were noted down.

Additionally, expert comments regarding the status of the litter transects and local anthropogenic settings (tourism infrastructure, crowd, dustbin locations, litter spread, etc.) were also noted down on-site. Transported samples were washed with fresh water to remove sand and unwanted organic material. Later, the samples were kept overnight under the fan to evaporate the moisture content and later differentiated into six different categories (loosely based upon Kaladharan et al., 2017), as given in Table 3.10.

Later on, each litter category was weighed separately using a top pan balance to know the relative weight and recorded as gm/transect.

Table-3.11 Categorization of Beach Litter.

Categories	Material
A	Nylon ropes and Rubber – part of fishing gear
B	Plastic (polyethylene bags, sachets, snack boxes, bottles, etc.)
C	Footwear (other than leather items)
D	Glass (liquor bottles, liquor drinking glass, and bulbs)
E	Metal (items containing a significant amount of any metal)
F	Thermocol (related packaging products)

First of all, the data was processed to determine litter quantity at each beach. Later, the entire litter was converted to a percentage to determine each litter category's share at each beach during different periods. Further, the relative litter weight was converted to g/m^2 by calculating the mean of beach litter quantity;

$$\frac{Total\ amount\ of\ litter\ at\ a\ beach\ (g)}{/Total\ area\ of\ all\ three\ transects\ \ (m^2)} \qquad (1)$$

$Total\ amount\ of\ litter\ at\ a\ beach\ (g)/Total\ area\ of\ all\ three\ transects\ \ (m2)$ (1)

Similarly, the Per capita share of beach litter was also calculated by;

$$\frac{The\ total\ amount\ of\ litter\ at\ a\ beach\ (g)}{/Total\ beach\ village\ population\ (counts)} \qquad (2)$$

$The\ total\ amount\ of\ litter\ at\ a\ beach\ (g)/Total\ beach\ village\ population\ (counts)$ (2)

Later, variations in litter amount in January 2021 and May 2020 was calculated as the percentage difference between the two;

$$\frac{V1-V0}{V0}\times 100, \qquad (3)$$

where, V1 = January 2021, V0 = May 2020.

In addition, six color codes were allocated to grade the studied beaches based on the mean quantity of beach litter found by following the literature (Kaladharan et al., 2017) (Fig.-3.6).

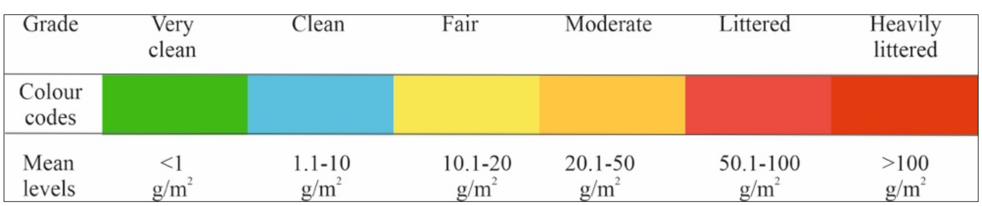

Fig- 3.6 Beach Color-Coding Scale (Adopted from Kaladharan et al., 2017).

Lastly, inferential statistical method Analysis of Variance (ANOVA) was computed using the statistical software, to determine the share of each of the litter categories during lockdown and unlock period.

3.5 Multi-Temporal Air Quality Analysis

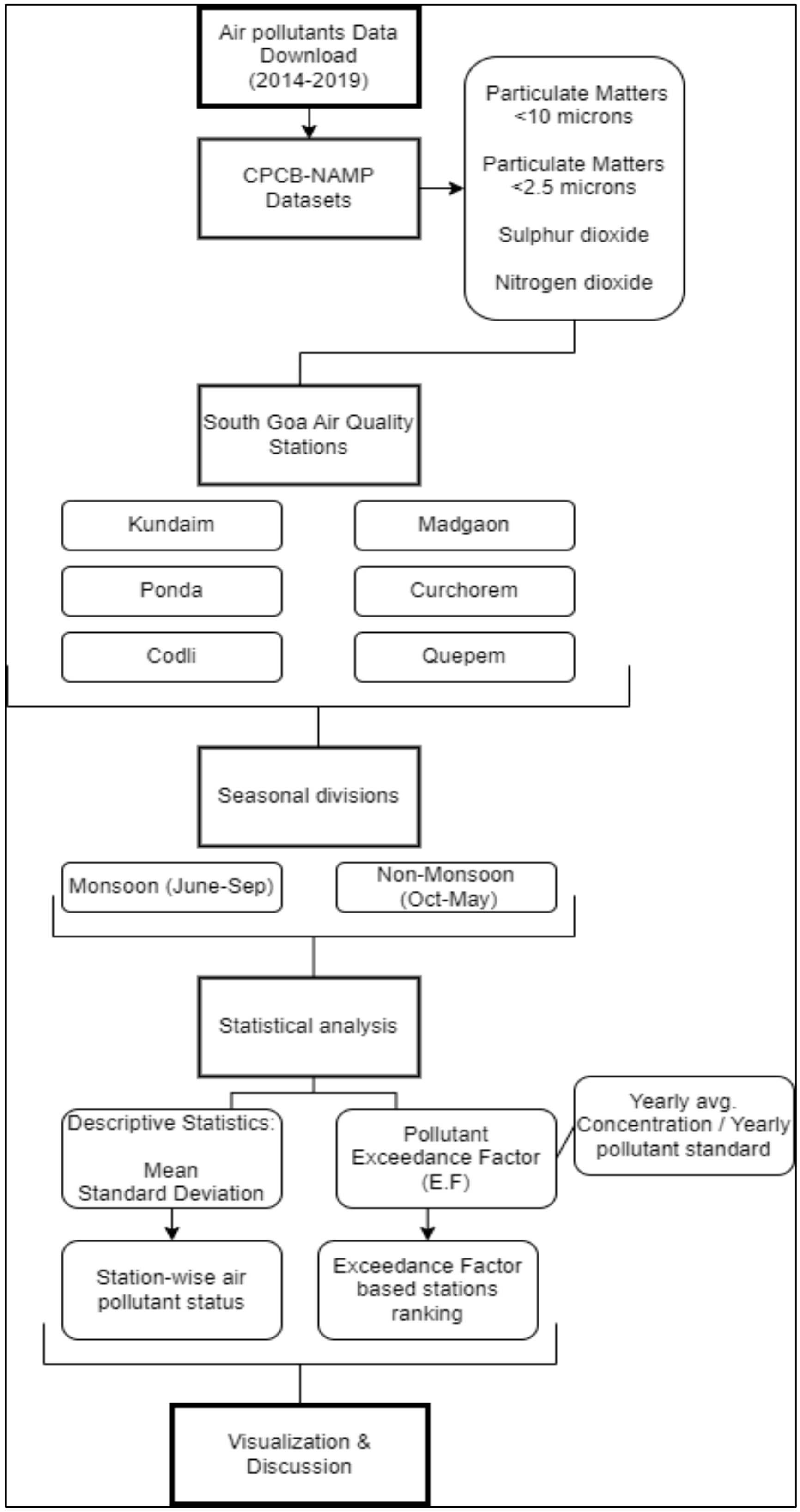

Fig- 3.7 Flowchart of the methodology of multi-temporal air quality analysis

The present study has broadly adopted the methodology given by Nigam and others (2021) in which the assessment was conducted based on the Central Pollution Control Broad (CPCB), NAMP datasets. In the present study, seven-year monthly air pollutant data (SO_2, $PM_{2.5}$ and PM_{10}) for eight different stations were downloaded from the Goa State Pollution Control Board (GSPCB) portal (http://goaspcb.gov.in/). The GSPCB provides pollutant data only from the manual monitoring network, due to which only the SO_2, $PM_{2.5,}$ and PM_{10} pollutant data were available.

Rainfall during the monsoon season in Goa plays a significant role in supporting agriculture, recharging groundwater, and influencing socio-economic conditions.

Yearly concentrations of $PM_{10,}$ $PM_{2.5,}$ SO_2 and NO_2 were downloaded from the GSPCB website for the year 2014 to 2020. Later, to separately determine the impact of weather on the pollutant concentrations, each year was assessed for two seasons: monsoon (June to September) and post-monsoon (October to May of the succeeding year).

The descriptive and inferential statistical methods consisting of mean, standard deviation, and mean difference in percentage were employed to perform the meta-analysis of continuous data.

The mean value of monthly data was computed to determine the annual mean values of each pollutant for each of the 7-year.

$$Mean = \frac{Xi}{N} \quad (1)$$

where X_i is the sum of the monthly pollutant value in a year and N is the total number of months in the year.

The standard deviation was computed to determine variation in the pollutant's concentration from its annual mean value.

$$Standard\ deviation\ \text{(SD)} = \sqrt{\frac{\Sigma(X\text{i}-\mu)^2}{N}} \quad (2)$$

where X_i is the monthly pollutant value in the year, μ is the mean pollutant value of a year and N is the total number of months in the season. For example, N=4 for monsoon, and N=8 for post-monsoon.

Further, the present study has also applied a method formulated by the CPCB, the EF of the air pollutants. EF is the "proportion of the yearly average concentration of a pollutant and its particular standard" (Haque and Singh, 2017). In other words, it is applied to show the intensity and the status of air quality at a particular place in comparison to annual standards of the pollutants given by the CPCB.

$$\boldsymbol{EF} = \frac{\text{Yearly average concentration of the pollutant}}{\text{Yearly standard for that particular pollutant}} \quad (3)$$

Based on equation (3), the air pollution levels can be categorized into four classes as follows. EF < 0.5: Low pollution; EF between 0.51-0.99: Moderate pollution (M); EF between 1 – 1.5: High pollution (H); and EF> 1.5: Critical pollution (C).

The meteorological data consisting of rainfall, maximum (T_{max}) and minimum (T_{min}) temperature was obtained from https://www.worldweatheronline.com.

3.6 Multi-Temporal Sea Level Rise Inundation Assessment

3.6.1 Data Collection

The present research has applied a modified version of the "bathtub" model (BTM), which includes considerations for the eight-sided hydrological connectivity (HC) instead of four-sided hydrological connectivity. HC refers to the way water flows across the landscape. There are two HC rules, Four-sided Rule: A grid cell in the DEM is considered hydrologically connected if any of its four cardinal directions (north, south, east, west) are connected to a flooded cell. Eight-sided Rule: Connectivity is considered in both cardinal and diagonal directions.

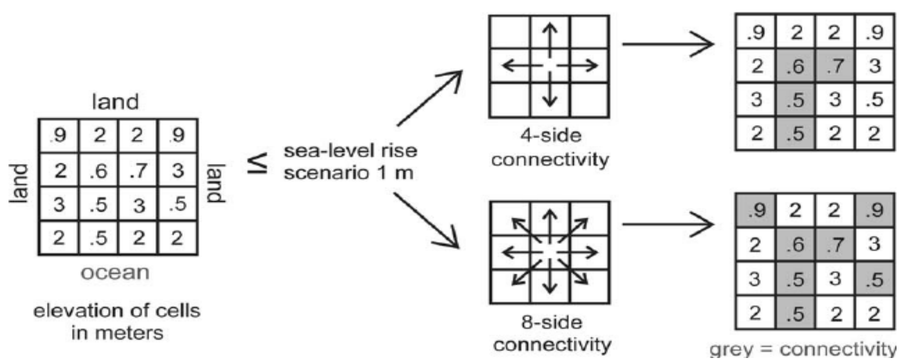

Fig-3.8 Showing the difference between a four side connectivity and eight side connectivity (Source: Sirianni et al., 2013)

The four-sided rule has the potential to underestimate coastal flooding impacts, while the “eight-sided” rule may have the potential to overestimate those impacts. Thus, going by this logic, the study chose the “eight-sided” rule simply because for planning purposes overestimation is usually more acceptable.

A medium resolution 30-meter SRTM DEM was downloaded from the NASA Earth Explorer to provide the elevation data for the study area to conduct hydrological modelling.

3.6.2 Creation of Sea Level Rise inundation scenarios

The study has postulated fourteen different plausible sea level rise inundation scenarios comprising of different coastal hazards, such as the SLR, storm surge, Higher High Water at Spring (HHWS) and Mean Higher High Water (MHHW) based on the estimates given by the IPCC and the Marmugao Port Trust (MPT). These water levels represent a range of plausible inundation scenarios for future sea-level rise and coastal hazards. They serve as a basis for modeling and assessing the extent of potential inundation.

Table- 3.12 Data Sources for Creating Plausible Sea Level Rise Inundation Scenarios.

Permanent Flooding			
AR6 SSP1 1.9 (Upper Limit)	0.59m (With 17-83% Confidence)	Best Case Scenario / Optimum	IPCC AR6
AR6 SSP5 8.5 (Upper Limit)	1.02m (With 17-83% Confidence)	Medium Case Scenario / Medium	IPCC AR6
AR6 SSP5 8.5 (Upper Limit)	1.61m (Low Confidence, .>17%)	Worst Case Scenario / Business As Usual	IPCC AR6
MHHW	0.6m	Embedded	Marmugao Port Trust
Episodic Flooding			
Storm Surge	4.5m	Episodic Flood	BMTPC, 2019
Higher High Water At Spring (HHWS)	1m	Episodic Flood	Marmugao Port Trust

Table-3.13 A Total of 14 Plausible Sea Level Rise inundation scenarios.

Scenarios	S No.	Compounding Factors	Elevation (in m)	Cumulative (in m)
Only SLR	1	SSP-1 + MHHW	0.55 + 0.6	1.15
	2	SSP-5 + MHHW	1.02 + 0.6	1.62
	3	SSP-5 (L) + MHHW	1.61 + 0.6	2.21
SLR + Highest High Spring Tide	4	SSP-1 + HHWS	0.55 + 1	1.55
	5	SSP-5 + HHWS	1.02 + 1	2.02
	6	SSP-5 (L) +HHWS	1.61 + 1	2.61
SLR + Storm Surge	7	SSP-1 + MHHW +SS	0.55 + 0.6 + 4.5	5.65
	8	SSP-5 + MHHW +SS	1.02 + 0.6 + 4.5	6.12
	9	SSP-5 (L) + MHHW +SS	1.61 + 0.6 + 4.5	6.71
	10	SSP-1 + HHWS + SS	0.55 + 1 + 4.5	6.05

SLR + Spring Tide + Storm Surge	11	SSP-5 + HHWS + SS	1.02 + 1 + 4.5	6.52
	12	SSP-5 (L) + HHWS + SS	1.61 + 1 + 4.5	7.11
Without SLR	13	MHHW + SS	0.6 + 4.5	5.1
	14	HHWS + SS	1 + 4.5	5.5

3.6.3 Inundation Modeling

The study used hydrological modeling techniques, particularly the BTM, to simulate how different scenarios of inundation (SLR, storm surge, etc.) would affect the study area. For each scenario, the relevant water level was subtracted from the DEM, and the chosen HC rule was applied. This process determined which areas would be considered inundated under each scenario. The inundation modelling was processed in the geo-processing environment of ESRI's ArcGIS 10.2.

Mean Higher High Water (MHHW) level of the study area was selected as the reference surface water level. MHHW represents the average higher high tide level, which serves as a starting point for assessing the potential impact of sea-level rise.

3.6.4 Inundation Mapping

After running the hydrological model for each scenario, the study generated inundation maps. These maps represent the areas that would be inundated under the water during coastal flooding under specific conditions. In total, 20 SLR inundation maps were generated (five each for a taluka), comprising of different clusters of inundation scenarios.

3.6.5 Comparison of Inundation Maps with LULC Maps

The inundation maps were further analyzed by overlaying them on the topographical maps and side-wise comparison with the LULC maps of the study area. This integration allowed the study to identify and assess which specific land use and land cover types would be impacted by coastal inundation under different scenarios. This information is crucial for understanding potential socio-economic and ecological consequences.

3.6.6 Analysis and Discussion

The study used the combined information from inundation maps, DEM data, HC rules, and LULC maps to conduct a detailed analysis, more robust than usual bathtub inundation modeling The resultant maps identify vulnerable areas and 'future hazard zones' in the study area, which are essential for coastal planning and management.

3.7 Coastal Vulnerability Index

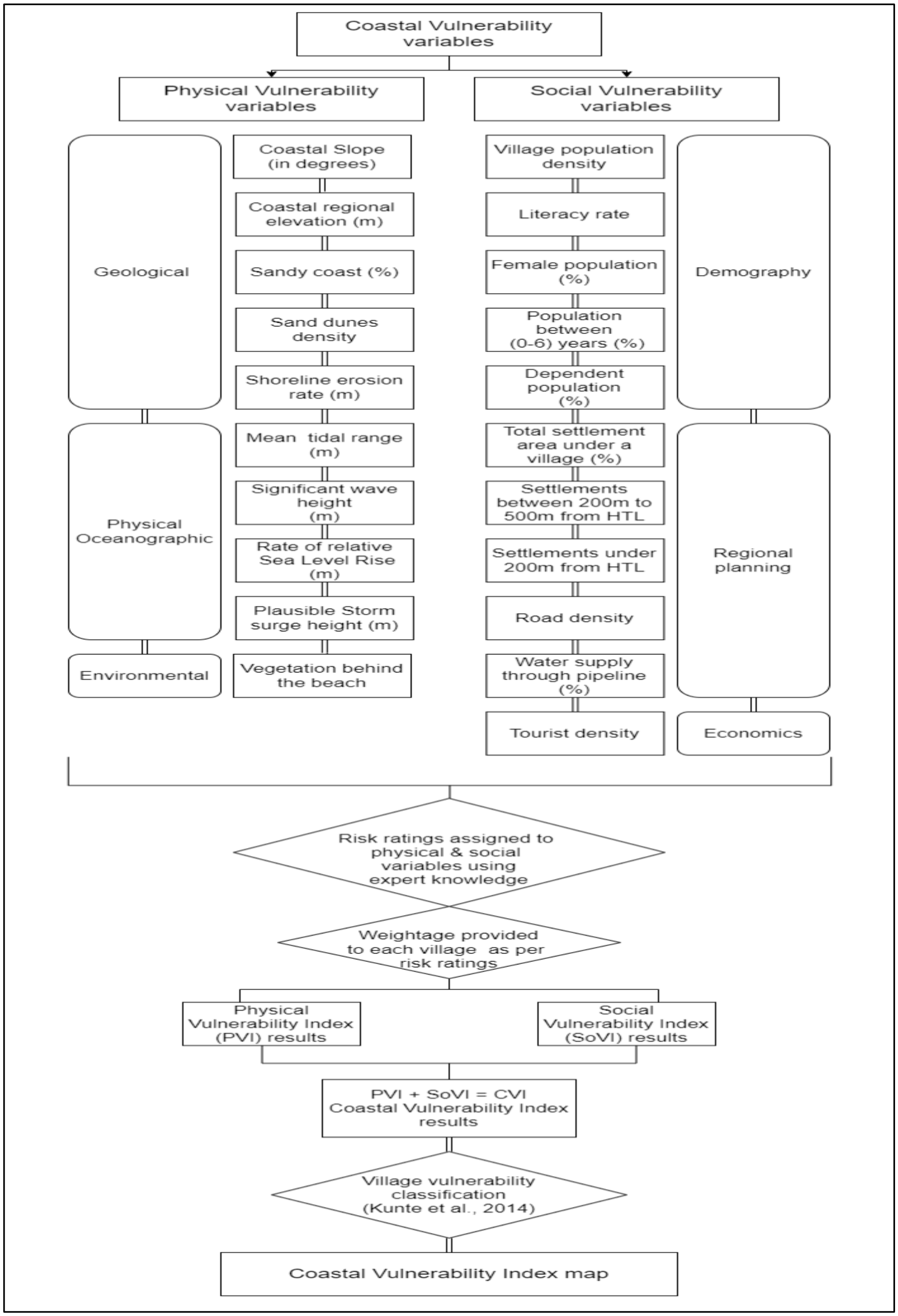

Fig-3.9 Flowchart of the Methodology of Coastal Vulnerability Index.

This assessment uses a modified version of the CVI methodology first published by the United States Geological Survey (USGS) (Thieler and Hammer-Klose, 1999, Thieler and Hammer-Klose, 2000b, Thieler and Hammer-Klose, 2000a), which assesses coastal vulnerability on the basis of six physical and geological variables.

In the current study, a Physical Vulnerability Index (PVI) is computed using 10 variables, including the six variables from the original USGS index, i.e.: rate of relative sea-level change, rate of shoreline change (erosion or accretion), mean tidal range, significant wave height, coastal slope and geomorphology, plus coastal regional elevation and other variables that have not yet been incorporated in CVI along the coast of India, that is percentage of sandy coast, sand dune density and vegetation behind the beach, or their use has yet been limited: plausible storm surge height. These latter thee variables were added because local morphological factors and vegetation can influence the degree of vulnerability.

The SoVI, for its part, comprises 11 social variables; Village population density, Road density, Total settlement area under village (%), Water supply through pipeline (%), Literacy rate (%), Dependent population (%), Female population (%), Population between (0-6 years) %, Tourist density, Settlement area under 500m HTL and Settlement area under 200m HTL.

Different methods are used to determine the values of the variables to comprising an index. The USGS methodology (Thieler and Hammer-Klose, 1999, Thieler and Hammer-Klose, 2000b, Thieler and Hammer-Klose, 2000a) consists of ranking each variable on an ordinal scale from one to five. Most studies, worldwide, have followed this ranking procedure but without necessarily using the same range for the ranking of the risk variables as no standards exist to determine what values should be considered as low, medium, or high when a three-category scale is used, for instance, nor is it the case when five ranking categories are used. Boruff et al. (2005), following the USGS methodology, ranked the variables as low, moderate, and high, while Kumar and Kunte (2012) classified the coastline of Chennai into three vulnerability categories. Likewise, this study has followed a linear scale from 1-3 to increase vulnerability from low to moderate to high (Table 2). With the help of expert knowledge, all the 21 variables were weighted accordingly (Table 3). Weightage score of 3 physical variables (rate of relative SLR, mean tidal range, and significant wave) is taken from Kunte et al. (2014) as changes in those variables along South Goa coastline are absent. Sand-dune density and Vegetation behind the beach along the study area’s coastline were ranked qualitatively based on the field observations taken by experts.

Table-3.14 Risk Ratings Assigned to 10 Physical Variables.

S. No.	Physical Variables	Low (1)	Medium (2)	High (3)
1	Coastal Slope (Degree)	>0.3	0.1-0.3	<0.1

2	Coastal Regional Elevation (M)	>50	20-50	<20
3	Sandy Coast (%)	<10	10-20	>20
4	Sand Dune Density	Rocky Coast, Low	Moderate	Sparse
5	Vegetation Behind The Beach	Dense	Moderate	Sparse
6	Rate Of Relative Slr (M)	--	1.29	--
7	Shoreline Erosion Rate (M)	<0.3	0.3-0.5	>0.5
8	Mean Tidal Range (M)	--	0.2-2.4	--
9	Significant Wave Height (M)	--	0.6-2.0	--
10	Plausible Storm Surge Height (M)	--	--	4.5

Table-3.15 Risk Ratings Assigned to 11 Social Variables.

S. No.	Social Variables	Low (1)	Medium (2)	High (3)
1	Village Population Density	<100	100-200	>200
2	Road Density	>100	50-100	<50
3	Total Settlement Area Under Village (%)	<15	15-30	>30
4	Water Supply Through Pipeline (%)	>80	40-80	<40
5	Literacy Rate (%)	>80	75-80	<75
6	Dependent Population (%)	<30	30-60	>60
7	Female Population (%)	<30	30-60	>60
8	Population Between (0-6) Years	<5	5-10	>10
9	Tourist Density (Person/Sq. Km)	<100	100-200	>200
10	Settlements Under 500m Htl (%)	<10	10-20	>20
11	Settlements Under 200m Htl (%)	-	-	>5

Table-3.16 Physical Variable Weightage Employed to Calculate the Physical Vulnerability Index in the Study Area.

Parameters	Vasco da Gama	Chicolna	Issorcim	Sancoale	Pale	Velsao	Cansaulim	Arrosim	Utorda
Dune Density	1	2	2	1	3	3	3	3	2
% of Sandy coast	2	2	2	1	3	3	3	3	3
Vegetation Behind	1	2	2	1	1	2	3	2	2
Historical rate of Shoreline	2	2	2	1	1	1	1	1	1
Coastal slope (Degrees)	3	3	3	3	3	3	3	3	3
Coastal Regional	2	2	1	1	3	3	3	3	3
Rate of relative	2	2	2	2	2	2	2	2	2
Mean Tidal	2	2	2	2	2	2	2	2	2
Significant Wave	2	2	2	2	2	2	2	2	2
Plausible Storm surge	3	3	3	3	3	3	3	3	3

Loutolim	Verna	Quellosim	Cortalim	Cavellosim	Varca	Benaulim	Sernabatim	Colva	Betalbatim	Gonsua	Majorda
3	3	3	3	1	1	2	1	3	1	3	2
3	3	3	3	3	3	3	3	3	3	3	3
2	3	3	3	2	2	3	3	3	2	2	2
1	1	1	1	2	2	1	1	1	1	1	1
2	1	2	2	3	3	3	3	3	3	3	3
3	2	3	3	3	3	3	3	3	3	3	3
2	2	2	2	2	2	2	2	2	2	2	2
2	2	2	2	2	2	2	2	2	2	2	2
2	2	2	2	2	2	2	2	2	2	2	2
3	3	3	3	3	3	3	3	3	3	3	3

Nagarcem-Chaudi	Agonda	Cola	Naquerim	Quitol	Curchorem	Chandor	Macasana	Curtorim	Raia	Rachol	Camurlim
3	3	3	1	1	3	3	3	3	3	3	3
3	2	2	1	1	3	3	3	3	3	3	3
3	3	2	1	1	2	1	1	2	2	2	3
2	2	1	1	1	1	1	1	1	1	1	1
3	3	3	3	3	1	2	1	1	2	3	2
3	3	2	1	1	3	3	3	3	3	3	3
2	2	2	2	2	2	2	2	2	2	2	2
2	2	2	2	2	2	2	2	2	2	2	2
2	2	2	2	2	2	2	2	2	2	2	2
3	3	3	3	3	3	3	3	3	3	3	3

Lolie m	Poinguini m
2	2
1	3
1	2
1	1
3	3
2	3
2	2
2	2
2	2
3	3

Table-3.17 Social Variable Weightage Employed to Calculate the Social Vulnerability Index in the Study Area.

Parameters	**Vasco da Gama**	**Chicol na**	**Issorcim**	**Sancoale**	**Pal e**	**Velsa o**
Tourist Density Person/sq. km	3	2	2	2	1	1
Village Population Density	3	3	3	3	3	3
Road Density	2	3	2	2	2	2
Population Under 6 Years	3	3	2	3	3	3
Literacy rate in %	1	2	2	2	1	1
Dependent Population In %	3	3	2	2	3	3
Water supply through Pipeline	1	1	1	1	1	1
Female Population in %	2	2	2	2	2	2
% of Settlement area under Village	3	3	3	3	3	3
% of Settlement under 500m from HTL	3	3	3	3	3	3
% of Settlement under 200m from HTL	3	2	3	2	3	3

Cortali	Cavellosim	Varca	Benaulim	Sernabatim	Colva	Betalbatim	Gonsua	Majorda	Utorda	Arrosim	Cansaulim
1	3	3	2	3	3	2	1	1	2	1	1
3	3	3	3	3	3	3	3	3	3	3	3
2	3	1	1	1	1	2	2	1	2	2	2
2	2	3	3	3	2	3	3	3	2	3	2
1	1	1	1	2	2	1	1	1	1	2	1
2	2	3	3	3	3	3	3	3	3	1	3
1	1	1	1	1	1	1	1	1	1	1	1
2	2	2	2	2	2	2	2	2	2	2	2
2	3	3	3	2	3	3	2	3	3	3	3
1	3	3	2	1	2	2	2	2	2	3	3
3	1	1	2	1	3	2	1	1	1	1	1

Cola	Naquerim	Quitol	Curchorem	Chandor	Macasana	Curtorim	Raia	Rachol	Camurlim	Loutolim	Verna	Quellosim
2	1	1	1	1	1	1	1	2	1	1	1	1
2	3	3	3	1	1	1	1	1	1	3	3	3
3	3	3	1	1	3	1	2	3	2	2	1	3
3	3	3	3	3	3	3	3	2	2	2	2	3
2	3	2	1	1	1	1	1	1	1	1	1	1
2	3	3	3	3	3	3	3	3	3	3	3	2
1	1	1	1	1	1	1	1	1	1	1	1	1
2	2	2	2	2	2	2	2	2	2	2	2	2
1	1	1	3	2	2	3	3	2	3	2	3	2
3	1	1	1	1	1	1	1	1	1	1	1	1
1	1	1	2	1	1	1	1	3	2	2	1	3

Parameters	Loliem	Poinguinim	Nagarcem-chaudi	Agonda
Tourist Density Person/sq. km	1	1	3	3
Village Population Density	2	2	2	3
Road Density	3	2	2	2
Population Under 6 Years	2	2	3	3
Literacy rate in %	1	2	2	2
Dependent Population	2	3	2	3
Water supply through	1	1	1	1
Female Population in %	2	2	2	2
% of Settlement area	1	1	2	3
% of Settlement under 500m from	1	3	3	2
% of Settlement under 200m from	1	2	3	2

The PVI and SoVI were calculated as the squared root of the product of the ranked variables divided by the number of variables as described in USGS (1999):

$$PVI = \sqrt{a1 * b1 * c1 * d1 * e1 * f1 * g1 * h1 * i1 * j1 / 10} \quad (1)$$

where a_1 = coastal slope, b_1 = Coastal regional elevation, refer to the geological variables, and represent the physical process variables. c1= Percentage of sandy coast, d1 = sand dunes density, e1 = vegetation density behind the beach, f1 = Rate of relative SLR, g1 = Shoreline erosion rate, h1 = mean tidal range, i1 = significant wave height, j1 = Plausible storm surge height.

$$\text{SoVI}= \sqrt{a2 * b2 * c2 * d2 * e2 * f2 * g2 * h2 * i2 * k2/11} \quad (2)$$

11 social variables: a2 = Village Population Density, b2 = Road Density, c2 =, Total settlement area under village (%), d2 = Water supply through Pipeline (%), e2 = Literacy Rate, f2 = Dependent Population, g2 = Female Population (%), h2 = Population between (0-6) years, i2 = Tourist density, j2 = Settlements under 500m High Tide Line (HTL) and k2 = Settlements under 200m HTL.

Then, the sum of the PVI and SoVi is calculated to determine the CVI, i.e.,

$$CVI = PVI + SoVI \tag{3}$$

The present study has followed the methodology given by Nigam et al., 2024 which have adopted the similar scale to classify CVI score as employed by Kunte et al., 2014, who also assessed similar coastal stretch but at much coarser spatial scale (at taluka level). The objective behind the use of similar scale for CVI values is to compare current study results (at village level) with Kunte et al., 2014, to highlight the importance of high spatial resolution CVI compared to low spatial resolution CVI.

Chapter-4

Multi-Temporal Climate Trend Analysis

4.1 Background

In the current times, climate change has accelerated the weather extremes, which have the highest attention of climate scientists (Shi et al., 2016). The most pressing issue is concerned towards weather extremes rather than the mean of weather phenomena because rapid changes in weather extremes are more significantly Impacting all the regions than the average weather (Choi et al., 2009), which even has a severe impact on human health and leading to loss of lives (Ebi and Bowen 2016; Zhang et al., 2017). The weather extremes are the maximum and minimum of any meteorological phenomena (Vega and Rohli, 2012). Temperature and DTR are the fundamental parts of the climate system, along with precipitation. Changes in these components normally negatively impact humans and the environment (McMichael et al., 2005).

Since the end of World war II, worldwide, the frequency of cold extremes has got reduced while the warm extremes have increased globally (IPCC, 2013). In addition, increasing mean temperature trends have also been detected regionally and globally during the same period (Jones and Moberg 2003; Hertig et al. 2010; Simolo et al. 2014; Abbasnia, 2019).

The global mean temperature is an important indicator denoting climate change phenomenon. However, the DTR provide more in-depth information than the mean because the changes in DTR could be due to changes in either the maximum or minimum end of temperature or relative change in both. Between 1906- 2005, the average annual global temperature increased by 0.74 ± 0.18 ◦C. However, major increments have been observed during 1910-1940 (0.35˚C) and since 1970 (0.55 °C) (IPCC, 2007). Unsurprisingly, globally, 1998 was recorded as the warmest year during the last 100 years, surpassed by 2009, then 2010, and finally, 2011 as the warmest year since 1850 and the decade of 1990 was observed as the warmest decade (Venkateshwaralu et al., 2011).

On the other hand, the diurnal temperature range (DTR) has been reducing since the 1950s over most of the regions around the world except for northern Eurasia, western North America, Australia and South Asia, where this pattern has been less consistent. However, in the regions where the DTR has reduced, it is due to lower warming in maximum temperature compared to minimum temperature (Karl et al., 1993; Zhou et al.). It is a well-known fact that urbanisation is imperative for transforming underdeveloped countries with socio-economic and ecological impacts (Bhat et al., 2017; Butsch et al., 2017; Sun et al., 2013). However, due to development, urban areas experience a rise in surface temperature, degrading air quality, loss of vegetation cover, urban heat island effect and climate variations (Chen et al., 2011; Estoque & Murayama, 2013; Gohain et al., 2020; Jenerette & Wu, 2001; Mohammad et al., 2019; Mohammad & Goswami, 2019; Malik et al., 2020; Tiwari et al., 2018; Yang et al., 2011).

In the case of haphazard development, India and South Asia are at the forefront. Indian economy is booming, due to which the urban part of the country constitutes 63% of the GDP, projected to increase to 75% by 2030 (Planning Commission, 2012). Increment in the economy is directly proportional to development and land use changes from natural to artificial. Hence, it has been reported that between 1901-2003, the annual T_{mean} increased at a rate of 0.05°C (per decade), while T_{min} showed a weak, statistically insignificant increasing trend. Moreover, between 1971-2003 accelerated warming in T_{mean} 0.22°C (10 yr.) has been observed (Kothawale and Kumar, 2005). Even there has been a significant increment in the DTR over India by 0.52˚ C (100 yr.) for 1901–2003) (Rai et al., 2012), while the decreasing trend has been observed in depicts decreasing trends in DTR monthly, seasonal (pre-monsoon and monsoon), and annual time scales in North East India (Jain et al., 2013). The primary causes of the increment in man temperature and DTR could be attributed to total cloud cover, precipitation and soil moisture.

Precipitation is an important factor concerning meteorology. It impacts the DTR, but erratic rainfall is associated with extreme events such as floods and landslides. Hence, understanding rainfall trends is paramount to formulating effective adaptation policies. In addition, low clouds have the largest impact on the DTR. Dai and others in 1999 observed a reduction in DTR by 25-50% over most of the land areas when coupled with precipitation and soil moisture. The amount of cloud cover is a significant factor because they dampen DTR as temperature decreases during the day by backscattering incident solar radiation but increasing the downwelling longwave radiation during both day and night (Vedecchia et al., 1994). Moreover, high soil moisture reduces the maximum temperature and DTR by increasing evaporation cooling by evapotranspiration.

The trends of record-breaking annual warming between 1946 and 1995 can be explained as anthropogenic forcing, while the forces behind the warming between 1896 and 1945 are the combination of anthropogenic, natural and internal variability (Braganza et al., 2004). Hence, urbanisation and concretization directly impact surface temperature. Even changes in land-use influence minimum temperature (Urban heat island). The reason is the high energy consumption, population heat and friction in the cities generate a significant amount of heat stored in the concrete structures. The stored heat energy in the infrastructure gets released at night and eventually makes the night warmer (Gadgil and Dhorde, 2005). Studies suggest that DTR can be influenced by changes in the LULC within a 10 km radius of an observation station. Urbanisation leads to changes in climatic parameters such as albedo, moisture, thermal inertia and the land-atmosphere interaction (Feddema et al., 2005).

Rapid haphazard development is directly leading to ever-increasing greenhouse gases and aerosols. LULC modifications may also impact the DTR trends at a regional level (Liu et al., 2018a; Sun et al., 2019). Increased aerosol concentration leads to decreasing DTR due to the cooling effect of aerosols (Huang et al., 2006; Gong et al., 2014; Xue et al., 2019) and aerosol-cloud interaction (Wang et al., 2013, 2015; Guo et al., 2019; Li et al., 2019). The impact of changes in DTR is detrimental as it would influence heat stress, agricultural failures (Lobell, 2007), droughts, increment in human mortality (Kan et al., 2007) and epidemics such as dengue, malaria (Liu-Helmersson et al., 2014; Ehelepola and Ariyaratne, 2016). The consequences of these changes have detrimental impacts on nature and society. These changes in the weather extremes can also increase hazard vulnerability and cause loss of lives and property, resulting in negative economic effects.

The need for the study lies in the fact that it is imperative to determine the current meteorological trends of temperature, DTR, rainfall etc., which are the most important factor leading to climatic variations. Coastal tracts of South Goa have seen rapid urbanisation and tourism development. Because of this, many lives and economics are at stake against climate variability.

Therefore, the present study aims to determine the current trends of meteorological variables in the study area over the last 40 years (1981-2020). Moreover, if any changes have occurred, then which meteorological and anthropogenic factors have been behind these changes.

4.2 Result

4.2.1 Correlation Coefficients of Rainfall And Mean Temperature

Table- 4.1 Correlation coefficients between the IMD and NASA POWER datasets during 1981-2020.

Month	Correlation Coefficient (Rainfall)	Correlation Coefficient (Mean Temperature)
January	0.27	0.62
February	0.56	0.73
March	0.93	0.55
April	0.25	0.78
May	0.70	0.42
June	0.28	0.51
July	0.65	0.41
August	0.71	0.70
September	0.83	0.80
October	0.72	0.60
November	0.73	0.49
December	0.71	0.47
Non-Monsoon (Oct-May)	0.54	0.59

Monsoon (June-Sept)	0.61	0.43
Annual	0.61	0.53

4.2.2 Climatic Variables Trend Analysis

4.2.2.1 Long-Term Trend Analysis (1981-2020)

- **Annual**

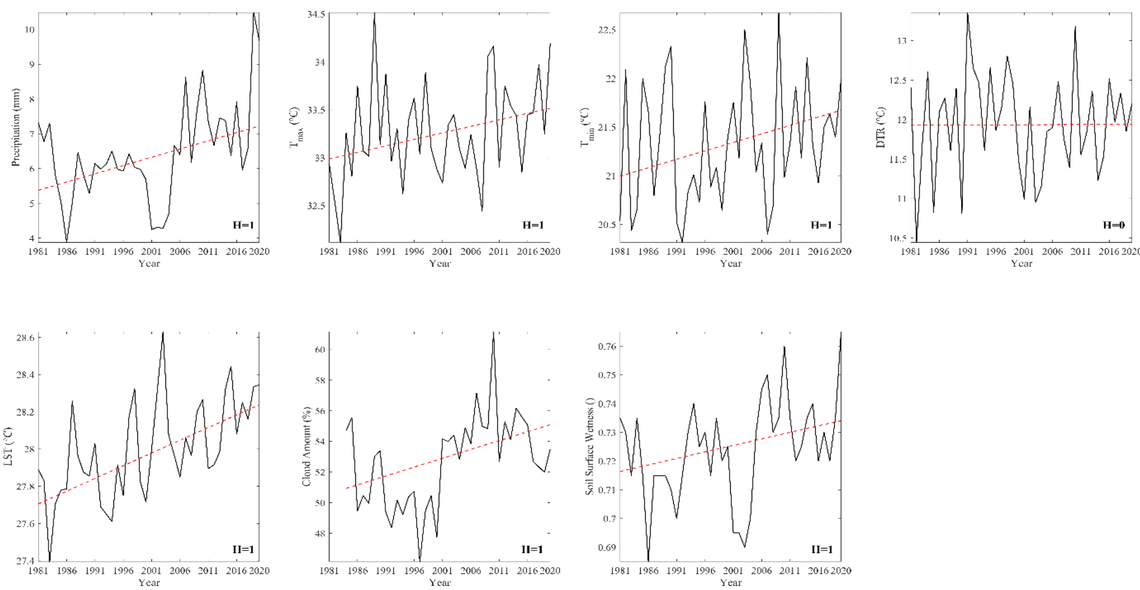

- **Non-Monsoon**

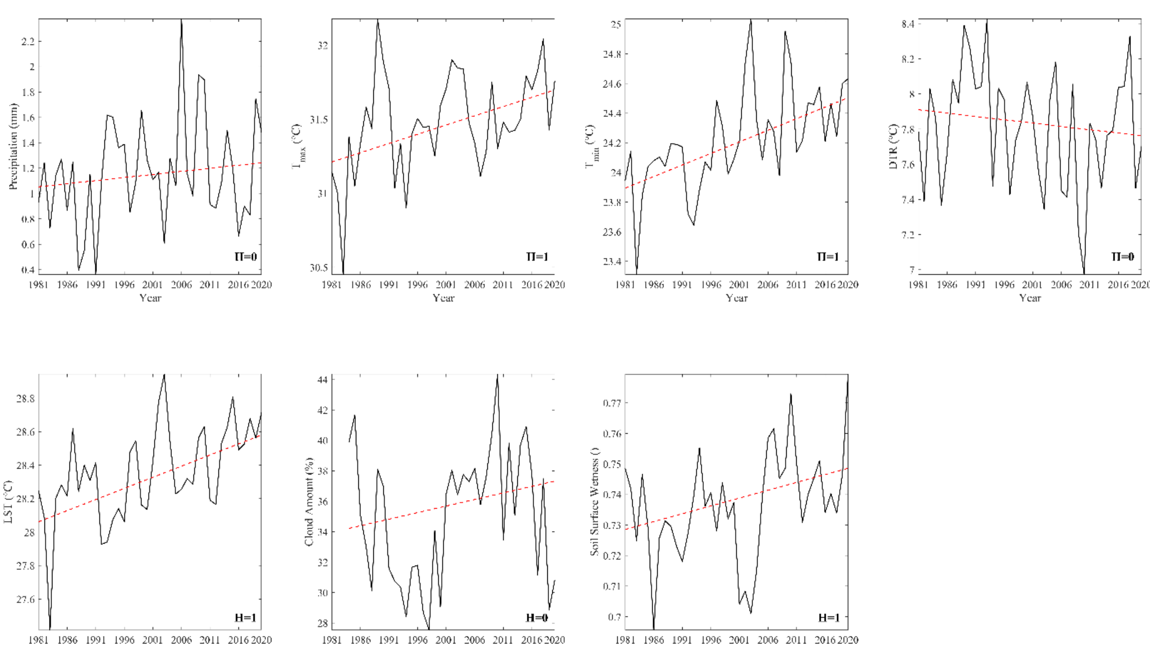

- **Monsoon**

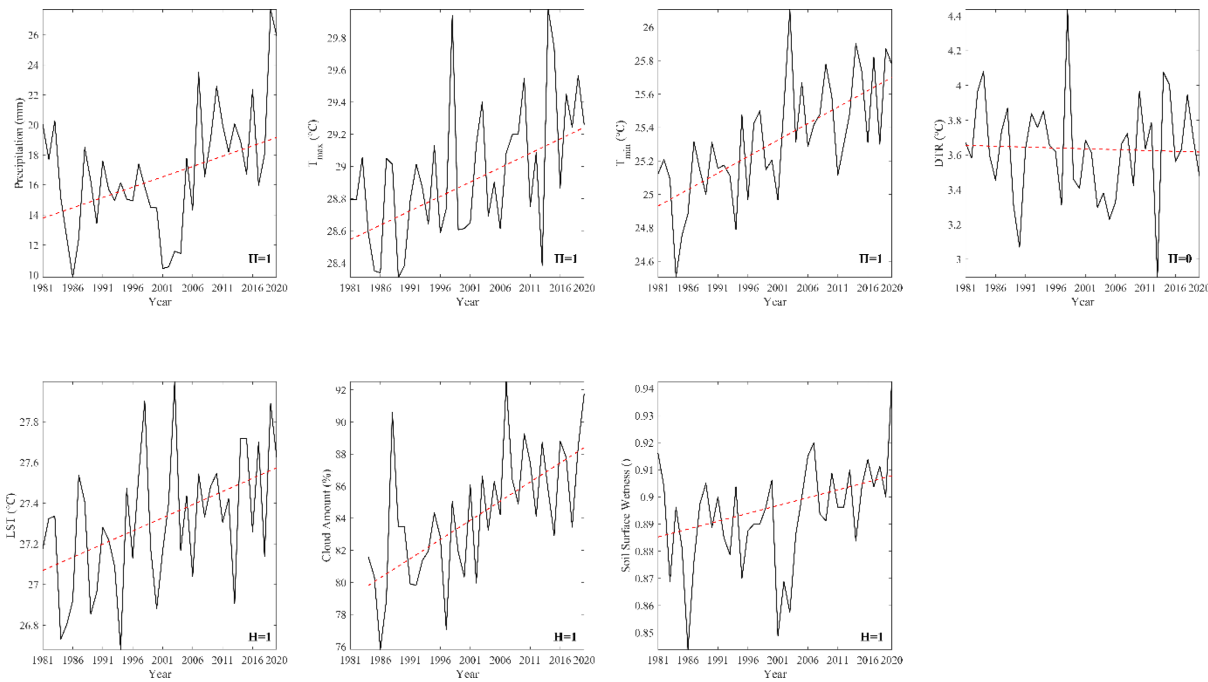

Fig-4.1 Plots Divided into Three Seasons (Annual, Non-Monsoon And Monsoon), showing the Trends Of Different Climatic Variables In South Goa Between 1981-2020.

Table- 4.2 Statistical Results of Annual and Seasonal Trend Analysis of South Goa District Between 1981-2020.

Variable	Hypothesis test (1 is significant @ 80% level) (h)	Significance level (p)	Sen Slope (Sen)	Z score (Z)	Mann-Kendall test (S)	Standard Deviation (S.D)	No. of values (n)
Annual							
Precipitation	1	0.007108	0.04742	2.691754	232	85.81764	40
T_{max}	1	0.047613	0.01359	1.98081	171	85.82346	40
T_{min}	1	0.110398	0.017374	1.596408	138	85.81764	40
DTR	0	0.990703	0.000179	0	1	85.82346	40
LST	1	6.12E-05	0.013675	4.008228	345	85.82346	40
Cloud amount	1	0.01076	0.115619	2.550382	196	76.45914	37
Soil Surface Wetness	1	0.023985	0.000455	2.257366	193	85.05488	40

Non-Monsoon							
Precipitation	0	0.40811	0.004865	0.827223	72	85.82929	40
T_{max}	1	0.008755	0.012468	2.621483	226	85.82929	40
T_{min}	1	2.73E-05	0.015643	4.194657	361	85.82346	40
DTR	0	0.441881	-0.00379	-0.76902	-67	85.82346	40
LST	1	0.000291	0.013295	3.623472	312	85.82929	40
Cloud amount	0	0.326634	0.086288	0.980916	76	76.45914	37
Soil Surface Wetness	1	0.018589	0.000514	2.353669	203	85.82346	40
Monsoon							
Precipitation	1	0.024535	0.13768	2.24865	194	85.82929	40
T_{max}	1	0.000698	0.017876	3.390451	292	85.82929	40
T_{min}	1	1.12E-05	0.019728	4.39244	378	85.82929	40
DTR	0	0.842992	-0.00099	-0.19807	-18	85.82929	40
LST	1	0.004468	0.012941	2.843045	245	85.82346	40
Cloud amount	1	7.40E-05	0.238679	3.962901	304	76.45914	37
Soil Surface Wetness	1	0.015781	0.000579	2.41395	208	85.75158	40

4.2.2.2 Short-Term Trend Analysis (1981-1999)

- **Annual**

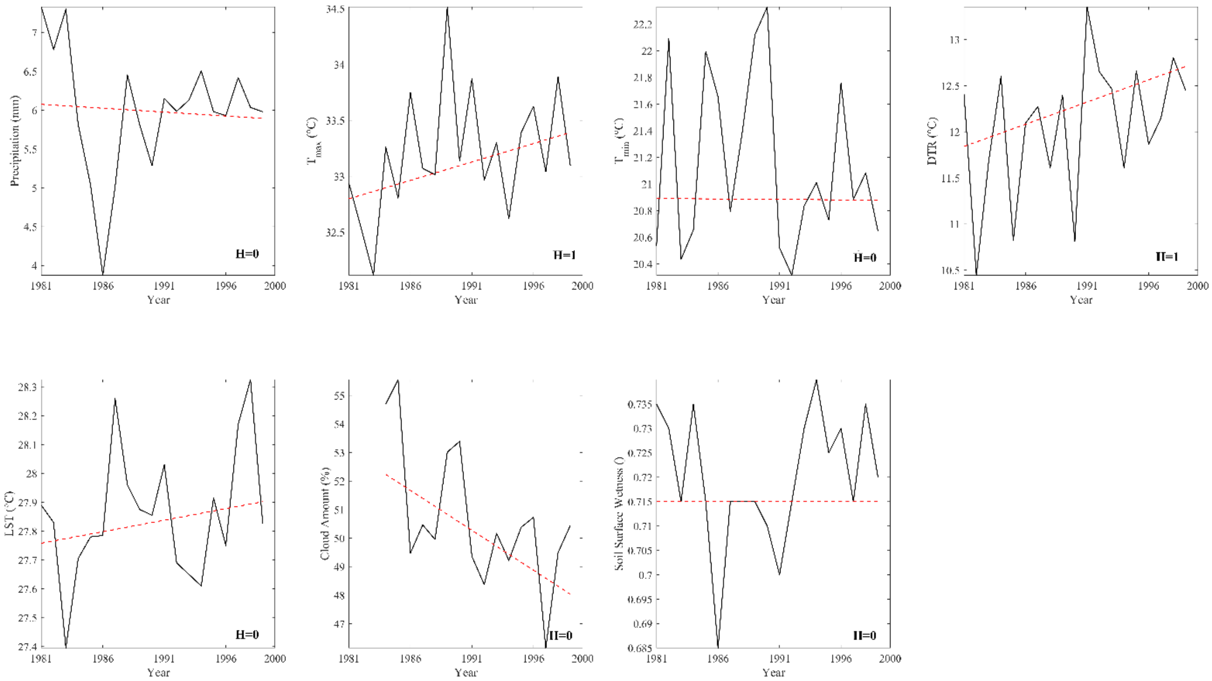

- **Non-Monsoon**

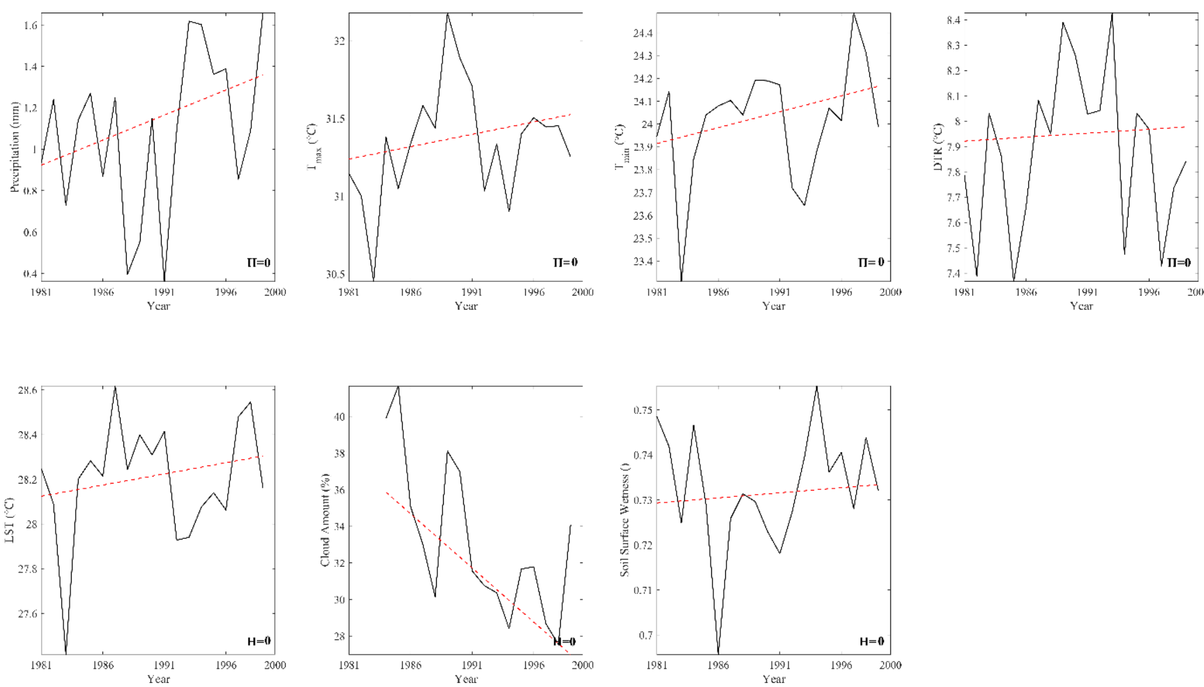

- **Monsoon**

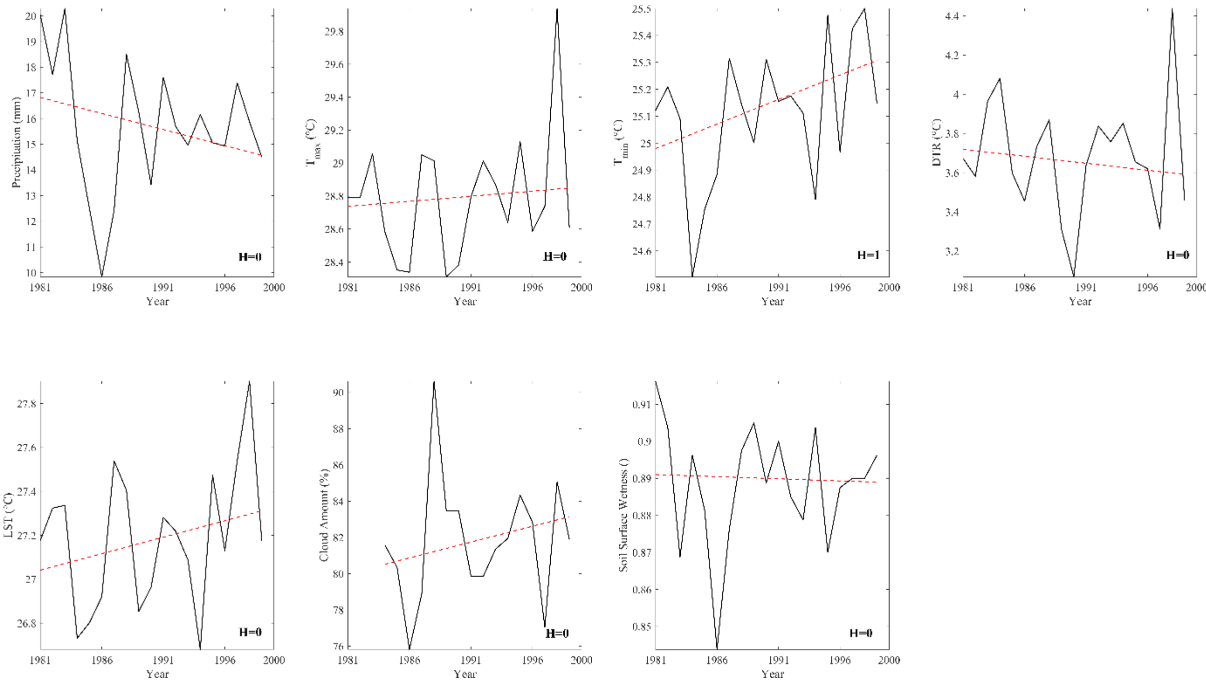

Fig- 4.2 Plots Divided into Three Seasons (Annual, Non-Monsoon and Monsoon), Showing The Trends of Different Climatic Variables in South Goa District Between 1981-1999.

Table- 4.3 Statistical Results of South Goa District Annual and Seasonal Trend Analysis between 1981-1999.

Variable	Hypothesis test (1 is significant @ 80% level) (h)	Significance level (p)	Sen slope (sen)	Z score (Z)	Mann-Kendall test (S)	Standard Deviation (S.D)	No. of values (n)
Annual							
Precipitation	0	0.752714	-0.31506	-10	28.56571	-0.00999	19
T_{max}	1	0.080243	1.749279	51	28.58321	0.032941	19
T_{min}	0	0.972091	0	-1	28.58321	-0.00067	19

DTR	1	0.115184	1.575315	46	28.56571	0.048122	19
LST	0	4.84E-01	0.699711	21	28.58321	0.007999	19
Cloud amount	0	0	0	0	0	0	0
Soil Surface Wetness	0	0.690911	0.397619	12	27.66466	0	19
Non-Monsoon							
Precipitation	0	0.207857	1.259481	37	28.58321	0.024167	19
T_{max}	0	0.262911	1.119538	33	28.58321	0.015885	19
T_{min}	0	3.45E-01	0.945189	28	28.56571	0.013958	19
DTR	0	0.726447	0.349856	11	28.58321	0.003125	19
LST	0	0.575637	0.559769	17	28.58321	0.009999	19
Cloud amount	0	0	0	0	0	0	0
Soil Surface Wetness	0	0.674612	0.419827	13	28.58321	0.000227	19
Monsoon							
Precipitation	0	0.293917	-1.04957	-31	28.58321	-0.12508	19
T_{max}	0	0.726447	0.349856	11	28.58321	0.006145	19
T_{min}	1	1.24E-01	1.539365	45	28.58321	0.018202	19
DTR	0	0.726447	-0.34986	-11	28.58321	-0.00713	19
LST	0	0.277826	1.085217	32	28.56571	0.014996	19
Cloud amount	0	0.00E+00	0	0	0	0	0
Soil Surface Wetness	0	0.944148	-0.07006	-3	28.5482	-0.00011	19

4.2.2.3 Short-Term Trend Analysis (2000-2020)

- **Annual**

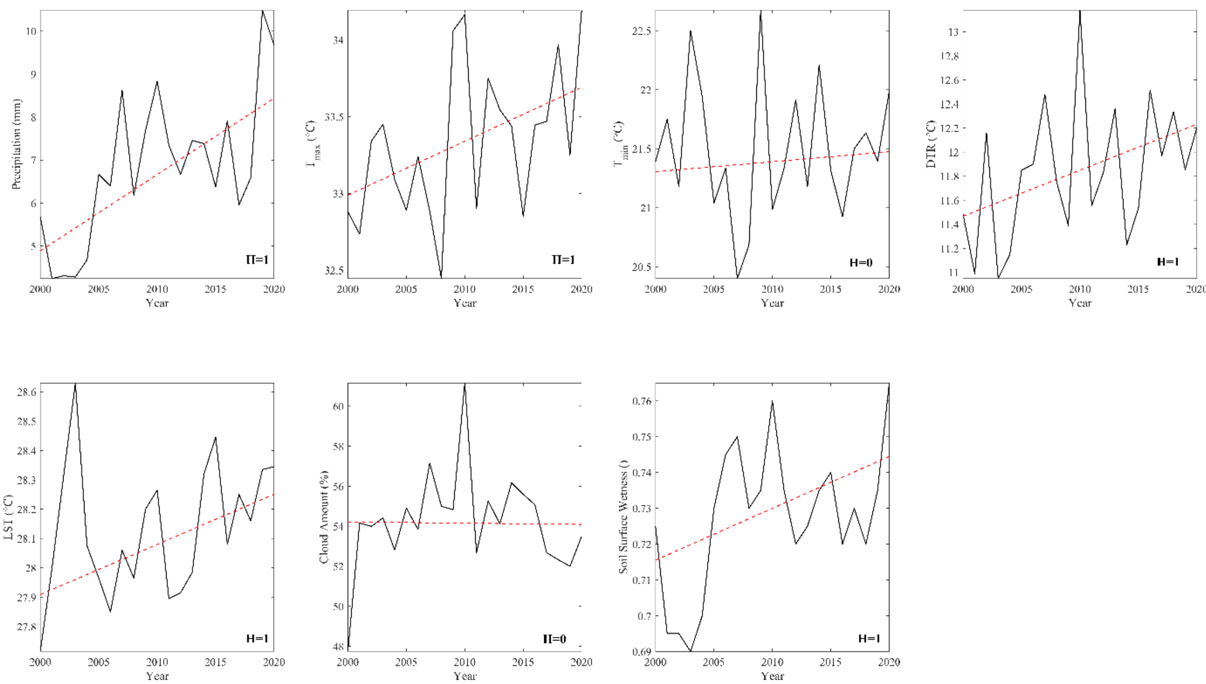

- **Non-Monsoon**

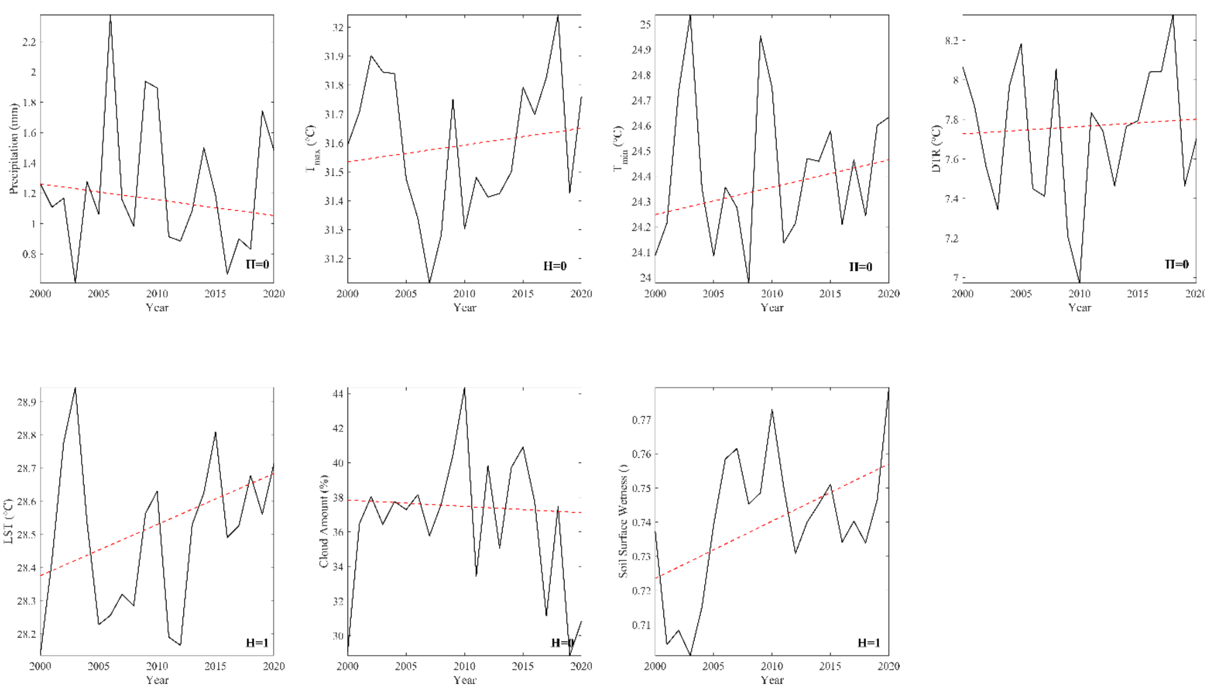

- **Monsoon**

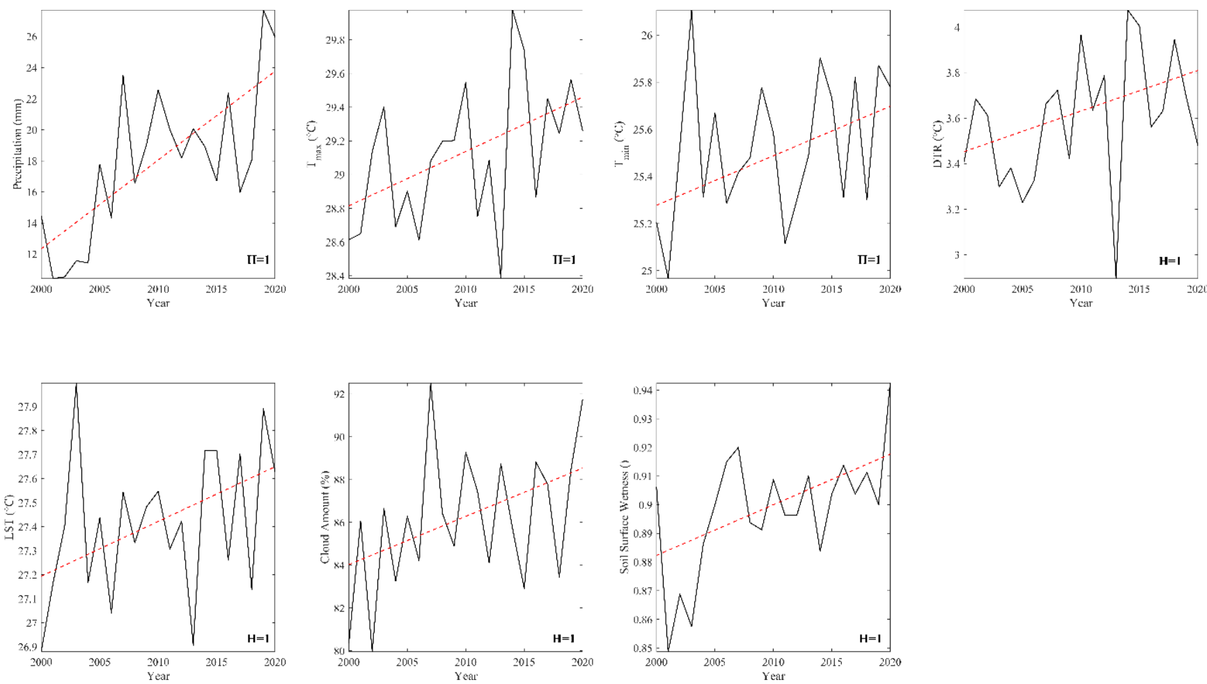

Fig- 4.3 Plot divided into three seasons (annual, non-monsoon and monsoon), showing the trends of different climatic variables in South Goa district between 2000-2020.

Table-4.4 Statistical results of South Goa district annual and seasonal trend analyses between 2000-2020.

Variable	Hypothesis test (1 is significant @ 80% level) (h)	Significance level (p)	Sen slope (sen)	Z score (Z)	Mann-Kendall test (S)	Standard Deviation (std)	No. of values (n)
Annual							
Precipitation	1	0.004514	2.839806	95	33.10086	0.177526	21
T_{max}	1	0.043053	2.023194	68	33.11596	3.52E-02	21
T_{min}	0	0.739535	0.332469	12	33.08575	8.44E-03	21
DTR	1	0.065473	1.842012	62	33.11596	0.038214	21
LST	1	5.71E-02	1.902406	64	33.11596	1.71E-02	21
Cloud amount	0	0.97591	-0.0302	-2	33.11596	-6.44E-03	21
Soil Surface Wetness	1	0.072427	1.796422	60	32.84306	1.45E-03	21
Non-Monsoon							
Precipitation	0	0.607708	-0.51335	-18	33.11596	-1.04E-02	21

T_{max}	0	0.694644	0.39256	14	33.11596	5.79E-03	21
T_{min}	0	3.81E-01	0.875711	30	33.11596	1.08E-02	21
DTR	0	0.879988	0.150985	6	33.11596	3.72E-03	21
LST	1	0.17419	1.358861	46	33.11596	1.54E-02	21
Cloud amount	0	0.694644	-0.39256	-14	33.11596	-0.0368	21
Soil Surface Wetness	1	0.057118	1.902406	64	33.11596	1.68E-03	21
Monsoon							
Precipitation	1	0.002289	3.049889	102	33.11596	0.571119	21
T_{max}	1	0.020063	2.325163	78	33.11596	3.22E-02	21
T_{min}	1	9.67E-02	1.660831	56	33.11596	2.10E-02	21
DTR	1	0.12355	1.540043	52	33.11596	1.79E-02	21
LST	1	0.109502	1.600437	54	33.11596	2.28E-02	21
Cloud amount	1	7.48E-02	1.781618	60	33.11596	0.225529	21
Soil Surface Wetness	1	0.0234	2.266837	76	33.08575	1.77E-03	21

4.2.3 Correlation Matrix of Seven Climatic Variables

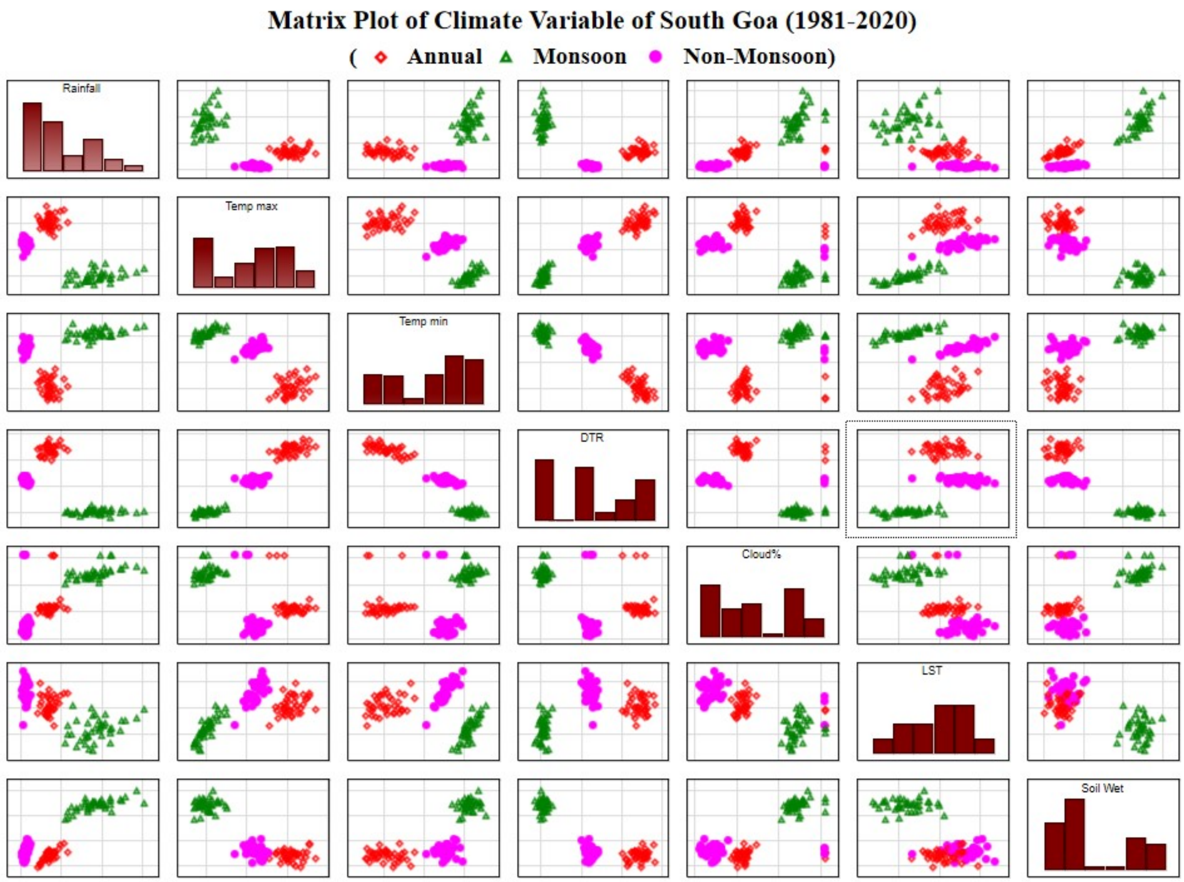

Fig-4.4 Matrix plot showing the climatic variables of South Goa between 1981-2020 during different seasons and annually.

4.3 Result interpretation

- **Datasets Correlation**

The correlation coefficient between IMD and NASA POWER's rainfall and temperature datasets was calculated for 40 years (1981-2020) for three periods (annual, non-monsoon and monsoon) (Table-4.1). It validates the efficacy of the NASA POWER gridded datasets available for the study area against sparsely available IMD dataset, which is the most preferred choice due to its network and reliability. The direction of relationship between the two is positive. The annual period has shown a moderately positive relationship (0.61) and (0.53) for rainfall and temperature variables respectively. While it more or less similar when the year is divided based on seasons with non-monsoon (0.54 & 0.59) and monsoon periods (0.61 & 0.43). However, during the second half of the year monsoon to post monsoon (July-Dec), when the rainfall effect is predominant in the region the relationship is 'fairly strong positive' but on the contrary, for the temperature variable, first half of the year (drier months) have relatively shown strong positive relationship between the IMD and NASA POWER datasets.

- **Climate trends**

In the study area, between 1981-2020, during annual period, the trend is fairly positive for all the climatic variable except for DTR for which no trend was found (Fig.-4.1 & Table-4.2). The Z-score was found to be highest for the LST (4.008) while it was only (1.59) for T_{min}, which shows the true characteristics of LST and T_{min} in a coastal area. While during non-monsoon months, all the variables have been found to have positive (increasing) trend except rainfall, DTR and cloud amount. The highlights were temperature (min and max), both have shown gradually uniform upward trends with a rate of (sen = 0.012 and 0.015) per year respectively. Monsoon months show positive upward trends in all the variables except the DTR which showed no trend. Cloud amount has shown most significant increment (S = 304) with the rate of (Sen = 0.238) percent per year with highest fluctuation (z score = 3.96) amongst all the variables. Consequently, rainfall has increased (S= 194, Sen=0.137) and the temperature (min and max) with the fastest rate (sen = 0.019 and 0.017) per year, amongst all the periods.

Annual climatic variable values during 1981-1999 in the study area (Fig.-4.2 & Table-4.3) were found to be very different from the long term analysis (1981-2020). Except T_{max} and DTR, no other variable showed any trend. T_{max} showed an upward trend (sen = 1.749, S = 51), which also resulted in sharp increment in DTR (sen = 1.575 and S = 46). Non-monsoon phase showed no trends in any of the variables. As well as, except for T_{min}, no other variable showed any upward or downward trend. T_{min} observed significant upward movement (sen = 1.54 and S = 45) during the phase.

Annual trend analysis of the last two decades (2000-2020) in the study area (Fig.-4.3 & Table-4.4) showed positive trend in all the variables except T_{min} and cloud amount which showed no trend. Rainfall has shown a significant upward trend with a magnitude of (sen = 2.84 and Z = 95) due to which soil wetness has also shown a positive trend (sen =1.8 and Z = 60). Similarly, T_{max} has also showed a significant upward trend (sen = 2.02 and Z =68) so as DTR (sen = 1.842 and Z = 62) and LST (sen = 1.90 and Z =64). Climatic variables during non-monsoon phase were statistically insignificant and showed no trends except LST (sen =1.35 and Z= 46) and Soil wetness (sen = 1.903 and Z = 64). The highest positive trends across all the periods and seasons is found in this monsoon phase. Rainfall showed significantly upward trend having magnitude (sen = 3.05) and (Z= 102) so as cloud amount (sen = 1.781 and Z= 60) and soil wetness (sen = 2.266 and Z= 76). Temperature (maximum and minimum) has also been found moving significantly upward (sen=2.32 and Z=78) and (sen= 1.660 and Z= 56) respectively. Consequently, upward movement in DTR magnitude (sen =1.54) and (Z=52) as well as LST (sen=1.6 and Z=54).

Chapter-5

Multi-Temporal Land Use Land Cover Assessment

5.1 Background

Pressure from a growing population and climate change results in changes in land use and land cover (LULC), which have the greatest negative effects on the environment through the vegetation cover, landform degradation, biodiversity loss, shoreline modification, seawater intrusion, groundwater pollution, and the deterioration of soils and air in coastal regions (Chandrasekar et al., 2001; Chauhan and Nayak, 2005; INCOIS, 2009; Kaliraj et al., 2014).

Around 43% of the earth's surface has been degraded by human activity (Daily, 1995), nearly 24% of it has seen a decline in ecosystem function and productivity over the past two decades (Kalensky et al., 2003). Also the demand is rising faster than the planet can sustainably meet it, which is leading to more serious long-term sustainability problems along the world's coasts (Xiuwan, 2002).

According to UNDP (2007), the population of coastal areas has doubled over the last 40 years and is expected to do so again in the subsequent 40 years. Due to the spread of settlements and infrastructure, rapid population growth has accelerated the rate of land transformation on the natural LULC features (Mujabar and Chandrasekar, 2012).

Changes in LULC as a result of numerous physical, climatic, and socioeconomic causes have a direct impact on the socioeconomic position of local inhabitants along the coastal zone in space and time. Rapid population expansion, urbanization, and tourism development activities are modifying the existing state of land use and land cover features (Clark, 1982; Chilar, 2000; Yuan et al., 2005; Joshi et al., 2011; Rawat et al., 2013; Prasad et al., 2023 (a); Shivkrishna et al., 2021), since coastal tourism represents the interaction of human elements and ecological systems, often generate several ramifications. It degrades coastal ecosystems and reduces coastal and marine biodiversity and productivity in most of the world's coastal locations (Naik, 2018).

The LULC changes in the coastal area have altered beachside landforms, sand dunes, agriculture, and vegetative cover due to the growth of towns and other infrastructures over the last decade. Natural processes such as waves, storm surge, cyclones, erosion and subsidence, and so on are also gradually changing the land use and land cover along the coast (Short and Trembanis, 2004; Zhang, 2011; Kaliraj and Chandrasekar, 2012; Mujabar and Chandrasekar, 2013) and eventually making them vulnerable to coastal hazards (Prasad et al., 2023 (b)).

The population growth rate along the Indian coastal tracts has increased from 11.42% in 1991 to 14.20% in 2014. It has a direct negative influence on land resources and generates rapid change of land cover into built-up areas, communities, and other recreational activities (Bhatta et al., 2010).

Due to the rapid growth on coastal habitats, problems cannot be put off or avoided. In context of this, it's critical to comprehend the LULC modification and how it will affect the coast. The review of the literature looks at a few studies (Brilliant et al., 2013, Yaw et al., 2014, Akshitha et al., 2015, and Kaliraj et al., 2017) that were largely conducted to evaluate the change in LULC and its effects on the environment and tourism in coastal zones.

In order to manage coastal zones sustainably, satellite images that provide a synoptic coverage of the earth's surface on both a spatial and temporal scale are used in the LULC change analysis. This enables us to comprehend how changes have occurred in different areas of the environment, including coastal areas (Misra et al., 2013). Consequently, under extreme population pressure, in order to enable proper coastal resource management planning at the national or regional level (Wu et al., 2002; Zoran, 2006; Zhang and Zhu, 2011) it has become imperative.

Large-scale changes in the geo-ecological setup and land use patterns have been caused by the introduction of tourism, increased mining operations, and population growth along with natural and anthropogenic changes brought on by contemporary societal demands. These changes have a direct impact on the human environment (Kotha, 2013).

South Goa's coastal tracts have seen notable changes in LULC features in recent decades as a result of the effects of marine and terrestrial forces, as well as human activity (Chandrasekar et al., 2013). There is an urgent need to protect coastal ecosystems and habitats, communities, historic towns, the environment, agriculture, and other resources for future generations.

The current study provides the basic information needed to comprehend trends in LULC change and transformation in the study area.

5.2 Result

(a) Marmugao

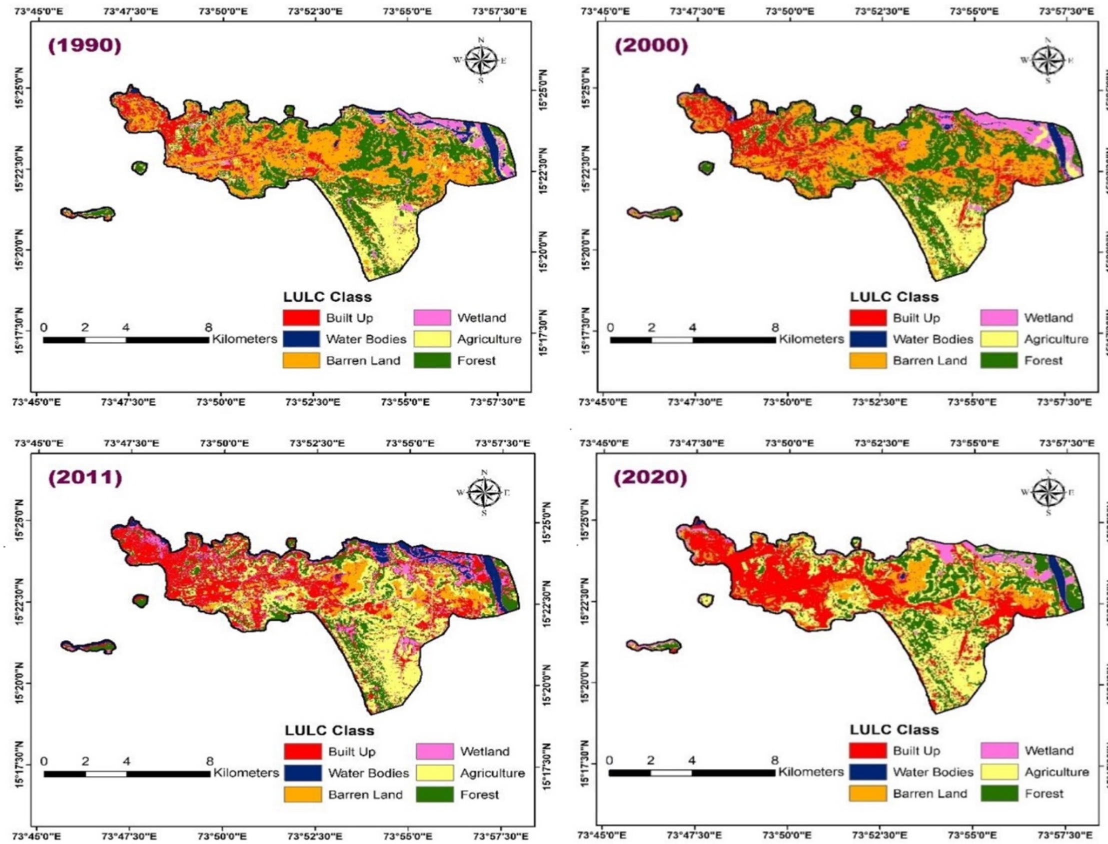
(1990)
(2000)
(2011)
(2020)
73°45'0"E
73°47'30"E
73°50'0"E
73°52'30"E
73°55'0"E
73°57'30"E
15°25'0"N
15°22'30"N
15°20'0"N
15°17'30"N
LULC Class
Built Up
Wetland
Water Bodies
Agriculture
Barren Land
Forest
0 2 4 8
Kilometers

(a) Salcete

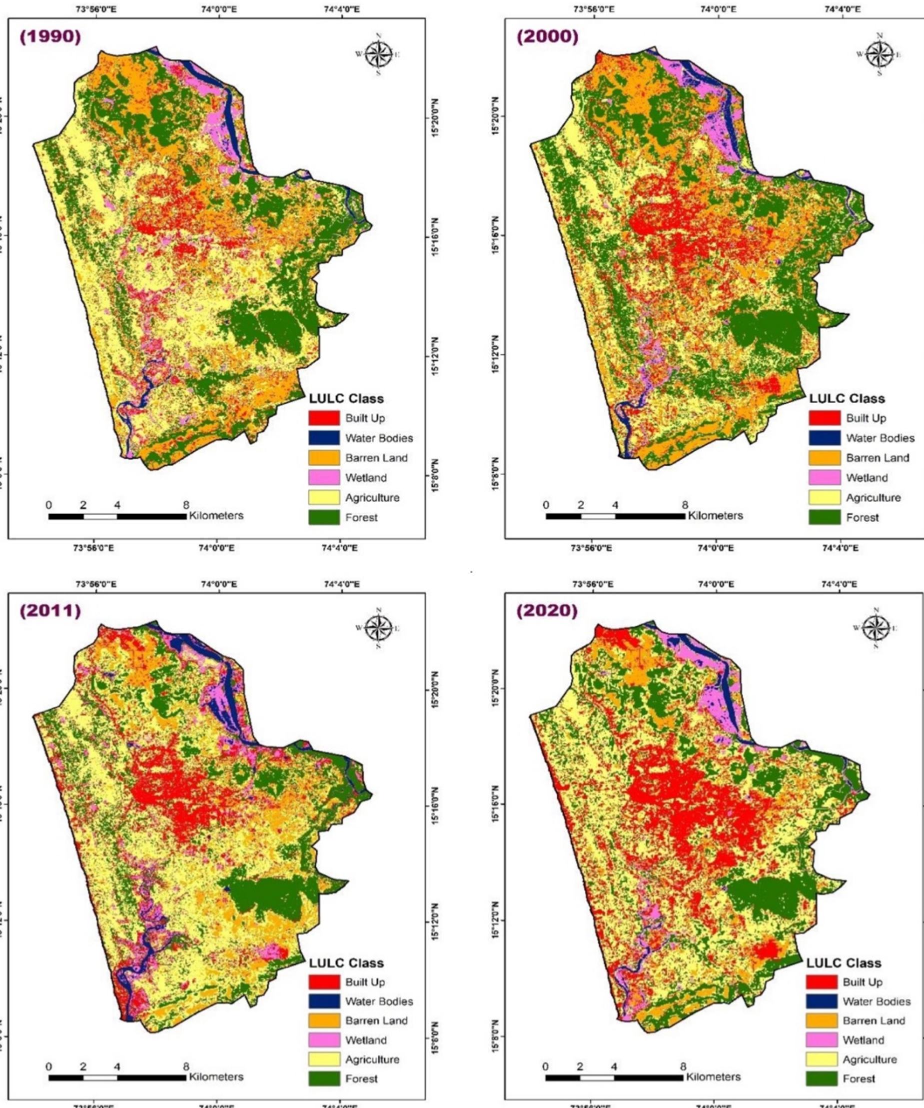
(1990)
(2000)
(2011)
(2020)
73°56'0"E
74°0'0"E
74°4'0"E
15°20'0"N
15°16'0"N
15°12'0"N
15°8'0"N
LULC Class
Built Up
Water Bodies
Barren Land
Wetland
Agriculture
Forest
0 2 4 8 Kilometers

(a) Quepem

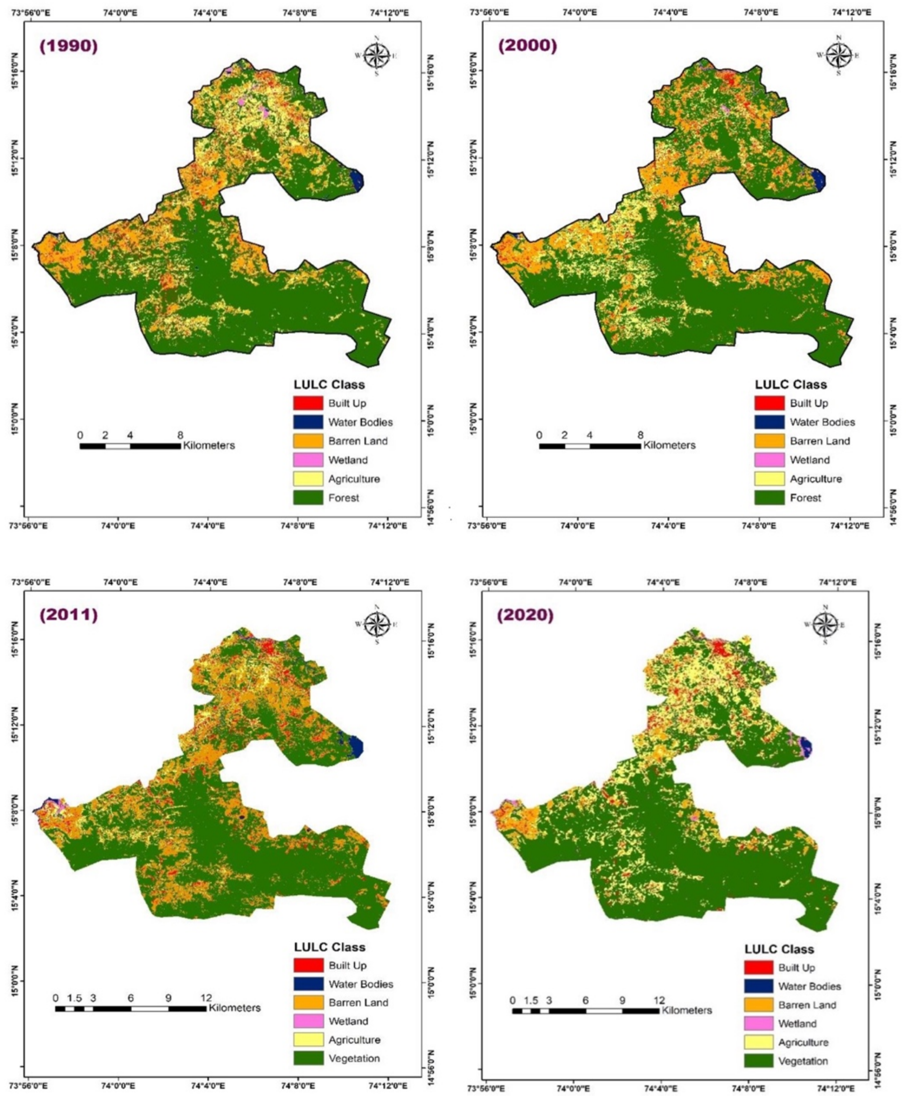
(1990)
(2000)
(2011)
(2020)
LULC Class
Built Up
Water Bodies
Barren Land
Wetland
Agriculture
Forest
Vegetation
Kilometers
73°56'0"E
74°0'0"E
74°4'0"E
74°8'0"E
74°12'0"E
15°16'0"N
15°12'0"N
15°8'0"N
15°4'0"N
15°0'0"N
14°56'0"N

(a) Canacona

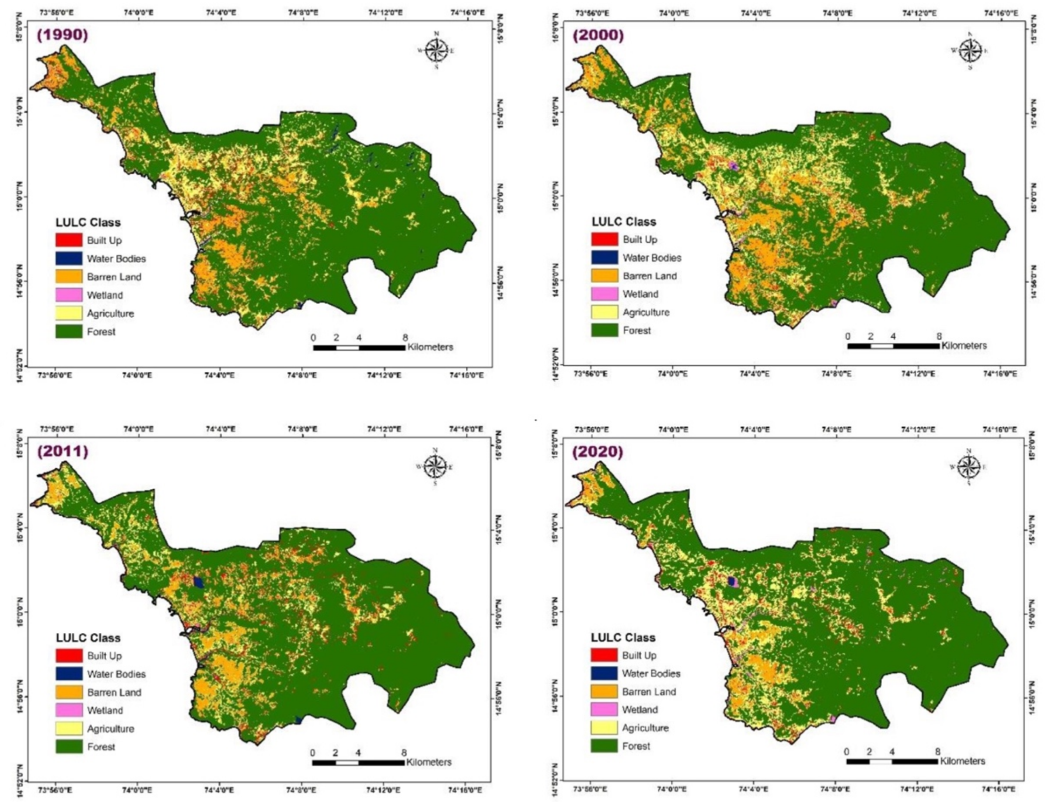

Fig-5.1 Decadal LULC change maps of Marmugao (a), Salcete (b), Quepem (c) and Canacona (d) for the year 1990, 2000, 2011 and 2020.

Table-5.1 Statistics of the LULC changes occurred in Marmugao, Salcete, Quepem and Canacona during the year 1990, 2000, 2011 and 2020. Changes in total area (sq. km), amount of change (% compared to total LULC changes during each year and percentage difference between the current and preceding year have been shown here.

	1990			2000			2011			2020		
	Sq. km	%	% diff	Sq. km	%	% diff	Sq. km	%	% diff	Sq. km	%	% diff
(a) Marmugao												
Agriculture	16.54	16	NA	11.12	12.23	-23.56	18.37	20.29	65.9	26.35	29.04	43.12
Barren Land	29.34	32.28	NA	30.44	33.49	3.74	12.48	13.79	-58.8	11.11	12.24	-11.24
Built Up	12.17	13.39	NA	16.02	17.62	31.74	25.22	27.86	58.1 1	29.49	32.51	16.69
Vegetation	23.76	26.14	0NA	23.99	26.39	0.95	15.42	17.03	-35.46	16.25	17.91	5.16
Water Bodies	4.16	4.57	NA	2.39	2.62	-42.66	4.17	4.6	75.57	1.61	1.77	-65.12
Wetland	4.90	5.39	NA	6.92	7.61	41.18	14.84	16.39	115.37	5.89	6.49	-60.40
(b) Salcete												

Agriculture	114.05	37.16	NA	98.24	32.01	-13.85	85.44	27.86	-12.96	91.84	29.93	7.43
Barren Land	56.65	18.46	NA	68.19	22.22	20.36	54.68	17.83	-19.75	56.50	18.41	3.25
Built Up	36.24	11.8	NA	44.70	14.56	23.38	54.83	17.88	22.8	74.44	24.26	35.68
Vegetation	76.87	25.05	NA	77.85	25.37	0.16	72.65	23.69	-6.62	64.31	20.96	-10.34
Water Bodies	5.78	1.88	NA	5.88	1.91	1.59	8.44	2.75	43.97	5.38	1.75	-36.36
Wetland	17.26	5.62	NA	11.97	3.9	-30.60	30.59	9.97	155.64	14.32	4.66	-53.25
(c) Quepem												
Agriculture	43.77	13.5	NA	42.45	13.1	-2.96	40.76	12.55	-4.19	43.88	13.5	7.56
Barren Land	58.05	17.91	NA	64.66	19.95	11.39	65.29	20.1	0.75	62.57	19.25	-4.22
Built Up	10.39	3.2	NA	11.63	3.58	11.87	12.94	3.98	11.17	15.79	4.85	21.85
Vegetation	207.46	64.02	NA	202.24	62.41	-2.51	200.59	61.76	-1.04	198.68	61.14	-1.03
Water Bodies	2.13	0.65	NA	1.90	0.58	-12.06	2.78	0.85	46.55	1.04	0.32	-62.35
Wetland	2.24	0.69	NA	1.16	0.35	-49.27	2.41	0.74	111.42	2.97	0.91	22.97
(d) Canacona												
Agriculture	49.52	12.68	NA	49.11	12.58	-0.78	28.64	7.32	-41.81	55.06	14.11	92.75
Barren Land	37.17	9.52	NA	40.95	10.49	10.17	65.60	16.78	59.96	38.24	9.8	-41.59
Built Up	9.55	2.44	NA	10.78	2.76	13.11	12.17	3.11	12.68	13.50	3.45	10.93
Vegetation	290.20	74.36	NA	285.64	73.19	-1.57	278.66	71.29	-3.41	277.90	71.22	-0.09
Water Bodies	2.46	0.63	NA	1.97	0.5	-20.63	3.16	0.8	60	0.80	0.2	-80
Wetland	1.36	0.34	NA	1.81	0.46	35.29	2.62	0.67	45.65	4.70	1.2	79.1

Table-5.2 Accuracy assessment of the multi-temporal LULC changes occurred in the study area during the year 1990, 2000, 2011 and 2020. Showing Producer's accuracy, User's accuracy and Kappa coefficient.

1990									
Class	Agricultural	Barren Land	Built up	Vegetation	Water Bodies	Wetland	Total	U. Accuracy	Kappa
Agricultural	16	0	0	0	0	3	19	0.842	0
Barren Land	0	14	0	1	1	1	17	0.824	0
Built up	0	1	8	0	0	1	10	0.8	0
Vegetation	0	1	0	50	2	0	53	0.943	0
Water Bodies	0	0	0	1	8	0	10	0.9	0
Wetland	0	1	0	0	0	9	10	0.9	0
Total	16	17	8	52	11	15	119	0	0
P. Accuracy	1	0.824	1	0.9	0.8	0.909	0	0.891	0

Kappa	0	0	0	0	0	0	0	0	0.850
2000									
Class	Agricultural	Barren Land	Built up	Vegetation	Water Bodies	Wetland	Total	U. Accuracy	Kappa
Agricultural	14	2	0	0	0	0	16	0.875	0
Barren Land	0	18	0	0	2	0	20	0.9	0
Built up	0	0	8	1	1	0	10	0.8	0
Vegetation	0	0	0	50	1	2	54	0.926	0
Water Bodies	0	0	0	0	10	0	10	1	0
Wetland	0	2	0	0	0	8	10	0.8	0
Total	14	22	8	51	14	11	120	0	0
P. Accuracy	1	0.727	1	0.875	0.943	0.818	0	0.9	0
Kappa	0	0	0	0	0	0	0	0	0.864
2011									
Class	Agricultural	Barren Land	Built up	Vegetation	Water Bodies	Wetland	Total	U. Accuracy	Kappa
Agricultural	10	1	1	0	0	0	12	0.833	0
Barren Land	0	18	0	3	0	0	21	0.857	0
Built up	0	1	8	1	0	0	10	0.8	0
Vegetation	2	2	0	46	0	1	51	0.902	0
Water Bodies	0	0	0	0	10	0	10	1	0
Wetland	0	0	0	1	1	8	10	0.8	0
Total	12	22	9	51	11	9	114	0	0
P. Accuracy	0.833	0.818	0.889	0.902	0.909	0.889	0	0.877	0
Kappa	0	0	0	0	0	0	0	0	0.832
2020									
Class	Agricultural	Barren Land	Built up	Vegetation	Water Bodies	Wetland	Total	U. Accuracy	Kappa
Agricultural	21	1	0	2	0	0	24	0.875	0
Barren Land	1	8	1	0	0	0	10	0.8	0
Built up	1	0	10	1	0	0	12	0.833	0
Vegetation	1	0	1	51	1	0	54	0.944	0
Water Bodies	0	0	0	0	10	0	10	1	0
Wetland	0	0	1	0	0	9	10	0.9	0
Total	24	9	13	54	11	9	120	0	0

P. Accuracy	0.875	0.889	0.769	0.944	0.909	1	0	0.908	0
Kappa	0	0	0	0	0	0	0	0	0.874

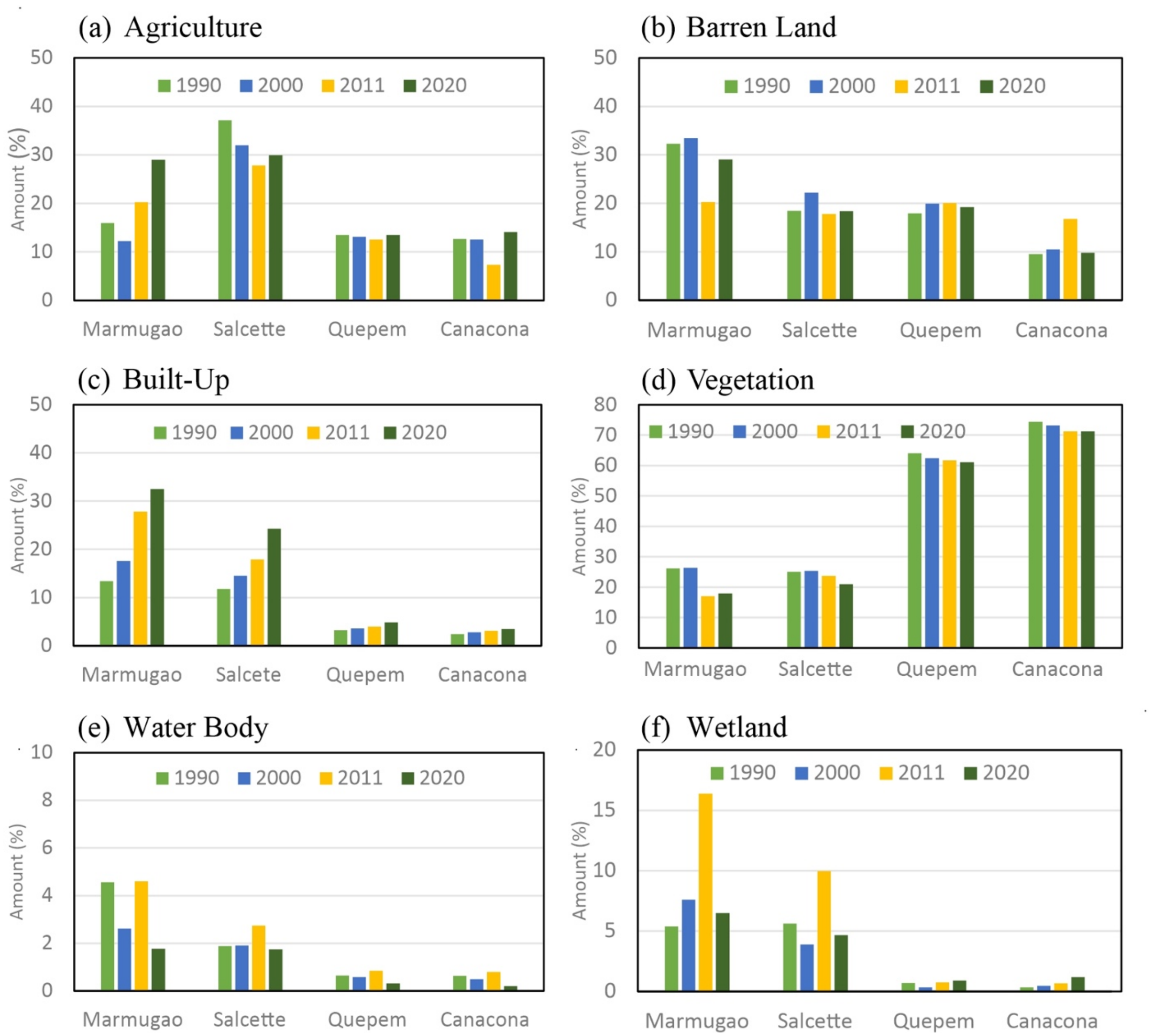

Fig-5.2 Bar graphs showing land-use wise decadal changes (in %) in each of the taluka(s) during the year 1990, 2000, 2011 and 2020.

Table-5.3 Amount of each land-use class (in sq. km) located at different Slope and Aspect categories for the year 2000 and 2020 in the study area.

Marmugao (2000)						
Slope	Agriculture	Built-Up	Barren land	Vegetation	Water body	Wetland

0-1	5.338	3.506	2.886	2.290	1.295	2.839
1-5	5.040	10.042	19.141	8.816	0.649	2.114
5-10	0.404	1.702	5.751	6.429	0.135	0.315
10-20	0.254	0.640	2.228	5.412	0.084	0.360
20-40	0.003	0.002	0.030	0.038	0.001	0.013
>40	0.000	0.000	0.000	0.000	0.000	0.000
Aspect	Agriculture	Built-Up	Barren land	Vegetation	Water body	Wetland
Plain	0.229	0.183	0.278	0.117	0.419	0.455
North	0.976	1.739	3.895	3.156	0.203	0.789
Northeast	1.680	1.773	3.401	3.735	0.351	0.846
East	1.538	1.718	3.362	2.419	0.214	0.545
Southeast	1.188	1.445	2.630	1.809	0.089	0.388
South	1.453	2.079	4.065	2.854	0.059	0.426
Southwest	1.487	2.491	4.171	3.137	0.254	0.614
West	1.418	2.174	4.139	2.847	0.339	0.707
Northwest	1.052	2.293	4.093	2.923	0.197	0.700
Salcete (2000)						
Slope	Agriculture	Built-Up	Barren land	Vegetation	Water body	Wetland
0-1	28.626	13.748	13.008	23.273	4.285	8.143
1-5	44.239	26.724	38.195	39.921	1.542	3.614
5-10	3.078	2.967	10.968	14.266	0.031	0.132
10-20	2.181	1.227	5.773	17.764	0.001	0.023
20-40	0.067	0.013	0.047	2.309	0.000	0.000
>40	0.000	0.000	0.000	0.000	0.000	0.000
Aspect	Agriculture	Built-Up	Barren land	Vegetation	Water body	Wetland
Plain	1.222	0.690	0.621	0.978	1.059	1.616
North	7.418	4.918	7.533	11.757	0.398	1.024
Northeast	9.680	4.697	8.244	13.584	0.872	1.738
East	11.347	4.229	7.436	12.745	0.619	1.240
Southeast	9.874	4.479	6.997	9.615	0.381	1.104
South	9.997	6.103	8.675	9.196	0.411	1.087
Southwest	10.592	6.568	10.388	14.113	0.962	1.467
West	9.662	6.526	9.003	13.812	0.800	1.386
Northwest	8.380	6.471	9.072	11.743	0.342	1.266
Quepem (2000)						

Slope	Agriculture	Built-Up	Barren land	Vegetation	Water body	Wetland
0-1	3.574	1.229	4.435	9.958	1.113	0.270
1-5	25.362	8.563	40.757	56.887	0.450	0.667
5-10	7.233	1.499	14.765	49.279	0.155	0.133
10-20	2.074	0.300	4.293	70.661	0.103	0.040
20-40	0.165	0.010	0.150	18.751	0.000	0.034
>40	0.000	0.000	0.000	0.000	0.000	0.000
Aspect	Agriculture	Built-Up	Barren land	Vegetation	Water body	Wetland
Plain	0.312	0.097	0.438	1.080	0.927	0.023
North	5.317	1.528	10.266	40.979	0.131	0.133
Northeast	4.915	1.322	8.229	32.420	0.228	0.187
East	4.309	1.164	6.711	20.586	0.148	0.164
Southeast	4.624	1.288	5.825	17.559	0.059	0.088
South	4.827	1.265	5.795	21.182	0.043	0.117
Southwest	4.534	1.381	7.160	19.764	0.087	0.160
West	4.225	1.663	9.369	21.440	0.096	0.118
Northwest	5.334	1.885	10.636	30.526	0.085	0.158
Canacona (2000)						
Slope	Agriculture	Built-Up	Barren land	Vegetation	Water body	Wetland
0-1	3.733	1.006	3.339	3.980	0.176	0.413
1-5	28.636	5.998	32.937	75.373	0.378	0.811
5-10	11.501	1.856	15.183	78.202	0.362	0.214
10-20	4.426	0.592	3.790	82.059	0.488	0.137
20-40	0.693	0.239	0.510	31.180	0.180	0.174
>40	0.002	0.018	0.012	0.159	0.008	0.016
Aspect	Agriculture	Built-Up	Barren land	Vegetation	Water body	Wetland
Plain	0.233	0.054	0.340	0.710	0.079	0.093
North	3.604	0.917	7.378	29.803	0.119	0.241
Northeast	4.013	0.774	5.101	28.998	0.111	0.170
East	4.793	0.791	3.840	24.727	0.028	0.096
Southeast	7.291	1.105	5.518	31.862	0.091	0.141
South	10.484	1.767	7.889	45.242	0.165	0.129
Southwest	9.046	1.859	9.979	47.429	0.374	0.228
West	5.394	1.449	8.606	32.363	0.288	0.319
Northwest	4.097	0.975	7.114	29.863	0.257	0.339

Marmugao (2020)						
Slope	Agriculture	Built-Up	Barren land	Vegetation	Water body	Wetland
0-1	6.002	5.583	0.991	2.820	1.022	1.723
1-5	11.605	18.877	7.583	5.546	0.362	1.802
5-10	5.340	3.287	1.986	3.567	0.033	0.525
10-20	2.764	1.302	0.477	3.769	0.063	0.601
20-40	0.021	0.029	0.000	0.016	0.002	0.017
>40	0.000	0.000	0.000	0.000	0.000	0.000
Aspect	Agriculture	Built-Up	Barren land	Vegetation	Water body	Wetland
Plain	0.303	0.354	0.104	0.214	0.402	0.298
North	2.921	3.302	1.457	2.117	0.089	0.870
Northeast	4.183	3.056	1.223	2.275	0.198	0.853
East	3.129	3.074	1.123	1.900	0.166	0.405
Southeast	2.652	2.336	0.984	1.268	0.057	0.249
South	3.436	3.971	1.303	1.971	0.023	0.224
Southwest	3.713	4.504	1.345	2.024	0.180	0.377
West	2.874	4.227	1.782	1.905	0.270	0.559
Northwest	2.551	4.205	1.712	2.075	0.079	0.640
Salcete (2020)						
Slope	Agriculture	Built-Up	Barren land	Vegetation	Water body	Wetland
0-1	36.787	23.531	5.631	12.048	3.924	9.149
1-5	65.616	44.561	17.701	20.294	1.415	4.637
5-10	9.079	4.201	5.204	12.637	0.025	0.293
10-20	6.018	1.803	1.923	17.076	0.006	0.144
20-40	0.213	0.026	0.015	2.167	0.000	0.016
>40	0.000	0.000	0.000	0.000	0.000	0.000
Aspect	Agriculture	Built-Up	Barren land	Vegetation	Water body	Wetland
Plain	1.574	1.104	0.234	0.575	0.976	1.726
North	11.820	7.645	3.211	8.748	0.396	1.225
Northeast	15.190	7.903	3.413	9.307	0.848	2.150
East	15.978	7.689	3.305	8.441	0.579	1.624
Southeast	13.542	7.920	3.311	6.109	0.348	1.223
South	13.595	10.221	3.890	6.223	0.350	1.188

Southwest	16.571	11.124	4.723	9.085	0.778	1.805
West	15.697	10.879	3.984	8.213	0.708	1.699
Northwest	13.773	9.592	4.401	7.506	0.375	1.626
Quepem (2020)						
Slope	Agriculture	Built-Up	Barren land	Vegetation	Water body	Wetland
0-1	8.547	1.911	2.215	6.534	0.892	0.477
1-5	43.182	10.804	13.227	63.831	0.073	1.540
5-10	10.982	1.634	3.369	56.567	0.026	0.467
10-20	2.809	0.336	0.648	73.382	0.001	0.291
20-40	0.157	0.072	0.008	18.723	0.000	0.148
>40	0.000	0.000	0.000	0.000	0.000	0.000
Aspect	Agriculture	Built-Up	Barren land	Vegetation	Water body	Wetland
Plain	0.669	0.138	0.136	0.968	0.821	0.139
North	8.808	1.908	3.168	44.071	0.017	0.373
Northeast	8.050	1.613	2.269	34.829	0.053	0.480
East	6.840	1.472	1.676	22.631	0.052	0.406
Southeast	7.819	1.633	1.746	18.003	0.006	0.229
South	7.987	1.697	1.548	21.784	0.010	0.199
Southwest	7.139	1.887	2.103	21.665	0.022	0.265
West	8.259	2.027	3.162	23.134	0.020	0.307
Northwest	10.087	2.364	3.692	31.959	0.006	0.507
Canacona (2020)						
Slope	Agriculture	Built-Up	Barren land	Vegetation	Water body	Wetland
0-1	4.132	1.486	1.564	4.810	0.269	0.380
1-5	32.743	7.990	13.154	88.371	0.234	1.630
5-10	13.391	2.335	3.155	87.390	0.082	0.955
10-20	3.810	0.911	0.283	85.623	0.116	0.752
20-40	0.823	0.522	0.046	30.919	0.015	0.659
>40	0.013	0.024	0.002	0.136	0.000	0.035
Aspect	Agriculture	Built-Up	Barren land	Vegetation	Water body	Wetland
Plain	0.262	0.107	0.159	0.794	0.134	0.052
North	5.141	1.133	2.678	32.524	0.048	0.535
Northeast	4.585	0.970	1.467	31.655	0.078	0.404
East	4.931	1.002	0.825	27.289	0.062	0.164
Southeast	7.545	1.640	1.372	35.136	0.075	0.234

South	10.380	2.543	1.926	50.454	0.075	0.296
Southwest	9.837	2.600	3.461	52.183	0.102	0.734
West	6.827	1.926	3.508	35.086	0.053	1.020
Northwest	5.389	1.268	2.808	32.211	0.073	0.893

5.3 Result Interpretation

Fourteen villages constituting the Mormugao taluka are Arossim, Cansaulim, Chicalim, Chicolna, Cortalim, Cuelim, Dabolim, Issorcim, Pale, Quelossim, Sancoale, São Jacinto and Sao Jorge Islands, and Velsao. Settlement areas dominate most regions in Chicolna, Sancoale, Dabolim, and Vasco-da-Gama. (Fig. 5.1(a) & Table 5.1) provide an overview of the computations. Overall, the taluka had the highest percentage of barren land at 32% and 33.5% during 1990 and 2000, reduced by 58.8% and 11.2% during 2011 and 2020, which was used to meet the increasing demand for settlement and commercial ventures. Build-up areas increased consistently from 13.4% in 1990 to 32.5% in 2020 due to demand for housing brought about by growth in Mormugao Port Trust, Dabolim airport, Vasco-da-Gama railway station, naval residential quarters in and around Dabolim, Verna industrial estate, and other business ventures. An increase in settlement areas happened from 2011 onwards, mainly in Dabolim, Mormugao, and coastal belts due to increased population and tourism activities. Agriculture activities, mostly carried out in Cansaulim, Cortalim, Pale, Quelossim, and Velsao, have increased from 16% in 1990 to 29%, with a drop of -23.56 in 2000. Vegetation which was nearly 23% between 1990 and 2000, dropped to about 17% from 2011 onwards, which could be attributed to its cut-down to make way for a four-lane highway linking the port at Mormugao to Verna and also sacrificed for settlement areas. Water bodies occupy the least area, which includes lakes. Areas of water bodies which were 4.57% in 1990, dropped to 1.77% in 2020, possibly to filling up with debris to change land use by selfish elements. Wetland areas, mostly in Sancoale and Cortalim, have increased from 5.39% in 1990 to 16.4% in 2011, with a drastic fall of 60.4% in 2020 which can be attributed to encroachment for selfish motives.

In Salcete taluka, agriculture is a widely practiced occupation, with rice and vegetables grown in the monsoon and winter seasons, respectively. With the highest percentage of area under cultivation in 1990 at 37.16%, it gradually fell to 29.9% in 2020. The vegetation area percentage dropped from 25% in 1990 to 29.9% in 2020. On the other hand, buildup areas almost doubled from 11.8% in 1990 to 24.2% in 2020, which is reflected in-and-around Margao city, which is the commercial capital of Goa and also along the coastal belt due to increased tourism activities from Majorda to Betul (Fig. 5.1(b) & Table-5.1). The percentage area of water bodies rose from 1.88% in 1990 to 2.75% in 2011 but was reduced in 2020 by 36.3%. Salcete has the highest wetland area among the four talukas considered in this work, which decreased from 17.26 sq. km. in 1990 to 11.97 sq. km in 2000; it increased to 30.59 sq. m and finally dropped by 53.2% in 2020. These changes are related to population pressure on the natural resources.

Quepem taluka is a hilly terrain with more than 60% forest area covering 207.4 sq. km. Over the 40 years, the vegetation has decreased by about 1%. Agriculture is practiced in over 13.5% of the area, which has increased by 7.56% in 2020. The percentage of barren land increased marginally, possibly due to deforestation cause by landslides during monsoon. The built-up area percentage has increased gradually due to the double tracking of the railway line and other commercial activities. The percentage of water bodies' area changed largely between 2011 and 2020, while the wetland area percentage dropped during this period (Fig.-5.1 (c) & Table-5.1).

In Canacona taluka, the percentage of agriculture area dropped by 41.8% during 2011, which doubled in size to 55.06 sq. km. in 2020. The barren land percentage showed a marginal increase from 1990 to 2011, which dropped by 41.59% in 2020. This drop is attributed to using some of the barren areas for agriculture. The buildup area percentage gradually increased from 2.44% in 1990 to 3.45% in 2020, particularly in the residential areas of Poingunim, Agonda, and Bali, in the coastal belt from Agonda to Galgibag and also due to the widening of the highway. Among all the talukas considered in this study, Canacona taluka had the highest vegetation cover of 290.2 sq. km. in 1990, dropping to 277.9% in 2020, which could be attributed to anthropogenic activities. The percentage of the area of water bodies also decreased from 0.63% in 1990 to 0.2% in 2020. The percentage of wetland areas increased four folds from 0.34% in 1990 to 1.2% in 2020 (Fig.-5.1 (d) & Table-5.1).

Chapter-6

Multi-Temporal Anthropogeomorphic Impact Assessment

6.1 Background: A Subject of Paramount Importance

In contemporary times, human activities as a catalyst for geomorphic changes are comparable to other natural geomorphic processes. While it falls behind endogenetic forces in terms of energy released, its dominance over exogenetic forces is undeniable (Lozy, 2010). Human civilization has witnessed substantial growth in tandem with technological advancements. Over the past 10,000 years, a significant portion of the global surface has undergone transformation from natural to manmade ecosystems, termed "Metahemerobic" (Bastian and Schreiber 1994), albeit at a modest rate until the 19th century. Technological advancements equipped humans with diverse tools for modifying the Earth, but it was the 19th-century industrial revolution that dramatically enhanced human capabilities (Lucas 2003), transforming them into highly active geomorphic agents (McCloskey 2003). Land surface transformation from "Ahemerobic" to "Metahemerobic" through anthropogenic measures occurs both indirectly (e.g., road construction leading to gully erosion on the sides) and directly (e.g., landfills, open-cast mining pits, etc.) (Rosza, 2020).

Whether through indirect or direct anthropogenic land transformation strategies, approximately 75% of ice-free areas and 66% of maritime regions have already undergone modification (WWF, 2020). Before the turn of the millennium, 2 million km2 of land had already been developed. Out of this, 15 million km^2 was converted into plantations and arable land, while 35 million km^2 was transformed into pasture areas (Loh & Wackernagel, 2004). Additionally, human activities have exploited 38 million km^2 of forest (Rozsa, 2007). The considerable scale of anthropo-geomorphic processes is evident through extensive land modification (AGP). Furthermore, the intense nature of AGP not only affects geomorphic assets but also heightens geohazard vulnerability (Pikelj and Juracic, 2013), disrupting the dynamic balance between landforms and processes. The origins of this transition can be traced back to the industrial revolution, human population growth, and rapid technological advancements aimed at meeting the world's ever-increasing economic needs (Weber and Sciubba, 2019).

Hooke (1994 & 2000), and Haff (2003) estimated that the amount of earth moved annually was about 111 billion/t/yr when all natural processes were considered, compared to 129 billion/t/yr by anthropic induced activities. This indicates that humans have unquestionably become the most powerful agent of geomorphic modifications even more than natural processes. Unprecedented growth in AGP stature has allowed it to carve out its own area of study in science. Anthropo-geomorphology, which is defined as "an applied science which studies the human role in creating geomorphologic landforms and modifying the geomorphological processes such as erosion, transportation, and deposition," covers the anthropogenic modifications of geomorphic landforms and processes (Szabo, 2010). This field evolved during the 1960s, when there was a paradigm change toward a quantitative approach and a focus on researching geomorphologic processes (Rosza, 2007).

In this context, the imperative to assess the impact of Anthropogenic Geomorphic Processes (AGP) is more crucial than ever, given the relentless advancement of technology and the burgeoning global population that continuously exerts pressure on extensive land resources and energy consumption. This undeniable trend has significantly altered natural geomorphology over the past century and is poised to persist in the near future.

While substantial research has been conducted in the field of anthropogeomorphology since the 1960s, pioneering efforts can be traced back to Marsh in 1864 (Rozsa, 2007). According to Rozsa (2007), Nir's 'Index of Potential Anthropogenic Geomorphology,' published in 1983, stands as a highly acclaimed model for quantifying human impact on geomorphology due to its simplicity and widespread availability of data. However, certain notions within Nir's index are subject to debate, such as the generalization of topographic and climatic factors for a larger area, assigning equal weightage to climate and terrain, and focusing solely on urban population (Rozsa, 2007). The model faces criticism for its inadequacy in quantifying AGP at the micro-level due to generalized parameters (Nigam et al., 2023). These parameters, being dynamic, undergo changes at different spatio-temporal scales, contributing to the ongoing debate in the field.

Numerous studies have tried to ranked or grade the geomorphic landforms according to the AGP impact modifications (Lausch and Herzog, 2002) along with their hazardous nature (Borgatti and Soldati, 2005). While some have come up with the quantification of anthropic impact upon geomorphic landforms in a comprehensive manner (Verstraeten et al. 2009; Vanwalleghem et al. 2017), most of others have covered often a specific type of anthropogenically impacted landform but in detailed manner, as for coastal and estuarine areas (Pye and Blott 2014; Ferrer-Valero et al. 2017), mining landforms (Harnischmacher and Zepp 2014; Byizigiro 2015; Dulias 2016), catchment areas (Slabá et al. 2015), and agriculture (Martinez-Casasnovas 2003; Houben et al. 2006; Chartin et al. 2013) in addition the impact quantification of transportation upon landforms has also been studied (Sofia et al. 2016).

With the growing body of work in the subject, a few review articles (Price et al. 2011; Brown et al. 2017) and comprehensive books (Szabó et al. 2010; Goudie and Viles 2016; Das et al., 2020) have appeared. Mapping of anthropogenically impacted landforms has also been carried out using a holistic approach that incorporates the underlying notion of earth movement. Hooke (1999) made a pioneering attempt in this area, calculating and mapping the amount of earth movement per year in the United States, while Pirkhoffer (2009) mapped anthropogenically impacted landforms in Hungary based on different land use categories. Recently, some pioneering attempts have been made to use geospatial technology to determine human impact on landforms using landscape metrics and the extent of anthropogenic modification (Tarolli, 2014; Tarolli et al., 2017).

Nonetheless, despite much research in the field, there is no universally acknowledged strategy or method for quantifying the influence of human activities on geomorphology (Rozsa, 2007).

The current study argues that there are still additional cross-disciplinary characteristics that play a crucial role in defining the AGP impact, and so they must be included to quantify the anthropo-geomorphic impact. Demography combined with geomorphometric factors, for example, are still unexplored paths. Because areas with a high population density and low socioeconomic development are more likely to exert pressure on the earth's surface than places with a low population density, higher income, and superior development. Similarly, local geomorphological characteristics such as rock type, slope, aspect, hazards, and the like play an essential role in the formation of an ecumene in a given area.

As a result, the current study presents a novel methodology for quantifying a region's AGP impact by assessing the pressure exerted by the ecumene and climate, as well as the fragility of local geomorphology. It uses a case study of coastal tracts in the South Goa district which have been rapidly transformed into high density human settlements since the turn of the century to demonstrate the frameworks' usefulness.

6.2 Result

Table-6.1 Results of Anthropogeomorphic Impact at ecumene for the year 2000 and 2020 in the study area.

Taluka	Year	Degree of Anthropic Pressure	Degree of Erosive susceptibility	AGI@E
Marmugao	2000	26.14	12.96	338.77
Marmugao	2020	27.23	13.16	358.34
Growth (%)		4.16	1.54	5.77
Salcete	2000	21.81	10.52	229.44
Salcete	2020	22.88	12.71	290.80
Growth (%)		4.9	20.81	26.74
Quepem	2000	11.47	7.42	85.10
Quepem	2020	11.95	8.69	103.84
Growth (%)		4.18	17.11	22.02
Canacona	2000	8.76	8.36	73.40
Canacona	2020	8.78	8.71	76.29
AGI@E Growth (%)		0.22	4.18	3.93

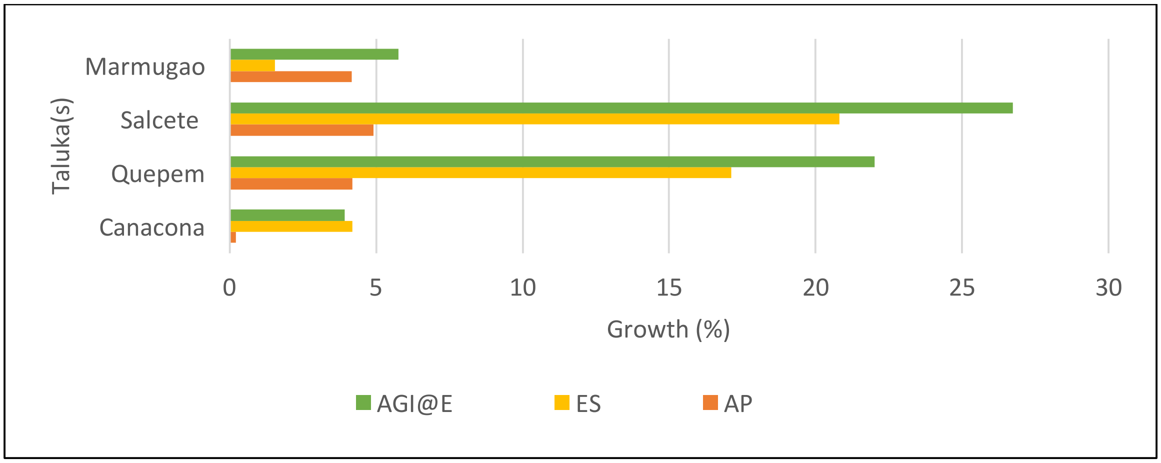

Fig-6.1 Plot showing the growth (%) encountered in the Amount of Anthropic Pressure (AP), Amount of Erosive Susceptibility (ES) and the AGI@E in different taluka(s) between 2000 and 2020.

6.3 Results Interpretation

The Nigam-Kotha model of AGI@E results (Fig.-6.1 & Table-6.1) of Marmugao were found to be the highest among its peers (338.77 & 358.34) during both the year (2000 & 2020). Salcete follows Marmugao with the AGI@E (229.44 & 290.80) during the similar years but showing fastest growth (26.74%) among all between the period 2000-2020. According to the model, both the taluka(s) are having severe impact upon the geomorphology. On the other hand, Quepem and Canacona have been found to be in their own league with Quepem (85.10 & 103.84) and Canacona (73.40 & 76.29) AGI@E during 2000 and 2020 respectively, having moderate AGP impact.

Likewise, the amount of anthropic pressure has been found to be highest in Marmugao (26.14 & 27.23) followed by Salcete (21.81 & 22.88) (Severe AGP impact) and Quepem (11.47 & 11.95) and Canacona (8.76 & 8.78) (moderate impact) during 2000 and 2020 which clearly suggests the negative significance of urbanization on geomorphology.

Similar trends have been observed for the erosive susceptibility where Marmugao (High AGP impact) tops the list, closely followed by Salcete (High AGP impact). Again, Quepem and Canacona have been found to be in a different league (Moderate impact) suggesting stable geomorphological aspects, resulting in less, compared to the remaining taluka(s). However, all the taluka(s) have shown positive growth trend between 2000 and 2020 in terms of anthropic pressure, erosive susceptibility and the AGI@E.

Chapter-7

Multi-Temporal Beach Litter Assessment

7.1 Background: A Major Environmental Concern due to Human Footprints

The coastal regions worldwide, recognized as highly productive environments supporting diverse marine life, have been integral to human settlements throughout history (Neumann et al., 2015). This longstanding human presence has given rise to some of the most significant urban centers along the coast (Griggs, 2020), contributing to the generation of substantial anthropogenic waste (Creel, 2003; McLachlan et al., 2013; Duarte et al., 2020; Grases et al., 2020). The disposal of land-generated litter into the sea occurs through various channels, including rivers, sewerage, wind, waves, currents, and spillage (William and Buitrage, 2019). Widespread and often disastrous for marine life and ecosystems, this litter, predominantly composed of plastic (>80%) in marine environments, has caused irreversible damages (Gallo et al., 2017; IUCN, 2020). To understand the spatial-temporal variations and assess the impact of litter pollution on the environment, numerous researchers have engaged in the study of marine litter (Xanthos and Walker, 2017; UNEP, 2017; Schnurr et al., 2018; Noelia et al., 2018; Mansui et al., 2020; Bellou et al., 2021; Morales-Caselles et al., 2021).

The increased awareness and growing concern surrounding the impacts of plastic pollution have spurred numerous researchers to delve into studies on marine litter, aiming to comprehend its sources and potential environmental implications. India, marked by rapid coastal development, a burgeoning beach tourism industry, and boasting some of the world's largest river systems, emerges as a significant contributor to marine litter. Investigations on litter monitoring assessments conducted across various segments of the Indian coastline unveil that inefficient waste management, especially in coastal areas, combined with population behavior towards waste disposal, serves as a primary cause of marine litter (Behera et al., 2021; Jayasiri et al., 2013; Jelil, 2013; Sharma and Pandey, 2020; Manickavasagam et al., 2020; Manickavasagam et al., 2021; Kaladharan et al., 2017, 2020; Vaz et al., 2017; Sridhar et al., 2007; Sulochanan et al., 2014; Sulochanan et al., 2019; Daniel et al., 2017; Ashwini and Varghese, 2020; Kaviarasan et al., 2020; Ramakritinan et al., 2015; Kumar et al., 2016; Veerasingam et al., 2016; Karthik, et al. 2018; Sathish et al., 2019; Jeyasantha et al., 2020; Vidyasakar et al., 2020; Dharani et al., 2003; Krishnakumar et al., 2020; Thorat et al., 2023).

In a recent study, Kaladharan et al. (2017) underscored the pivotal role of coastal tourism in contributing to beach litter. Goa, renowned as one of the world's most popular tourist destinations, not only stands out for its vibrant tourism industry but also registers the highest amount of beach litter, including the greatest quantity of plastic among all Indian coastal states. Leveraging the unique circumstance presented by the COVID-19 pandemic, this study seized the opportunity to monitor and assess beach litter along Goa's coastline. The survey covered eight different beaches, four in each of the north and south districts, during two distinct periods: May 2020, marked by a standstill in tourism-related activities due to the COVID-19 lockdown, and January 2021, a period of peak tourism activity in Goa under normal circumstances.

The objective of this study is to measure beach litter during the absence of tourism activity resulting from the lockdown and subsequently compare it with the peak tourism season. The aim is to gain insights into the impact of tourism on litter generation along the Goa coast. This chapter, in particular, delves into a multi-temporal assessment of beach litter, exploring its evolution, spatial distribution, implications on coastal ecosystems and most importantly, its occurance as the proxy of human presence.

Table-7.1 Characteristics of the Beaches in the study area.

S. No	Beach	Location	Sediment Type	Significance
a.	Baina, Marmugao	15.392124 N, 73.806836 E	Fine to medium Sand	Urban beach located on the outskirts of the Vasco-da-Gama city, which is known for fishing activity. Frequently visited by locals. Litter is generated by many households situated on the shoreside.
b.	Velsao, Marmugao	15.354617 N, 73.884208 E	Fine sand	Part of the longest continuous sandy beach stretch in south Goa is used for fishing using canoes and visited by locals. No commercial activities (Shrivastava, 2020).
c.	Colva, Salcete	15.276226 N, 73.913626 E	Fine sand	The most popular and crowded beach in South Goa which is known as the queen of beaches. Lots of commercial activity on the shore side (India.com, 2020).
d.	Palolem, Canacona	15.011469 N, 74.021420 E	Fine sand beach	World-renowned beach which is popular among high-end international tourists. Known for water sports. Shacks crowded on the shoreside (Oliver Wakefield, 2018)

Fig- 7.1. Visualization of the UAV (Drone) reconnaissance survey for detecting beach litter hotspots in the study area for the selection of beaches (a. Baina, b. Velsao, c. Colva, and d. Palolem (The insets display complete stretch of the beaches).

7.2 Results

Table-7.2 Litter density at different beach locations during May 2020 and January 202.

Beach	Total Area (sq. m)	May 2020		January 2021		Difference
		Total litter (g)	Litter (g/m^2)	Total litter (g)	Litter (g/m^2)	Change in Litter (Jan 2021 w.r.t. May 2020, %)
Baina	9800	9936	1.01	37725	3.85	+281.18
Velsao	17100	6978	0.41	16563.15	0.97	+136.58
Colva	14100	16289	1.16	38308.2	2.72	+134.48
Palolem	7700	2103	0.27	23711	3.08	+1040.74

Table-7.3 Per capita share of beach litter among the population of respective coastal villages.

Beach		May 2020		January 2021		Difference
	Village population	Total litter (g/m^2)	Litter per person (kg/head)	Total litter (g/m^2)	Litter per person (kg/head)	Increment in Jan 2021 w.r.t. May 2020 (%)
Baina	77243	9936	0.13	37725	0.49	+276.92
Velsao	1520	6978	4.59	16563.15	10.90	+137.47
Colva	3141	16289	5.19	38308.2	12.20	+135.06

Palolem	4547	2103	0.46	23711	5.21	+1032.60

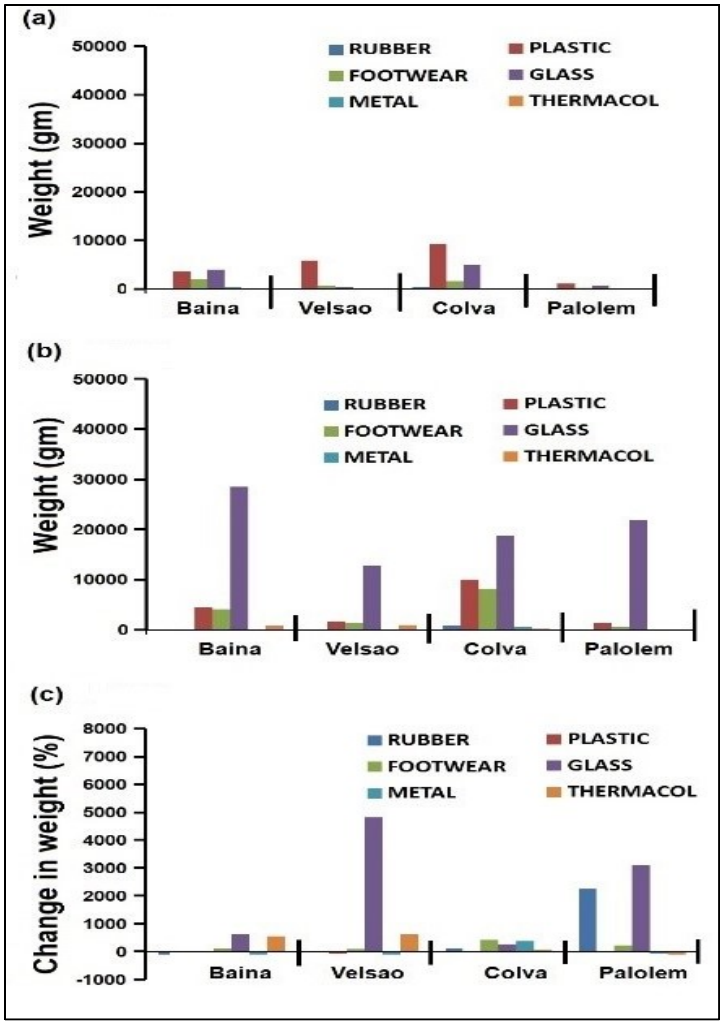

Fig- 7.2 Different litter categories during lockdown (May 2020) and unlock (January 2021), cumulative of all transects at each beach.

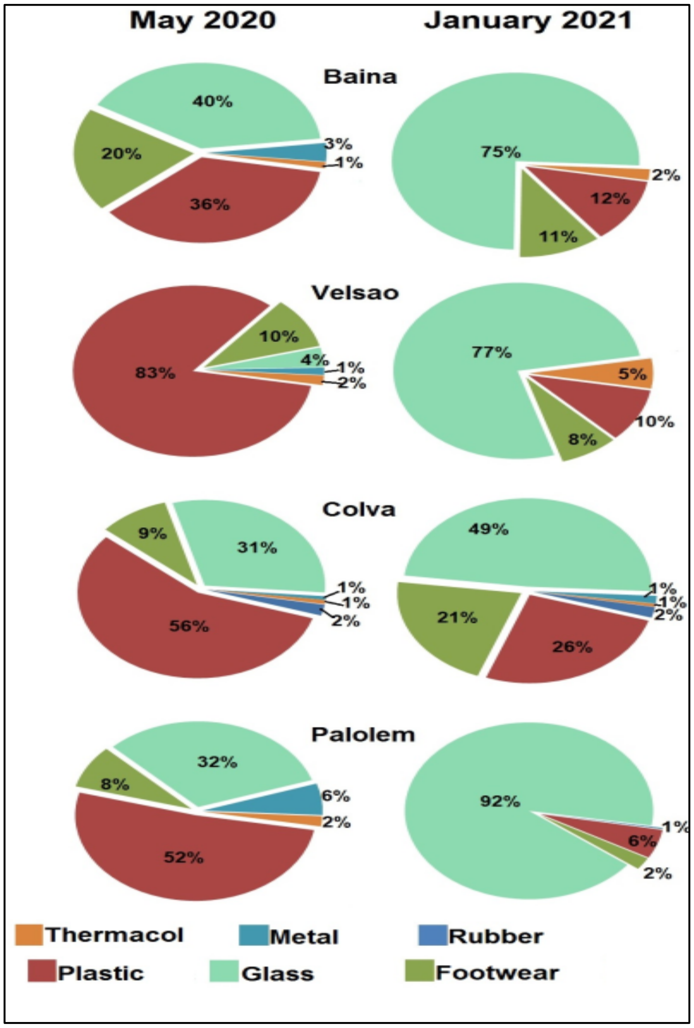

Fig- 7.3 Breakup of beach litter categories at each beach during lockdown (May 2020) and unlock (January 2021).

Table-7.4 Interpreted Color coding indicator for beach cleanliness.

Beach	Litter (g/m^2) May 2020	Litter (g/m^2) January 2021
Baina	1.01	3.85
Velsao	0.41	0.97
Colva	1.16	2.72
Palolem	0.27	3.08

Table-7.5 ANOVA results of litter data at the selected beaches in the study area. The relatively higher *F* value (2.13821) in the table, verifies the significant increase in beach litter from lockdown to unlock periods. The litter types: Glass, Footwear, and plastic, show a substantial variation contributing towards total litter (also refer to Fig.-7.3).

	Test of SS Whole Model vs. SS Residual										
	Multiple R	**Multiple R^2**	**Adjusted R^2**	**SS**	**df**	**MS**	**SS**	**df**	**MS**	**F**	**p**
Rubber	0.345	0.119	0.056	723775.6	1	723775.5	5347601.1	14	381971.5	1.895	0.190
Plastic	0.123	0.015	-0.055	2133414.4	1	2133414.4	139556631.8	14	9968330.8	0.214	0.651
Footwear	0.366	0.134	0.072	9610426.3	1	9610426.3	62121562.6	14	4437254.5	2.166	0.163
Glass	0.697	0.486	0.449	1495674311.9	1	1495674311.9	1581567547.1	14	112969110.5	13.240	0.003
Metal	0.160	0.025	-0.044	36130.4	1	36130.4	1381267.3	14	98662.0	0.366	0.555
Thermocal	0.369	0.136	0.074	365233.2	1	365233.2	2318580.2	14	165612.9	2.205	0.160
Total	0.676	0.458	0.419	1980219206.1	1	1980219206.1	2346856778.4	14	167632627.0	11.813	0.004
Litter Density	0.474	0.225	0.170	20.0	1	20.0	69.0	14	4.9	4.067	0.063

EFFECT	**Multivariate Tests of Significance: Sigma-restricted parameterization**					
	Test	**Value**	**F**	**Effect**	**Error**	**p**
Intercept	Wilks	0.077425	17.87359	6	9	0.000157
Period	Wilks	0.412291	2.13821	6	9	0.146923

Fig-7.4 Scatter Matrix Plot of Litter variables for the Lockdown and Unlock periods.

7.3 Result Interpretation

The beaches in the study area mainly showed an increase in litter after lockdown. For Baina, except for a decrease in metal (100%), all items exhibited an increase with glass, thermocol, and footwear by 624%, 552%, and 107%, respectively. For Velsao beach, the glass litter was highest (4818 %), followed by thermocol (621%) and footwear (85%). Interestingly, plastic and metal litter were correspondingly reduced by 72% and 95%. Colva beach exhibited an increase in all the categories of litter ranging from 8% (plastic) to 429% (footwear). Glass litter increased (3103%) followed by rubber (2140%) and footwear (213%) for Palolem beach, while metal and thermocol showed a decrease by more than 70% (Table-7.2).

For plastic litter exceeding 2 kg, Colva beach ranked top, followed by Baina (Table-7.2). For footwear litter exceeding 1 kg for both periods, the assessment found at Colva, Baina. Glass litter exceeding 1 kg for all beaches in post-lockdown. Packaging materials like thermocol, Velsao, Baina, and Colva exhibited more than 0.1 kg of litter.

Beach-wise variation in litter categories is further interpreted statistically to understand the relationship between the litter categories within and among beaches. Untreated raw data of beach litter categories are used as input data for the statistical interpretation (Schulz et al., 2013). The summary of the relationships between all litter variables is presented in a scatterplot matrix (Fig.

7.4), a graphical plot equivalent of the correlation matrix. The scatterplot portrays a clear separation of lockdown versus unlock periods. Further, the matrix plot shows the relationship (graphically) of each of the litter variables. The litter data was subjected to statistical analyses ANOVA to understand the changes quantitatively during and post-lockdown periods.

Chapter-8

Multi-Temporal Air Quality Analysis

8.1 Background

While the industrial revolution marked a monumental achievement in technology, societal progress, and enhanced services, it also introduced significant quantities of pollutants into the water we drink, the air we breathe, and the soil supporting plant growth. Environmental pollution and degradation have evolved into a global public health concern, encompassing multifaceted dimensions such as social, economic, and legislative considerations. The surge in industrialization, escalating urbanization, and associated anthropogenic activities have reached unprecedented levels worldwide, precipitating a critical scenario in urban and semi-urban regions, particularly in developing countries (Sharma and Patil, 2016). Scientific evidence underscores the prevalence of poor air quality (AQ) in both megacities and small towns across Asia (IAQP, 2010). Anthropogenic air pollution stands as one of the most significant global public health hazards, contributing to approximately 9% of annual deaths (Louati et al., 2018; Son and Louati, 2016). Deterioration in urban AQ emerges as a paramount concern amidst environmental degradation in urban and semi-urban areas, directly impacting human health (Tandon et al., 2008) and, consequently, the overall quality of life (Dadhich et al., 2018). Air pollution, recognized as one of the top five global risk factors for mortality (HEI, 2019), is linked to compromised lung function, cardiovascular diseases, neuropsychological issues, and, critically, loss of life (Gupta, 1999; WHO, 2005). In this chapter, we delve into a multi-temporal analysis of air quality, exploring its evolution, spatial distribution, and the far-reaching consequences on human health and well-being.

Air pollution comprises of various gaseous and dust particles such as Carbon dioxide (CO_2), Sulphur dioxide (SO_2), Oxides of Nitrogen (NO_x), Carbon Monoxide (CO), Ozone, Methane, Particulate Matter (PM), etc. Their major sources are power stations, the chemical and fertilizer industries, metallurgical and other industrial plants, construction activities, open-cast mining, fossil fuel-based vehicles, and municipal incineration. These possess different intensities of adverse effects on human health. SO_2, which is formed from the combustion of fossil fuels and thermal power stations (Darryl, 2017), causes significant health complications such as substantial reduction in lungs efficiency, Asthma, Inflammation, and irritation in the respiratory tract and eyes, cardiovascular disease, etc. PM is another ubiquitous air pollutant dominating the urban and semi-urban regions, which occurs as a cocktail of solids and liquid particles of various sizes floating in the air. The primary source of PM is dust particles, diesel soot, while the gaseous form of sulfate and nitrate transform physic-chemically and become the secondary source of the PM (Limaye and Salvi, 2010). The PM has different effects on human health depending on the size

(Kim et al., 2015). The $PM_{2.5}$ can remain in the atmosphere for a longer time (days to weeks); as such, they can be transported over longer distances. These have a very high level of penetrability in the lungs, which can eventually cause premature deaths. The coarser PM_{10} quickly settle down due to gravity or are washed out by precipitation.

Pollutants have differences in chemical and physical properties, which cause inconsistency in their capacity to produce toxic effects. According to GBD MAPS Working Group (2018), $PM_{2.5}$ pollutants was responsible for 0.99 million and 0.78 million in 1990 and 2016, respectively. India has an even more grim situation in terms of pollution Exceedance Factor (EF). During 1998, 27% of 640 districts of India were found to be above the annual standard value of 40 $\mu g/m^3$ of air pollution, which deteriorated even more in 2010 when 45% of the Indian districts had air pollution that exceeded the annual standard value (Guttikunda et al. 2019). It is estimated that 0.62 million deaths occurred due to high air pollution and deteriorating AQ in India (Lim *et al.*, 2012). In 2019, nine cities from India were under the top 10 most polluted cities in the world ranking list (Yuda 2019).

Goa is the smallest Indian state located on the west India coast and forms a narrow strip of low land sandwiched between the Arabian Sea in the west and the Western Ghats in the east. The majority of the state has been under a good amount of vegetation; however, since the past four decades, haphazard urbanization and rapid economic growth due to extensive tourism activities, open-cast mining, and construction activities have degraded the environment (Nigam et al., 2020). The compounded annual growth rate of Green House Gases (GHG) emission between 1980 and 2005 for Goa was found to be 5.59% for CO_2. It provides clear evidence of subsequent growing energy consumption and future demand in Goa (Jamir and De, 2013). This can be attributed to rapid growth in tourism, transport, and mining activities. A quick increment in vehicular traffic is becoming a significant source of air pollution in Goa, as fuel consumption shows a growth of 8.5% (Sharma and Patil, 2016).

The study area is still in the nascent stage of gaseous pollutant emission; however, the PM_{10} concentration is the most dominant pollutant because of gross violations of transport vehicles construction companies' operating protocol and mining firms. The increase in pollutant emissions in Goa can also be attributed to a large influx of tourists who commute from other states with their own diesel-operated vehicles. The tourist demands, such as energy consumption, vehicular movement, etc., increase exponentially and creates more pollution (Sharma and Patil, 2016) and leads to increment in trash generation during the peak tourism season (Nigam et al., 2021). While the tourism activities are significantly less in the hinterland of Goa, iron-ore mining and transportation is the primary source of economic activity. It contributes to air pollution in the hinterland and along the iron-ore transportation routes, which is usually done using diesel-operated trucks. However, the mining activity has been banned in the state by the Supreme Court of India since 2018 due to violation of the Environmental Protection Act, The Forest Conservation Act, Mines and Minerals Act by the mining companies.

South Goa's beautiful beaches and unique cultural heritage attract tourists from around the world, so much so that many people from other places have settled, and some have even bought a holiday home in this picturesque state. This has led to more urbanization, enhanced trash, and pollution due to more vehicular traffic, and has inflated the cost of living. In this background, the present work asses the level of air pollution by analyzing the inter-annual variability of SO_2, $PM_{2.5}$, and PM_{10} at eight different pollution monitoring stations which cover commercial/economic centers, township/residential areas, and mining pockets situated in the study area over the period 2014-2020. The goals are to address the inter-annual variability of the AQ and the role of environmental variables like precipitation and air temperature in modulating the changes in the AQ during monsoon and post-monsoon seasons. It is anticipated that the outcome of this study would be useful to determine increasing human influence nearby the meteorological stations and also to the authorities to plan mitigation control measures to combat air pollution in order to arrest the environmental degradation.

8.2 Results

Fig-8.1 The inter-annual distribution of seasonal average (monsoon and post-monsoon) SO_2, $PM_{2.5}$, PM_{10}, seasonal average rainfall, seasonal average minimum and maximum temperature along with the Exceedance Factor for the stations; (a) Vasco da Gama (Marmugao), (b) Margao (Salcete), (c) Quepem (Quepem) and (d) Curchorem (Quepem).

(a) Vasco da Gama

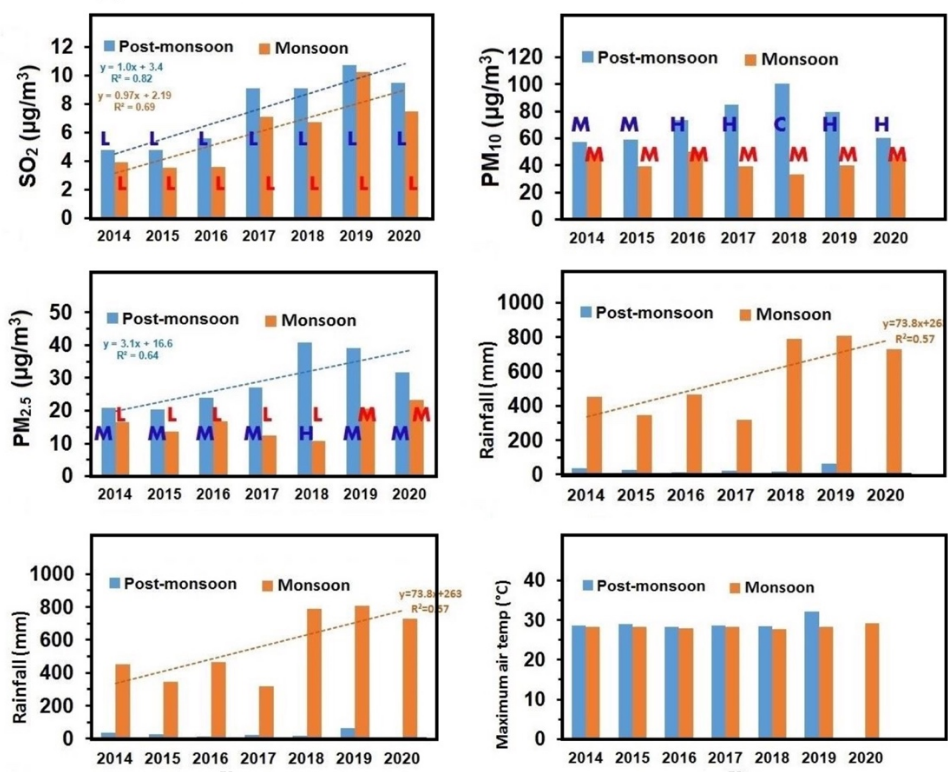

(b) Margao

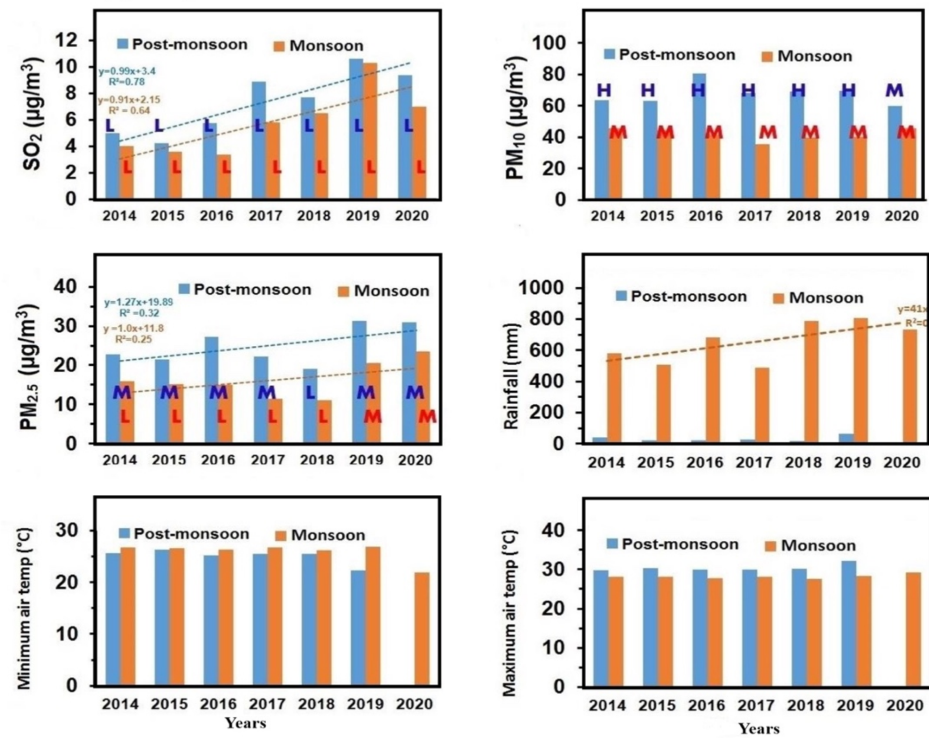

(c) Quepem

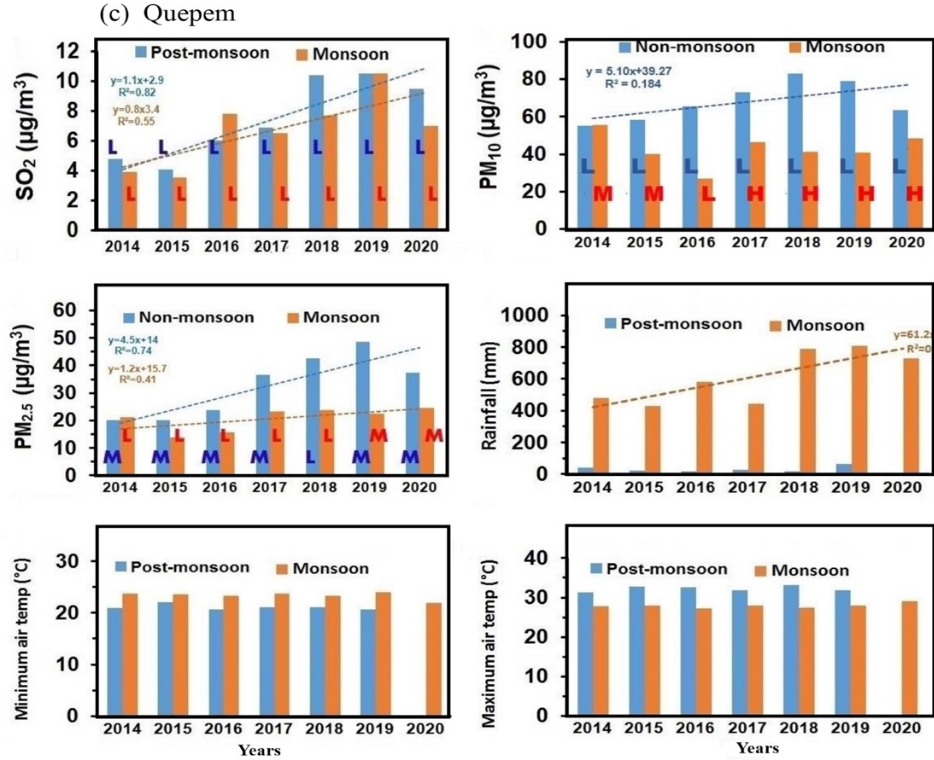

(d) Curchorem

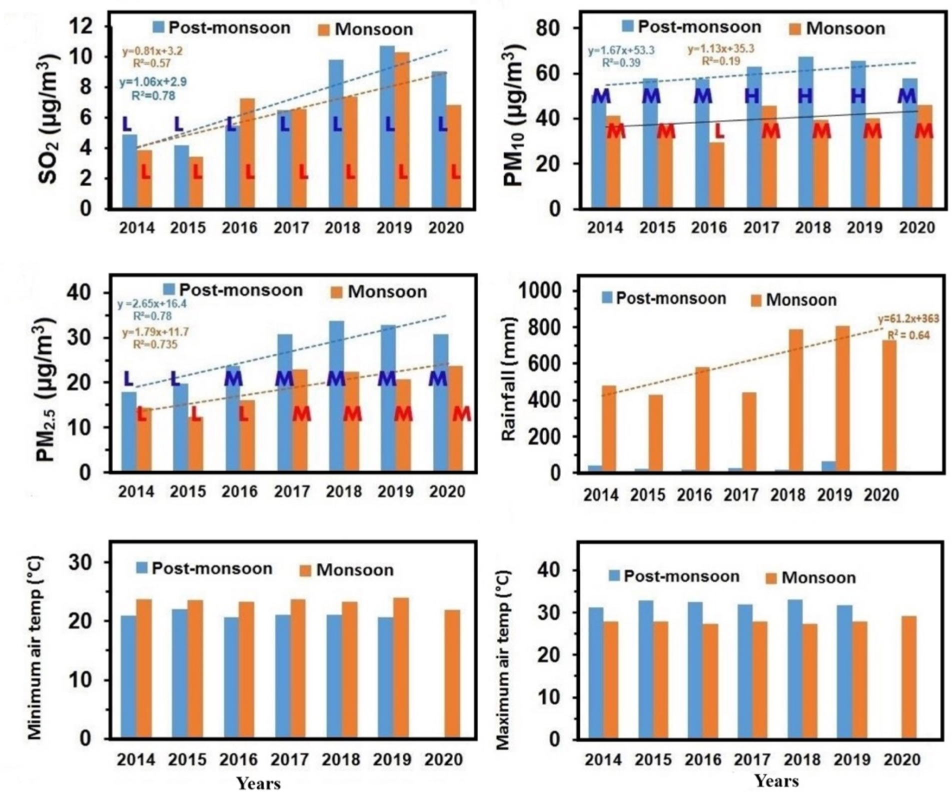

Table-8.1 Statistical results showing the Mean, Standard Deviation, Mean difference (in %) of the pollutants (SO_2, PM_{10} and $PM_{2.5}$) for the towns (Vasco-da-Gama, Margao, Quepem and Curchorem) located in the study area.

Vasco da Gama									
	SO_2			PM_{10}			$PM_{2.5}$		
Year	Mean	Std. Deviation	Mean Difference In (%)	Mean	Std. Deviation	Mean Difference In (%)	Mean	Std. Deviation	Mean Difference In (%)
2014 (N.M)	4.8	0.61	NA	57.3	4.06	NA	20.8	2.74	NA
2014 (M)	3.92	0.36	NA	46.74	1.81	NA	16.43	0.9	NA
2015 (N.M)	4.8	0.07	-12.5	59.2	7.9	3.31	20.3	3.35	-2.40
2015 (M)	3.55	0.36	-9.43	39.23	5.48	-16.06	13.55	1.43	-17.52

2016 (N.M)	5.6	1.9	16.66	73.7	24.39	24.49	23.9	6.8	17.73
2016 (M)	3.6	0.18	1.40	49.9	1.62	27.19	16.7	0.76	23.24
2017 (N.M)	9.1	1.96	62.5	85.1	14.64	15.46	27.14	10.28	13.55
2017 (M)	7.1	0.75	97.22	39	4.77	-21.84	12.37	0.97	-25.92
2018 (N.M)	9.1	0.98	0	100.13	53.45	17.66	40.83	4.46	50.44
2018 (M)	6.7	0.86	-5.63	33.2	3.23	-14.87	10.63	1.5	-14.06
Margao									
	SO_2			PM_{10}			$PM_{2.5}$		
Year	Mean	Std. Deviation	Mean Difference In (%)	Mean	Std. Deviation	Mean Difference In (%)	Mean	Std. Deviation	Mean Difference In (%)
2014 (N.M)	5.01	0.7	NA	63.79	4.4	NA	22.73	1.2	NA
2014 (M)	4	0.32	NA	45.6	8.24	NA	15.9	3.44	NA
2015 (N.M)	4.23	0.1	-15.56	63.19	12.6	-0.94	21.56	4.9	-5.14
2015 (M)	3.6	0.13	-10	44.2	3.93	-3.07	15.1	1.61	-5.03
2016 (N.M)	5.76	1.9	36.17	80.59	1.9	27.53	27.23	3	26.29
2016 (M)	3.4	0.31	-5.55	41.5	9.05	-6.1	15	3.99	-0.66
2017 (N.M)	8.89	1.4	54.34	68.2	14.5	-15.37	22.23	5.6	-18.36
2017 (M)	5.8	0.91	70.58	35.6	2.05	-14.21	11.4	0.67	-24
2018 (N.M)	7.68	0.2	-13.61	69.24	11	1.52	19.04	4.2	-14.34
2018 (M)	6.5	0.36	12.06	39.8	10.32	11.79	11	1.42	-3.50
Quepem									
	SO_2			PM_{10}			$PM_{2.5}$		
Year	Mean	Std. Deviation	Mean Difference	Mean	Std. Deviation	Mean Difference	Mean	Std. Deviation	Mean Difference

			In (%)			In (%)			In (%)
2014 (N.M)	4.8	0.64	NA	55.1	11.55	NA	20.1	4.3	NA
2014 (M)	3.9	0.24	NA	55.46	7.75	NA	21.27	2.38	NA
2015 (N.M)	4.1	0.09	-14.58	58.2	8.53	5.62	20	3.24	-0.49
2015 (M)	3.55	0.26	-8.97	40.15	2.24	-27.60	13.88	0.75	-34.74
2016 (N.M)	6	2.06	46.34	6.4	10.07	-89	23.8	3.23	19
2016 (M)	7.8	0.66	119.71	26.83	5.68	-100	15.73	1.66	13.32
2017 (N.M)	6.9	0.78	15	72.9	7.2	1039.06	36.67	4.81	54.07
2017 (M)	6.525	0.17	-16.34	47.32	6.2	NA	23.3	2.9	48.12
2018 (N.M)	10.38	1.06	50.43	82.80	16.57	13.58	42.52	8.96	15.95
2018 (M)	7.7	0.83	18	41.13	8	-13.09	23.66	6.8	1.54
Curchorem									
	SO_2			PM_{10}			$PM_{2.5}$		
Year	Mean	Std. Deviation	Mean Difference In (%)	Mean	Std. Deviation	Mean Difference In (%)	Mean	Std. Deviation	Mean Difference In (%)
2014 (N.M)	4.9	0.7	NA	50.6	8	NA	18	2.5	NA
2014 (M)	3.88	0.314	NA	41.17	3.62	NA	14.49	1.22	NA
2015 (N.M)	4.2	0.1	-14.28	58	10.1	14.62	19.8	3.7	10
2015 (M)	3.43	0.16	-11.59	36.68	3.15	-10.90	12.43	0.81	-14.21
2016 (N.M)	5.5	1.5	30.95	57.6	13.9	-0.68	23.7	2.2	19.69
2016 (M)	7.25	0.82	111.37	29.65	3.4	-19.16	16.1	1.5	29.52
2017 (N.M)	6.5	0.6	18.18	63	3.5	9.37	30.7	2.8	29.53
2017 (M)	6.55	0.15	-9.65	45.55	4.39	53.62	22.9	1.9	42.23
2018 (N.M)	9.82	1.16	51.07	67.58	3.74	7.26	33.7	2.81	9.77
2018 (M)	7.4	0.12	12.97	39.43	6.99	-13.42	22.33	5.4	-2.48

Table-8.2 Statistical results showing the level of Exceedance Factor and the air quality in relation to the pollutants (SO_2, PM_{10} and $PM_{2.5}$) in the towns (Vasco-da-Gama, Margao, Quepem and Curchorem) located in the study area.

Vasco da Gama						
	SO_2		PM_{10}		$PM_{2.5}$	
Year	Exceedance Factor (E.F)	Air Quality	Exceedance Factor (E.F)	Air Quality	Exceedance Factor (E.F)	Air Quality
2014 (N.M)	0.09	L	0.95	M	0.52	M
2014 (M)	0.07	L	0.77	M	0.41	L
2015 (N.M)	0.09	L	1.08	H	0.51	M
2015 (M)	0.07	L	0.65	M	0.33	L
2016 (N.M)	0.11	L	1.22	H	0.59	M
2016 (M)	0.07	L	0.83	M	0.41	L
2017 (N.M)	0.18	L	1.41	H	1.01	H
2017 (M)	0.14	L	0.65	M	0.30	L
2018 (N.M)	0.18	L	1.66	C	1.02	H
2018 (M)	0.13	L	0.55	M	0.26	L
Margao						
	SO_2		PM_{10}		$PM_{2.5}$	
Year	Exceedance Factor (E.F)	Air Quality	Exceedance Factor (E.F)	Air Quality	Exceedance Factor (E.F)	Air Quality
2014 (N.M)	0.1002	L	1.06	H	0.56825	M
2014 (M)	0.08	L	0.76	M	0.3975	L
2015 (N.M)	0.08	L	1.05	H	0.53	M
2015 (M)	0.07	L	0.73	M	0.37	L
2016 (N.M)	0.11	L	1.34	H	0.68	M
2016 (M)	0.068	L	0.69	M	0.37	L
2017 (N.M)	0.17	L	1.13	H	0.55	M
2017 (M)	0.11	L	0.59	M	0.28	L
2018 (N.M)	0.15	L	1.15	H	0.47	L
2018 (M)	0.13	L	0.66	M	0.27	L
Quepem						
	SO_2		PM_{10}		$PM_{2.5}$	
Year	Exceedance Factor (E.F)	Air Quality	Exceedance Factor (E.F)	Air Quality	Exceedance Factor (E.F)	Air Quality
2014 (N.M)	0.09	L	0.91	M	0.51	M

2014 (M)	0.07	L	0.92	M	0.53	M
2015 (N.M)	0.08	L	0.97	M	0.51	M
2015 (M)	0.07	L	0.66	M	0.34	L
2016 (N.M)	0.12	L	0.10	L	0.59	M
2016 (M)	0.15	L	0.44	L	0.39	L
2017 (N.M)	0.13	L	1.21	H	0.91	M
2017 (M)	0.13	L	0.78	M	0.58	M
2018 (N.M)	0.20	L	1.38	H	1.01	H
2018 (M)	0.15	L	0.68	M	0.59	M
Curchorem						
	SO_2		PM_{10}		$PM_{2.5}$	
Year	Exceedance Factor (E.F)	Air Quality	Exceedance Factor (E.F)	Air Quality	Exceedance Factor (E.F)	Air Quality
2014 (N.M)	0.09	L	0.84	M	0.45	L
2014 (M)	0.07	L	0.68	M	0.36	L
2015 (N.M)	0.08	L	0.96	M	0.49	L
2015 (M)	0.06	L	0.61	M	0.31	L
2016 (N.M)	0.11	L	0.96	M	0.59	M
2016 (M)	0.14	L	0.49	L	0.40	L
2017 (N.M)	0.13	L	1.05	H	0.76	M
2017 (M)	0.13	L	0.75	M	0.57	M
2018 (N.M)	0.19	L	1.12	H	0.84	M
2018 (M)	0.14	L	0.65	M	0.55	M

8.3 Result Interpretation

For Vasco-da-Gama station (Table-8.1 (a) & 8.2 (a) & Fig-8.1 (a)), the SO_2 concentration for post-monsoon varied from 4.8±0.6 μg/m^3 in 2014 to 10.7±0.6 μg/m^3 in 2019. Likewise, it varied from 3.9±0.4 μg/m^3 in 2014 to 10.3±0.4 μg/m^3 for monsoon (Fig. 8a), which led to an increasing trend of 0.97 μg/m^3/year and 1 μg/m^3/year for post-monsoon and monsoon, respectively. The pollution level was found to be low across the years. The PM_{10} concentration increased at the rate of 11.1 μg/m^3/year from 57±4.1 μg/m^3 to 100±53.5 μg/m^3, from 2014 to 2018, which was followed by a decreasing trend (Fig. 8b). On the other hand, its concentration showed a marginal decreasing trend of 0.6 μg/m^3/year for monsoon season. It is a matter of concern as the pollution level jumped from medium to high in 2017 to critical in 2018 for pot-monsoon. The $PM_{2.5}$ concentration varied from 20.8±2.7 μg/m^3 to 39±12 μg/m^3 from 2014 to 2019, exhibited a trend of 3.1 μg/m^3/year for post-monsoon (Fig. 8c). On the other hand, the mean concentration varied within 10 μg/m^3 over the 7-year period.

For the commercial city of Margao (Table-8.1 (b), 8.2 (b) & Fig-8.1 (b)), the SO_2 concentration steeped up from 4.2±0.1 (4±0.32) μg/m^3 in 2014 to 4±0.32 (10.3±0.43) μg/m^3 in 2019 for post-monsoon (monsoon) season. The trend was found to be 0.99 (0.91) μg/m^3/year for the post-monsoon (monsoon) season. The pollution level was classified as low across the years. The PM_{10} concentration varied from 63.8±4.4 (45.6±8.2) in 2014 to 69.3±20.4 (40.1±4.6) in 2019, which led to an insignificant negative trend of -0.4 (-0.41) μg/m^3/year for post-monsoon and monsoon season. The pollution level was high/medium for the post-monsoon/monsoon period. The $PM_{2.5}$ concentrations also exhibited an increasing trend of 1.27 (1.0) μg/m^3/year. For the monsoon period, the concentration was found below 20 μg/m^3. The pollution level varies between low and medium for both seasons. The lower concentration in PM was attributed to higher rainfall was seen across the years.

For Quepem station (Table-8.1 (c), 8.2 (c) & Fig.-8.1 (c)), the SO_2 concentration increased 1.1 (0.8) μg/m^3/year for post-monsoon (monsoon). The pollution level was found to be low across the years (Fig. 8a). Interestingly, the SO_2 concentration for 2019 was nearly the same (10.4±0.4 μg/m^3). The PM_{10} concentration showed an increasing but insignificant trend of 5.1 μg/m^3/year for post-monsoon (Fig. 8b). The pollution level was shifted from low in 2016 to high after 2017 for the monsoon period but was consistently at a low level for the post-monsoon season. The $PM_{2.5}$ concentration depicted an increasing trend of 4.5 μg/m^3/year for post-monsoon (Fig. 8c). The pollution level was moderate for 2019-2020 for both seasons. Heavy rainfall during 2018-2020 dropped the concentration of PM drastically (Fig. 8 b, c & d).

For Curchorem station (Table-8.1 (d), 8.2 (d) & Fig-8.1 (d)) which is situated in the township area, the SO_2 concentration showed an increase from 4.9±0.7 (3.88±0.3) μg/m^3 in 2014 to 10.7±0.5 (10.28±0.43) μg/m^3 in 2019, which dropped to 9±1.5 (6.8±1) μg/m^3 in 2020 for post-monsoon (monsoon) season. The trend in its concentration was found to be 1.06 (0.81) μg/m^3/year for post-monsoon (monsoon), and the pollution level was found to be low. The PM_{10} concentration showed an increasing trend of 1.67 (1.13) μg/m^3/year for the post-monsoon (monsoon) season. The pollution level was high during 2017-2019 post-monsoon and mostly medium for the monsoon period. The $PM_{2.5}$ concentration showed an increasing trend of 2.65 (1.79) μg/m^3/year for post-monsoon (monsoon). The pollution level shifted from low to medium for 2017-2020.

Chapter-9

Multi-Temporal Sea Level Rise Inundation Assessment

9.1 Background: The Interconnected Impact of Greenhouse Gases and Sea Level Rise

Greenhouse gases and aerosols play a pivotal role in climate dynamics by altering solar and thermal radiation, influencing Earth's energy balance. Various atmospheric gases and particles contribute to the warming or cooling of the climate system (IPCC, 2007). Human activities, dating back to the industrial age, have significantly warmed the climate (Gabriel et al., 2019), surpassing the influence of natural processes (Chu et al., 2017).

Human-induced global warming has raised the average global temperature by approximately 1°C since the industrial revolution (IPCC, 2014). The last decade stands as the warmest on record, with a current rise exceeding 1.2°C per decade (World Meteorological Organization, 2020). Beyond temperature increase, climate change affects interconnected Earth systems, leading to sea level rise (SLR) at various scales and putting coastal communities at risk (IPCC, 2007).

SLR, a visible consequence of climate change, has far-reaching economic and socio-demographic implications, causing coastal erosion and flooding (World Bank, 2007; Sarkar et al., 2014). The rise in global mean sea level results from thermal expansion and ocean mass gain, particularly due to declining land-ice mass (Mimura, 2013). Antarctica and Greenland's ice sheets are losing mass, contributing to a substantial increase in sea level (Perkins, 2022; Leuliette and Nerem, 2016).

Oceanic heat retention, responsible for one-third to one-half of global sea level rise, has intensified in recent decades, marked by the warmest ocean temperatures and increased tropical cyclone activity (Cheng et al., 2020; Ginis, 2021; Sharma, 2022). Rising sea levels, coupled with storm surges, pose immediate threats, evidenced by a surge in cyclonic events in India and temperature-related changes in the Arabian Sea (Kabir et al., 2022; D'Mello and Kumar, 2017).

Long-term projections indicate the acceleration of global mean sea level, driven by ice melt and thermal expansion. Anthropogenic forces, notably since 1970, have been the primary contributors to this rise (Oppenheimer et al., 2019). Projections suggest a rise between 0.43 m and 0.84 m by 2100, with variations based on emission scenarios (Oppenheimer et al., 2019; AR6, 2021). Regional disparities in sea level rise, affecting populations within 10 meters of mean sea level, highlight the urgency for adaptation measures (IPCC, 2019; Merkens et al., 2016).

Asia, home to 75% of the world's population, faces increased threats of inundation and erosion (Dumenu & Obeng, 2016; Smith, 2011). Coastal risks, exacerbated by extreme events, are reported globally, impacting infrastructure, livelihoods, and agriculture (Hallegatte et al., 2013; Woodruff et al., 2013; Clark et al., 2016, Prasad et al., 2023c). In Goa, socio-economic factors and anthropogenic activities heighten vulnerability to SLR and Extreme Sea Level events (IPCC AR-6, 2019).

Without significant adaptation efforts, SLR-related risks, including erosion and flooding, are expected to intensify along low-lying coasts by the century's end. Non-climatic drivers and demographic patterns contribute to the exposure and vulnerability of coastal communities in Goa to SLR and ESL events (IPCC AR-6, 2019). The dynamic nature of coastal risk emphasizes the need for proactive strategies to address the escalating challenges posed by climate change.

With regard to the study area, Goa has witnessed a remarkable surge in its population, primarily attributed to robust economic development propelled by tourism (Sawkar et al., 1998; Desousa, 1999). As of the 2001 census, Goa boasts the highest urban population in the country, constituting 62%, marking a significant increase from 49% (Sawkar et al., 1998). However, this unprecedented urbanization has given rise to a myriad of challenges, including the improper conversion of agricultural lands to non-agricultural uses, extensive deforestation, demolition of ancestral estates, and substantial investments in tourism-driven concrete infrastructure. Notably, large-scale conversions of dune belts have led to irreversible alterations in the coastal landscape, causing damage to dune flora, permanent loss of coastal sand dunes, and limited beach erosion (Goa Herald, 2019).

Looking ahead, the impact of climate change is poised to exacerbate existing challenges in Goa. Anticipated sea level rise (SLR) and heightened intensity and frequency of severe storm events in the coming decades will introduce new vulnerabilities to the coastal areas (Prasad et al., 2021) of Goa, necessitating proactive measures. In response, this study seeks to delineate 'future hazard zones' by calculating the spatial extent of coastal flooding resulting from expected SLR by 2100 AD in South Goa's coastal tracts. Additionally, the study aims to quantify the escalation of SLR-induced vulnerability within the study area over the last two decades. This comprehensive analysis is crucial for developing strategies to mitigate the dual challenges of rapid economic development and the impending impacts of climate change in Goa.

9.2 Results

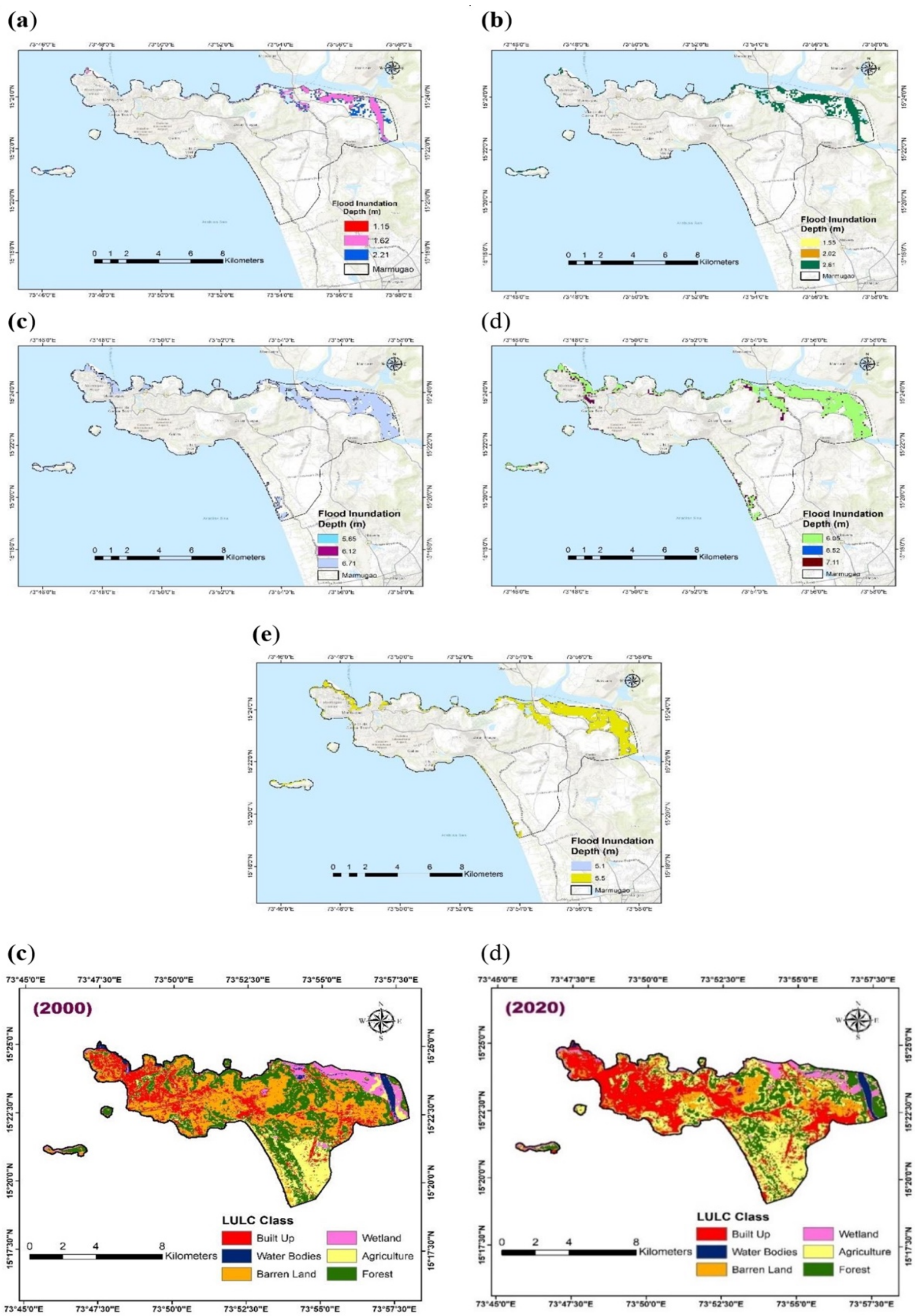

Fig- 9.1 Sea level rise inundation maps and LULC maps (2000 and 2020) of Marmugao. Showing the clusters of different inundation scenarios; (a) Only SLR, (b) SLR + Highest high spring tide, (c) SLR + Storm surge, (d) SLR + Spring tide + Storm surge, (e) Without SLR, (f) LULC-2000, (g) LULC-2020.

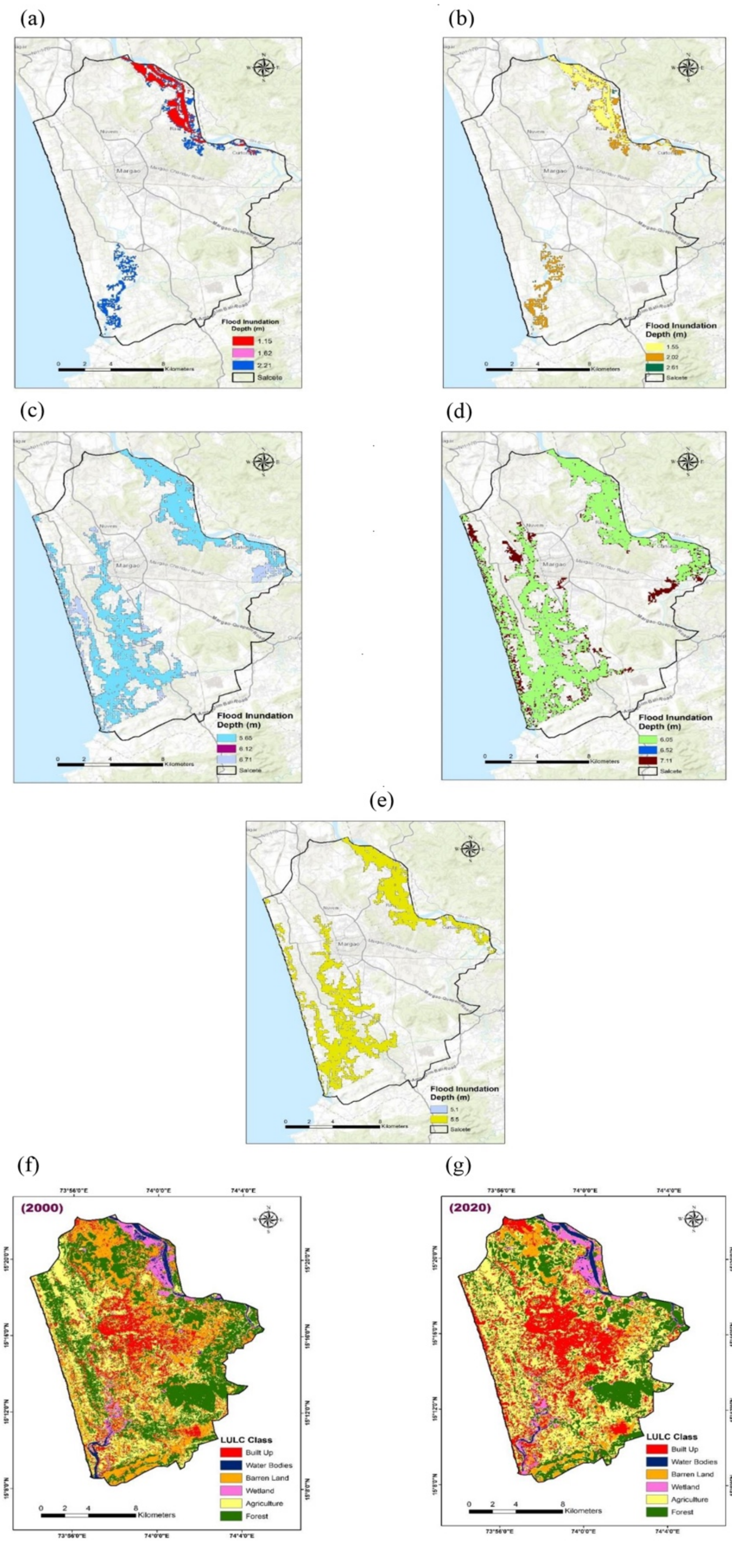

Fig- 9.2 Sea level rise inundation maps and LULC maps (2000 and 2020) of Salcete. Showing the clusters of different inundation scenarios; (a) Only SLR, (b) SLR + Highest high spring tide, (c) SLR + Storm surge, (d) SLR + Spring tide + Storm surge, (e) Without SLR, (f) LULC-2000, (g) LULC-2020.

(a)

No impact observed

(b)

No impact observed

(c)

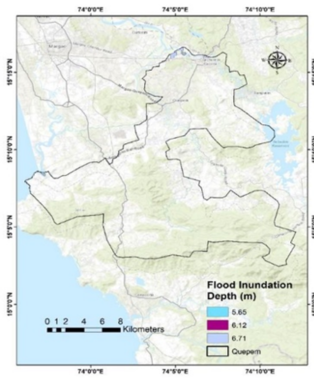

(d)

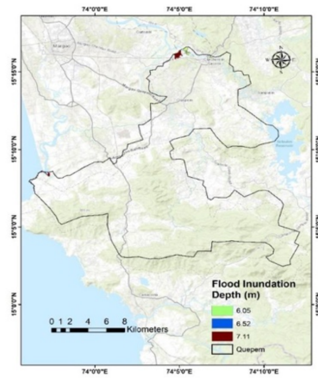

(e)

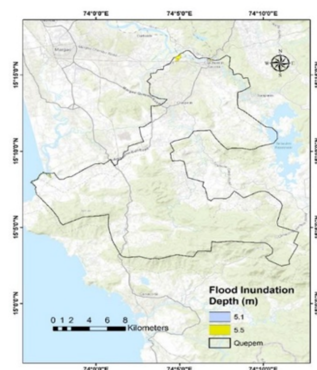

(f)

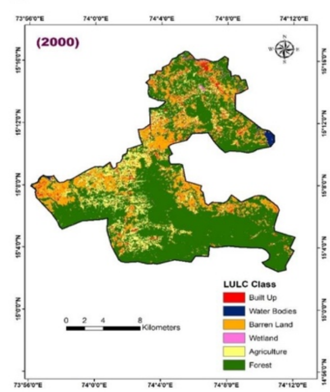

(g)

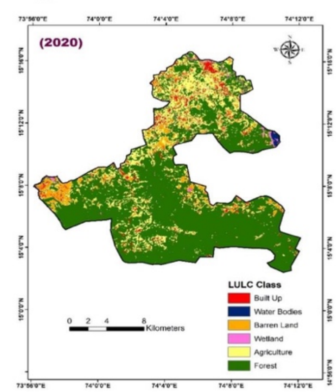

Fig- 9.3 Sea level rise inundation maps and LULC maps (2000 and 2020) of Quepem. Showing the clusters of different inundation scenarios; (a) Only SLR, (b) SLR + Highest high spring tide, (c) SLR + Storm surge, (d) SLR + Spring tide + Storm surge, (e) Without SLR, (f) LULC-2000, (g) LULC-2020.

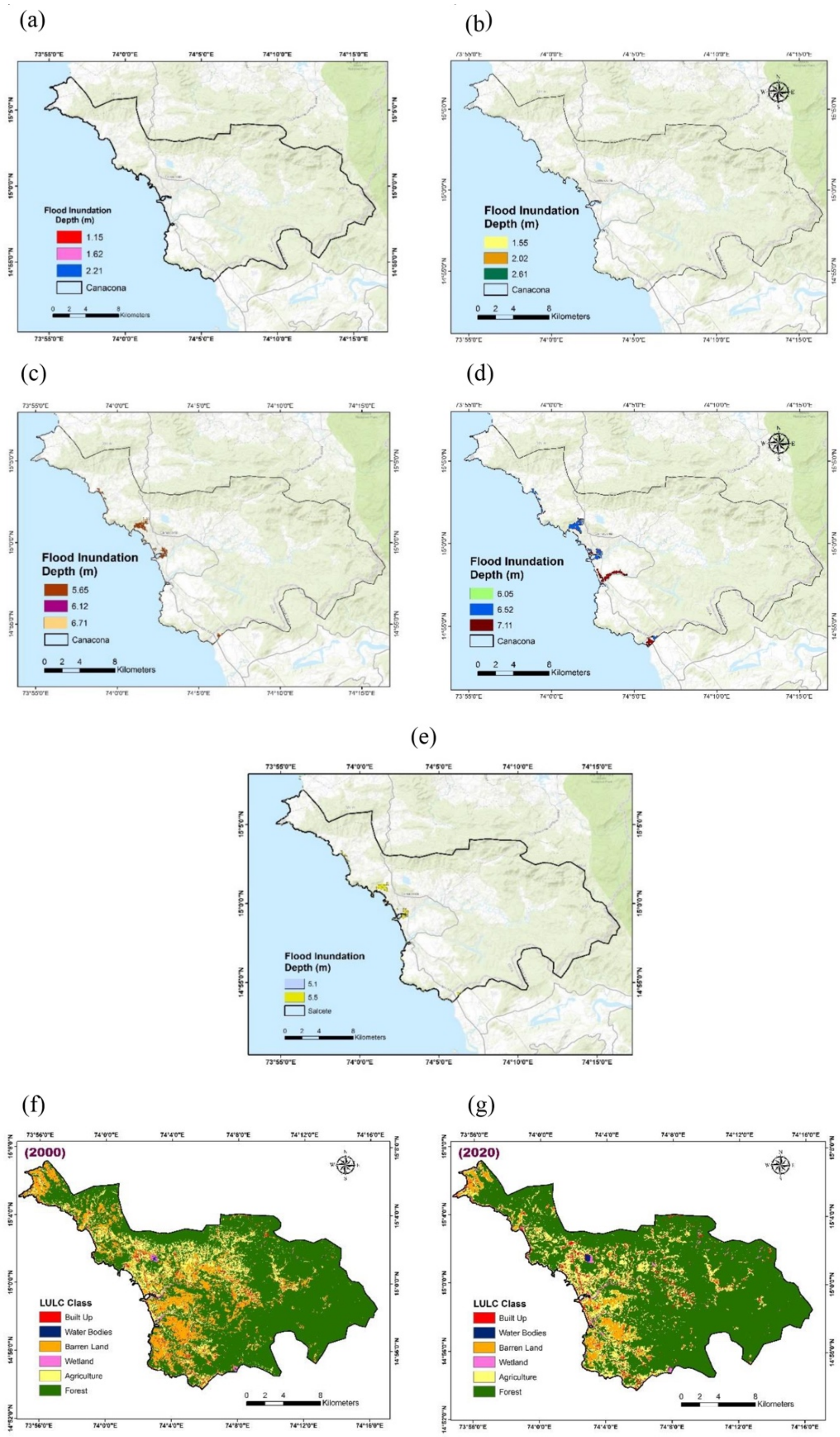

Fig- 9.4 Sea level rise inundation maps and LULC maps (2000 and 2020) of Canacona. Showing the clusters of different inundation scenarios; (a) Only SLR, (b) SLR + Highest high spring tide, (c) SLR + Storm surge, (d) SLR + Spring tide + Storm surge, (e) Without SLR, (f) LULC-2000, (g) LULC-2020.

Table-9.1 Amount of inundated area (in sq. km) and Vulnerability Growth Rate (in %) under different sea level rise inundation scenarios, on the basis of 2000 and 2020 LULC settings in Marmugao

Scenario-1 (Only SLR)	Built Up	Water Bodies	Wetland	Agriculture	Forest	Barren Land
1.15m						
2000	0.025	1.107	1.521	0.017	0.161	0.037
2020	0.068	1.078	1.071	0.185	0.403	0.015
VGR	172	-2.61	-29.58	988.23	150.31	-59.45
1.62m						
2000	0.025	1.107	1.521	0.017	0.161	0.037
2020	0.068	1.078	1.071	0.185	0.403	0.015
VGR	172	-2.61	-29.58	988.23	150.93	-59.45
2.21m						
2000	0.066	1.286	2.604	0.124	0.365	0.103
2020	0.177	1.166	1.897	0.360	0.846	0.045
VGR	168.18	-9.33	-27.15	190.32	151.78	-56.31
Scenario-2 (SLR + Highest high spring tide)	Built Up	Water Bodies	Wetland	Agriculture	Forest	Barren Land
1.55m						
2000	0.025	1.107	1.521	0.017	0.161	0.037
2020	0.068	1.078	1.071	0.185	0.403	0.015
VGR	172	-2.61	-29.58	988.23	150.31	-59.45
2.02m						
2000	0.066	1.286	2.604	0.124	0.365	0.103
2020	0.177	1.166	1.897	0.360	0.846	0.045
VGR	168.18	-9.33	-27.15	190.32	131.78	-56.31
2.61m						
2000	0.066	1.286	2.604	0.124	0.365	0.103
2020	0.177	1.166	1.897	0.360	0.846	0.045
VGR	168.18	-9.33	-27.15	190.32	131.78	-56.31
Scenario-3 (SLR + Storm surge)	Built Up	Water Bodies	Wetland	Agriculture	Forest	Barren Land
5.65m						
2000	0.545	1.732	4.544	0.939	1.028	0.464
2020	1.081	1.345	3.100	0.977	2.494	0.181
VGR	98.34	-22.34	-31.77	4.04	142.6	-60.99
6.12m						
2000	0.769	1.824	4.750	1.265	1.263	0.660

Marmugao (2020)	1.484	1.381	3.294	1.344	2.721	0.210
VGR	92.97	-24.28	-30.65	6.24	115.43	-68.18
6.71m						
2000	0.769	1.824	4.750	1.265	1.263	0.660
2020	1.484	1.381	3.294	1.344	2.721	0.210
VGR	92.97	-24.28	-30.65	6.24	115.43	-68.18
Scenario-4 (SLR + Spring tide + Storm surge)	Built Up	Water Bodies	Wetland	Agriculture	Forest	Barren Land
6.05m						
2000	0.769	1.824	4.750	1.265	1.263	0.660
2020	1.484	1.381	3.294	1.344	2.721	0.210
VGR	92.97	-24.28	-30.65	6.24	- 115.43	-68.18
6.52m						
2000	0.769	1.824	4.750	1.265	1.263	0.660
2020	1.484	1.381	3.294	1.344	2.721	0.210
VGR	92.97	-24.28	-31.28	6.24	- 115.43	-68.18
7.11m						
2000	1.184	1.893	4.915	1.484	1.661	0.923
2020	2.155	1.399	3.455	1.762	2.902	0.259
VGR	82.01	-26.09	-29.70	18.73	-74.71	-71.93
Scenario-5 (Without SLR)	Built Up	Water Bodies	Wetland	Agriculture	Forest	Barren Land
5.1m						
2000	0.545	1.732	4.544	0.939	1.028	0.464
2020	1.081	1.345	3.100	0.977	2.494	0.181
VGR	98.34	-22.34	-31.77	4.04	142.6	-60.99
5.5m						
2000	0.545	1.732	4.544	0.939	1.028	0.464
2020	1.081	1.345	3.100	0.977	2.494	0.181
VGR	98.34	-22.34	-31.77	4.04	142.6	-60.99

Table-9.2 Amount of inundated area (in sq. km) and Vulnerability Growth Rate (in %) under different sea level rise inundation scenarios, on the basis of 2000 and 2020 LULC settings in Salcete

Scenario-1 (Only SLR)	Built Up	Water Bodies	Wetland	Agriculture	Forest	Barren Land
1.15m						

2000	0.018	3.062	3.486	0.144	0.268	0.011
2020	0.042	3.026	3.527	0.170	0.085	0.066
VGR	133.33	1.17	1.17	18.05	-68.28	500
1.62m						
2000	0.020	3.056	3.473	0.144	0.269	0.012
2020	0.044	3.023	3.510	0.174	0.085	0.066
VGR	120	-1.07	1.06	20.83	-68.40	450
2.21m						
2000	0.908	4.327	5.864	1.454	2.154	0.664
2020	1.233	4.059	6.474	1.554	1.295	0.657
VGR	35.79	-6.19	10.40	6.87	-39.97	-1.05
Scenario-2 (SLR + Highest high spring tide)	Built Up	Water Bodies	Wetland	Agriculture	Forest	Barren Land
1.55m						
2000	0.023	3.045	3.514	0.143	0.147	0.014
2020	0.047	3.013	3.543	0.121	0.030	0.068
VGR	104.34	-1.05	0.82	-15.38	-79.59	385.71
2.02m						
2000	0.908	4.327	5.864	1.454	2.154	0.664
2020	1.233	4.059	6.474	1.554	1.295	0.657
VGR	35.79	-6.19	10.4	6.86	-39.87	-1.05
2.61m						
2000	0.917	4.332	5.916	1.462	2.210	0.669
2020	1.244	4.059	6.534	1.590	1.318	0.658
VGR	35.65	-6.3	10.44	8.75	-40.36	-1.64
Scenario-3 (SLR + Storm surge)	Built Up	Water Bodies	Wetland	Agriculture	Forest	Barren Land
5.65m						
2000	5.765	5.176	9.842	14.676	10.025	6.248
2020	9.040	4.841	11.263	17.201	6.640	2.842
VGR	56.8	-6.47	-99.88	17.2	-33.76	-54.51
6.12m						
2000	6.946	5.292	10.345	20.485	13.453	8.206
2020	11.716	4.963	11.900	23.702	9.097	3.447
VGR	68.67	-6.21	-99.88	15.7	-32.37	-57.99
6.17m						
2000	6.946	5.292	10.345	20.485	13.453	8.206
2020	11.716	4.963	11.900	23.702	9.097	3.447
VGR	68.67	-6.21	15.03	15.7	-32.37	-57.99
Scenario-4 (SLR + Spring tide + Storm surge)	Built Up	Water Bodies	Wetland	Agriculture	Forest	Barren Land
6.05						

2000	6.946	5.292	10.345	20.485	13.453	8.206
2020	11.716	4.963	11.900	23.702	9.097	3.447
VGR	68.67	-6.21	15.03	15.17	-32.37	-57.99
6.52						
2000	6.946	5.292	10.345	20.485	13.453	8.206
2020	11.716	4.963	11.900	23.702	9.097	3.447
VGR	68.67	-6.21	15.03	15.17	-32.37	-57.99
7.11						
2000	8.330	5.370	10.733	26.275	16.708	10.131
2020	14.661	5.019	12.326	31.279	10.594	3.878
VGR	76	-6.53	14.84	19.04	-36.59	-61.77
Scenario-5 (Without SLR)	Built Up	Water Bodies	Wetland	Agriculture	Forest	Barren Land
5.1m						
2000	5.765	5.176	9.842	14.676	10.025	6.248
2020	9.038	4.844	11.263	17.197	6.642	2.842
VGR	56.77	-6.41	14.43	17.17	-33.74	-54.51
5.5m						
2000	5.765	5.176	9.842	14.676	10.025	6.248
2020	9.038	4.844	11.263	17.197	6.642	2.842
VGR	56.77	-6.41	14.43	17.17	-33.74	-54.51

Table-9.3 Amount of inundated area (in sq. km) and Vulnerability Growth Rate (in %) under different sea level rise inundation scenarios, on the basis of 2000 and 2020 LULC settings in Quepem

Scenario-1 Only SLR	Built Up	Water Bodies	Wetland	Agriculture	Forest	Barren Land
1.15m						
2000	0	0.010	0	0	0.009	0
2020	0	0.005	0.005	0.004	0.003	0
VGR	0	-50	500	400	-300	0
1.62m						
2000	0	0.010	0	0	0.009	0
2020	0	0.005	0.005	0.004	0.003	0
VGR	0	-50	500	400	-66.66	0
2.21m						
2000	0.002	0.037	0.008	0	0.005	0.004
2020	0.003	0.010	0.045	0.001	0.002	0
VGR	50	-72.97	462.5	100	-60	-100

Scenario-2 (SLR + Highest high spring tide)	Built Up	Water Bodies	Wetland	Agriculture	Forest	Barren Land
1.55m						
2000	0	0.010	0	0	0.009	0
2020	0	0.005	0.005	0.004	0.003	0
VGR	0	-50	500	400	-66.66	0
2.02m						
2000	0.002	0.047	0.009	0	0.005	0.004
2020	0.003	0.010	0.152	0.001	0.002	0
VGR	50	-78.72	1588.88	100	-60	-100
2.61						
2000	0.002	0.047	0.009	0	0.005	0.004
2020	0.003	0.010	0.053	0	0.001	0.002
VGR	50	-78.72	488.88	0	-80	-50
Scenario-3 (SLR + Storm surge)	Built Up	Water Bodies	Wetland	Agriculture	Forest	Barren Land
5.65m						
2000	0.009	0.123	0.039	0.024	0.305	0.010
2020	0.016	0.015	0.152	0.144	0.174	0.005
VGR	77.77	-87.8	289.74	500	-42.95	-50
6.12m						
2000	0.019	0.168	0.078	0.044	0.472	0.039
2020	0.030	0.031	0.220	0.209	0.292	0.025
VGR	57.89	-81.54	182.05	375	-38.13	-35.89
6.71m						
2000	0.019	0.168	0.078	0.044	0.472	0.039
2020	0.030	0.031	0.220	0.209	0.292	0.025
VGR	57.89	-81.54	182.05	375	-38.13	-35.89
Scenario-4 (SLR + Spring tide + Storm surge)	Built Up	Water Bodies	Wetland	Agriculture	Forest	Barren Land
6.05m						
2000	0.019	0.168	0.078	0.044	0.472	0.039
2020	0.030	0.031	0.220	0.209	0.292	0.025
VGR	57.89	-81.54	182.05	375	-38.13	-35.89
6.52						
2000	0.019	0.168	0.078	0.044	0.472	0.039
2020	0.030	0.031	0.220	0.209	0.292	0.025
VGR	57.89	-81.54	182.05	375	-38.13	-35.89
7.11m						
2000	0.012	0.154	0.028	0.046	0.410	0.019

2020	0.028	0.014	0.173	0.252	0.186	0.003
VGR	133.33	-90.9	517.85	447.82	-54.63	-84.21
Scenario-5 (Without SLR)	Built Up	Water Bodies	Wetland	Agriculture	Forest	Barren Land
5.1m						
2000	0.009	0.123	0.039	0.024	0.305	0.010
2020	0.016	0.015	-	0.144	0.174	0.005
VGR	77.77	-87.18	-100	500	-42.95	-50
5.5m						
2000	0.009	0.123	0.039	0.024	0.305	0.010
2020	0.016	0.015	-	0.144	0.174	0.005
VGR	77.77	-87.18	-100	500	-42.95	-50

Table-9.4 Amount of inundated area (in sq. km) and Vulnerability Growth Rate (in %) under different sea level rise inundation scenarios, on the basis of 2000 and 2020 LULC settings in Canacona

Scenario-1 Only SLR	Built Up	Water Bodies	Wetland	Agriculture	Forest	Barren Land
1.15m						
2000	0.002	0.020	0.008	0.006	0.009	0.017
2020	0.018	0.001	0.017	0.019	0.003	0.003
VGR	800	-95	112.5	216.66	-66.66	-82.35
1.62m						
2000	0.001	0.020	0.008	0.003	0.009	0.004
2020	0.014	0.001	0.017	0.010	0.003	-
VGR	1300	-95	112.5	233.33	-66.66	0
2.21m						
2000	0.004	0.078	0.018	0.005	0.013	0.014
2020	0.031	0.017	0.060	0.012	0.004	-
VGR	675	-78.2	233.33	140	-69.2	-100
Scenario-2 (SLR + Highest high spring tide)	Built Up	Water Bodies	Wetland	Agriculture	Forest	Barren Land
1.55m						
2000	0.002	0.020	0.008	0.006	0.009	0.017
2020	0.018	0.001	0.017	0.019	0.003	0.003
VGR	800	-95	112.5	216.66	-66.66	-82.35
2.02m						

2000	0.004	0.078	0.018	0.005	0.013	0.014
2020	0.031	0.017	0.060	0.012	0.004	-
VGR	675	-78.2	235.33	140	- 69.23	-100
2.61m						
2000	0.004	0.078	0.018	0.005	0.013	0.014
2020	0.031	0.017	0.060	0.012	0.004	-
VGR	675	-78.2	233.33	140	- 69.23	100
Scenario-3 (SLR + Storm surge)	Built Up	Water Bodies	Wetland	Agriculture	Forest	Barren Land
5.65m						
2000	0.228	0.328	0.157	0.653	0.139	0.376
2020	0.442	0.055	0.426	0.751	0.147	0.079
VGR	93.85	-83.23	171.33	15	5.75	-78.98
6.12m						
2000	0.336	0.412	0.185	0.957	0.199	0.501
2020	0.647	0.063	0.531	1.100	0.184	0.093
VGR	92.55	-84.7	187.02	-88.5	-7.53	-81.43
6.71m						
2000	0.336	0.412	0.185	0.957	0.199	0.501
2020	0.647	0.063	0.531	1.100	0.184	0.093
VGR	92.55	-84.70	187.02	14.94	-7.53	-81.43
Scenario-4 (SLR + Spring tide + Storm surge)	Built Up	Water Bodies	Wetland	Agriculture	Forest	Barren Land
6.05m						
2000	0.336	0.412	0.185	0.957	0.199	0.501
2020	0.647	0.063	0.531	1.100	0.184	0.093
VGR	92.55	-84.17	187.02	14.94	-7.53	-81.43
6.52m						
2000	0.336	0.412	0.185	0.957	0.199	0.501
2020	0.647	0.063	0.531	1.100	0.184	0.093
VGR	92.55	-84.17	187.02	14.94	-7.53	-81.43
7.11m						
2000	0.598	0.572	0.392	1.832	0.487	0.806
2020	1.098	0.117	0.815	2.005	0.517	0.162
VGR	83.61	-79.54	107.9	9.4	6.16	-79.9
Scenario-5 (Without SLR)	Built Up	Water Bodies	Wetland	Agriculture	Forest	Barren Land
5.1m						
2000	0.228	0.328	0.157	0.653	0.139	0.376
2020	0.442	0.055	0.426	0.751	0.147	0.079
VGR	93.85	-83.23	171.33	15	5.75	-78.79

5.5m						
2000	0.228	0.328	0.157	0.653	0.139	0.376
2020	0.442	0.055	0.426	0.751	0.147	0.079
VGR	93.85	-83.23	171.33	15	5.75	-78.79

9.3 Result Interpretation

Vulnerability Growth Rate (VGR) is simply the growth rate in the amount of a specific LULC category between the current and preceding year. Therefore, it is to be understood here that, the positive growth in the VGR is a concern only for the land use classes such as; built-up, agriculture, barren land. But, on the other hand, negative growth in the land cover classes such as; forest, water bodies and wetland is a concern. Because in this case, coastal vulnerability would increase when the land cover classes would get reduced. Thus, in other words, increasing VGR is a threat to the land-use categories and decreasing VGR is a threat to land cover category.

- **Sea Level Rise Inundation Assessment - Marmugao**
- **Scenario-1 (Only SLR)**

Under all three inundation depths (1.15 m, 1.62 m & 2.11 m), there is an increase in the Built Up, indicating urbanization and population growth. This trend suggests that more land is being converted for Built-up purposes, which could get effected in the event of coastal flooding up to 2.21 m elevation. The agriculture shows an increasing trend across scenarios which could indicate potentially increased demand for vegetables and rice. The forests cover also indicates an increase across all scenarios, suggesting conservation initiatives. The Barren Land shows reduction across scenarios possibly due to land development. We found consistent patterns in vulnerability changes. In terms of VGR, Built-Up and Agriculture consistently experience high VGR, while Water Bodies, barren land and wetland show a decreasing trend which clearly suggests encroachment due to human activities. Among all the classes, only the forest increment is a silver lining in reducing the VGR.

- **Scenario-2 (SLR + Highest High Spring Tide)**

Across all scenarios (1.55 m, 2.02 m & 2.61 m), an increment in built-up is found, indicating urban expansion and development. Similarly, across all scenarios, agricultural land has increased. This suggests agricultural expansion driven by changes in land use practices due to improving economic factors. The forest area has been found to be generally increased across all scenarios, indicating afforestation efforts or natural re-growth in certain areas. Reduction in the area of water bodies in found under all the inundation scenarios. This could be due to land reclamation for increasing demand of land resources. Likewise, the VGR exhibits an increasing trend mainly in human-influenced land use.

- **Scenario-3 (SLR + Storm Surge)**

In all three scenarios (5.65 m, 6.12 m, and 6.71 m), there is a consistent trend of increasing built-up areas between the years 2000 and 2020 suggesting rapid urbanization in Mormugao. While, reduction in both Water Bodies and Wetland has been found across all three scenarios, pointing towards challenges related to wetland conservation. The forest category has shown an increase across the three scenarios. The agriculture and barren land exhibit smaller changes compared to other land use categories.

- **Scenario-4 (SLR + Spring tide + Storm surge)**

In all cases (6.05 m, 6.52 m, 7.11 m), the vulnerability of built-up areas has increased significantly. The growth rate of vulnerability is consistently increasing across the different scenarios. Water bodies, wetlands and Barren land have generally shown a decrease in growth across the different scenarios, indicating reduction in above mentioned categories due to anthropogenic factors. The agricultural land vulnerability has increased, but the rates of increase vary between the different scenarios. The forest areas which are situated on elevated regions consistently show a significant decrease in the VGR.

- **Scenario-5 (Without SLR)**

Across both scenarios (5.1 and 5.5 m) the amount of inundation area is found to be similar. The built-up areas have expanded from 2000 to 2020. Water bodies and wetland areas have decreased, suggesting urbanization or land use changes behind the reduction of these ecologically valuable areas. Agricultural land area seems relatively stable between 2000 and 2020, with minor changes. However, there is a positive VGR. The forest areas have experienced a significant decrease in the VGR, while barren land areas have seen an increase in the VGR. This suggests potential changes in land management.

Despite variations in land use categories, there is a consistent trend of increased vulnerability for Built-up areas, Water bodies, and Wetlands. This point directly to increasing human influence impacting these categories.

- **Sea Level Rise Inundation Assessment - Salcete**
- **Scenario-1 (Only SLR)**

In all scenarios (1.15m, 1.62m & 2.11m), there is a consistent increase in built-up from 2000 to 2020. This indicates ongoing urbanization and development in the Salcete. The agricultural land also shows a general trend of growth in all scenarios also suggesting that agriculture is expanding in the region over time, possibly due to changes in land use practices. The VGR for vegetation is consistently negative across all scenarios which implies that the vegetation cover has significantly declined over time, possibly due deforestation, land degradation and land-use change. Water bodies and wetland areas has also shown reduction across the different scenarios however, these categories have not seen dramatic shifts over the years. Barren land, similar to Built-up areas, shows an increase in all scenarios. This could indicate disturbances or changes in land conditions that have led to the expansion of barren land.

- **Scenario-2 (SLR + Highest High Spring Tide)**

All scenarios (1.55m, 2.02m and 2.61m) have experienced increment in built-up between 2000 and 2020. In two out of three scenarios (2.02 and 2.61 m), there was a decrease in Water body areas but not in lowest inundation scenario. This decline could be due land reclamation. In all three scenarios, Wetland areas have exhibited increment indicating efforts towards wetland conservation or natural expansion of these areas. The agriculture areas have shown mixed trends. While the agriculture decreased in 1.55 m scenario, it shows an increasing trend in 2.02 m and 2.61 m scenarios suggesting changing agricultural practices and responses to changing land use patterns. Significant decrease found in forest areas across the scenarios, indicating deforestation due to agricultural expansion, logging, or land clearing. The vulnerability growth rates showed variations, but generally, Built Up and Agriculture have been positive over time.

- **Scenario-3 (SLR + Storm surge)**

Across all three time periods (5.65m, 6.12m, and 6.71m), there is a consistent trend of an increase in "Built Up" areas and a common trend of decreased water bodies and wetland between 2000 and 2020 in the first scenarios, potentially due to human activities and changes in land use. Agriculture shows some variation, there is an increment in the first two scenarios followed by a slight decrease in the third scenario reflecting changing agricultural practices and land use priorities. Contrary to Agriculture, the Forest class show a decline in the first two scenarios a slight increase under third scenario. This suggests potential efforts towards reforestation or conservation at slightly higher elevations.

- **Scenario-4 (SLR + Spring tide + Storm surge)**

The Built-up increased over the years in all scenarios (6.05m, 6.52m, and 7.11m). The VGR for built-up areas are significantly positive, indicating a higher vulnerability. Water bodies and Forest area generally showed a decline over time under scenarios 6.05m and 6.52m, but the area increased under scenario of 7.11m and so inversely its VGR. On the contrary, Wetland increased under scenarios 6.05m and 7.11m, but showed a slight decrease under scenario 6.52m.

Agricultural land has increased under all the scenarios, showing a trend of expansion and so as its VGR. While Barren land area decreased over time under all scenarios.

- **Scenario-5 (Without SLR)**

In both scenarios (5.1m and 5.5m) the results have been found to be similar, the percentage of built-up land (urban areas) increased significantly from 2000 to 2020. This suggests a common trend of urban expansion over the years. The amount of water bodies decreased, which could be due to urbanization and pollution. Increment in the amount of agricultural land suggesting agricultural activities expanded over the years, driven by population growth. Both scenarios show a decrease in forest and barren land, suggesting deforestation and urbanization. The VGR for each land use category show that built-up areas, wetlands, and agricultural lands became more vulnerable in both scenarios. This could be due to potential degradation and increasing human influence at his elevation.

- **Sea Level Rise Inundation Assessment - Quepem**
- **Scenario-1 Only SLR**

Scenario 1.15m and 1.62m are found to be completely similar with reduction in water bodies and vegetation and increment in agriculture and wetland, clearly indicating human impact in the area.

Although no built-up has been developed between 2000 and 2020, not even under scenario 2.21m and barren land found to be similar under all scenarios. However, there is a decrease in water bodies and increment in wetland, agriculture, forest land cover categories under 2.21m scenario.

- **Scenario-2 (SLR + Highest High Spring Tide)**

1.55m scenario has been found to be similar to 1.15m and 1.62m scenarios discussed in the above section. However, under scenarios 2.02m and 2.61m Built-up land increased by 50% from 2000 to 2020. This suggests a common trend of urbanization. We find a reduction in Water Bodies area and proportion by approximately 78.72% is found. Barren land decreased by 50% under the scenario 2.61m but no changes found under 2.02m scenario. The Agriculture area has remained constant under both the scenarios

- **Scenario-3 (SLR + Storm Surge)**

Under 5.65m, 6.12m and 6.71m scenarios**,** the proportion of built-up has increased and also the VGR with the highest increase in vulnerability under the 5.65m scenario, which suggest increment in built-up areas below 5.65m elevation. However, water bodies and barren land and forest decreased in all three scenarios and so as their VGR. While, the proportion of wetland and agriculture has increased significantly under all conditions from 2000 to 2020.

- **Scenario-4 (SLR + Spring tide + Storm surge)**

In all three scenarios 6.05m, 6.52m and 7.11m, an increase in the proportion of Built Up and agriculture cover from 2000 to 2020 suggesting development, driven by factors population growth and infrastructure expansion. While reduction in water bodies and forest is observed across all three scenarios but the wetland proportion has increased.

- **Scenario-5 (Without SLR)**

Under both scenarios (5.1m and 5.5m), an increase in Built Up areas and significant increment in agriculture is observed, indicating urbanization and population growth in the region. While, a significant decrease in water bodies, wetland, forest and barren land have been observed under both the scenarios, clearly indicating significant increment in VGR in all the land use.

- **Sea Level Rise Inundation Assessment - Canacona**
- **Scenario-1 Only SLR**

Built up areas have increased under all three inundation scenarios (1.15m, 1.62mm, and 2.2m), indicating growth in urbanization and development. Water bodies have increased in 1.15m indicating land reclamation and slightly increased under the 1.62m to 2.21m scenarios. The overall trends of wetland suggest an increase in wetland under 1.62m to 2.21m scenarios. While there is a notable increase in forest and barren land VGR under 1.15m and 1.62m scenarios but a slight decrease under 2.21m scenario, suggesting afforestation. However, the amount of LULC getting affected by these plausible inundation scenarios is negligible, as Canacona is predominantly hilly.

- **Scenario-2 (SLR + Highest High Spring Tide)**

In terms of VGR, Built-up, wetland areas have increased from 2000 to 2020 in all three cases (1.55m, 2.02m, and 2.61m). Under 1.55m scenario, small decrease in water bodies, while in the 2.02m and 2.61m scenario it has increased. There is an increase in agriculture in the 1.55m and 2.61m scenarios but a decrease in the 2.02m scenario. While forest have increased VGR in the 1.55m and 2.61m scenarios but decreased slightly in the 2.02m scenario and barren land stayed relatively constant. However, the amount of LULC getting affected by these plausible inundation scenarios is negligible, as Canacona is predominantly hilly.

- **Scenario-3 (SLR + Storm surge)**

In terms of VGR, across all scenarios (5.65m, 6.12m, and 6.71m), there is a significant growth in built-up areas. Both Water Bodies and Barren Land areas show consistent reduction in their extents which could be attributed to urban expansion, resulting in decreased natural and open areas. Wetland have consistently shown an increase in extent over time. Agriculture have generally increased in extent across the years, with varying vulnerability growth rates. Forest have exhibited mixed trends with both positive and negative changes in extent, indicating fluctuations in natural vegetation cover however. However, the amount of LULC getting affected by these plausible inundation scenarios is negligible, as Canacona is predominantly hilly.

- **Scenario-4 (SLR + Spring Tide + Storm Surge)**

In terms of VGR, under all three scenarios (6.05m, 6.52m, and 7.11m) increasing built up and agriculture is observed suggesting urban development and population growth have been a major driving force across the years. Water bodies and Barren and have decreased significantly. Wetland areas have experienced increment over the years. The VGR of Barren Land has consistently increased over the years, suggesting conversion of land use. However, the amount of LULC getting affected by these plausible inundation scenarios is negligible, as Canacona is predominantly hilly.

- **Scenario-5 (Without SLR)**

In terms of VGR, in both scenarios follows somewhat similar patterns across land use categories. However, the amount of LULC getting affected by these plausible inundation scenarios is negligible, as Canacona is predominantly hilly.

Chapter -10

Coastal Vulnerability Index

10.1 Background: Climate Change and Coastal Vulnerability: A Multifaceted Analysis

Climate change, driven by escalating greenhouse gas emissions, poses a substantial global challenge with far-reaching consequences. The rise in greenhouse gases contributes to higher sea surface temperatures (SST), sea-level rise (SLR), and alterations in ocean currents, adversely impacting coastal regions and augmenting their vulnerability (Oppenheimer et al., 2010). The augmented risk of storm surges linked to tropical cyclones, intensified by warmer SSTs, could lead to severe consequences for coastal areas, compounding the existing challenges posed by higher sea levels (Knutson et al., 2010). These potential scenarios further amplify the vulnerability of low-lying coastal areas (Oppenheimer et al., 2010).

In September 2019, the Intergovernmental Panel on Climate Change (IPCC) projected a global SLR between 61 cm and 1.1 m by A.D. 2100, marking a 10 cm increase from the 2013 IPCC report (Oppenheimer et al., 2019). While these estimates are considered conservative, they underscore the growing threat to coastal regions. Concurrently, rapid urbanization, particularly in developing countries, adds another layer of complexity. Approximately 40% of the global population now resides in coastal areas, with projections indicating greater population growth in these regions than inland locations (United Nations, 2017; Neumann et al., 2015).

The state of Goa, renowned for its beaches, has witnessed a surge in urbanization, with the urban population increasing from 49% to 62% in the decade leading to the 2011 census (Census, 2011). This trend is mirrored in the coastal tracts of South Goa, fueled by tourism and developmental pressures along the coastline. The interplay between sea level rise and storm surge heightens the vulnerability of coastal regions, particularly those with sandy beaches, estuaries, and floodplains, housing valuable recreational and ecological assets (IPCC, 2014).

Current vulnerability assessments often lack spatial resolution, relying on administrative units like talukas and failing to capture the complexity of diverse coastal environments. This doctoral work addresses this gap by proposing modifications to the Coastal Vulnerability Index (CVI) methodology. The goal is to enable village-level vulnerability assessments, allowing for a more granular understanding of coastal vulnerability. By aggregating village CVI scores, taluka, and district-level vulnerability can also be determined.

Additionally, the doctoral work adopts a holistic approach, considering a comprehensive set of variables. Unlike traditional CVI assessments that focus mainly on physical and geological parameters, this work incorporates 10 such parameters alongside 11 socio-economic variables, recognizing the intricate interplay between different factors in influencing coastal vulnerability (Nigam et al., 2023, in press). This comprehensive analysis aims to contribute valuable insights for local adaptation efforts in the face of coastal hazards and long-term climatic changes.

10.2 Results

Table-10.1 Village-wise scores of Coastal Vulnerability Index (CVI), Social Vulnerability Index (SoVI) and Physical Vulnerability Index (PVI). Scores visually denoted by color coding: Green (<10) (Low level of vulnerability), Yellow (10-20) (Moderate level of vulnerability) and Red (>20) (High level of vulnerability).

Marmugao			
Village	**SoVI**	**PVI**	**CVI**
Vasco da Gama	24.64	10.4	35.04
Chicolna	27.69	13.14	40.83
Issorcim	19.18	14.7	33.88
Sancoale	21.7	2.68	24.38
Pale	16.27	14	30.27
Velsao	16.27	19.7	35.97
Cansaulim	7.67	24.14	31.81
Arrosim	7.67	19.71	27.38
Utorda	8.86	16.1	24.96
Majorda	5.42	16.1	21.52
Marmugao	15.53	15.06	30.6
Salcete			
Village	**SoVI**	**PVI**	**CVI**
Gonsua	6.26	19.7	25.96
Betalbatim	15.34	11.38	26.72
Colva	18.79	24.14	42.93
Sernabatim	7.67	14	21.67
Benaulim	10.85	19.7	30.55
Varca	11.51	16.1	27.61
Cavellosim	13.29	16.1	29.39
Cortalim	5.36	19.71	25.07
Quellosim	7.67	34.15	41.82
Verna	3.28	11.38	14.66
Loutolim	5.11	27.88	32.99
Camorlim	3.79	19.71	23.5
Rachol	6.26	19.71	25.97
Raia	3.13	16.09	19.22
Curtorim	2.21	11.38	13.59

Macasana	3.28	8.04	11.32
Chandor	1.8	11.38	13.18
Salcete	7.38	17.67	25.06
Coastal Salcete	11.95	17.03	29.26
Riverine Salcete	4.18	17.94	22.13
Quepem			
Village	**SoVI**	**PVI**	**CVI**
Curchorem	6.64	36.88	43.52
Quitol	5.42	2.68	8.1
Naquerim	6.64	2.68	9.32
Quepem	6.23	14.08	20.31
Coastal Quepem	6.03	2.68	8.71
Riverine Quepem	6.64	36.88	43.52
Canacona			
Village	**SoVI**	**PVI**	**CVI**
Cola	8.8	13.1	21.9
Agonda	26.5	27.8	54.3
Nagarcem-Chaudi	21.7	34.1	55.8
Poinguinim	7.2	16	23.2
Loliem	2.08	5.36	7.44
Canacona	13.25	19.27	32.52

(Score classification adopted from Kunte and others (2014))

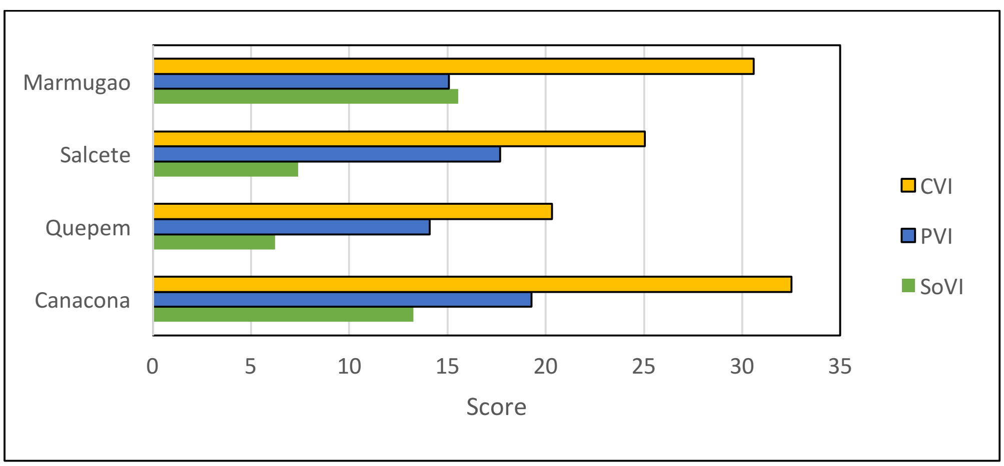

Fig 10.1 Clustered bar graph showing the CVI, PVI and SoVI score of each of the taluka(s) in the study area.

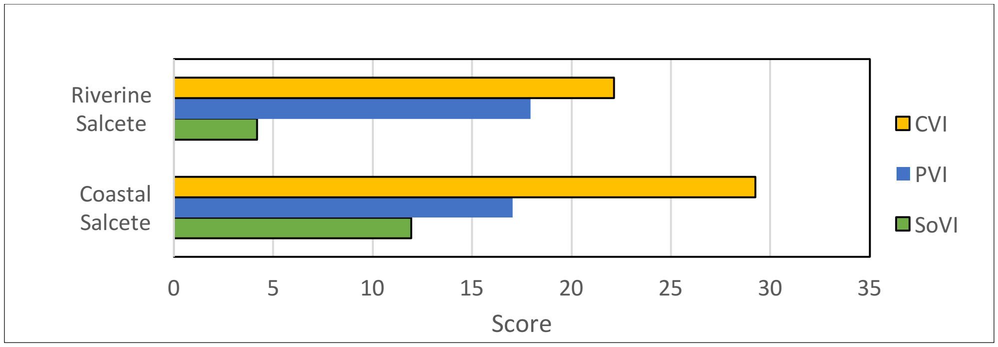

Fig 10.2 Clustered bar graph showing the difference between the CVI, PVI and SoVI scores of Riverine Salcete and Coastal Salcete regions.

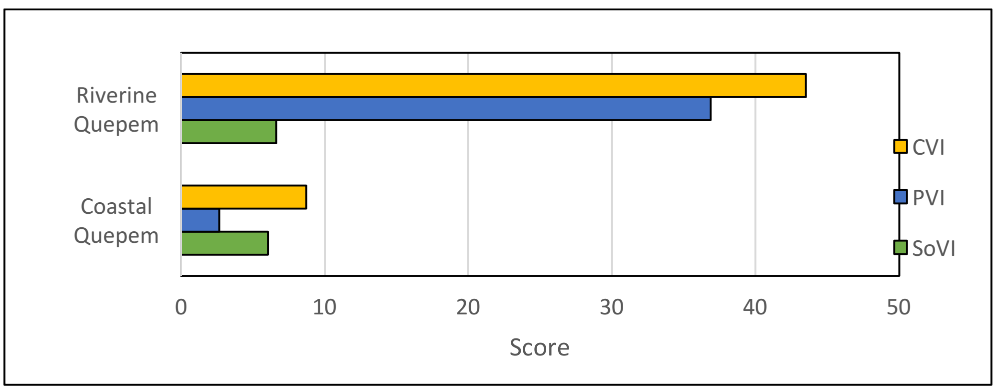

Fig 10.3 Clustered bar graph showing the difference between the CVI, PVI and SoVI scores of Riverine Quepem and Coastal Quepem regions.

10.3 Result Interpretation

- **Marmugao**

- In terms of SoVI, Chicolna, Vasco da Gama and Sancoale, located on the Marmugao headland have been found to have highest SoVI, while Pale, Velsao and Issorcim have moderate level of social vulnerability. Cansaulim, Arrosim, Utorda and Majorda, all located in along the linear coast of Marmugao have been found to be low on social vulnerability.
- In terms of PVI, only Sancoale was found to have low physical vulnerability. While Vasco da Gama, Assorcim, Utorda, Pale have moderate physical vulnerability. Cansaulim, Velsao and Arrosim have been categorized under high physical vulnerability, according to the results.

- In terms of CVI, all the villages in Marmugao taluka have been found to have high CVI scores. Consequently, Marmugao CVI is 30.6 (Table-10.1 & Fig.-10.1).

- **Salcete**

- Social vulnerability in Salcete taluka have been found under low SoVI category for all the villages except for Colva, Benaulim, Betalbatim, Cavellosim and Quellosim. These five taluka have high concentration of settled and tourist population. Cumulative SoVI in whole taluka and the riverine belt is under low category while in coastal belt its in moderate category.
- Physical vulnerability in Salcete taluka have been found to be low only in Macasana. Moderate in Gonsua, Betalbatim, Sernabatim, Benaulim, Varca, Cavellosim and also along the bank of Zuari river, Cortalim, Verna, Raia, Curtorim, Chandor, Camorlim, Chandor, Rachol. High PVI values have been found in Colva (estuary on the beach), Quellosim (low lying) and Loutalim (Khazan lands) being the primary reasons. Cumulative PVI in whole taluka and the riverine belt and in coastal belt is found to be in moderate category.
- Coastal Vulnerability in Salcete taluka has been found to be in high category from Gonsua in the north to Cavellosim in the south, along the Arabian coast and also in the low lying villages of Rachol, Camorlim and Loutilim. While the other villages, Verna, Raia, Curtorim, Macasana and Chandor have been found to be under moderate CVI category. Consequently, cumulative CVI in whole taluka, riverine belt and in coastal belt is found to be in moderate category (Table-10.1, Fig. 10.1 & 10.2).

- **Quepem**

- SoVI in Quepem taluka has been found to be under low category for all three villages and coastal Quepem region.
- However, the PVI is high in Curchorem and low in Quitol and Naquerim (along the coast) and moderate in Quepem.
- In terms of CVI, Curchorem, Quepem taluka and Riverine Quepem have been found to be under high CVI category (Table-10.1, Fig. 10.1 & 10.3).

- **Canacona**

- SoVI in Canacona taluka has been found to be low in Cola, Poinguinim and Loliem and high in Agonda and Nagercem-Chaudi, both of which are predominantly visited by tourists along with substantial infrastructural development. However, the SoVI for Canacona is under moderate category.
- Physical vulnerability in Canacona has been found to be under low category in Agonda, Nagercem-Chaudi and Loliem while in Cola, Poinguinim and Canacona taluka are under moderate PVI category.

- The CVI has been found to be under high category in the villages of Cola, Agonda, Nagercem-Chaudi and Poinguinim and also in Canacona taluka while the CVI is low in Loliem due to its location on the top of the cliff (Table-10.1 & Fig. 10.1).

Chapter-11

Discussion and Synthesis

11.1 Multi-Temporal Climate Trend Analysis

The goal of the current study was to identify the multi-temporal trends of the diurnal temperature range in the coastal tracts of South Goa district between 1981 and 2020, as well as the influence of other meteorological factors on the DTR, such as rainfall, temperature, land surface temperature, cloud cover, and cloud amount (See Chapter-4).

The study made use of the NASA POWER database, which are capable of reliably forecasting the majority of weather variables. NASA POWER's raw measurements of high and low temperatures and solar radiation are reliable and consistent (Rodriguez and Braga, 2021). Italian researchers Negm and others., Bai and others, in China and Monteiro et al. in Brazil made similar findings for different climatic variables. Similar findings were published by White et al. for the continental United States and Aboelkhair et al. for Egypt. Both groups concluded that NASA POWER datasets can reliably predict maximum and minimum temperatures.

The current work has demonstrated using the NASA POWER records, that there is a direct relationship between several climatic variables that affect one another at a specific location and time. The findings show that soil surface moisture is substantially influenced by rainfall, which is influenced by cloud cover, affecting T_{max}, T_{min}, DTR, and LST in the research area. T_{max} and T_{min}, on the other hand, have a significant impact on the DTR and LST. DTR, LST, and soil surface moisture are thus strongly influenced by tidal temperature, precipitation, and cloud cover (Fig.-4.4).

Climatic trends are continuous and subtle, covering a larger area with homogenous climatic characteristics. Hence, coastal climate is primarily influenced by the marine phenomena such as wind, currents and sea surface temperature. (Chiyyadri, 2021) which does not usually show stark differences in diurnal temperatures due to the influence of large water body.

11.1.1 Long-Term (1981-2020)

The current study has found increases in rainfall, T_{max} and T_{min}, LST, cloud amount, and soil surface wetness throughout the 40 years between 1981 and 2020, except DTR, which did not show any trend because both T_{max} and T_{min} are showing positive trend over this period, indicating that the difference between them is not changing (Table-4.2 & Fig.-4.1).

However, an increase in the Arabian Sea's sea surface temperature substantially impacts changes in rainfall, temperature, and cloud cover. Since 1980, the SST has increased significantly (Murakami et al., 2017). Since mid-1990s, warming rate has accelerated (from 7.7 milli-degrees/year to 13.4 milli-degrees/year) (Kumar et al., 2009). In the deeper ocean layers, which are known as the ocean heat content, warming is also observed in addition to the upper layers. 2009 (Kumar et al.). The elevated SST impacts the length, frequency, and intensity of cyclones and storms in the Arabian Sea. The frequency and strength of cyclones and storms over the Arabian Sea have increased significantly between 1982 and 2019. In particular, *"A 52% increase in cyclonic storm frequency, an 80% increase in cyclonic storm duration, and an increase in cyclonic storm severity of roughly 20% in the pre-monsoon period and 40% post-monsoon"* (Deshpande et al., 2021). Arabian Sea cyclones are strengthening as the SST and ocean heat content rise (Kumar et al., 2009).

Due to the intensity and increased frequency of cyclones, more clouds are forming, which eventually move to the Indian west coast during the southwest monsoon and provide heavy rain along the coastal area. Due to the increase in rainfall over the past few decades, this phenomenon is no longer just limited to the monsoon season. Additionally, increased cloud formation contributes to increased rainfall and soil surface moisture by contributing to increased cloud formation.

Additionally, it is impossible to deny human effect on shifting climatic patterns given the research area's rapid anthropogenic development. Coastal tracts of South Goa are a popular tourist destination with a significant influx of visitors and migrants, especially after the turn of the century. As a result, the coastal areas have seen haphazard tourism infrastructure construction. Furthermore, Goa is the most urbanised state in India, with 62.8% of its residents living in urban areas (Business Goa, 2018). Over the past two decades, this has altered the state's land-use pattern by turning forest and agricultural regions into built-up areas. These anthropogenic landscape modifications justify the recent upward Trends in LST.

11.1.2 Short Term (1981-1999)

Only T_{max} and DTR have showed positive trends throughout the short-term (1981-2020) timeframe, whereas all other climatic indicators have not (Table-4.3 & Fig.-4.2). The explanation for the positive trend in DTR is the rapid increase in T_{max} during this period compared to T_{min}, which increased the range between diurnal T_{max} and T_{min}. The most significant reason for the remaining climatic variables showing no trends, on the other hand, is that this 20-year period marked the beginning of changes in meteorological processes in the Arabian Sea (Murakami et al., 2017) and anthropic driven pressure in the research area.

On the other hand, the bigger picture is imperative to be understood to find out the climate trends of the coastal tracts of South Goa, which is a subset of Goa state. The anthropogenic pressure had begun to build up in the state of Goa by this time. The population of Goa state was 10,07,749 in 1981, but it increased by 33.7% to 13,47,668 in 2001. (Census of India, 2001). The tourism growth rate increased during the 1990s (Achrekar, 2019). The number of tourists arriving in 1981 (7,75,000), 1990 (8,81,000), 1995 (11,08,000), and 2000 (12,69,000) increased at a five-year growth rate of 13.67%, 25.76%, and 14.53%, respectively (Bremmer and Beech, 2004). Goa had

281 hotels and lodges in 1988, which climbed to 400 in 1994 and 436 in 1996. Approximately 77% of local and 95% of foreign tourists stayed in coastal locations (Kamat, 2003).

The statistics described above show that the local population, tourist population, and tourism infrastructure had little impact in Goa state till this period, because the tourism industry was just being established at the time. This suggests that throughout this time, the physical process of the Arabian sea warming and the anthropogenic pressure on the study area had begun to evolve, which explains the lack of trends in rainfall, T_{min}, LST, cloud quantity, and soil surface wetness. The increase in temperature is the first change in a region's weather that happens when changes in the climatic system begin to take place, therefore the upward trend in T_{max} can indeed be linked to changes in these physical and anthropogenic processes, even though they were still in the early stages. This time frame can be referred to as "the consolidation phase" of changing climatic and anthropogenic processes in the research area.

11.1.3 Short-term recent (2000-2020)

Since the turn of the millennium, the state of Goa has witnessed drastic increments in infrastructure development, tourism activities, vehicular traffic and migrant population (Business Goa, 2018).

The rapid expansion of tourism operations in the state has resulted in an expansion of other socio-economic and demographic aspects. Unprecedented rise in tourism happened during this period due to an increase in domestic tourists' disposable income, improved accessibility (Airport expansion, Konkan trains were operational), and according to Bremmer and Beech (2004), Goa's clean beaches and western lifestyle drew millions of tourists each year. Goa received 12,69,000 tourists in 2000, which increased to 23,00,000 in 2005 (81.24% increase). The following decade saw exceptional tourist growth, such as in 2010 (25,41,00), 2015 (53,00,000), and 2019 (Pre-COVID 80,00,000) (Govt. of Goa, 2021)., with five-year growth rates of 14.82%, 100.68%, and 50.94%, respectively.

Hosting an ever-increasing population in this compact coastal tract was never intended, resulting in an exponential rise of lodging infrastructure. This was accomplished by turning vast agricultural and wetland sections into built-up areas for developing tourism infrastructure (See Chapter-4).

According to Achrekar, 2018 *"Due to tourism and rapid urbanisation, there has been a tremendous pressure to convert land for non-agricultural use. As a result, land available for cultivation has declined hence the same limited cultivated land is used for sowing more than once".* The land unavailable for cultivation has almost doubled from 5.5% in 1961 to 10.28 in 2013-14 (Achrekar, 2018).

In 2015, there were 3358 hotels, an increase of 55.75 % since 2005, when there were 2156 total hotels, nearly a 10-fold increase since 1987. It is important to note that the informal hospitality industry has grown rapidly in addition to the emergence of hotels of the finest quality (Achrekar, 2018). These establishments are now the primary forces behind the haphazard development and concretisation in regions like the Baga-Candolim belt, North Goa, Palolem-Patnem and South Goa, which has also contributed to a significant rise in the amount of traffic in the state.

Tourism has also contributed to a general increase in the cost of living for the local inhabitants. Based on the fluctuations in the Consumer Price Index (CPI) for urban white collared employees, with 1982 as the base year index, the CPI for middle class workers was 245 in 1991-92, 554 in 2004-05, and 1182 in 2014-15. (Government of Goa, 2015). This resulted in locals migrating from the tourist belt to the hinterland regions, resulting in deforestation and conversion of agricultural fields to built-up hinterland areas. As a result of uncontrolled infrastructure development during the previous two decades, Goa has seen an extraordinary increase in land-use conversion, urbanisation, vehicular traffic, and concretisation, demonstrating conclusively the upward trend in LST during the 2000-2020 period. Increased LST, together with increased pollution from vehicular traffic and related tourism and mining operations in the state, promotes a positive trend in T_{max} (Table-4.4 & Fig.-4.3).

On the other hand, the Arabian Sea has experienced an increase in cyclonic activity during the past ten years, and as a result, cyclones have started to occur more frequently, annually, indicating a change in pattern. The primary evidence of a sharp increase in cyclone activity in the Arabian Sea is provided by Nilofar (2014), Chapala and Megh (2015), Vayu (2019), Nisarga (2020), and Tautkae in 2021 (Dasgupta, 2021). The current analysis also discovered that, between 1982 and 2020, there were 13 years (33%) with above-average rainfall per day (>18mm/day), and 11 of the 13 occurrences (84.61%) happened within the previous 14 years (Fig.-11.1). The amount of rainfall increases when cyclone frequency increases (EPA, 2017).

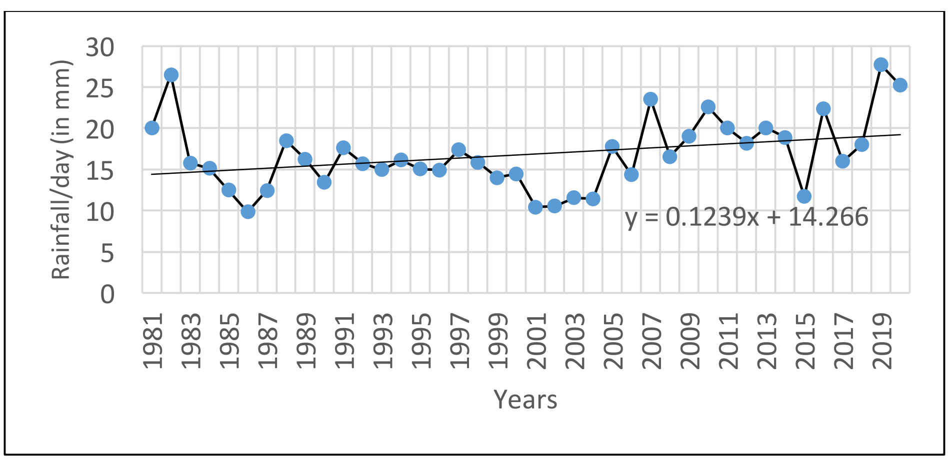

Fig-11.1 Rainfall/day (in mm) during monsoon period (June-September) between 1982-2020. (Source: NASA POWER)

As a result, the increase in SST in the Arabian Sea has increased the frequency of cyclones (Murakami et al., 2017), which is the leading cause of the positive trends in rainfall, cloud amount, and the resultant soil surface wetness, as well as T_{min} (due to greenhouse effect from copious quantities of cloud cover during monsoon), over the past 20 years.

11.2 Multi-Temporal Land Use Land Cover Assessment

This multi-temporal assessment has been carried out to delineate the decadal changes in LULC pattern using satellite data. Modern strategies for managing natural resources and tracking environmental changes rely heavily on changing land use and cover (Masroor, 2013; Ashbindu, 1989). Socioeconomic factors, such as land policy, property rights, institutions, population migration, urbanization, other economic activities, have a significant impact on land-use change. As a result, research in the field of LULC favors a holistic viewpoint and calls for an interdisciplinary approach. Any research on LULC must have a thorough grasp of the causes of land-use or land-cover changes.

The increase in the build-up area in all the four talukas has been at the cost of agricultural land or water bodies/wetland encroachment (Table-5.1 & Fig.-5.1). This is expected given the fact the Goa in a tourist destination and more and more people invest in constructions which has higher price tag compared to the agricultural produce.

The loss in vegetation is also due to converting the land to settlement by vested interest. The loss in vegetation is remarkable in talukas where the land gradient is low. For example, the loss in vegetative areas in Quepem and Canacona (Table 5.1 (c) & (d)) & (Table-5.3) were minimum during the four decade compared to Mormugao and Salcete (Table 5.1 (a) & (b)) & (Table-5.3). The government acquires agriculture lands at lower rates to use them for development for roads, structures and other facilities for citizens which is the root cause for dropping percentage of agriculture land. Most of the localities in Salcete are hosting commercial activities so the pressure on agriculture land is more.

Wetland and water bodies form an important part of the ecosystem that supports fresh water life and also provides employment to people involved in pisciulture, salt farming, etc. A decrease in the area by more than 60% in area occupied by water bodies in Mormugao and Quepem during 2011 to 2020 is alarming (Table 5.1 (a) & (c)) & (Fig.-5.2). Likewise, decrease in area of wetland by more than 50% in the aforementioned talukas during the same period is a matter of concern. Most of the wetland and water bodies are encroached by weeds. Weeds are unwanted aquatic plants of uncontrolled growth which generate gases like H_2So_4 and CH_4 that pose threat to the productive potential of the aquatic body.

Canacona is a global tourist destination which is visited by 77,041 tourists (total population of taluka 45,172). The coastline of Canacona is known for stunning, breath-taking and spectacular coastal landforms and beaches. The vegetation areas showing no change in the Canacona taluka are due to the presence of wildlife sanctuaries such as Cotigao wildlife Sanctuary which are under protection under wild life act. The increase in the buildup area at an average rate of 11% and decrease in barren land in 2011-2020 (Table-5.1(d)) & (Fig.-5.2) is attributed to increase in guesthouses, small hotels to accommodate tourists and making provisions for parking of vehicles, respectively. Likewise, beautiful beaches like Colva, Sernabatim, Velsao, along the coastal tracks of Salcete are home to millions of tourists, so the buildup areas have increased exponentially.

11.3 Anthropogeomorphic Impact Assessment

11.3.1 Variables of the Nigam-Kotha model of AGI@E

Many alternative methodologies have been proposed to quantify the AGP impact, but none appear to provide comprehensive data. Although Nir's index of Anthropic stress has been identified as the most useful model for dealing with the problem (Rozsa, 2007), it also has some flaws that are discussed in the preceding section.

According to Rozsa (2007), the potential influence of AGP on the ecosystem and the earth's surface is decided by technological advancement and population expansion. In other words, as the population grows, more land resources are required to meet its demands (e.g. farmland for agriculture, mining for industrial development, grazing land and suitable land for habitat development). As a result, an increase in ecumene expansion results in a direct modification of geomorphology.

In order to determine the ecumene expansion, geospatial approaches are the most efficient way since they can offer multi-temporal changes in an ecumene at different spatial resolutions. However, determining the geomorphic impact of ecumene expansion is outside the limits of geospatial technology; so, this novel model has been proposed to assess the influence of ecumene on geomorphology, which uses remote sensing to calculate the ratio of ecumene to natural habitat.

The novel model has incorporated a total of ten parameters. Four corresponds to the “Anthropic Stress” which are further divided into two; “Amount of Anthropic Pressure” (Ecumene In %, Population Density in Ecumene) and “Amount Of Lack Of Perception” (Illiteracy in %, Population Below Poverty Line in %). On the other hand, remaining six parameters indicates “Geomorphological Susceptibility” to modification by defining the “Degree of Deformation Susceptibility” which also comprises of two different sub-parts; Geomorphic setting (Rock Constant, Slope Constant and Rain & Sun Aspects) and “Erosive Susceptibility” (climate and hazard). Rationale behind incorporating all these ten parameters in the model is provided in (Supplementary table-1, in Appendices) and each of the parameters have been discussed below:

- **Ecumene**

The term is derived from an ancient Greek word "oecumene" which referred to the known world or the habitable world. In modern times ecumene refers to any inhabited land or “the area under human influence” (Jefferson, 1934). As Jefferson argued *“Egypt for instance, is most densely populated. It has over a thousand people per square mile. But a square mile of what? Not desert,* *off course, but irrigable land by the Nile. Egypt's fourteen million people on her area of 386,000 square miles amounts to less than forty people to the mile, say ten families. That is not the right picture of Egypt. The desert is not Egypt. It merely belongs to Egypt. The people are crowded on the delta and flood-plain. That is all we should count. It is Egypt's ecumene. The contrast between desert and ecumene is sharp"* (Jefferson, 1934). *Therefore, in context of the AGP, Direct* Human influence upon geomorphology only takes place when an uninhabited land area comes under the usage of anthropogenic activities such as; settlement, agriculture, terrestrial transportation network. This causes land transformation as per the land use modification intensity.

As a result, in the context of the AGP, human influence on geomorphology occurs only when an uninhabited wilderness region is subjected to anthropogenic activities such as settlement, agriculture, and terrestrial transportation networks. This results in land transformation based on the intensity of land use alteration. The direct impact of anthropogeomorphic processes is visible only in the ecumene region, not in the non-ecumene region, because the absence of human activities leads to the absence of an ecumene; thus, absence of ecumene leads to no direct AGP impact, and indirect or cascading effects of AGP in non-ecumene area is beyond the scope of this model. (Refer to Appendix section, Supplementary Table-1 & Table-2 to read about the rationale behind each variables and impact of different land-use and human activities on geomorphology respectively).

- **Population density**

Human population growth puts more strain on the land (Garg, 2017), because humans need land resources to survive. The model incorporates this variable based on this simple reasoning since the higher the human density, the greater the strain on landforms, processes, and limited terrestrial resources. Furthermore, rather than incorporating the crude value of population density of an administrative area, the model has used a novel concept of 'ecumene population density' because the population density of a whole administrative unit (sub-district, district, or state) may be insignificant in terms of the pressure exerted by human population on the concerned land. An administrative unit can also have areas that are unaffected by human activities; therefore, only the ecumene zone is the part of an administrative unit where the population resides and exerts pressure on the land, and this is where the AGP operates.

- **Illiteracy**

Illiteracy indicates a lack of education, which is required to build a public perspective in order to use limited land resources in a sustainable manner (Nir, 1983). Illiteracy is a crucial factor in reducing the influence of AGP in a community. To begin with, an illiterate individual or society would struggle to comprehend the concepts of sustainable use of available resources and sustainable growth (Marope, 2017). Lack of understanding would result in an intentional or unintentional increase in the AGP impact. Furthermore, illiteracy promotes a lack of perception (Nir, 1983; Vagvolgyi et al., 2017), which may impede mitigation of the AGP's already detrimental consequences.

- **Population Below Poverty Line**

The population living below the poverty line is commonly defined as a segment of society that lacks the bare necessities (financial and materialistic) to sustain a decent standard of living. It becomes a major determinant in limiting the AGP consequences since it stimulates over-exploitation of resources (such as land & water) to meet requirements and discourages the use of resources in a sustainable manner wherever possible (Khan et al., 2022).

- **Rock type**

Rock is the parent element that forms a landform. Thus, rock erodibility defines how stable or fragile a landform is against the operating processes. Varying rocks (hard rock and soft rock) have different ability to withstand erosion caused by geomorphic processes (Duszyski et al., 2022). The rock building substance influences rock erodibility. The idea behind including this variable is that if the erodibility of the rock is high, it will be eroded faster, causing the landform to deteriorate faster. If the AGP is operating on a landform with a high erodibility rate, the AGP's influence will be significantly greater than on low erodibility rock formations.

- **Slope**

The gradient between the highest and lowest point at a given position on the surface is referred to as slope (steepness) (Saunders and Young, 1983). The lower the degree of steepness, the better for anthropogenic operations since it provides stability against gravitational force, whereas the higher the degree of slope, the more prone to landslides (Haijun et al., 2018). As a consequence, there is more erosion. The slope is included in the model because the higher the degree of slope of an ecumene, the higher the AGP pressure because less force is necessary to initiate the erosion. As a result, the magnitude of landform modifications would be larger as well as detrimental to anthropogenic activity.

- **Aspect (Rain)**

Due to the orographic rainfall phenomenon, the 'windward side' of a landform receives more rainfall than the 'leeward side' (Shrivastava et al., 2022) As a result of strong rainfall penetration, the windward side of an ecumene becomes especially prone to chemical weathering and erosion (Bosdorf and Stadle, 2015), which is a function of natural process. When the AGP is operating on it, this aids in landform deterioration. As a result, windward aspect multiplies the AGP stress many times. On the other hand, the intensity of rainfall decreases away from the windward side, resulting in low chemical weathering and consequently less assistance from rainfall in erosion.

- **Aspect (Solar)**

Solar insolation raises the temperature of the rock's surface during the day, while the absence of sunlight causes the rock to lose heat at night. This process occurs on a daily basis, and ultimately the top layers of the rock begin exfoliating, a process known as exfoliation (onion) weathering, which weakens the rock over time (Jain, 2014). Exfoliation weathering is more common in regions (landforms) that get direct sunlight for a longer duration of the day because they experience a greater range of temperature change during the day and night than areas that do not receive direct sunlight. Similarly, to the rain aspect, if the AGP is also active in an area where exfoliation weathering is active, an increase in AGP stress is guaranteed (compared to partially solar facing or non-facing) because exfoliation weathering will work hand in hand with the AGP, resulting in rapid modification of landforms by increasing weathering rate.

- **Climate**

Climate has a significant impact on geomorphic processes (Parsons et al., 2009). However, the intensity with which these processes are fed varies among regions. In other words, along with the AFP, climate (exogenetic forces) is the primary cause of landform changes. Climatic agents such as precipitation, temperature, and wind, to mention a few, are the causes of many geomorphic processes such as fluvial, glacial, marine, and aeolian. These processes shape a region's landforms and determine its geomorphology (Parsons et al., 2009). For example, a humid tropical environment yields the most rain in the world, resulting in the highest rate of erosion since moving water is one of the most powerful agents of erosion. Hot and dry desert climates, on the other hand, have one of the lowest erosion rates of all climate types due to the presence of the slowest geomorphic agents (solar and wind). As a result, the strength of landform erosion varies with climate.

- **Hazard**

Natural hazards are just natural processes (exogenetic or endogenetic) that have existed since the earth's inception, but these natural processes have become dangers when they inflict damage to any anthropogenic belongings (Khan et al., 2008). The presence of various natural hazards which can occur in a particular region and act on a landform as a geomorphic process is described by the hazard factor in the model. However, if the AGP is also dominant in the given area, the damage could be magnified enormously. When the hazard(s) and AGP interact, they might cause significant changes across the region.

11.3.2 Case study – Coastal tracts of South Goa

According to Rozsa (2007), built-up activities are one of the most intensive land alteration processes, resulting in the greatest anthropogeomorphological impact. Similarly, AGI@E model results suggest that Marmugao and Salcete have the highest degree of Anthropic pressure, which is mostly influenced by study area's land-use (Table-6.1 & Fig.-6.1). The study area (primarily Marmugao and Salcete) has seen unimaginable built-up activities (amount of anthropic pressure) (Fig-11.3 (a) & (b)) to cater to ever-increasing coastal tourism and urbanisation activities since the turn of the millennium. It had 83.13 km^2 of built-up area in 2000, which expanded to 133.22 km^2 in 2020, a 60.25% growth, with the majority of it in the taluka(s) of Marmugao and Salcete. On the other hand, agricultural land got reduced by 8.1% during the similar period and also the forest and water bodies (Fig-11.3 (a) & (b)).

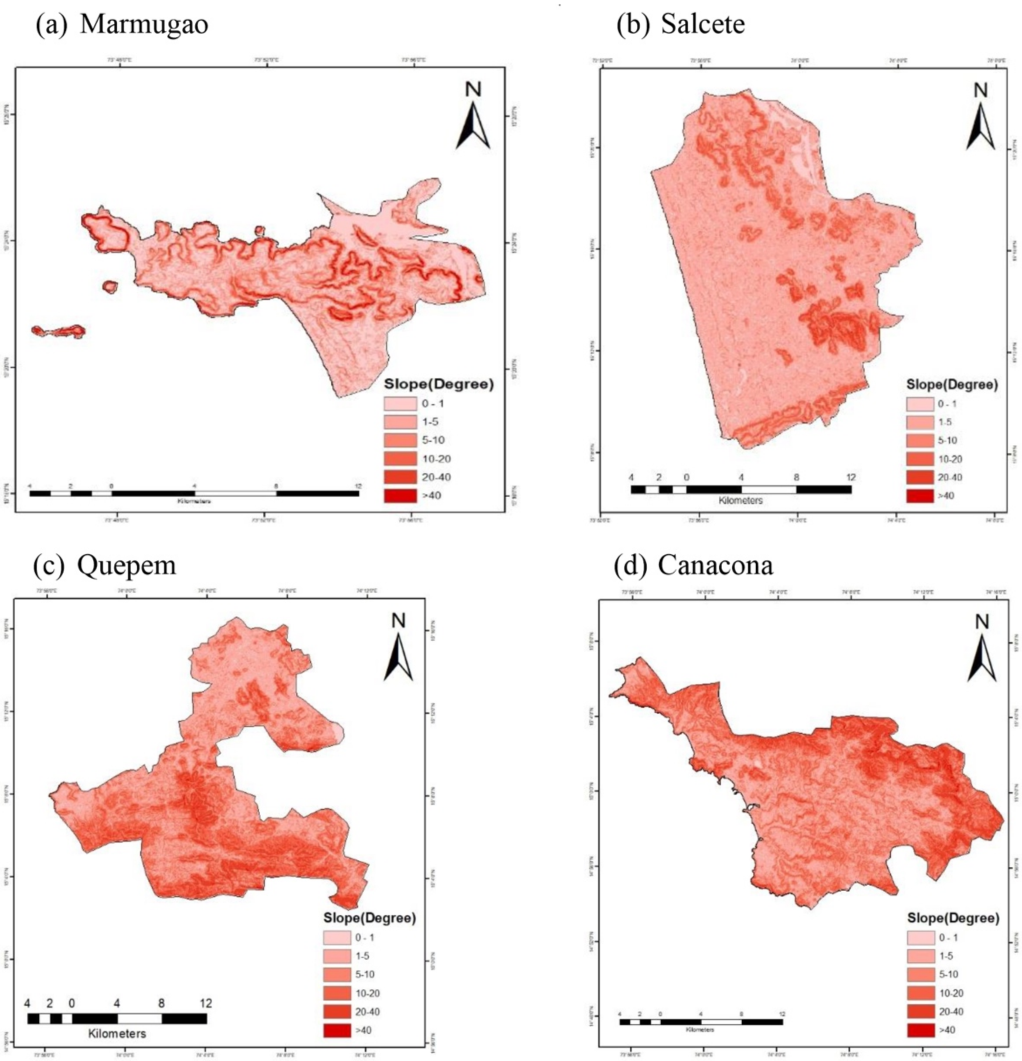

Fig-11.2 Slope maps of all the four taluka(s) in the study area.

Marmugao

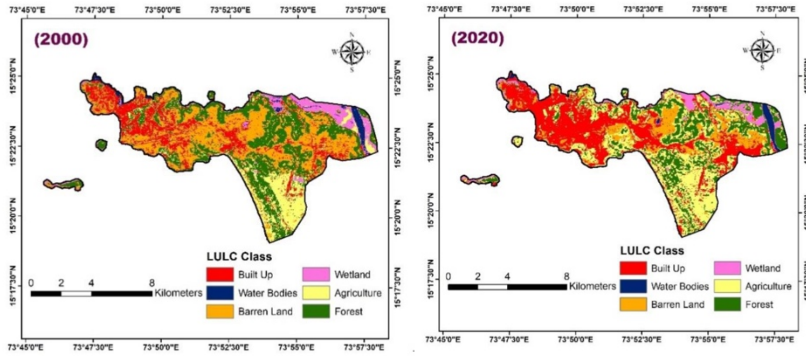

Salcete

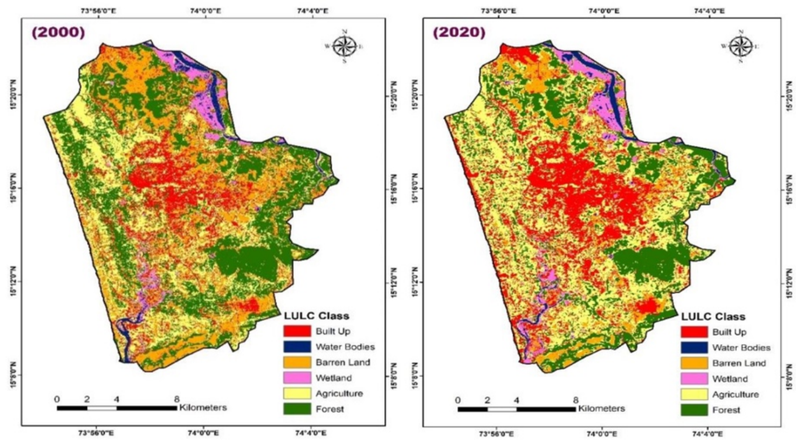

Quepem

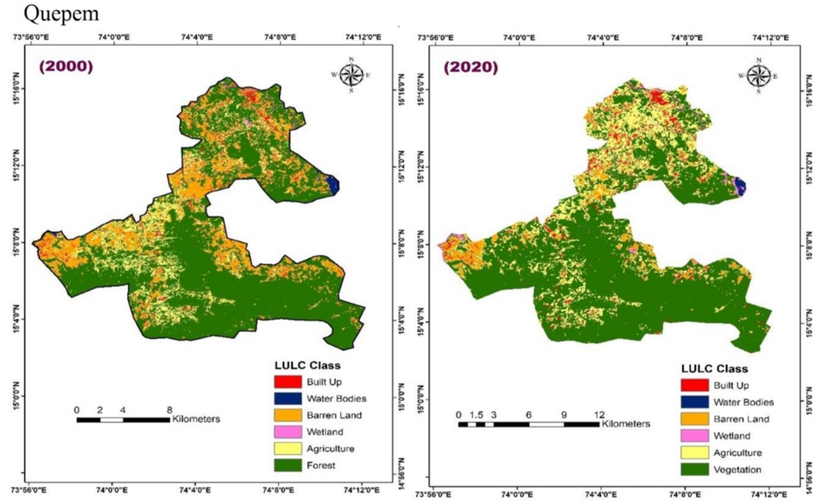

Canacona

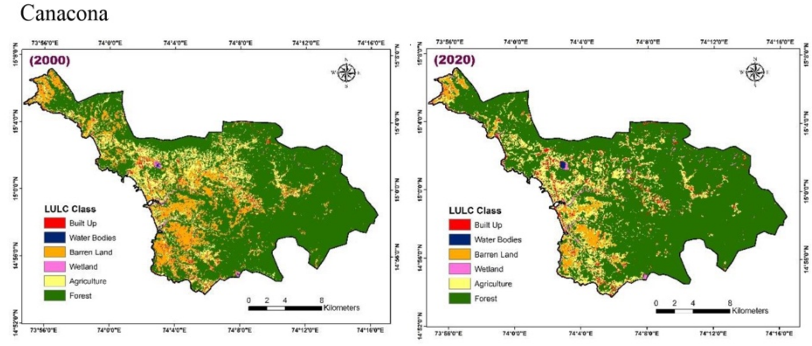

Fig-11.3 Land Use Land Cover maps of the four taluka(s) located in coastal South Goa during 2000 and 2020 (Refer to Appendix section, Supplementary Table -3 for the LULC statistics).

Moreover, Hooke (1994) regarded Gross National Product as one of the proxies to evaluate deliberate human geomorphological effect in any given nation. Similarly, Goa's National State Domestic Product was Rs. 26418 in 1996-97, Rs. 44110 in 2001-02, and Rs. 259444 in 2011-12 (RBI, 2019). This implies that the increase in NSDP is directly proportional to technological improvement, which is one of the primary drivers of intentional human geomorphological effect in the region (Rozsa, 2007). Under the degree of anthropic pressure, the novel model AGP@E findings completely justify this theory.

According to Nir (1983), Mitra (1984), and Ngondya (2011), the illiteracy rate and anthropogeomorphic impact are directly proportional to each other since illiteracy generally leads to a negative perception of curtailing erosion caused by human land-use activities and vice versa. Marmugao taluka has the highest illiteracy rate and slum areas of all of the talukas. Furthermore, the majority of the population in these slum neighborhoods is below poverty line (mainly immigrants). The outcomes of this unique model AGI@E strongly justify the current scenario in the study area, as Marmugao tops the list in terms of the “Degree of Anthropic Pressure”, which is also influenced by illiteracy and poverty.

Marmugao 2000

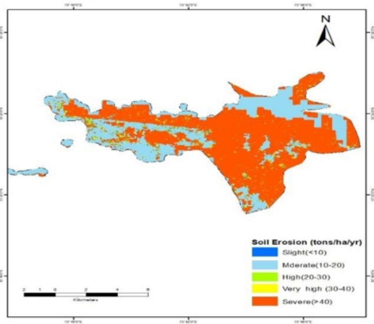

Marmugao 2020

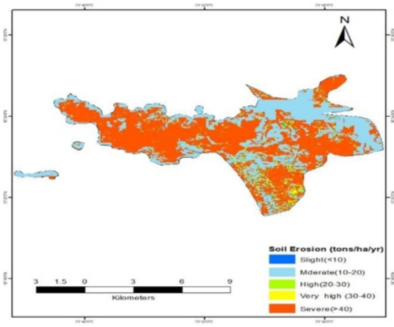

Salcete 2000

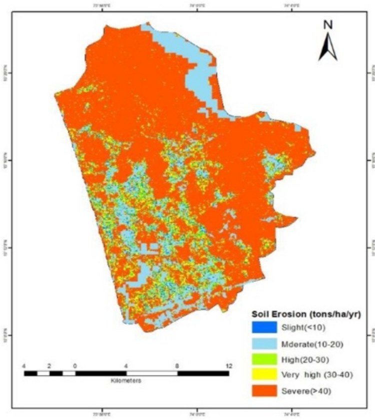

Salcete 2020

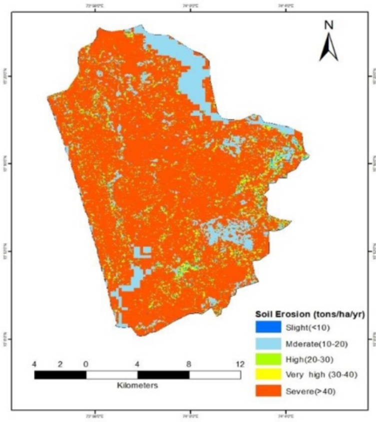

Quepem 2000

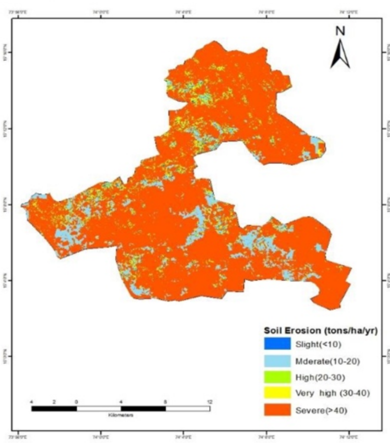

Quepem 2020

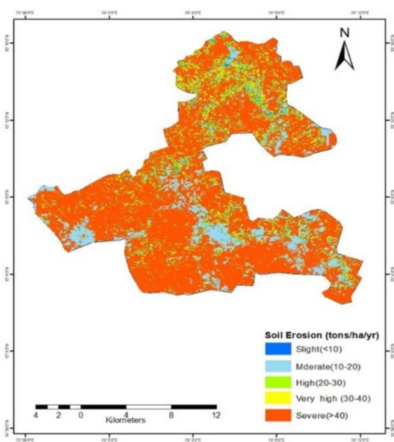

Canacona 2000

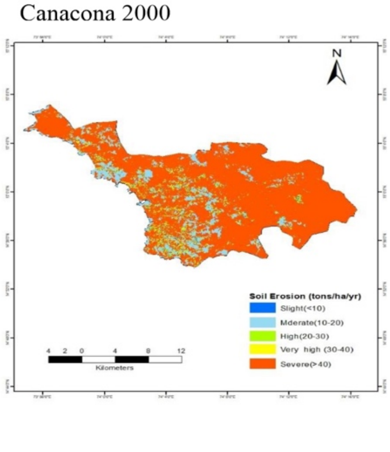

Canacona 2020

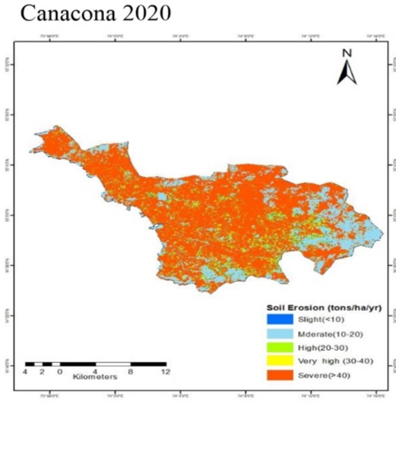

Fig-11.4 Soil loss maps of the four taluka(s) located in the study area during 2000 and 2020 (Refer to Appendix section, Supplementary Table - 4 for soil loss statistics).

Soil erosion in Marmugao and Salcete taluka(s) is 'moderately high' in the state but the highest in the study area, according to the status of soil loss in the study area (Fig-11.4 & Supplementary Table - 4). Marmugao is at the top of the list because it is located on a lateritic headland (Reddy et al., 2016), whereas Salcete has gentle, low-lying Zuari river flood plains formed by unconsolidated particles (Fig-11.2 (a) & (b)). Both the taluks(s) are naturally prone to erosion, but growing urbanisation has resulted in a very significant human impact on relatively unconsolidated land. The results of the novel model AGI@E confirm this, with Marmugao and Salcete earning the highest values of the 'degree of erosive susceptibility' and, as a result, a significantly higher AGI@E compared to Quepem and Canacona who have extensively hard bedrock compared to the other two.

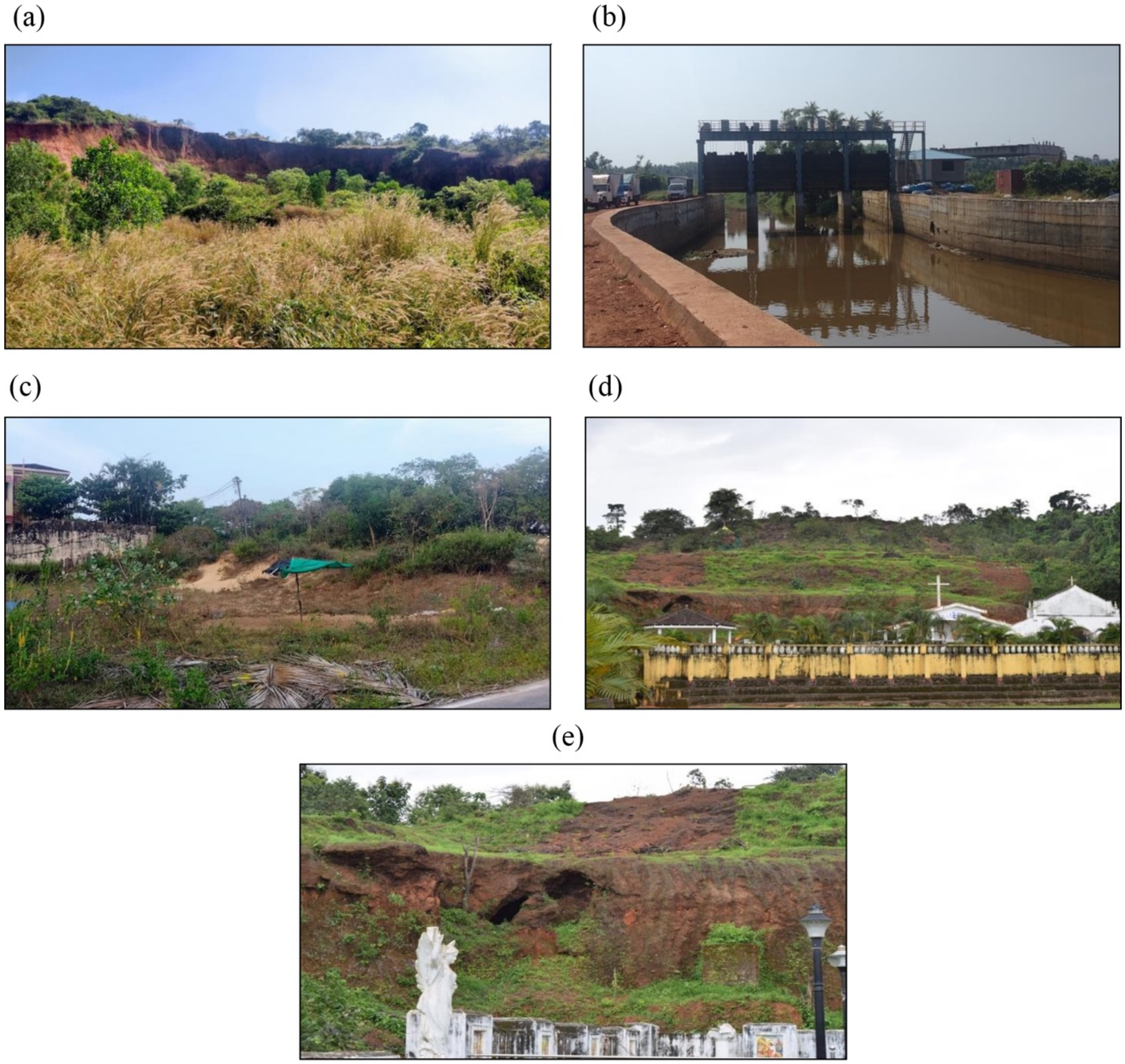

Fig –11.5 Some examples of the Anthropogeomorphic impacts in the study area. (a) Hill cutting and ground planation for urban expansion at Fatorda, Margao city, Salcete. (b) Channelization of Sal river near western bypass, Margao city, Salcete. (c) Sand dune destruction and ground levelling for the construction of houses at Gonsua village, Salcete, (d) Human induced terracing and ground levelling of the northern lateritic slope of Verna plateau, Quellosim, Salcete and (e) Zoomed-in image showing severe erosion making the terrace fragile at the same location.

(a)

(b)

Fig –11.6 Massive hill cutting and ground levelling along the National Highway – 66 at Poinguinim, Canacona.

High water erosion is caused by excessive rainfall (Kulimushi et al., 2023) and windward side aspects (erosive susceptibility) (Fig.-11.2). It accounted for 58.2% of total erosive processes functioning in the study area in 2005-06. In addition, in 2005-06, the second most dominating process in the research region was anthropo-geomorphic, with a share of 19.08% spanning an area of 81.20 sq. km. However, in 2015-16, the share of anthropo-geomorphic processes increased to 88.23 sq. km (20.50%) (Fig.-11.3, Fig.-11.5 & Fig. 11.6) whereas the share of water erosion processes declined to 247.32 sq. km (57.46%) (NRSC, 2018). The findings show that the AGP is gradually rising to become the most important geomorphic process in the study area.

This fact further reinforces the validity of the robust model AGI@E, explaining why Marmugao and Salcete had greater ‘erosive susceptibility' values than Quepem and Canacona. It is so because Marmugao and Salcete ecumene have a higher proportion of directional aspects which face south-west rains, despite the fact that all four taluka(s) fall under the same climatic and hazard classifications.

11.4 Multi-Temporal Beach Litter assessment

Several researchers have undertaken a study of the nature and abundance of marine litter and its impact on the coastal environments of India to understand the source. Kaladharan et al. (2017) observe that coastal tourism playing a prominent source of beach litter. The spatiotemporal distribution, composition, and beach quality based on 17 beaches of Northeast India (Mugilarasan et al., 2021), suggested that the type of marine litter were representatives of household, tourism, and fishing activities.

The microplastic litter occurrence, distribution, and characterization suggest considerable pollution along the coastal stretch of Karnataka state (south of the present study area) and recommends the implementation of a regular and permanent waste management system for beach protection (Yarnal et al., 2021). A substantially high overall abundance of plastic litter in the beaches of the Mumbai coast resulting from coastal recreational and other anthropogenic activities was reported by Jayasiri et al. (2013). Behera et al. (2021) observe that coastal recreation is the primary source of marine litter pollution along the coastal stretch of Northern Gujarat. More microplastics in the highly productive and bio-diversified coastal ecosystems off the southeast coast of India, especially in regions dominated by tourists and fishing activity, has been detected elsewhere (James et al., 2021). Widespread occurrence of microplastics in the sediments of the Kanyakumari coastal stretch of southernmost India has been reported. Sunder et al. (2021), while providing baseline data on the beach litter along the Southeastern Coast of India, identifies a relationship between human activities and microplastic concentrations as most of the litter is found associated with sediments in the vicinity of harbors and tourist beaches.

The awareness towards reducing marine pollution is growing in the scientific community and local governments. Several schemes introduced in India, such as the Circular Economy Solutions Preventing Marine Litter in Ecosystems- which aims to follow R3 (Reduce, Reuse and Recycle) for the plastic items, particularly in the states of Kerala, Tamil Nadu, and Uttar Pradesh, to quantify and monitor marine litter. The deposit fund scheme for plastic bottles is also currently being implemented in various parts of India (Henzlar et al., 2019).

Among the most secluded and tranquil beaches covered under the study is Velsao. Amenities are commonly owned by local residents, which can be considered as the primary source of beach litter for urban beaches. Baina is primarily an urban beach located in business city of Vasco-Da Gama. Baina observed a reduction of 288.18% during the lockdown period. As the beach is centrally located, which strongly indicates that locals and tourists were unable to visit these beaches; resultantly huge reduction in beach litter occurred.

South Goa's highest tourist inflow occurs Colva, and Palolem beaches. These beaches also cater to a significant number of local tourists. Palolem beach witnessed the highest reduction in beach litter amount during the lockdown, as compared to post lockdown (1040.74%). In contrast, Colva observed a (134.48%) of reduction. The multi-temporal observations revealed that these beaches sustain totally upon tourism activities (D'Souza, 2021) and do not have a significant local population who visit these beaches. Total restriction on tourist inflow during lockdown could be the most prominent factor that reduced litter, which suggests that tourism activity is the primary source of litter. Besides, the main aspects of litter at urban beaches is also slum development along the Baina beach (Table-7.1 & Fig.-7.1).

The complacent behavior of tourists plays a significant role in beach litter generation (Table-7.1 & Fig.-7.1). On the other hand, the burden of maintaining cleanliness relies on the local population. Per-capita litter reduction (Table-7.3) during the lockdown in comparison to the post-lockdown period was found to be highest for Palolem (1032.60%), Baina (276.92%), Velsao (137.47%) and

Colva (135.06%). This study also reveals that a significant reduction in the mean litter along the South Goa coast, 28.31 g/m^2 during peak tourism period, and reduced to 10.04 g/m^2 during lockdown period. Both the values are significantly lower than the litter density of 205.75 g/m^2 reported by Kaladharan and others (2017) during October 2013-January 2014 along the coast of Goa, which declared that the coast is the most littered among the coastal states in India. However, the results indicate a remarkable improvement in containing beach litter and maintaining beach hygiene.

Anthropogenic beach litter once discarded, makes its own journey and can be found in high numbers especially where the human influence is higher. It is a clear indicator of human footprints. Primarily, at tourism dominant spots, specific type of litter can provide an idea about the anthropogenic pressure on the specific part of coastline. This implies that, floating population is major source of beach litter because of their sheer numbers which clearly indicates towards higher burden on the limited and already under pressure coastal resources. Resultantly, this phenomenon is increasing the exposure of inherent vulnerability in the study area and thus the coastal vulnerability.

11.5 Multi-Temporal Air Quality Analysis

Air pollution levels may vary to a great extent with the geography, demography, and socio-economic factors of the region, which determine the source and dispersal of the pollutants. The climate and topography of a region also influence the atmospheric processes thereby, modulating the circulation of pollutants and their effects on the environment and subsequently on human health. SO_2 and PM concentrations have been related to meteorological factors (Chao, 1990). A high correlation between the mean dust concentration and several meteorological factors in Osaka City has been found (Miyazaki and Yamaoka, 1991). Tirabassi and others (1991) found a close relationship between wind speed, SO_2, and particle concentrations in the coastal city of Ravenna, while Cuhadaroglu and Demirci (1997) used multiple linear regression analysis to evaluate the relation of pollutant concentrations with several meteorological factors. In the study presented by Bridgman and others (2002), the relationship of SO_2 concentrations with the major meteorological parameters such as wind speed and direction, solar radiation, relative humidity, pressure, and the temperature was investigated. Their results revealed that SO_2 concentrations were strongly related to a colder temperature. On the other hand, there is another way around too. Increasing air pollution also suggest the increasing human influence in the region.

In the present analysis, different contributors have led to steep pollution levels in Goa (Table-8.1& Fig.-8.1 (a)). The state highway witnesses heavy traffic consisting of trucks/lorries, interstate buses, and other vehicles that pass through Vasco da Gama city. Vasco Da Gama has predominantly been found to be on the top of the list of most polluted towns in Goa. GSPCB in 2018 stated the reason behind critical pollution status in the city which includes the high amount of infrastructure construction, as well as the explosion in the number of vehicles plying on the roads of this congested city devoid of space (Navhind Times, June 6, 2018). In addition, one of the largest concentration of the slums across the state is in Vasco, who are devoid of modern home appliances and sustainable living standards. It is strongly believed and experienced since the turn of this century that the coal handling operations at the Marmugao Port located in Vasco city is the major source of pollution pertaining to Particulate Matters (PM_{10} and $PM_{2.5}$) because the coal is transported on the trucks passing through the sole major road of the town and the coal filled railway wagons mostly stationed in the town waiting for their turn. This phenomenon is clearly indicated in the present study as the increasing trend of $PM_{2.5}$ and "High" to "Critical" level of PM_{10} and $PM_{2.5}$ between 2017-2020 period (Table-8.2).

The other indirect but very significant health implication of coal dust is through the leakage and spillage from the barges during transportation into the Vasco bay, which also indicates increasing human presence in the once preserved estuarine area. This bay is the fishing ground of villagers from Kharewado, Baina and Desteiro. This pose a great danger of ingestion of coal dust and other pollutants by the local population through edible fishes. Adding to the crisis, these villagers are threatened to be displaced from their village due to expansion of the port area, which will further deteriorate the pollution levels in Vasco da Gama. The use of biomass material for water heating and cooking is the major source of pollution in the city (Herald, March 29, 2019) whose dispersal in the air in a true proxy of human influence in the neighbouring areas as well.

For Margao, the pollution has been attributed to an increase in the number of road vehicles, construction debris, and incineration of waste in the open air. Most of the vehicles pass through these cities as a part of interstate connectivity, so diesel vehicles top the list contributing to PM, SO_2, CO, etc. (Table-8.1 & Fig.-8.1 (b)). Rampant construction activities, including public works have increased in Margao, Mapusa and Ponda which has also deteriorated the AQ in the past five years when interstate highway widening works were undertaken by clearing of roadside trees and cutting and leveling of hills and dumping of debris in the low lying areas as a filling material for road making. Margao is one of the major railway terminals where at least 30 long-distance and ten local trains running on diesel makes a scheduled stop, which also adds to the air pollution. Though the incineration of waste is banned since 2016 by the National Green Tribunal, there are instances wherein plastic, tires, and other domestic wastes are burned on a small scale in the countryside.

Partly, in the township areas in Curchorem, the mining dust from the mining rejects and ore dumps contribute a significant share to the PM (Table-8.1 & Fig.-8.1 (d)). The ore to the ore-burden ratio in Goa is 1:3, which means for every tonne of ore excavated, about three tonnes of overburden material is generated and is treated as mountains of rejects/ dumps. Major sources of atmospheric emissions from open-cast mining activity include land clearing, removal of dumps, and vehicular movement on the haul roads, excavation, loading and unloading of ore materials, as well as overburden (Singh and Perwez, 2015). Dust emanating from the haul roads contributes considerably to the PM in the atmosphere (Singh and Perwez, 2015). With the Supreme Court allowing auctioning of the mined ore for the last three years, the exhaust from the trucks and the dust generated during transportation to the barge landing points adds to the air pollution. However, heavy rainfall in these region is a blessing in disguise to flush out the PM. Most of the area in Quepem is hilly with thick cashew plantation, which is a cash crop, so the PM settles down on the vegetation, reducing the fruit-bearing capacity. Coal dust blown from the cargo trains running through Curchorem also contributes to the PM, and people with cases of asthma and respiratory ailments have gone up in the recent past.

Goa being a tourist attraction, many tourists from the neighboring states visit Goa on weekends by driving in their vehicles. Rent-a-bike and rent-a-car are also popular, which significantly adds to the air pollution, besides generating trash (Nigam et al., 2022) and putting pressure on resources like infrastructure, drinking water, etc. Goa has a vehicle density of 625 vehicles for every 100 people and is ranked fifteenth in the world in terms of vehicle density. Several chartered flights would land in Goa, which also had a share in pushing up the air pollution levels. Eateries/hotels/beach shacks cater to the increasing demands of the tourists by getting the raw materials like vegetables, poultry, meat, fruits from the neighboring states, which are transported by diesel-run trucks almost every day; this further deteriorates the AQ in terms of PM, SO_2, CO, NOx, etc. Likewise, construction material and finished products are procured from across the country by availing road transport. Hence, it is crystal clear that increasing pollution is directly proportional to increasing human influence in the region. This also clarifies the increasing perimeter of the ecumene and thereby inherent vulnerability in the low lying coastal tracts of South Goa.

11.6 Multi-Temporal Sea Level Rise Inundation Assessment

Total area of Marmugao is 109 km² including 43.50 km² rural area and 65.62 km² urban area. Marmugao taluka has a population of 1,54,561 persons, out of which urban population is 1,32,329 while rural population is 22,232. Marmugao is an important region because of two important commercial activities. There is a harbor run by the Marmugao Port Authority and Dabolim Airport (GOI). These generate an income of USD per year, on average, to the country. In fiscal year 2022-2023, the airport handled around 8.5 million passengers including several European charter airlines. The airport is centrally located which brings 1200 international flights per year accounting for some 93% of India's international charter tourist flights that fly to Goa seasonally, typically between November and May months. It is estimated that about 300-350 thousand international tourists arrive at Dabolim on charter flights that supports the local economy and provides an international/national link to air passengers. In 2006, the government upgraded the airport by constructing a new international passenger terminal and adding several more aircraft stands over an area of about 4 hectares. Since support facilities are required for these government establishments, there increasing trend in built-up areas between the years 2000 and 2020 due to rapid urbanization (Fig.-9.1 (f) & (g)). This could be one of the reasons that there is a consistent trend of increased inundation vulnerability for Built-up areas, Water bodies, and Wetlands (Table-9.1 & Fig.-9.1). The latter two have been encroached by private individuals. Among all the classes, there is an increment in forest area mostly in the hilly Sancoale, Loutolim, and Verna. Traditionally this taluka is known for agriculture (Fig.-11.7) which is now showing an increasing trend, possibly due to escalating price of vegetables brought in from bordering states.

Fig –11.7 Low lying Khazan lands in Marmugao taluka.

Total area of Salcete is 298 km² including 145.11 km² rural area and 153.05 km² urban area. The Sal River and its backwaters dominate its landscape. The topography of the region is an intermix of mountains (35% of area) and plateau where agriculture is widely practiced. Margao serves as the administrative headquarters and the commercial capital of Goa. The land use change from agriculture/barren land to settlement/commercial is the main cause of increased concrete structures with a higher vulnerability for built-up areas (Fig.-9.2 (f) & (g) & Fig.-11.8). Water bodies and Forest area generally showed a decline over time due to rampant encroachment. On the contrary, Wetland increased under scenarios 6.05m and 7.11m, but showed a slight decrease under scenario 6.52m. The agricultural land has increased under all the scenarios indicating an expansion and higher VGR, while Barren land area decreased over time under all scenarios (Table-9.2), possibly brought under cultivation of rice, vegetables, and other crops including kidney peas and watermelons in 35 villages. The farmers use and maintain traditional ponds/wetland for irrigation of crops (using electric pump). Many hotels along the coastal zone constitute the Build-up area that cater to tourists who come to visit some fine beaches, some of which are Varca, Velsao, Arossim, Benaulim, Cavelossim, Mobor, Senabatim, Majorda, Utorda, Fatrade. The River Sal flows in south-western direction for 16 kilometers passing through the villages of Nuvem, Mongul, Seraulim, Colva, Margao, Benaulim, Navelim, Varca, Orlim, Carmona, Dramapur, Chinchinim, Assolna, Cavelossim, Mobor and drains itself into the Arabian Sea at Betul. The Arabian Sea and River Sal pose a high vulnerability for built-up areas along those structures along the river front and those in the coastal zone (Fig.-11.8).

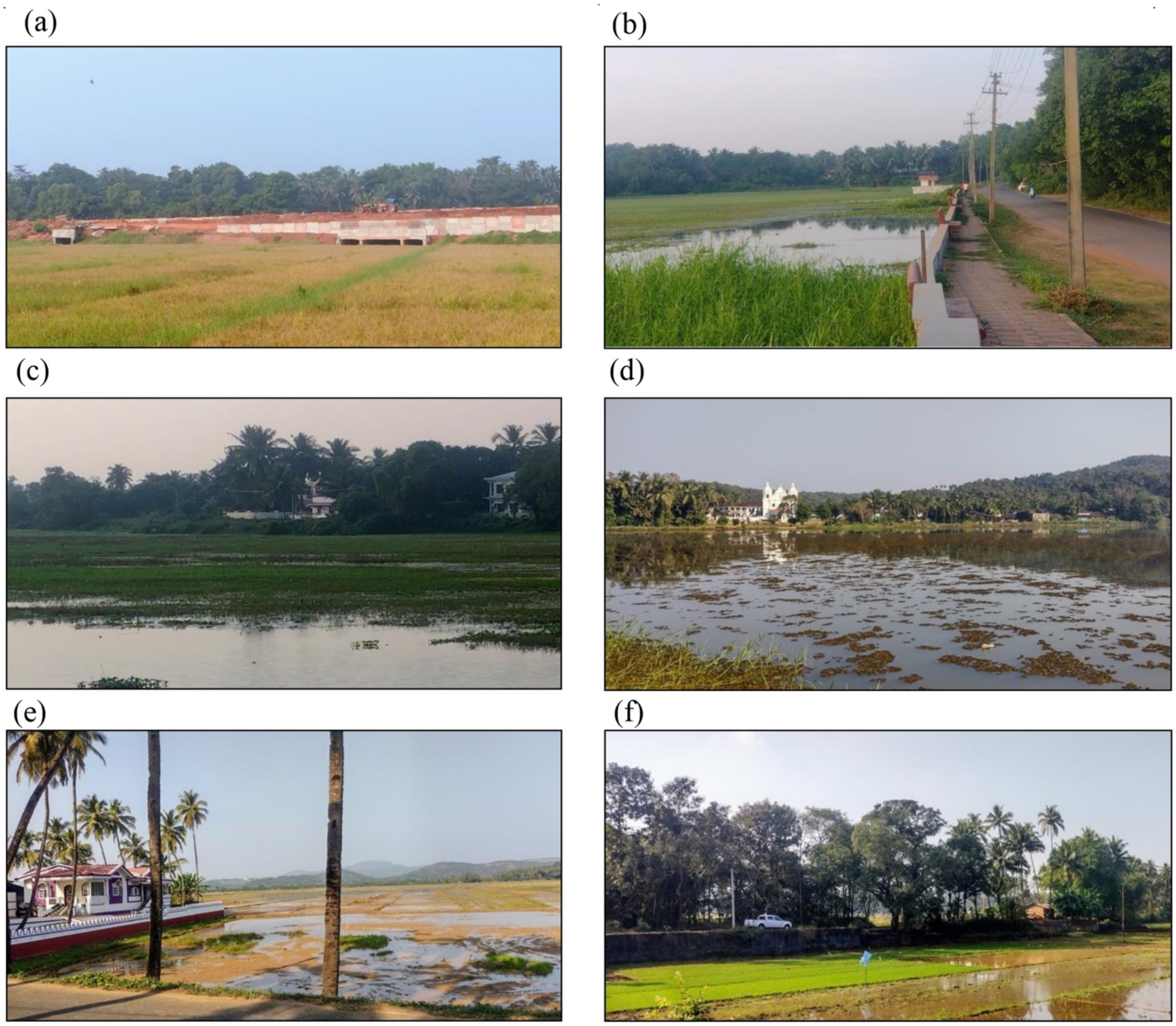

Fig –11.8 Ongoing development in the low-lying regions of Salcete taluka. (a) Western bypass construction in Sal floodplains, west of Margao city, (b) Benaulim-Margao road along the low-lying Khazan lands, (c) Houses constructed in Benaulim after filling up the Khazan lands, (d) Curtorim church and old houses along the bank of the lake, connected to Khazan lands, (e) A house constructed by encroaching in the khazan lands, Curtorim and (f) Road to Handi-khuris, constructed on embankment, in the midst of sea level high Khazan lands.

The topography of Quepem is mostly hilly, with the height varying from 1m to a maximum of 681m. Total area of Quepem taluka is 318 km² including 271.58 km² rural area and 46.66 km² urban area. As of 2011, it has a population of 81,193 persons, out of which urban population is 44,959 while rural population is 36,234. There are 35 villages and 3 towns in Quepem. Nanda Lake admeasuring an area of 644664 m^2 notified as a wetland. All scenarios for Quepem indicate an increase in Built Up and agriculture cover from 2000 to 2020 (Table-9.3 & Fig.-9.3), propelled by population growth and infrastructure such as highway expansion. While reduction in water bodies area can be attributed to debris from landslides which promotes soil erosion leading to decrease in forest cover across all three scenarios. The wetland consisting of Xeldem lake, Cottombi lake and Nanda lake proportion has increased due to regulation of developmental activities within the wetland as well as within its zone of influence following the conservation and management Rules 2017 of the Central government. The regulations have prohibited activities within the wetland boundaries including setting up of any industry and expansion of existing industries with the exception of modernization of existing industries which will not affect the ecological balance of the wetland under consideration, no construction, demolition, hazardous, electronic or other waste can be dumped in a wetland, discharge of untreated wastes and effluents, plastic or solid waste, extraction of sand or mud for commercial purpose, etc. Furthermore, activities like agriculture cultivation, fishing, religious practices, removal of water for domestic consumption, plantation of trees are permitted within the wetland boundaries.

The total area of Canacona is 352.04 km2 with population density of 128 per km2. Out of total population, 72.47% of population lives in urban area and 27.53 in rural areas. Increasing Built up and agriculture is observed suggesting urban development and population growth across the years. Modern amenities like Canacona bus stand opened in 2004, earlier, highway route NH17 connecting Mumbai to Ernakulam passes through Chaudi locality and connects to Salcete-Margao and Panaji. The newly constructed Canacona bypass in November 2019 has the Talpona, Galgibag and Mashem bridges. When it comes to agriculture, Canacona's net sown area has decreased from 10253 hectares in 1987 to roughly 9000 hectares in 2021. Land that was once cultivated is now left barren and unproductive. Canacona taluka is blessed with a long coastline, 3 estuarine rivers, and backwater systems (Fig.-11.9). Our study showed that Water bodies and Barren and have decreased significantly, while Wetlands areas have experienced increment over the years. Many places, particularly low-lying areas and barren fields experience flash floods that occurred in Oct. 2009 and Oct. 2017. However, the inundation vulnerability is negligible being a hilly locality. The shoreline of Canacona is dotted with about good beaches including Palolem, Patnem and Agonda beaches which attract domestic and international tourists due to their decent infrastructure, located in low-lying coastal areas (Fig.-9.4).

(a)

(b)

Fig –11.9 Low lying areas in Canacona taluka. (a) An estuary meeting to the Arabian sea at low lying Agonda village, with high density tourist infrastructure around it and (b) A house constructed (light green, right-centre) after clearing mangrove plantation along the bank of Galgibaga river.

11.7 Coastal Vulnerability Index

11.7.1 A Robust Methodology of Coastal Vulnerability Index

The novelty of the present study lies in the incorporation of a total of 21 physical, geological and socio-economic variables, which have never been adopted together to compute relative coastal vulnerability, that too at the smallest possible spatial administrative unit. Resultantly, the CVI results obtained in this assessment are much more robust than any previous CVI studies, it provides the field status in depth more than ever. Gornitz and other (1994) had introduced six physical variables; geomorphology, coastal slope, relative SLR rate, shoreline erosion rate, mean tide range and mean wave height which are well documented. In addition, the current study has introduced four more physical variables, novel to CVI assessments namely; plausible storm surge height, vegetation density behind the beach, percentage of sandy coast and coastal regional elevation.

Storm surge height refers to the plausible highest elevation of a wave during a storm along the coast. Its significance becomes undeniable when a storm strikes at a low elevation coastal area. If a wave surge of this height of gets generated and hit the coast then it is quite plausible that it would extensively erode sandy coasts or even submerged its inland areas, although temporarily. High population density areas could face devastation if these waves actually occurs. This is a low frequency high magnitude phenomenon.

While the vegetation density behind the beach generally refers to mangrove, casuarina and coconut tree plantations developed naturally or anthropogenically behind sandy beaches. It is a well established fact that the vegetation behind the beach acts as a protective belt between the sea and inland areas. When a cyclone, storm or Tsunami occurs, this belt has been proven to be effective to drastically reduce the wave intensity thus, protects inland areas quite effectively. Hence, higher the vegetation density lowers the vulnerability behind this belt. After 2004 Indian Ocean tsunami stuck the Coromondal coast of India, the state government made it mandatory to plant casuarina in between the coast and the habitable land behind. It is largely visible along the East coast road. In addition, Bangladesh is primarily protected by mangrove vegetation, which proves the protective ability of vegetation from the waves and storm.

Sand characteristics may refer to percentage of sandy coast or sand dunes. A general coastal geomorphology of the sandy coasts has lower elevation along with gradual slope having fast eroding material and cliffed coast have higher elevation and steep slope. Low elevation, gradual slope along with unconsolidated material makes sandy coast most susceptible to coastal erosion and submergence. Thus, high amount of sandy coast along with low regional elevation along a coastline, would make it high vulnerable to any coastal hazard. Hence, determining the area under sandy coast at low elevation is quite essential to demarcate vulnerable coastal zones. e.g. Chittagong coast, Bangladesh is highly vulnerable to coastal erosion as its coast is predominantly sandy in nature along with low regional elevation. On the other hand, Sand dunes in any coastal stretch always plays an essential role in restricting high tides and storm surge to reach beyond them. As they mark a breaker where the wave loses its intensity and gets perished (Refer to Appendices, Supplementary Table-3 for the rationale behind physical variables).

Vulnerability of the coast does not only belong to the physical processes, geology and topography of the coast. It is significantly influenced the people residing there, the level of infrastructural development, anthropogenic activities, income, quality of life to name a few, also play an important role in defining coastal vulnerability. This concept is similar to hazard and disaster concept where a hazard is defined as a natural process of the earth which has been occurring since the earth's inception. However, the similar hazard, a natural process, becomes a disaster when it affects human lives or human property. Hence, anthropogenic involvement in defining coastal vulnerability is pretty clear. Otherwise, why aren't we more concerned about the coastal vulnerability of any uninhabitable coastal tract of the mainland or an island? It is because human population or any of its property is absent in those areas and possibly it doesn't lure human interest. Therefore, coastal vulnerability assessment is incomplete without a variety of in-depth socio-economic variables, which could provide the information about the current state of coastal human settlements and their functioning (Refer to Appendices, Supplementary Table-4 for the rationale behind social variables).

11.7.2 Coastal Vulnerability Index of the Study Area

- **Marmugao**

A predominant part of Marmugao is situated at the headland area along the Arabian Sea. It can be considered as the commercial capital of Goa as it hosts the Marmugao port, Dabolim airport and a bustling town like Vasco da Gama which is experiencing rapid population growth due to tourism and economic opportunities. However, its villages, located outside the headland, along the low lying coastal tracts are at different stage in terms of socio-economic exploitation of the region.

SoVI reveals that Chicolna, Vasco da Gama, and Sancoale exhibit the highest social vulnerability, influenced by a dense population (Table-10.1 & Fig.-11.10) and the presence of marginalized communities (highest amount of slums in Goa state). In contrast, Pale, Velsao, and Issorcim have moderate levels, suggesting more balanced social conditions (low commercial activities and low population density but low on socio-economic facilities). Cansaulim, Arrosim, Utorda, and Majorda, situated along the linear coast, display low social vulnerability due to better access to resources such as roads, better health care facilities, proximity to Margao city as well as low population density and higher per capita income (due to high-end tourist resorts) as compared to the villages located at Marmugao headland.

Fig –11.10 High rise buildings located at the headland in Marmugao, seen from Velsao beach.

On the physical vulnerability front, only Sancoale boasts low vulnerability, indicative of its location at a cliff on higher elevation and higher degree of coastal slope (Fig.-11.11). Assorcim, Utorda Pale and Vasco da Gama fall within the moderate range, because of their geographical characteristics (low lying areas are densely populated such as Baina; obliterated sand dunes in Utorda etc.). Cansaulim, Velsao, and Arrosim (adjacent villages along the coastline) are categorized as having high physical vulnerability, primarily due to to their proximity to the coastline, less dense vegetation behind the beach, encroached sand dunes, low coastal slope etc. which increases susceptibility to storms and flooding (Table-10.1 & Fig.-10.1).

All villages in Marmugao taluka score high in CVI, resulting in an overall CVI of 30.6. This indicates a clear sense of risk in the coastal tract of Marmugao taluka. The interplay between the geographical setting of the region and the rapid development underway is heavily imbalanced. Marmugao is generally seen as safe in terms of coastal risk all due to its higher elevation headland but it is mostly forgotten that a majority of its part is located in low lying areas, down the headland slope (sprawling Vasco da Gama town). Concentration of transportation facilities has primarily added to this menace because the influx of people seeking employment opportunities has shaken the socio-economic web in the taluka, as it now hosts the largest slum area in the state. In addition, haphazard development, traffic congestion along the main arterial roads have only added to increased social vulnerability which pushes to understand the importance of the dynamics of population growth and economic activity in the context of vulnerability in Marmugao.

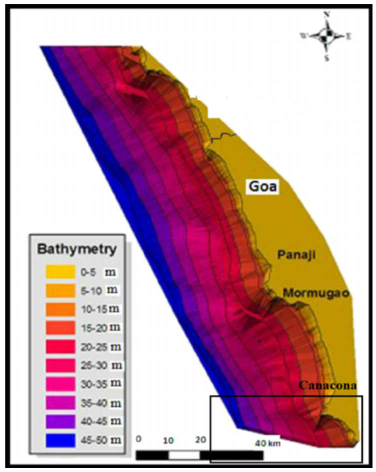

Fig-11.11 Near-shore bathymetry of the Goa coast (Source: Kunte et al., 2014).

- **Salcete**

Further south of Marmugao, is Salcete taluka. It's a significant taluka in the study area in terms of industrial development, demographics and extensive tourism infrastructure. Salcete is the most populated taluka with highest population density in the study area where the majority of population is settled near to the coastline and in the Zuari floodplains which both are highly sensitive to coastal vulnerability. Margao is the largest city in taluka, located inland but its outskirts host numerous villages of Zuari floodplain which have been found be highly vulnerable to coastal hazards.

However, the present study found that most villages in Salcete as having low social vulnerability which reflects a strong sense of community, better infrastructure, better health facilities, higher literacy rate, excellent road network thus, resilience. However, Colva, Benaulim, Betalbatim, Cavellosim are located along the coastline, where there is a high concentration of settled and tourist populations. Colva-Benaulim belt is a popular tourist destination, dotted with high concentration of hotels and resorts, thereby attracts high number of Indian tourist population (Fig.-11.12). Cavellosim is a high-end tourist village, located on a barrier beach between the Arabian sea and Sal river. Due to dense infrastructure and road connectivity constraint along the narrow belt, it exhibits high social vulnerability. Quellosim, on the other hand located in Zuari floodplain, hosts high population density and due to its proximity to Verna industrial estate. All these factors significantly influence social vulnerability in Salcete taluka (Table-10.1 & Fig.-10.2).

Fig –11.12 Status of sand dunes at various beaches in the study area. (a) Destructed dunes at Colva beach, Salcete (b) Protection barriers (sand bags) to save infrastructure constructed on razed sand dunes, Colva beach, Salcete (c) Way to Velsao beach, Marmugao without razing stabilized sand dunes, (d) Way to Betalbatim beach, Marmugao constructed after razing stabilized sand dunes, (e) Protected vegetation (Casaurina plantation) and sand dunes with minimal tourist infrastructure at Gonsua beach, Salcete and (f) Showing limited connectivity, a Lone road connecting high-end tourist destinations of Cavellosim and Mobor villages, Salcete with the mainland.

Physical vulnerability in Salcete has very different story where, Macasana, located in Zuari floodplains (having thick mangroves as buffer and higher gradient towards the river) is the only village with low physical vulnerability and all other in the Zuari floodplain (Fig.-11.13) have either moderate or high physical vulnerability which can be directly attributed to low-lying areas with gentle slope towards the river and conversion of wetlands to agricultural field and subsequent infrastructural development in these areas of Salcete taluka. Along the coastline, Gonsua, Betalbatim, Sernabatim, Benaulim, Varca, and Cavellosim have moderate PVI scores which is influenced by their geographical characteristics such as, presence of sand dunes, vegetation behind the beach, sparse construction in the proximity to the HTL to name a few. However, Colva, a neighbouring village of Benaulim boasts high PVI because of an estuary joining the sea and extensive tourism activities which have led to the destruction of geographical characteristics discussed above (Fig.-10.2).

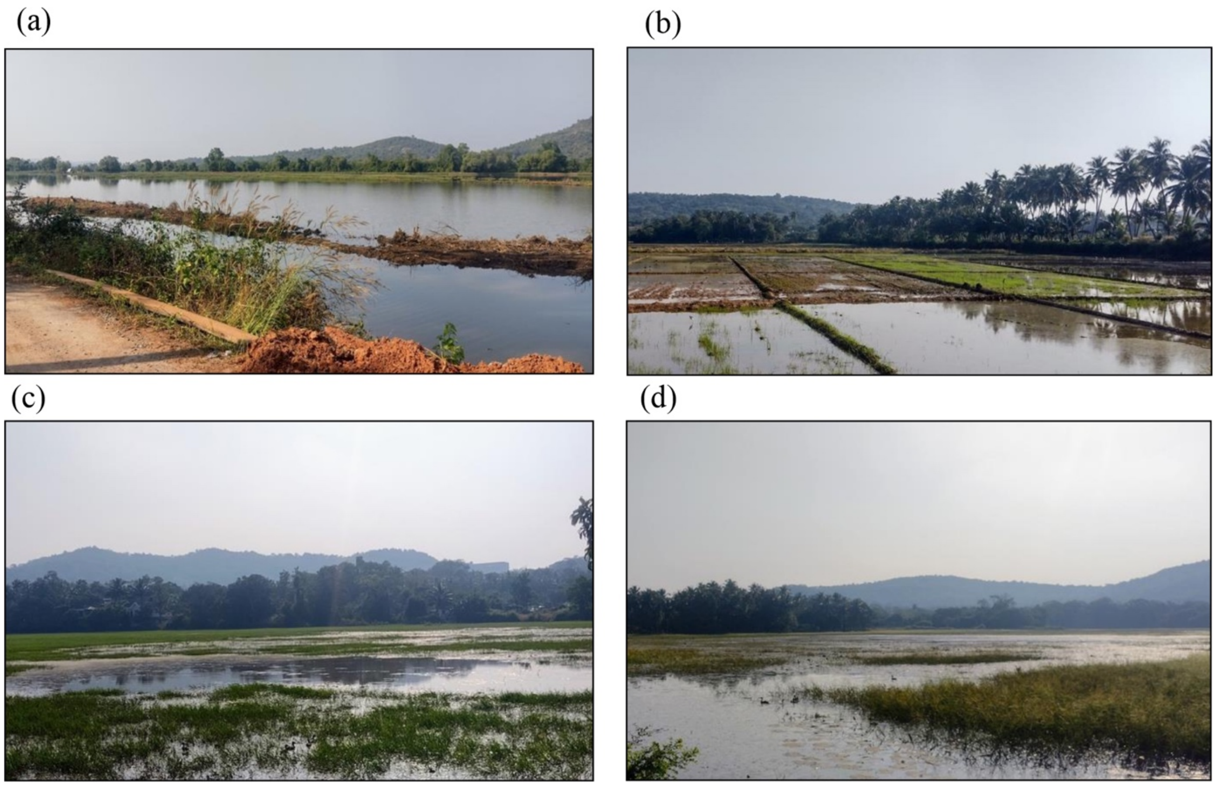

Fig-11.13 Low-lying floodplains of Zuari river, located in Marmugao and Salcete taluka(s), flooded during high tides.

The comparison between the coastal villages Zuari floodplain villages (Fig-11.13) portrays an interesting picture of coastal vulnerability. It suggests that, although the villages situated in Zuari floodplain are away from the Arabian sea, but they posses much higher physical coastal vulnerability than the villages located adjacent to the coastline. The findings clarify that the cause behind this situation are several factors such as, gentle gradient towards the river, absence of sand dune as a protection barrier, destruction of wetlands and vegetation in the floodplains etc (Fig.-10.2). This suggests that a majority of natural protection measures have be destructed along the

Zuari floodplain which is already a gently sloping and low lying region which has led to a concerning situation adversely impacting the future of the villages located in the Zuari floodplain, highlighting the need for targeted adaptation strategies.

- **Quepem**

Quepem demonstrates low social vulnerability across all three villages and mainly in the coastal region which is located a higher elevation on the cliff and sparsely populated (Table-10.3 & Fig.11-14). However, PVI varies significantly, with high vulnerability in Curchorem, located along the Zuari bank and low vulnerability in Quitol and Naquerim (located along the coast) (Fig.-10.3). The reason can be significantly attributed to the difference in regional elevation and slope gradient (low in Curchorem and high in Quitol and Naquerim) as well as similar geographical constraints for Curchorem face by Salcete's villages located in Zuari floodplain.

Kunte and others (2014) had ranked the taluka of Quepem as the least vulnerable to erosion due to the presence of rocky cliffs, exposed rocks, and mesas. They also have low population density and do not attract many tourists (Kunte et al., 2014). On the other hand, the present study considered grass-root level vulnerability assessment, which has revealed that this contrast in vulnerability score amongst the two village locations (Curchorem and Quitol) in Quepem taluka highlights the importance of understanding the physical aspects of small pockets (such as Curchorem) as well, although it is located in a predominantly hilly taluka.

Fig –11.14 Tourist resort constructed on the steep slope of a cliff, facing the Arabian sea at Canaguinim village, Quepem

- **Canacona**

Canacona displays a similar pattern, with low SoVI in Cola, Poinguinim, and Loliem, and high SoVI in Agonda and Nagercem-Chaudi, primarily due to tourism and infrastructure development (Fig.11.15). The region's overall SoVI falls within the moderate category. Tourism, in particular, has transformed Agonda and Nagercem-Chaudi into tourist hotspots, driving population growth and development (Table-10.1). They are the most vulnerable coastal villages in Canacona. It is because they have low lying topography such as; very high proportion of sandy beach stretch and low regional elevation world-renowned sandy beaches (Agonda, Palolem) of South Goa

(Fig.11.15). The land use land cover is drastically changed in the last two decades due to increased tourist activity. Due to the availability of low-cost accommodation in comparison to North Goa beaches, tourism has thrived here. However, to cater the need, haphazard development with congested roads in the coastal tracts has resulted in high social vulnerability scores. As a result, it is not only the geographical factors but also the economic and social dynamics that shape vulnerability in these villages.

Fig-11.15 Tourist infrastructure along the coastline of Canacona taluka. (a) Excessive infrastructure constructed along the beach after razing sand dunes and vegetation at Agonda beach, (b) Concrete construction using bricks and mortar, stabilized sand dunes completely razed and levelled at Agonda beach, (c) Low-end tourist infrastructure, located at the fringe of Colamb beach, (d) Congested way to seaside tourist accommodations located at Patnem beach, (e) Drone imagery showing haphazard development without Casaurina cover along the Palolem beach, Nagercem village and (f) Drone imagery showing extensive cliffed coast along Cola village coastline.

On the other hand, Loliem is completely on the opposite site (Table-10.1). Its geological settings are much safer to coastal hazards (high elevation, rocky coast). Socio-economically as well it has low population density, open roads, less traffic congestion, less population to serve to etc. So fundamentally, local level variables like type of coastline, regional elevation, high population and tourist density, and settlement pattern, play a crucial role in defining coastal vulnerability at the most localized level.

In addition, it has also come to light that the administrative centres located along the coast generally serve to a larger population from the nearby towns and villages, which consequently leads to the development of other public amenities such as; high density commercial areas, transportation facilities, residential projects etc. in those administrative centres. Resultantly, these centres attract more people who prefer to live there to avail these amenities and this kind of immigration increases pressure on the natural resources of administrative centres, e.g. Vasco da Gama, Nagercem-Chaudi, Curchorem are the primary examples of these kind of influence on coastal vulnerability in a town or village. Thus, when an administrative centre such as discussed above is having geological settings (low elevation, gentle slope, river bank with tidal influence, sandy coast, sparse vegetation along the coastline etc.) then coastal vulnerability could increase by manifolds compared to the town which have no administrative liabilities (other villages in the study area) thus does not attract population due to this specific reason. Therefore, localized CVI variables can differentiate one village from another in terms of slightest difference in coastal vulnerability and also make a strong case to consider village-level coastal vulnerability assessments as an important tool to determine coastal vulnerability.

The Complex Interplay of Elements Shaping Coastal Vulnerability: A Comprehensive Synthesis

11.8 Elements Shaping a Coastal Region

Coastal regions are located at the intersection of the land and sea (Brocx et al., 2009), which are intricate and complicated interfaces where the various competing forces of nature and human activities interact and intertwine in a manner (Reckermann et al., 2022) which is extraordinary. This convergence of nature and human activities is actually the convergence of vastly different yet extremely interconnected worlds, which results in the creation of unique landscapes that are characterized by their ecological richness and social significance (Allam and Jones, 2019).

The climate dynamics encompasses a variety of meteorological factors such as temperature, wind patterns, atmospheric pressure, and precipitation, which cumulatively create the distinct local meteorological conditions, exclusively found in coastal areas (Awour et al., 2008). The proximity to expansive water bodies effects sea breezes and temperature gradients. These meteorological variations are the quintessential factors that shape and define the microclimates of the coastal areas (Ramamurthy and Sangobanwo, 2016). The interplay, which exists between air masses and humidity, not only governs but also dictates weather patterns that play a vital role in influencing the rates of evaporation, cloud cover, and storm occurrence (Trenberth et al., 2003). These meteorological relationships, in turn, impacting and influencing plant growth, water availability, and soil stability, thereby forming a foundational layer of coastal dynamics (Hobohn et al., 2021), that is deeply interrelated.

The intricate web of coastal regions is greatly influenced by the crucial link formed by geomorphology. The movement of sediment is steered by the various geomorphological processes, which in turn creates beaches, dunes, cliffs, headlands, valleys, marshes, estuaries etc (Viles and Spencer, 2014). These coastal landforms play a significant role in regulating sediment transport, erosion rates, and the distribution of habitats (Jackson and Nordstrom, 2011. The web of coastal ecosystems is deeply interconnected by the complex mechanisms of geomorphology (Viles and Spencer, 2014).

Forests play a crucial role in connecting local meteorology, geomorphology, and the coastal environment (Alongi, 2022), acting as a bridge between these interconnected systems, they hold a pivotal position. The forest canopy has the ability to regulate temperatures in the local area, both through shading and transpiration (Rahman et al., 2020. Additionally, the intricate root systems of forests are able to stabilize soil, combatting erosion and landslides (Pramova et al., 2012). The significance of forests extends beyond their physical attributes, as they are also able to influencing microclimates (Ewers, 2013). These lush ecosystems are an essential component in maintaining the delicate equilibrium of the coastal environment, forming a critical thread that binds together various elements.

Wetlands play an integral role in the interconnected dynamics of coastal environments, influencing various factors such as meteorology, geomorphology, forests, and overall resilience (Lopes et al., 2022), thereby having the ability to moderate local weather patterns, stabilize temperatures, and impact nearby areas, thereby playing a crucial role in the overall ecosystem. Wetlands are also responsible for shaping landforms and habitats, and their sediment-trapping abilities have a major impact on coastal geomorphology (Reed et al., 2009), Additionally, they support biodiversity and ecological interactions, thereby enhancing forests (Viles and Spencer, 2014). Also, wetlands act as natural defenses against natural calamities, such as storms and tsunamis, by absorbing water and dissipating wave energy (Ostling et al., 2014), thus mitigating erosion.

The convergence of local meteorology, geomorphology, and forests results in the coastal environment, which serves as a nexus (Ward et al., 2016). Due to their proximity to the ocean, coastal regions are highly susceptible to meteorological shifts, such as sea-level rise and storm surges (Karim and Mimura, 2008). The imprint of geomorphology is readily apparent in the formation of shorelines, which impact sediment dynamics, erosion rates, and habitat availability (Viles and Spencer, 2014). Coastal forests serve as natural guardians, protecting the coasts from erosion, stabilizing dunes, and contributing organic matter to adjacent marine ecosystems (Alongi, 2022). These complex relationships culminate in an ecosystem that facilitates a variety of life forms, human activities, and ecological functions. It is important to recognize and appreciate the relationships of these interactions (Allam and Jones, 2019), as they play a crucial role in maintaining the health and vitality of the coastal environment.

Moreover, the complex interrelationship of various factors such as local meteorology, geomorphology, forests, and the coastal environment is not just a static framework but a dynamic web of relationships that continuously evolve. The interactions among these elements can have far-reaching implications for coastal vulnerability, resilience and the overall health of ecosystems (Naylor et al., 2017). Furthermore, these interconnected elements play a critical role in molding the coastal environment and its ability to withstand natural hazards (Pelling and Uitto, 2001). It is therefore essential to understand the delicate balance between these factors to ensure the long-term health and sustainability of the coastal ecosystem.

11.9 Imbalances and Increasing Coastal Vulnerability

However, human influence is the biggest factor affecting the coastal environment and causing imbalance. With the increasing human population, the dynamics of local meteorology, geomorphology, forests, and the coastal environment are becoming more complex (Michenar et al., 1997). Urban growth leads to the destruction of natural habitats such as forests, wetlands, and sand dunes. This exacerbates imbalances in ecosystems and geomorphology (Nicholls et al., 2007).

As more land is cleared for housing, infrastructure, and industries, the protective functions of coastal forests are getting compromised (Lewsey and Kruse, 2004). This is especially problematic as these forests help to regulate weather patterns and stabilize the surrounding land. Additionally, the filling and draining of wetlands due to human activity disrupts their hydrological balance, their protective functions are compromised and increasing the vulnerability of coastal areas to erosion, flooding and habitat loss (Moomaw et al., 2018). This all disrupts coastal environmental vital functions which is causing unpredictable changes in microclimates.

High population densities in coastal urban areas result in the formation of "urban heat islands", which are characterized by temperatures that are considerably higher than those in nearby rural areas (Silva et al., 2018). These heat islands have a significant impact on local meteorological patterns, including wind flows and cloud cover (He, 2018). As a result, the altered local meteorology affects the coastal areas by influencing storm tracks and precipitation (Karl et al., 1997).

Also, haphazard development in the low lying areas is the primary driving force behind coastal modifications, such as seawalls, land reclamation etc. Though the primary goal of these projects is to safeguard human assets however, the impact of such interventions lead to unintended consequences, such as the alteration of coastal geomorphology, modified coastal hydrodynamics, and eventually alter local meteorology and the influence of erosion patterns (Zhang et al., 2015). Resultantly, it leads to an increased vulnerability neighboring areas. These changes can have far-reaching consequences on coastal ecosystems and the communities that rely on them, highlighting the complex interactions between these elements.

On the top of it, at the global scale, climate change is a powerful amplifier of coastal vulnerability at the regional level, notably in the tropical and subtropical areas. The release of greenhouse gases has resulted in rising temperatures, sea-level rise, and changes in precipitation patterns (Kjellstrom and McMichael, 2013), these changes have an impact on all interrelated parts.

The presence of feedback loops and cascading effects is a fundamental component of these interrelated processes. When one ingredient is disrupted, it triggers off a sequence of events that exacerbate the disruption (Linkov and Trump, 2018). For example, changes in precipitation patterns might result in more violent and frequent storms, which impact other local meteorological variables, biodiversity, and geomorphology in an area. This cycle can generate a self-reinforcing loop, making it more difficult to restore natural equilibrium; also, the combination of these elements adds to an increased risk of extreme weather events and coastal hazards.

11.10 Case Study of the Coastal Tracts of South Goa

Without a doubt, the coastal regions of South Goa are a perfect illustration of this complex interplay, where the interconnected strings of natural processes and human activity are deeply shaping the risk profile of the study areas.

Over the last two decades, from 2000 to 2020, coastal regions in South Goa have seen substantial and diverse transformations. During this time, the region's landscape saw tremendous transformation, owing to influences ranging from urbanisation and tourism to population shifts and environmental changes.

An upsurge in tourism activities, credited to South Goa's clean coastline and cultural attraction, brought in a wave of socioeconomic effect and demographic shifts, as migrants sought employment in the expanding tourism industry. However, this population transition brought with it new issues in urban planning and cultural preservation. The natural landscape has changed as a result of these developments, with agricultural and wetland regions being converted into urban areas. Climate change has played a significant effect, with rising temperatures, shifting rainfall patterns, and increased cyclonic activity in the Arabian Sea exacerbating vulnerabilities, particularly in coastal and urbanised areas.

11.10.1 Synergistic Effects Between Climate Trends and Anthropogeomorphic Impacts

The AGP study of Mormugao taluka indicates a significant degree of human influence induced by urbanisation and industrial activity. This dense human presence directly adds to the urban heat island effect, which leads to higher Land Surface Temperatures (LST) and Maximum Temperatures (Tmax) as discovered in the climatic trends analysis. Heat retention is amplified by the dense built environment and industrial zones, altering local microclimates and compounding the observed temperature rise. Additionally, changes in land cover caused by anthropogenic activity can influence local wind patterns, influencing temperature distribution and humidity levels. Thus, the interaction between AGP effects and climate changes highlights a localised feedback loop in Mormugao, where urbanisation pushes greater temperatures and changed climatic conditions.

The climatic trends investigation showed a significant increase in Land Surface Temperature (LST) and Maximum Temperature (Tmax) in Salcete (around Margao city, where urbanisation and infrastructure expansion are important AGP influences. The increase in urbanisation intensifies the urban heat island effect, increasing heat retention in densely populated regions. As a result, urbanised areas experience greater temperatures than neighbouring areas, resulting in a localised climatic impact. The synergy between AGP effects and climatic trends is visible in how faster human activities contribute to changing microclimates, validating the idea that rapid urbanisation exacerbates the local warming effect in Salcete.

The specific AGP effect pattern of Quepem taluka, with higher recorded geomorphological alterations, matches to localised climatic patterns. The modest rise in Land Surface Temperature (LST) and Maximum Temperature (Tmax) corresponds to the landscape's moderate anthropogenic effect. The less visible human changes result in weaker localised temperature fluctuations. The synergy in Quepem shows how the extent of AGP effects is closely related to the extent of climate deviations, highlighting the significance of understanding localized variances between human activity and climatic responses.

The complex AGP impacts find alignment with localized climatic patterns in Canacona. Canacona's balanced human-induced geomorphological changes correspond to a slight rise in Land Surface Temperature (LST) and Maximum Temperature (Tmax). The interaction here shows how the complex linkages between human activities and the surrounding environment result in relatively quantifiable climate variations. This complex synergy demonstrates how even little AGP influences can lead to detectable local climate patterns.

Therefore, the localized synergistic effects of climate trends and AGP impacts show how human activities, such a urbanization and agriculture, strongly alter microclimates and climatic indicators in South Goa's coastal tracts. The link between human activities and climate reactions is not consistent, but rather varies according to the strength and type of anthropogenic impacts in different talukas.

11.10.2 Synergistic Effects Between Climate Trends and Coastal Vulnerability

There is a definite synergistic impact between the two assessments, Climate trends and Coastal vulnerability in the coastal tracts of South Goa. These two points of view interact to create a more complete picture of the region's dynamics.

The first study focuses on climate trends and identifies shifting patterns in climatic indicators. It revealed the changing meteorological processes in the study area, as well as the impact of human activity on these patterns. This data serves as the foundation for comprehending the larger context of the region's climate variations.

The second study concerned with coastal vulnerability, puts into perspective these detected climatic changes in terms of potential threats and issues. This study highlights the real-world consequences of the shifting climatic trends revealed in the first analysis by examining vulnerabilities to variables such as sea-level rise, and storm surges arising due to the influence of human activities. The initial analysis' findings provide critical inputs for understanding how shifting climate trends may contribute to vulnerabilities in the region.

These two analyses work in unison to provide a powerful synergy. The first study provides information regarding changing climatic conditions that may have an influence on the region's susceptibility. The second study analyses those climatic changes and projects their effects on the area's susceptibility. The two viewpoints complement and enrich one another, providing a more comprehensive and inclusive analysis of the difficulties and opportunities confronting South Goa's coastal areas. This synergistic impact eventually directs researchers, and policymakers in developing comprehensive solutions that take into account both climate trends and vulnerabilities in order to create a more sustainable and resilient future.

11.10.3 Synergistic Effects Between LULC Changes and Coastal Vulnerability

The complicated relationship between the two studies reveals an explanation of urbanization-driven vulnerability in Marmugao taluka. The depiction of haphazard built-up area development in the first study corresponds strikingly with the vulnerability patterns shown in the second analysis. Urban growth increases exposure to coastal disasters. As settlements encroach on natural buffers like wetlands and forests, the area becomes more vulnerable to sea-level rise and storm surges. This loss can be observed in the first study' negative vegetation cover changes, revealing the concrete impact on ecosystem resilience. According to the first investigation, vulnerability growth rates in the built-up and agricultural categories reflect the increasing vulnerability stated in the second analysis.

The dynamics of Salcete taluka display a relationship between urbanization and vulnerability. The first investigation highlights the increase of built-up regions as a result of the ever-increasing tourism industry and urban development, repeating the vulnerability patterns shown in the second analysis. The urban expansion on natural land cover like wetlands and forests confirms the area's higher vulnerability to coastal disasters. This ecological conversion is consistent with the first investigation's conclusions, emphasizing the significance of protecting these habitats. The first investigation found mixed trends in forest cover vulnerability, emphasizing conservation potential. The delicate relationship between urban growth, ecological change, and vulnerability emphasizes the need for a coordinated strategy in order to address the growing coastal vulnerabilities.

Quepem provides a detailed examination of the interaction of natural processes, human influence, and vulnerability. The modest decline in vegetation cover discussed in the first study is linked to the vulnerability dynamics discussed in the second. While the area's geography and forest cover may make vulnerability levels appear to be lower, the potential for disturbance due to human activity is clear. The first investigation identified patterns of slight agricultural expansion, which added to vulnerability concerns. The observed vulnerability growth rates in different categories are also consistent with the modest changes in land use practices. This exacerbated link represents the delicate equilibrium between natural resistance and human-caused alterations in determining vulnerability in Quepem.

Canacona taluka, as underlined by both investigations, encompasses an intriguing report of human-induced vulnerability. The oscillations in agricultural patterns, deforestation, and land-use changes indicated in the first study closely match to the increased vulnerability patterns outlined in the second analysis. The change of natural environments in the low lying areas particularly wetlands and forests to built-up regions and agricultural land significantly increases its vulnerability to coastal hazards. The insufficiency of planning methods and development, as revealed in the first investigation, corresponds strongly with the identified vulnerabilities in Canacona. To successfully address the rising issues in Canacona, quick and informed solutions that account for the delicate interaction of sustainable development and human-caused vulnerabilities are required.

An investigation of the synergistic impacts of the two methods reveals a complex web of interconnection in each of the four talukas. The fragile relationship between urbanization, ecological shift, climate change, and growth agendas highlights the difficult challenges of managing coastal vulnerabilities. These links highlight the importance of holistic strategies that thoughtfully integrate environmental preservation and developmental priorities, emphasizing the need for strategic interventions to protect South Goa's coastal tracts from the escalating impacts of sea-level rise, storm surges, and evolving human influence.

11.10.4 Synergistic Effects Between Anthropogeomorphic Impacts and Coastal Vulnerability

The effects of anthropogenic activity in Marmugao, as indicated in the first investigation, reveals that human influence has left a substantial impact on the landscape. The AGP@E model has classified Marmugao as having "severe" effect due to urbanisation, infrastructural growth, and industrial activity which identified urban expansion as a primary driver of influence coincides with the vulnerability assessment findings in the second investigation. The rapid development of built-up areas, as evidenced by increased vulnerability growth rates, demonstrates how urbanisation increases these regions' vulnerability to coastal hazards.

Salcete highlights different patterns of human influence, as seen in the first investigation, with AGP impact ratings indicating significant increases over time. This acceleration is consistent with the results of the vulnerability assessment and is linked to dynamic factors like urbanisation and infrastructure development primarily in the low lying areas of Zuari floodplains. The increased vulnerability growth rates in Built-Up regions highlight how vulnerable people are affected by more urban growth. A result of human activity identified in the impact analysis is the conversion of ecosystems like wetlands and water bodies to built-up areas, which is consistent with the vulnerability assessment's worries about encroachment on important ecosystems. Thus, the findings of the two studies coincide to highlight the need of addressing how urbanisation shapes vulnerability as well as the need to protect ecological components.

According to the first investigation, Quepem has relatively moderate AGP impact ratings, indicating more modest levels of anthropogenic geomorphological alterations. This is consistent with the vulnerability assessment findings that a lesser percentage of land in Quepem was impacted. However, the impact study highlights that human influence can result in alarming land use changes and declining land cover even in places with minimal impact, increasing vulnerability. Due to this synergy, it is clear that even relatively little anthropogenic influences can have an impact on vulnerability.

The AGP impact research highlights the complex relationship between human activity and the natural landscape of Canacona. The result of the first investigation is consistent with the vulnerability assessment. Together, the three primary effect drivers of urbanisation, deforestation, and land use changes lead to increased vulnerability to sea level rise. The vulnerability assessment underlined the concern that the conversion of wetlands and forests into populated areas and agricultural land increases vulnerability and disturbs the natural environmental balance. The vulnerability assessment makes note of the effects analysis's discussion of inadequate planning and development practices, which contribute to a lack of resilience to sea-level rise.

11.11 Summing-up

The comprehensive and methodical evaluation presented in the current thesis serves as a compelling call for immediate action, highlighting the critical need for strategic interventions that can cautiously balance environmental preservation, development and social equity. As the vulnerable surroundings shifts and evolves, a requirement to promote and reinforce community resilience, as well as inclusive access to crucial resources, is becoming a necessity that requires immediate attention.

The complexity of coastal vulnerability in low-lying coastal areas is not only touched upon in this thesis, rather, it is investigated in a comprehensive manner, revealing the multiple dimensions of the problem and its complicated interrelationship with ecology, development, and significant socioeconomic factors. This highlights the fundamental interconnectedness of these factors, which all need to be carefully integrated in coordinated attempts to address and mitigate the complex problems caused by the complex interactions between coastal hazards and the widespread impact of human activity. This study serves as a call for intervention for an integrated, holistic, and interdisciplinary strategy, to provide a thorough plan for tackling all the possibilities and challenges coming from the growing vulnerable coastal environment.

Chapter-12

Conclusion and Recommendations

12.1 Conclusion

This doctoral study comprehensively investigates the coastal vulnerability of South Goa in the face of global environmental challenges, particularly focusing on the UN Decade on Ecosystem Restoration (2021-2030). Utilizing a holistic and interdisciplinary approach, the research addresses the complex dynamics of coastal ecosystems, emphasizing the urgency of understanding and mitigating potential consequences of hazards. The analysis covers climate trends, land use changes, anthropogenic impacts on geomorphology, beach litter, air quality, sea-level rise, and social vulnerability. Results reveal intricate relationships between meteorological processes, human activities, and the region's climate trends, emphasizing the need for strategic interventions. The study also introduces the AGI@E model, assesses beach litter as a proxy for human influence, analyzes air quality as an indicator of increasing human presence, and evaluates vulnerability to sea-level rise. Social vulnerability is addressed, filling a crucial research gap. Specific vulnerabilities and recommendations are outlined for each taluka in South Goa, emphasizing the importance of sustainable development, environmental protection, and proactive measures. Various points regarding the conclusion are as follow:

- **Interdisciplinary Approach**
  The holistic and interdisciplinary approach provides a comprehensive view of South Goa's coastal vulnerability, incorporating diverse parameters to ensure a thorough understanding.

- **Climate Trends and Human Influence**
  Climate trend analysis highlights the evolving meteorological parameters over four decades, showcasing the impact of urbanization, tourism, and population growth on temperature patterns. Increasing cyclonic activities are linked to rising sea surface temperatures, influencing rainfall.

- **Land Use Changes and Development**
  Anthropogenic-induced developmental activities contribute to land use changes, emphasizing the struggle between economic growth and environmental preservation. Tailored approaches for each taluka are essential for effective decision-making.

- **AGI@E Model**
  The newly derived "Nigam-Kotha model of AGI@E" proves robust in assessing anthropo-geomorphic processes, validating its accuracy in South Goa. Different talukas exhibit varied levels of impact, necessitating strategic interventions.

- **Beach Litter and Air Quality**
  Beach litter serves as a proxy for human influence, revealing the impact of COVID-19 lockdowns on coastal vulnerability. Air quality analysis indicates increasing pollution levels, emphasizing the need for improved waste disposal practices.

- **Sea-Level Rise Vulnerability**
  Vulnerability assessments highlight the dynamic nature of vulnerability across talukas, accentuated by urbanization, deforestation, and land use changes. The urgency of addressing mounting vulnerabilities is emphasized.

- **Social Vulnerability Assessment**
  The comprehensive social vulnerability assessment, through the Composite Vulnerability Index (CVI), offers insights into spatial variability. Villages in floodplains show higher physical vulnerability, necessitating tailored interventions.

- **Taluka-Specific Vulnerabilities**
  Taluka-specific vulnerabilities are outlined, emphasizing the need for strategic interventions in Marmugao, sustainable urban planning in Salcete, balanced development in Quepem, and community-based initiatives in Canacona.

- **Importance of Sustainable Development**
  The findings underscore the importance of sustainable development, environmental protection, and proactive measures. Balancing economic growth with ecological preservation is crucial for mitigating coastal vulnerability.

- **Role in Decision-Making**
  The study provides a robust framework for determining coastal vulnerability, offering essential data for informed decision-making, disaster management, and environmental planning at various governance levels.

In conclusion, the study highlights the intricate relationships shaping South Goa's coastal vulnerability, underscoring the need for immediate action to foster resilience and sustainable development in the face of escalating environmental challenges.

12.2 Recommendations

The following comprehensive recommendations are tailored to tackle the specific challenges and vulnerabilities unearthed in this doctoral study, with the aim of fostering more sustainable and resilient development in the coastal tracts of South Goa.

- **Sustainable Urban Development:**

In talukas such as Mormugao, Salcete, and the coastal tracts of Canacona experiencing rapid urbanization, sustainable practices are imperative. This involves strategic land use planning that harmonizes economic growth with environmental preservation. Measures include zoning regulations prioritizing green spaces, incentives for sustainable development, and infrastructure projects aligned with local geomorphology and ecosystems to safeguard critical ecosystems and wetlands.

- **Conservation of Natural Ecosystems:**

Talukas like Quepem and Canacona, characterized by significant forest cover, hilly terrain, and coastal and riverine floodplains, necessitate a focus on conserving natural ecosystems. Enforcing stringent regulations against deforestation, land degradation, and encroachments into water bodies and wetlands is pivotal for mitigating vulnerability.

- **Coastal Flooding Preparedness:**

Enhanced preparedness for coastal flooding, triggered by storm surge and sea-level rise, is essential. This entails developing coastal defenses like sand dune conservation and embankments, along with adaptive strategies for coastal communities. Integrating sea-level rise threats into urban planning and infrastructure projects across talukas is vital for resilience.

- **Resilient Infrastructure:**

Given climate trends and heightened coastal vulnerability, investments in resilient infrastructure are critical. Timely aid facilities must be consolidated along coastal tracts and floodplains. This includes infrastructure capable of withstanding extreme weather events and preserving coastal ecosystems, such as sand dunes, dune vegetation, and wetlands, which act as natural buffers.

- **Air Quality Improvement:**

The study identifies an increase in $SO2$ and Particulate Matter (PM), especially post-monsoon. To improve air quality, particularly in towns like Vasco da Gama, measures should be implemented. This involves promoting renewable energy sources, cleaner transportation options, and effective waste management. Additionally, curbing open-air waste incineration, prevalent in the study area's villages, requires efficient management.

- **Litter Reduction Campaigns:**

Recognizing the impact of tourism-related litter on the coastal environment, a focus on responsible waste disposal and eliminating single-use plastics is essential. Litter reduction campaigns can significantly mitigate beach litter and its adverse effects on the coastal ecosystem.

- **Community Engagement:**

Engaging local communities, social workgroups, college students, and NGOs is pivotal in monitoring and addressing environmental issues. Volunteers can contribute to keeping beaches clean, raising awareness about reforestation, wetland conservation, waste management, and addressing local and global environmental problems. Promoting environmental education through online courses, regular webinars, and virtual initiatives can effectively sensitize the local population for the overall betterment of their neighborhoods.

References

1. A., Vidyasakar., K., Neelavannan., S., Krishnakumar., G., Prabaharan., T., Sathiyabama, Alias, Priyanka., N., S., Magesh., Prince, S., Godson., Seshachalam, Srinivasalu. (2018). Macrodebris and microplastic distribution in the beaches of Rameswaram Coral Island, Gulf of Mannar, Southeast coast of India: A first report. Marine Pollution Bulletin, 137:610-616. doi: 10.1016/J.MARPOLBUL.2018.11.007
2. Abbasnia, M. (2019) Climatic characteristics of heat waves under climate change: A case study of mid-latitudes, Iran; Environ. Dev. Sustain. 21(2) 637–656. DOI: 10.1007/s10668-017-0052-4
3. Abbasnia, M., & Toros, H. (2020). Trend analysis of weather extremes across the coastal and non-coastal areas (case study: Turkey). Journal of Earth System Science, 129, 1-13. Retrieved from https://www.ias.ac.in/article/fulltext/jess/129/0095
4. Aboelkhair, H.; Mostafa, M.; El Afandi, G. (2019). Assessment of Agroclimatology NASA POWER reanalysis datasets for temperature types and relative humidity at 2 m against ground observations over Egypt. *Adv. Space Res.*, *64*, 129–142. DOI:
5. Abou-Mahmoud, M. M. E. (2021). Assessing coastal susceptibility to sea-level rise in Alexandria, Egypt. The Egyptian Journal of Aquatic Research, 47(2), 133-141. DOI: https://doi.org/10.1016/j.ejar.2021.04.002
6. Achrekar, G. (2018). Tourism Development in Goa: Trends, Importance and Challenges. International Journal of Multidisciplinary in Management and Tourism Vol. 3. DOI: https://doi.org/10.14456/10.14456/ijmmt.2021.1
7. Adger, W. N. (1999) Social Vulnerability to Climate Change and Extremes in Coastal Vietnam, World Development, 27 (2), 249-269). DOI: https://doi.org/10.1016/S0305-750X(98)00136-3
8. Aggarwal, D., & Lal, M. (2001). Vulnerability of Indian coastline to sea level rise. New Delhi, India. Proceedings of the 14th Biennial Coastal Zone Conference, New Orleans, Louisiana, July 17 to 21, 2005. Retrieved on Aug 20, 2021 from https://research.fit.edu/media/site-specific/researchfitedu/coast-climate-adaptation-library/asia-amp-indian-ocean/india-amp-sri-lanka/Dwivedi-and-Sharma.-2005.-SLR--Coastal-Wetlands-of-India.pdf
9. Aguilar, R. G., Owens, R., & Giardino, J. R. (2020). The expanding role of anthropogeomorphology in critical zone studies in the Anthropocene. Geomorphology, 366, 107165. DOI: 10.1016/j.geomorph.2020.107165
10. Ahsan, M. N. & Warner, J. (2014). The Socioeconomic Vulnerability Index: A Pragmatic Approach For Assessing Climate Change Led Risks–A Case Study In The South-Western Coastal Bangladesh. International Journal Of Disaster Risk Reduction, 8, 32-49. Retrived from https://research.fit.edu/media/site-specific/researchfitedu/coast-climate-adaptation-

library/asia-amp-indian-ocean/bangladesh/Ahsan--Warner.--2014.--socioeconomic-vulnerability-index-A-pragmatic-approach-for-assessing-CC-led-risks.pdf.pdf

11. Ajai., & Nayak, S., (2012). Coastal Zones of India. Space Application Center (ISRO), Ministry of Environment & Forests, Govt. of India. Retrieved on Aug 28, 2021 from https://iomenvis.nic.in/indexx.aspx?langid=1&slid=3536&mid=2&sublinkid=253
12. Akshitha, H., Bhat, G., & Naveenchandra, B. (2015). Land Use Land Cover Change Detection Study in parts of Mangalore Taluk, Karnataka using multi-temporal remotely sensed data and GIS Techniques. Proceedings of GITA-2K15 held at SMVITM, Bantakal, Udupi.
13. Albert, S., Abernethy, K., Gibbes, B., Grinham, A., Tooler, N., & Aswani, S. (2013). Cost-effective methods for accurate determination of sea level rise vulnerability: A Solomon Islands example. Weather, Climate, and Society, 5(4), 285-292. DOI: https://doi.org/10.1175/WCAS-D-13-00010.1
14. Ali, I., Shaik, R., Maruthi, A. Y., Azman, A., Singh, P., Bala, J. D., ... & Hossain, K. (2020). Impacts of climate change on coastal communities. In Decision Support Methods for Assessing Flood Risk and Vulnerability (pp. 42-59). IGI Global. DOI: 10.4018/978-1-5225-9771-1.ch003
15. Allam, Z., & Jones, D. (2019). Climate change and economic resilience through urban and cultural heritage: The case of emerging small island developing states economies. *Economies*, *7*(2), 62. DOI: https://doi.org/10.3390/economies7020062
16. Allen, M.R., O.P. Dube, W. Solecki, F. Aragón-Durand, W. Cramer, S. Humphreys, M. Kainuma, J. Kala, N. Mahowald, Y. Mulugetta, R. Perez, M. Wairiu, and K. Zickfeld, 2018: Framing and Context. In: *Global Warming of 1.5°C. An IPCC Special Report on the impacts of global warming of 1.5°C above pre-industrial levels and related global greenhouse gas emission pathways, in the context of strengthening the global response to the threat of climate change, sustainable development, and efforts to eradicate poverty* [Masson-Delmotte, V., P. Zhai, H.-O. Pörtner, D. Roberts, J. Skea, P.R. Shukla, A. Pirani, W. Moufouma-Okia, C. Péan, R. Pidcock, S. Connors, J.B.R. Matthews, Y. Chen, X. Zhou, M.I. Gomis, E. Lonnoy, T. Maycock, M. Tignor, and T. Waterfield (eds.)]. Cambridge University Press, Cambridge, UK and New York, NY, USA, pp. 49-92, doi:10.1017/9781009157940.003.
17. Allen, M.R., O.P. Dube, W. Solecki, F. Aragón-Durand, W. Cramer, S. Humphreys, M. Kainuma, J. Kala, N. Mahowald, Y. Mulugetta, R. Perez, M.Wairiu, and K. Zickfeld, (2018). Framing and Context. In: Global Warming of 1.5°C. An IPCC Special Report on the impacts of global warming of 1.5°C above pre-industrial levels and related global greenhouse gas emission pathways, in the context of strengthening the global response to the threat of climate change, sustainable development, and efforts to eradicate poverty [Masson-Delmotte, V., P. Zhai, H.-O. Pörtner, D. Roberts, J. Skea, P.R. Shukla, A. Pirani, W. Moufouma-Okia, C. Péan, R. Pidcock, S. Connors, J.B.R. Matthews, Y. Chen, X. Zhou, M.I. Gomis, E. Lonnoy, T. Maycock, M. Tignor, and T. Waterfield (eds.)]. Cambridge

University Press, Cambridge, UK and New York, NY, USA, pp. 49-92. DOI: https://doi.org/10.1017/9781009157940.003.

18. Alongi, D. M. (2022). Impacts of climate change on blue carbon stocks and fluxes in mangrove forests. *Forests*, *13*(2), 149. DOI: https://doi.org/10.3390/f13020149
19. Alvear, O., Zema, N.R., Natalizio, E., Calafate, C.T., 2017. Using UAV-based systems to Monitor air pollution in areas with poor accessibility. J. Adv. Transp., 8204353. https://doi.org/10.1155/2017/8204353.
20. Amal L, Son LH, Chabchoub H (2018) SGA: spatial GIS-based genetic algorithm for route optimization of municipal solid waste collection. Environ Sci Pollut Res 25:27569–27582. DOI: https://doi.org/10.1007/ s11356-018-2826-0
21. Amarnath, G. & Ahalacoon,N. & Smakhtin,V. & Aggarwal, P. (2017). Mapping multiple climate-related hazards in South Asia, Volume 170 of IWMI Research Report. International Water Management Institute (IWMI)., 2017. https://books.google.co.in/books?id=BpQnDwAAQBAJ&source=gbs_navlinks_s
22. Amosu, A. O., Bashorun, O. W., Babalola, O. O., Olowu, R. A., & Togunde, K. A. (2012). Impact of climate change and anthropogenic activities on renewable coastal resources and biodiversity in Nigeria. URL: http://hdl.handle.net/10566/2304
23. Anderies, J. M., & Barreteau, O. (2019). Governance principles for robust and resilient coastal systems in the face of global change. Regional Environmental Change, 19(7), 1831-1833. DOI:10.1007/s10113-019-01542-3
24. Andrews, G., 2012. Plastics in the Ocean affecting human health. Teach the Earth, Geology and Human Health, Health case studies. Retrieved on March 6, 2021, from https://serc.carleton.edu/NAGTWorkshops/health/case_studies/plastics.html#:~:text=Of%20the%20most%20devastating%20elements,food%20chain%2C%20threatening%20human%20health.
25. Anil K.R. Coastal Communities and Climate Change: A Case Study in Gujarat, India. Environ Anal Eco stud. 2(1). EAES.000527.2018. DOI: 10.31031/EAES.2018.02.000527
26. Anil, N. C., Rao, J. M., Sankar, J. G., Gireesh, G. A., Sailaja, U., & Kumar, S. A. (2012). Monitoring of urban land use/land cover (lulc) changes in parts of Greater Visakhapatnam Municipal Corporation (GVMC) and surrounding areas, ap-using remote sensing and GIS techniques. International Journal of Geomatics and Geosciences, 2(4), 974. Retrieved from https://www.semanticscholar.org/paper/Monitoring-of-urban-Land-UseILand-cover-(LULC)-in-N.C-Rao/65e83c80470050d0eaf893c882b5c1d693decfc8
27. Ara, S., Alif, M. A. U. J., & Islam, K. A. (2021). Impact of tourism on LULC and LST in a coastal island of Bangladesh: A geospatial approach on St. Martin's Island of Bay of Bengal. Journal of the Indian Society of Remote Sensing, 49(10), 2329-2345. DOI: 10.1007/s12524-021-01389-4
28. Arns, A., Dangendorf , S., Jensen, J. et al. Sea-level rise induced amplification of coastal protection design heights. Sci Rep 7, 40171 (2017). https://doi.org/10.1038/srep40171

29. Arya, A.S. (2019). Vulnerability atlas of India. Building materials and technology promotion council (BMTPC), Ministry of Housing and Urban Affairs, Government of India. Retrieved from: http://bmtpc.org/topics.aspx?mid=56&Mid1=180
30. Ashbindu, Singha (1989). Review Article Digital change detection techniques using remotely-sensed Data, International Journal of Remote Sensing, Vol. 10, No. 6. DOI: https://doi.org/10.1080/01431168908903939
31. Ashwin, S., Prashanth Kumar, K., & Vinay, D. C. (2021). Rainfall trend analysis in coastal region of karnataka. Trends in Civil Engineering and Challenges for Sustainability: Select Proceedings of CTCS 2019, 823-833. DOI:10.1007/978-981-15-6828-2_60
32. Ashwini, S. K., Varghese, G. K., 2020. Environmental forensic analysis of the microplastic pollution at "Nattika" Beach, Kerala Coast, India. Environ. Forensics 21:1, 21-36, https://doi.org/10.1080/15275922.2019.1693442.
33. Awuor, C. B., Orindi, V. A., & Ochieng Adwera, A. (2008). Climate change and coastal cities: the case of Mombasa, Kenya. *Environment and urbanization*, *20*(1), 231-242. DOI: https://doi.org/10.1177/0956247808089158
34. Aydin, C., Guven, O., SALİHOĞLU, B., & KIDEYŞ, A. (2016). The influence of land use on coastal litter: an approach to identify abundance and sources in the coastal area of Cilician Basin, Turkey. Turkish Journal of Fisheries and Aquatic Sciences, 16(1). DOI:10.4194/1303-2712-v16_1_04
35. Ayyam, V., Palanivel, S., Chandrakasan, S., Ayyam, V., Palanivel, S., & Chandrakasan, S. (2019). Climate Change and Its Impact on the Coastal Region. Coastal Ecosystems of the Tropics-Adaptive Management, 219-245. ISBN 978-981-13-8926-9
36. Bahinipati, Chandra Sekhar. (2014). Assessment of vulnerability to cyclones and floods in Odisha, India: A District-level analysis. Current science. 107. Retrieved from https://www.unisdr.org/preventionweb/files/41736_19971.pdf
37. Bai, J.; Chen, X.; Dobermann, A.; Yang, H.; Cassman, K.; Zhang, F. Evaluation of NASA satellite- and model-derived weather data for simulation of maize yield potential in China. *Agron. J.* 2010, *102*, 9–16. DOI: DOI:10.2134/agronj2009.0085
38. Basanna, R., & Wodeyar, A. K. (2013). Supervised classification for LULC change analysis. International Journal of Computer Applications, 66(21). Retrieved from https://research.ijcaonline.org/volume66/number21/pxc3886438.pdf
39. Basheer Ahammed, K. K. & Pandey, A. C. (2019). Coastal Social Vulnerability And Risk Analysis For Cyclone Hazard Along The Andhra Pradesh, East Coast Of India. Kn - Journal Of Cartography And Geographic Information, 69, 285-303. DOI: https://doi.org/10.1007/s42489-019-00029-9
40. Bastian, O. and Schreiber, K.-F. 1999. Analyse und ökologische Bewertung der Landschaft. Spektrum, Heidelberg, Germany. Baume, O., Bastian, O. and Röder, M. 1994. Entwicklung und Stand der geographischen Landschaftsforschung in Kuba. Petermanns Geograph. Mitt. 138: 235–244. DOI: https://doi.org/10.1023/A:1014412915534
41. Behera, D.P., Kolandhasamy, P., Sigamani, S., Devi, L.P., Ibrahim, Y.S., 2021. A

preliminary investigation of marine litter pollution along Mandvi beach, Kachchh, Gujarat. Mar. Poll. Bull. 165, 112100. https://doi.org/10.1016/j.marpolbul.2021.112100.

42. Behera, D.P., Kolandhasamy, P., Sigamani, S., Devi, L.P., Ibrahim, Y.S., 2021. A preliminary investigation of marine litter pollution along Mandvi beach, Kachchh, Gujarat. Mar. Poll. Bull. 165, 112100. https://doi.org/10.1016/j.marpolbul.2021.112100.
43. Bellou, N., Gambardella, C., Karantzalos, K. et al. Global assessment of innovative solutions to tackle marine litter. Nat Sustain 4, 516–524 (2021). https://doi.org/10.1038/s41893-021-00726-2
44. Bergmann, M., Gutow, L., & Klages, M. (2015). Marine anthropogenic litter (p. 447). Springer Nature. DOI:10.1007/978-3-319-16510-3
45. Bertler, N. A., & Barrett, P. J. (2010). Vanishing polar ice sheets (pp. 49-83). Springer Netherlands. DOI:10.1007/978-90-481-8716-4_4
46. Betts, R. A., Falloon, P. D., Goldewijk, K. K., & Ramankutty, N. (2007). Biogeophysical effects of land use on climate: Model simulations of radiative forcing and large-scale temperature change. Agricultural and forest meteorology, 142(2-4), 216-233. DOI: 10.1016/j.agrformet.2006.08.021
47. Bhat, P. A., Shafiq, M. U., Mir, A. A., & Ahmed, P. (2017). Urban sprawl and its impact on landuse/land cover dynamics of Dehradun City, India. International Journal of Sustainable Built Environment, 6(2), 513–521. https://doi.org/10.1016/j.ijsbe.2017.10.003
48. Bhatta, B., Saraswati, S., Bandyopadhyay, D., 2010. Urban sprawl measurement from remote sensing data. Appl. Geogr. 30, 731–740. DOI: https://doi.org/10.1016/j.apgeog.2010.02.002
49. Bhunia, G. S., Chatterjee, U., Lalmalsawmzauva, K. C., & Shit, P. K. (Eds.). (2022). Anthropogeomorphology: A geospatial technology based approach. ISBN 978-3-030-77571-1. Springer Nature. DOI: https://doi.org/10.1007/978-3-030-77572-8
50. Black, K.P., Mathew, J. and Anjali, S. (2017). The Maharashtra Shoreline Management Plan. Sanctuary Beach (Singapore), Sustainable Coastal Protection and Management Investment Program – Tranche 1, Maharashtra Maritime Board, Mumbai, India. Accessed on Sepetember 15, 2021 from https://www.scribd.com/document/366556954/Coastal-Protection-Plan-2017
51. Blackburn, S., Pelling, M., & Marques, C. (2019). Megacities and the coast: global context and scope for transformation. In Coasts and Estuaries (pp. 661-669). Elsevier. DOI:10.1016/B978-0-12-814003-1.00038-1
52. BorgattI, l. and soldatI, M. (2005): Geomorphological hazard and human impact in mountain environment. In: Geomorphology 66, 7–11. https://doi.org/10.1016/j.geomorph.2004.10.001
53. Borsdorf, A., & Stadel, C. (2015). *The Andes: A geographical portrait*. Springer International Publishing, 2015. xiv + 368 pp. ISBN 978-3-319-03529-1. DOI:10.1659/mrd.mm180

54. Boruff, B. J., Emrich, C., & Cutter, S., L. (2005). Erosion Hazard Vulnerability of Us Coastal Counties. Journal of Coastal Research, 215, 932-942. DOI: DOI:10.2112/04-0172.1
55. Boruff, B., Emrich, C., & Cutter, S. L. (2005). Erosion Hazard Vulnerability of US Coastal Counties. *Journal of Coastal Research*, *21*(5), 932-942. https://doi.org/10.2112/04-0172.1
56. Braganza, K., Karoly, D. J., & Arblaster, J. M. (2004). Diurnal temperature range as an index of global climate change during the 20th century. Geophysical Research Letters. https://doi.org/10.1029/2004gl019998
57. Brammer, N. & Beech, J. (2004). Use and abuse of tourism: The Goan experience. Tourism Culture & Communication. 5. 23-35. 10.3727/1098304042781508.
58. Breda, A., Saco, P. M., Sandi, S. G., Saintilan, N., Riccardi, G., & Rodríguez, J. F. (2021). Accretion, retreat and transgression of coastal wetlands experiencing sea-level rise. Hydrology and Earth System Sciences, 25(2), 769-786. DOI: https://doi.org/10.5194/hess-25-769-2021
59. Bridgman, H. A., Davies, T. D., Jickells, T., Hunova, I., Tovey, K., Bridges, K., Surapipith, V. (2022). Air pollution in the Krusne Hory region, Czech Republic during the 1990s, Atmospheric Environment, 36(21), 3375-3389. DOI:10.1016/S1352-2310(02)00317-5
60. Brilliant, R., Varghese, V. M., & Pradeepkumar, A. P. (2013). Landuse/Land Cover Evaluation for Sustainable Coastal Tourism Development of Varkala, Kerala. International Journal of Plant, Animal and Environmental Sciences, 3(1). Retrieved from https://www.fortunejournals.com/ijpaes/admin/php/uploads/273_pdf.pdf
61. Brocx, M., & Semeniuk, V. (2009). Coastal geoheritage: encompassing physical, chemical, and biological processes, landforms, and other geological features in the coastal zone. *Journal of the Royal Society of Western Australia*, *92*, 243. Retrieved from https://www.semanticscholar.org/paper/Coastal-geoheritage%3A-encompassing-physical%2C-and-and-Brocx-Semeniuk/e163de760beb4c7581e7fe875a2d21294c629746
62. Brooks, N. (2003). Vulnerability, risk and adaptation: A conceptual framework. Tyndall Centre for climate change research working paper, 38(38), 1-16. Accessed from https://gsdrc.org/document-library/vulnerability-risk-and-adaptation-a-conceptual-framework/
63. Brown, A. G., Tooth, S., Bullard, J. E., Thomas, D. S. G., Chiverrell, R. C., Plater, A. J., Murton, J., Thorndycraft, V., Tarolli, P., Rose, J., Wainwright, J., Downs, P., & Aalto, R. (2017). The geomorphology of the Anthropocene: emergence, status and implications. Earth Surface Processes and Landforms, 42(1), 71-90. https://doi.org/10.1002/esp.3943
64. Brown, A. G.; Tooth, S.; Bullard, J. E.; Thomas, D. S. G; Chiverell, R. C.; Plater, A. J.; Murton, J.; Thorndycraft, V. R.; Tarolli, P.; Rose, J.; Wainwright, J.; Downs, P. And Aalto, R. (2017): The geomorphology of the Anthropocene: emergence, status and implications. In: Earth Surface Processes and Landforms 42, 71–90. https://doi.org/10.1002/esp.3943

65. Bulleri, F., & Chapman, M. G. (2010). The introduction of coastal infrastructure as a driver of change in marine environments. Journal of Applied Ecology, 47(1), 26-35. doi: 10.1111 /j. 1365-2664.2009
66. Burton, I., Huq, S., Lim, B., Pilifosova, O. and Schipper, E. L. (2002) From impacts assessment to adaptation priorities: the shaping of adaptation policies, Climate Policy, 2, 145-159. DOI: 10.3763/cpol.2002.0217
67. Business Today. (June 7, 2019). "Cyclone Fani caused loss of over Rs 9,000 crore in Odisha; 1.6 crore people affected," Accessed June 15, 2019. https://www.businesstoday.in/current/economy-politics/ cyclone-fani-news-odisha-fani-cyclone-disaster-total-loss-due-tocyclone-fani/story/354287.html.
68. Business Goa. (November 1, 2018). Goa's growing urbanization. Ecomania, Business Goa. Retrieved on December 2, 2022 from https://businessgoa.in/goas-growing-urbanisation/
69. Butsch, C., Kumar, S., Wagner, P., Kroll, M., Kantakumar, L., Bharucha, E., & Kraas, F. (2017). Growing 'smart'? Urbanization processes in the Pune urban agglomeration. Sustainability, 9(12), 2335. https:// doi.org/10.3390/su9122335
70. Byizigiro, R. V., Raab, T. And Maurer, T. (2015): Small-Scale Opencast Mining: An Important Research Field For Anthropogenic Geomorphology. In: Die Erde 146 (4), 213–231. DOI: DOI:10.12854/erde-146-21
71. Byizigiro, R. V., Raab, T. And Maurer, T. (2015): Small-Scale Opencast Mining: An Important Research Field for Anthropogenic Geomorphology. In: Die Erde 146 (4), 213–231. DOI:10.12854/erde-146-21
72. Cabral, P., Augusto, G., Akande, A., Costa, A., Amade, N., Niquisse, S., & Santha, R. (2017). Assessing Mozambique's exposure to coastal climate hazards and erosion. International journal of disaster risk reduction, 23, 45-52. DOI: https://doi.org/10.1016/j.ijdrr.2017.04.002
73. Camedda, A., Coppa, S., Palazzo, L., Marra, S., Massaro, G., Serrentino, F., ... & de Lucia, G. A. (2021). Characterization and assessment of micro and macroscopic litter in sardinian beaches (Western Mediterranean Sea). Water, Air, & Soil Pollution, 232, 1-14. DOI:
74. Census of India (2011), Primary Census Abstracts, Registrar General of India, Ministry of Home Affairs, Government of India, Available at: http://www.censusindia.gov. in/2011census/PCA/pca_highlights/pe_data. html, Accessed on 14 July 2013.
75. Census of India. (2011). Primary Census Abstract Highlights. Office of the Registrar General & Census Commissioner, India, Ministry of Home Affairs, Government of India. Retrieved on March 6, 2021 from https://censusindia.gov.in/2011census/PCA/PCA_Highlights/PCA_Data_highlight.html.
76. Chachadi, G. & Ferraira, J.P.L. (2002). Assessing aquifer vulnerability to sea-water intrusion using GALDIT method. The Fourth Inter-Celtic Colloquium on Hydrology and Management of Water Resources, Universidade do Minho, Guimarães July 11-13, 2005. Retrieved from https://aprh.pt/celtico/PAPERS/26.PDF

77. Chandra, S. & Singh, S.S. & Meena, S. & Vijayalakshami, G. (2016). status report on coastal protection and development in India. Retrieved from: http://old.cwc.gov.in/CPDAC-Website/Paper_Research_Work/Status_Report_on%20_Coastal_Protection_and%20_Development_in%20_India_2016.pdf
78. Chandrasekar, N., Cherian, A., Rajamanickam, M., Rajamanickam, G.V. (2001). Influence of Garnet sand mining on beach sediment dynamics between the Periathali and Navaladi coast, India. India. J. Indian Assoc Sedimentol. 20 (2), 223–233. Retrieved from https://www.researchgate.net/publication/230729477_Influence_of_Garnet_sand_mining_on_beach_sediment_dynamics_between_Periyathalai_and_Navaladi_Coast_Tamil_Nadu
79. Chandrasekar, N., Joevivek, V., Saravanan, S., 2013. Coastal vulnerability and shoreline changes for southern tip of India-Remote sensing and GIS approach, Earth Sci. Clim. Change. DOI: 10.4172/2157-761711000144
80. Chandrasekar, N.; Joevivek, V. John Prince Soundaranayagam., Divya, C. (2011). Geospatial Analysis of Coastal Geomorphological Vulnerability along Southern Tamil Nadu Coast; Geospatial World Forum. Accessed on September 15, 2021 from https://geospatialworldforum.org/2011/proceeding/pdf/N.%20ChandrasekarFullPaper.pdf
81. Chandrasekaran, R., SEELAM, J., Gowthaman, R., Jishad, M., Yadhunath, E. M., Pednekar, P. (2014). Sand spit and shoreline dynamics near Terekhol River mouth, Goa, India. Indian Journal of Geo-Marine Sciences. 43. 1311-1315. http://drs.nio.org/drs/handle/2264/7634
82. Chandrashekar, V. D., & Shetty, A. (2018). Trends in extreme rainfall over ecologically sensitive Western Ghats and coastal regions of Karnataka: an observational assessment. Arabian Journal of Geosciences, 11, 1-13. DOI:10.1007/s12517-018-3700-6
83. Change detection studies in coastal zone features of Goa, India by remote sensing. Current Science. vol.91(6), 816-820p. http://drs.nio.org/drs/handle/2264/437
84. Chao, Z. (1990). Urban climate and air pollution in Shangai, Energy Build., 15-16, 673-676. Retrieved from https://hero.epa.gov/hero/index.cfm/reference/details/reference_id/1704430
85. Chartin, C.; Evrard, O.; Salvador-Blanes, S.; Hinschberger, F.; Van Oost, K.; Lefèvre, I.; Daroussin, J. and Macaire, J-J. (2013): Quantifying and modelling the impact of land consolidation and field borders on soil redistribution in agricultural landscapes (1954–2009). In: Catena 110, 184–195. https://doi.org/10.1016/j.catena.2013.06.006
86. Chartin, C.; Evrard, O.; Salvador-Blanes, S.; Hinschberger, F.; Van Oost, K.; Lefèvre, I.; Daroussin, J. and Macaire, J-J. (2013): Quantifying and modelling the impact of land consolidation and field borders on soil redistribution in agricultural landscapes (1954–2009). In: Catena 110, 184–195. https://doi.org/10.1016/j.catena.2013.06.006

87. Chauhan, H.B., Nayak, S., 2005. Land use/land cover changes near Hazira region, Gujarat using remote sensing satellite data. J. Indian Soc. Remote. 33 (3), 413– 420. DOI: https://doi.org/10.1007/BF02990012
88. Chen, Y., Li, X., Zheng, Y., Guan, Y., & Liu, X. (2011). Estimating the relationship between urban forms and energy consumption: A case study in the Pearl River Delta, 2005–2008. Landscape and Urban Planning, 102(1), 33–42. https://doi.org/10.1016/j.landurbplan.2011.03.007
89. Cheng, L., Abraham, J., Trenberth, K.E. *et al.* Upper Ocean Temperatures Hit Record High in 2020. *Adv. Atmos. Sci.* 38, 523–530 (2021). DOI: https://doi.org/10.1007/s00376-021-0447-x
90. Chenthamilselvan, S., & Kankara, R.S., & Rajan, B., (2014). Assessment of shoreline changes along Karnataka coast, India using GIS & Remote sensing techniques. Indian Journal of Geo-Marine Sciences, Vol. 43(7), July 2014, pp. Retrived from https://nopr.niscpr.res.in/bitstream/123456789/34441/1/IJMS%2043(7)%201286-1291.pdf
91. Chilar, J., 2000. Land cover mapping of large areas from satellites: status and research priorities. Int. J. Remote Sens. 21 (67), 1093–1114. DOI: https://doi.org/10.1080/014311600210092
92. Chinowsky, P., & Helman, J. (2021). Protecting Infrastructure and public buildings against sea level rise and storm surge. Sustainability, 13(19), 10538. DOI: https://doi.org/10.3390/su131910538
93. Chittibabu, P., (1999). DEVELOPMENT OF STORM SURGE PREDICTION MODELS FOR THE BAY OF BENGAL AND THE ARABIAN SEA. Retrieved from: http://eprint.iitd.ac.in/bitstream/handle/12345678/2650/TH-2676.pdf?sequence=2

94. Chiyyadri, R, S. (2021). Effect of Climate Change in Coastal Areas. J Marine Sci Res Dev 11: 298. DOI: 10.4172/2155-9910.100029.

95. Choi G, Collins D and Ren G et al. 2009 Changes in means and extreme events of temperature and precipitation in the Asia-PaciBc Network region, 1955–2007; Int. J. Climatol. 29(13) 1906–1925. DOI: DOI:10.1002/joc.1979
96. Chowdhary, R., & Gowthaman, R & Kumar. V.S., (2013). Shoreline change detection from Karwar to Gokarna - South West coast of India using remotely Sensed data. International Journal of Earth Sciences and Engineering ISSN 0974-5904, Vol. 06, No. 03, June 2013, pp. 489-494. Retrieved from https://drs.nio.res.in/drs/bitstream/handle/2264/4386/Int_J_Earth_Sci_Eng_6_489.pdf?sequence=1&isAllowed=y
97. Chowdhury, P., & Behera, M. R. (2015). A Study on Regional Sea Level Variation Along the Indian Coast. 1078-1084. Paper presented at 8th International Conference on Asian and

Pacific Coasts, Chennai, India. https://doi.org/10.1016/j.proeng.2015.08.348

98. Chu, E. W., & Karr, J. R. (2017). Environmental Impact: Concept, Consequences, Measurement. *Reference Module in Life Sciences*, B978-0-12-809633-8.02380-3. DOI: https://doi.org/10.1016/B978-0-12-809633-8.02380-3
99. Church, J. A., Gregory, J. M., Huybrechts, P., Kuhn, M., Lambeck, K., Nhuan, M. T., & Woodworth, P. L. (2001). Changes in sea level. In , in: JT Houghton, Y. Ding, DJ Griggs, M. Noguer, PJ Van der Linden, X. Dai, K. Maskell, and CA Johnson (eds.): Climate Change 2001: The Scientific Basis: Contribution of Working Group I to the Third Assessment Report of the Intergovernmental Panel (pp. 639-694). Accessed from https://epic.awi.de/id/eprint/4506/
100. Clark, D., (1982). Urban Geography: An Introductory Guide. Croom Helm, London, pp. 200–220. DOI: https://doi.org/10.4324/9780203796641
101. Clark, P., Shakun, J., Marcott, S. *et al.* Consequences of twenty-first-century policy for multi-millennial climate and sea-level change. *Nature Clim Change* 6, 360–369 (2016). DOI: https://doi.org/10.1038/nclimate2923
102. Claudia, T., Benjamin, H. S., & Chris, E. Z. (2012). Modelling sea level rise impacts on storm surges along US coasts. *Environmental Research Letters*, *7*(1), 014032. DOI 10.1088/1748-9326/7/1/014032
103. Coast (n.d.) *The American Heritage Dictionary of the English Language (4th ed.). 2000. Archived from* the original *on 2009-02-01*. Retrieved on June 22, 2021 from https://www.etsy.com/listing/1213217369/american-heritage-dictionary-of-the
104. Coastal and Marine Environment Pollution Prevention, CMEPP-99: Advanced International Training Programme, April 15-May 20, Sweden, 10 p. http://drs.nio.org/drs/handle/2264/1905
105. Coastal Zone Management in India. (1989). New Delhi: Indian Association for the Advancement of Science;145-147. http://drs.nio.org/drs/handle/2264/7280
106. Comiso, J. C., & Hall, D. K. (2014). Climate trends in the Arctic as observed from space. Wiley Interdisciplinary Reviews: Climate Change, 5(3), 389-409. DOI: https://doi.org/10.1002/wcc.277
107. Cook, P.J. 1996. Social trends and their impacts on the coastal zone and adjacent seas. Rep. 3, British Geological Survey. Natural Environment Research Council (NERC), VF 2392. Retrieved on Oct 10, 2022 from https://library.sprep.org/content/societal-trends-and-their-impact-coastal-zone-and-adjacent-seas
108. Corbau, C., Lazarou, A., Gazale, V., Nardin, W., Simeoni, U., & Carboni, D. (2022). What can beach litter tell about local management: A comparison of five pocket beaches of the North Sardinia island (Italy). Marine Pollution Bulletin, 174, 113170. DOI: 10.1016/j.marpolbul.2021.113170

109. Creel, L. (2003). Ripple effects: Population and coastal regions. Population, Health and Environment Program. Retrieved on March 9, 2021 from https://www.prb.org/rippleeffectspopulationandcoastalregions/.

110. Csorba P, Zsadányi E (2003) Veränderungen des Characteristikums der Naturnahen Vegetation in den Letzten 30 Jahren in dem Halbbecken von Bodrogkeresztúr. Acta Geogr Debrecina 36: 121–140. DOI: https://doi.org/10.1007/978-90-481-3058-0

111. Cuhadaroglu, B., and Demirci, E. (1997). Influence of some meteorological factors on air pollution in Trabzon city, Energy and Build., 25, 179-184. DOI: https://doi.org/10.1016/S0378-7788(96)00992-9

112. Curtis, S. (2019). Means and long-term trends of global coastal zone precipitation. Scientific Reports, 9(1), 5401. DOI: https://doi.org/10.1038/s41598-019-41878-8

113. Cutter, S. L., & Finch, C. (2008). Temporal and spatial changes in social vulnerability to natural hazards. *Proceedings of the National Academy of Sciences of the United States of America*, *105*(7), 2301–2306. DOI: https://doi.org/10.1073/pnas.0710375105

114. D'Mello, Joshua & Kumar, S. Prasanna. (2017). Processes controlling the accelerated warming of the Arabian Sea. International Journal of Climatology. 38. DOI: 10.1002/joc.5198.

115. D’Souza, M., 2020. Tourists Arrival Statistics. Department of Tourism, Government of Goa. Retrieved on March 9, 2021 from https://www.goatourism.gov.in/statistics/

116. Dadhich, A, P., Goyal, R., & Dadhich, P, N. (2018). Assessment of Spatio-Temporal Variations in Air Quality of Jaipur City, Rajasthan, India. The Egyptian Journal of Remote Sensing and Space Sciences 21 (2018) 173–181. DOI: http://dx.doi.org/10.1016/j.ejrs.2017.04.002

117. Dai, A., K.E. Trenberth, T.R. Karl. (1999) Effects of clouds, soil moisture, precipitation, and water vapour on diurnal temperaturerange, J. Climate, 12, 2451-2473. DOI: https://doi.org/10.1175/1520-0442(1999)012<2451:EOCSMP>2.0.CO;2

118. Dailidienė, I., Davulienė, L., Kelpšaitė*, L., & Razinkovas, A. (2012). Analysis of the climate change in Lithuanian coastal areas of the Baltic Sea. Journal of Coastal Research, 28(3), 557-569. DOI: https://doi.org/10.2112/JCOASTRES-D-10-00077.1

119. Dale, V. H. (1997). The relationship between land-use change and climate change. Ecological applications, 7(3), 753-769. DOI: https://doi.org/10.1890/1051-0761(1997)007[0753:TRBLUC]2.0.CO;2

120. Daniel, D.B., Thomas, S.N. and Thomson, K.T., 2020. Assessment of fishing-related plastic debris along the beaches in Kerala Coast, India. Mar. Pollut. Bull. 150,

110696. https://doi.org/10.1016/j.marpolbul.2019.110696.
121. Darryl, D., M. (2017). India Climate Dialogue. Retrieved from https://indiaclimatedialogue.net/2017/11/24/india- biggest-emitter-so2/
122. Das, Balai & Ghosh, Sandipan & Islam, Aznarul & Roy, Suvendu. (2020). Anthropogeomorphology of Bhagirathi-Hooghly River System in India. CRC Press, Boca Raton. https://doi.org/10.1201/9781003032373
123. Das, S., & Angadi, D. P. (2020). Land use-land cover (LULC) transformation and its relation with land surface temperature changes: A case study of Barrackpore Subdivision, West Bengal, India. Remote Sensing Applications: Society and Environment, 19, 100322. DOI: https://doi.org/10.1016/j.rsase.2020.100322
124. Dasgupta D, Laplante B, Meisner C, Wheeler D, Yan J. The impact of sea level rise on developing countries: a comparative analysis. Word Bank Policy Research Working Paper. 2007;4136:51. Accessed from http://wwwwds.worldbank.org/servlet/WDSContentSer ver/WDSP/IB/2007/02/09/00001640620070209161430/Rendered/PDF/wps4136.pdf
125. Dasgupta, A. (June 17, 2021). Arabian Sea emerging as a cyclone hotspot. News feature, nature India. *DOI:* https://doi.org/10.1038/d44151-021-00061-7.
126. Dasgupta, S., Laplante, B., Meisner, C., Wheeler, D., Yan, J. (2007). The Impact of Sea Level Rise on Developing Countries: A Comparative Analysis. Policy Research Working Paper; No. 4136. World Bank, Washington, DC. © World Bank. https://openknowledge.worldbank.org/handle/10986/7174 License: CC BY 3.0 IGO."
127. Dasgupta, S., Laplante, B., Meisner, C., Wheeler, D., & Yan, J. (2007). The impact of sea level rise on developing countries: a comparative analysis. Climatic Change 93, 379–388. DOI: https://doi.org/10.1007/s10584-008-9499-5
128. Dávid L, Patrick, C. (1998). Quarrying as an anthropogenic geomorphological activity. In: Szabó J, Wach J (Eds.), Anthropogenic Aspects of Geographical Environment Transformation. University of Silesia, Faculty of Earth Sciences, Sosnowiec, Kossuth Lajos University, Debrecen, Debrecen-Sosnowiec. https://www.researchgate.net/publication/26503966_Quarrying_an_anthropogenic_geomorphological_approach
129. Dávid, L. (2000). A kobányászat, mint felszínalakító tevékenység tájvédelmi, tájrendezési és terület- ″ fejlesztési vonatkozásai Mátra-hegységi példák alapján (Landscape Protection, Landscape Management and Regional Development Aspects of Quarrying as a Surface-Forming Activity Based on Examples from the Mátra Mountains). Debreceni Egyetem, Debrecen
130. David, L., Szilagyi, Z, L., & Baros, Z. (2010). The impact of tourism and sports activities. (Eds.) Anthropogenic Geomorphology, A Guide to Man-Made Landforms, pp. 233-254. Springer, ISBN 978-90-481-3057-3. DOI: 10.1007/978-90-481-3058-0
131. Davidson-Arnott, R., Bauer, B., & Houser, C. (2019). Introduction to coastal processes and geomorphology. Cambridge university press.

132. de Andres, M., & Barragan, J. M. (2015). Development of coastal cities and agglomerations: pressure and impacts on coastal and marine ecosystems. Coastal Cities and Their Sustainable Future, 148, 63-71. DOI: 10.2495/CC150061

133. da Silva RM, Santos CAG, de Macedo MLA, Pereira e Silva L and Freire PKMM (2013) Space—time variability of rainfall and hydrological trends in the Alto São Francisco River basin. *IAHS-AISH publication*, NA(NA): 177-182. Retrieved from https://api.semanticscholar.org/CorpusID:133343876

134. De Sherbinin, A. & Bardy, G. (2015). Social Vulnerability To Floods In Two Coastal Megacities: New York City And Mumbai. Vienna Yearbook Of Population Research, 13, 131-165. Retrieved from DOI:10.1553/populationyearbook2015s131

135. Deepa, J. S., & Gnanaseelan, C. (2021). The decadal sea level variability observed in the Indian Ocean tide gauge records and its association with global climate modes. Global and Planetary Change, 198, 103427. DOI: https://doi.org/10.1016/j.gloplacha.2021.103427

136. Defeo, O., McLachlan, A., Armitage, D., Elliott, M., Pittman, J. (2020). Sandy beach socialecological systems at risk: regime shifts, collapses and governance challenges. Front. Ecol. Environ. (in press).

137. Deidun, A., Gauci, A., Lagorio, S., Galgani, F. (2018). Optimising beached litter monitoring protocols through aerial imagery. Mar. Pollut. Bull. 131, 212–217. https://doi.org/10.1016/j.marpolbul.2018.04.033.

138. Deng, H., & Mendelsohn, R. (2021). The effect of urbanization on air pollution damage. Journal of the Association of Environmental and Resource Economists, 8(5), 955-973. DOI: http://dx.doi.org/10.1086/714415

139. Deshpande, M., Singh, V. K., Ganadhi, M. K., Roxy, M. K., Emmanuel, R., & Kumar, U. (2021). Changing status of tropical cyclones over the north Indian Ocean. Climate Dynamics, 57, 3545-3567. DOI: 10.1007/s00382-021-05880-z

140. Deshpande, M., Singh, V.K., Ganadhi, M.K. *et al.* Changing status of tropical cyclones over the north Indian Ocean. *Clim Dyn* 57, 3545–3567 (2021). DOI: https://doi.org/10.1007/s00382-021-05880-z

141. Deshpande, Medha & Singh, Vineet & Mano Kranthi, Ganadhi & Koll, Roxy & Rongmie, Emmanuel & Kumar, Umesh. (2021). Changing status of tropical cyclones over the north Indian Ocean. Climate Dynamics. 57. DOI: 10.1007/s00382-021-05880-z.

142. DeSousa, S., N. (1999). Effect of mining rejects on the nutrient chemistry of Mandovi Estuary, Goa. Indian Journal of Marine Sciences. 28. Retrieved from https://nopr.niscpr.res.in/bitstream/123456789/25708/1/IJMS%2028%284%29%20355-359.pdf

143. Dharani, G., Nazar, A. K., Ravindran, M. (2003). Marine Debris in Nicobar. Curr. Sci. 85, 574-5775.

144. Dhiman, R., VishnuRadhan, R., Eldho, T.I., Inamdar, A. (2019). Flood risk and

adaptation in Indian coastal cities: recent scenarios. Applied Water Science. DOI: 9. 10.1007/s13201-018-0881-9.

145. Di Febbraro, M., Frate, L., de Francesco, M. C., Stanisci, A., Tozzi, F. P., Varricchione, M., & Carranza, M. L. (2021). Modelling beach litter accumulation on Mediterranean coastal landscapes: an integrative framework using species distribution models. Land, 10(1), 54. DOI: https://doi.org/10.3390/land10010054

146. Diez, P.G., Perillo, G.M.E. and Piccolo, C.M. (2007) Vulnerability to Sea-Level Rise on the Coast of the Buenos Aires Province. Journal of Coastal Research, 23, 119- 126. https://doi.org/10.2112/04-0205.1

147. Dinesh Kumar, P. K. (2006). Potential vulnerability implications of sea level rise for the coastal zones of Cochin, Southwest coast of India. Environmental Monitoring and Assessment 123, 333-344. DOI: https://doi.org/10.1007/s10661-006-9200-2

148. Dolan, A. H., & Walker, I. J. (2006). Understanding vulnerability of coastal communities to climate change related risks. Journal of Coastal research, 1316-1323. Retrieved from https://www.jstor.org/stable/25742967

149. Duarte, C.M., Agusti, S., Barbier, E., Britten, G.L., Castilla, J.C., Gattuso, J.P., Fulweiler, R.W., Hughes, T.P., Knowlton, N., Lovelock, C.E., Lotze, H.K., Predragovic, M., Poloczanska, E., Roberts, C., Worm, B. (2020). Rebuilding marine life. Nature 580, 39–51. DOI: 10.1038/s41586-020-2146-7

150. Dube, S.K., & Murthy, T.S., & Feyen, J.C., & Cabrera, R., & Harper, B.A., & Belse, J.D., & Amer, S. (2010). Storm Surge Modeling and Applications in Coastal Areas. DOI: 10. 1142/9789814293488_0012.

151. Dube, S.K., & Sinha, P.C., & Rao, A.D., & Rao, G.S., (1984). Numerical modelling of Storm surges in Arabian sea. Appl. Math. Modelling, 1985, Vol. 9, August, 1984. DOI: https://doi.org/10.1016/0307-904X(85)90067-8

152. Duc, K. N., Ancev, T., & Randall, A. (2019). Evidence of climatic change in Vietnam: Some implications for agricultural production. Journal of Environmental Management, 231, 524-545. DOI: 10.1016/j.jenvman.2018.10.011

153. DulIas, r. (2016): The impact of mining on the landscape. A study of the Upper Silesian coal basin in Poland. Cham. https://doi.org/10.1007/978-3-319-29541-1

154. DulIas, r. (2016): The impact of mining on the landscape. A study of the Upper Silesian coal basin in Poland. Cham. https://doi.org/10.1007/978-3-319-29541-1

155. Dumenu, W. K., & Obeng, E. A. (2016). Climate change and rural communities in Ghana: Social vulnerability, impacts, adaptations and policy implications. *Environmental Science & Policy*, *55*, 208–217. DOI: https://doi.org/10.1016/j.envsci.2015.10.010

156. Duszyński, F., Ford, D, C., Goudie, A., & Migoń, P. (2022). Rock properties and rock-controlled landforms. Geological Society, London, Memoirs, Volume 58Pages 151 – 171. DOI: https://doi.org/10.1144/M58-2021-1

157. Datta B. (2018). Controlling Dust Pollution in Goa. Home, Opinion, Commentary, Navhind Times. Retrieved from

https://www.navhindtimes.in/2018/01/20/opinions/opinion/controlling-dust-pollution-in-goa/

158. Duttagupta, S. (May 24, 2017). Calangute Beach. Time travel, Travel, Calangute beach. Retrieved on July 13, 2021 from https://timesofindia.indiatimes.com/travel/Calangute/Calangute-Beach/ps58822359.cms
159. Dwarakish G. S., Vinay S. A., Natesan, U., Asano, T., Kakinuma, T., Venkataramana, K., Jagadeesha, P. B., and Babita, M. K., 2009. Coastal Vulnerability Assessment of the Future Sea-Level Rise in Udupi Coastal Zone of Karnataka State, West Coast of India. Ocean and Coastal Management, DOI: 10.1016/ j.ocecoaman.2009.07.007.

160. Dwarakish, G. S., Vinay, S. A., Dinakar, S. M., Pai, J. B., Mahaganesha, K. & Natesan, U. 2008. Integrated Coastal Zone Management Plan For Udupi Coast Using Remote Sensing, Geographical Information System And Global Position System. Journal Of Applied Remote Sensing, 2, 023515. DOI:10.1117/1.2919101
161. Dzurik, A. A. (1984). Environmental Conflicts in a Rapidly Growing Coastal Economy: The Case of South Florida. Water Science and Technology, 16(3-4), 659-666. Retrieved from https://na.unep.net/siouxfalls/publications/Conflicts.pdf
162. Ebi K L and Bowen K 2016 Extreme events as sources of health vulnerability: Drought as an example; Wea. Clim. Extrem. 11 95–102. DOI: https://doi.org/10.1016/j.wace.2015.10.001.
163. Efthymiadis, D. A., & Jones, P. D. (2010). Assessment of maximum possible urbanization influences on land temperature data by comparison of land and marine data around coasts. Atmosphere, 1(1), 51-61. DOI: https://doi.org/10.3390/atmos1010051
164. Eger, A. M., Earp, H. S., Friedman, K., Gatt, Y., Hagger, V., Hancock, B., ... & Reeves, S. (2022). The need, opportunities, and challenges for creating a standardized framework for marine restoration monitoring and reporting. Biological Conservation, 266, 109429. DOI: https://doi.org/10.1016/j.biocon.2021.109429
165. Ehelepola, N.D.B., Ariyaratne, K., 2016. The correlation between dengue incidence and diurnal ranges of temperature of Colombo district, Sri Lanka 2005-2014. Glob. Health Action 9. DOI: https://doi.org/10.3402/gha.v9.32267, 32267-32267.
166. Elhacham, E., & Alpert, P. (2021). Temperature patterns along an arid coastline experiencing extreme and rapid urbanization, case study: Dubai. Science of the Total Environment, 784, 147168. DOI: 10.1016/j.scitotenv.2021.147168

167. ElNesr (2010) Temperature Trends and Distribution in the Arabian Peninsula. *American Journal of Environmental Sciences*, 6(2): 191-203 doi:10.3844/ajessp.2010.191.203
168. Estoque, R. C., & Murayama, Y. (2013). Landscape pattern and ecosystem service value changes: Implications for environmental sustainability planning for the rapidly

urbanizing summer capital of the Philippines. Landscape and Urban Planning, 116, 60–72. DOI: https://doi.org/10.1016/j.landurbplan.2013.04.008

169. Evan, A.T., & Camargo, S.J., (2010), A Climatology of Arabian Sea Cyclonic Storms. Journal of Climate, Volume 24, DOI: 10.1175/2010JCLI3611.1.

170. Ewers, R. M., & Banks-Leite, C. (2013). Fragmentation impairs the microclimate buffering effect of tropical forests. *PLOS one*, *8*(3), e58093. DOI: 10.1371/journal.pone.0058093

171. Feddema, J. J., Oleson, K. W., Bonan, G. B., Mearns, L. O., Buja, L. E., Meehl, G. A., & Washington, W. M. (2005). The importance of land-cover change in simulating future climates. Science, 310(5754), 1674–1678. DOI: https://doi.org/10.1126/science.1118160

172. Ferdig, M. A. (2007). Sustainability leadership: Co-creating a sustainable future. Journal of Change Management, 7(1), 25-35. https://doi.org/10.1080/14697010701233809

173. Ferrer-valero, n.; Hernández-calvento, l. and Hernández-cordero, a. I. (2017): Human impacts quantification on the coastal landforms of Gran Canaria Island (Canary Islands). In: Geomorphology 286, 58–67. https://doi. org/10.1016/j.geomorph.2017.02.028

174. Ferrer-valero, n.; Hernández-calvento, l. and Hernández-cordero, a. I. (2017): Human impacts quantification on the coastal landforms of Gran Canaria Island (Canary Islands). In: Geomorphology 286, 58–67. https://doi. org/10.1016/j.geomorph.2017.02.028

175. Fischer, J., Riechers, M., Loos, J., Martin-Lopez, B., & Temperton, V. M. (2021). Making the UN decade on ecosystem restoration a social-ecological endeavour. Trends in Ecology & Evolution, 36(1), 20-28. DOI: https://doi.org/10.1016/j.tree.2020.08.018

176. Flanagan, B. E., Gregory, E. W., Hallisey, E. J., Heitgerd, J. L. & Lewis, B. 2011. A Social Vulnerability Index For Disaster Management. Journal Of Homeland Security And Emergency Management, 8, 23. DOI:10.2202/1547-7355.1792

177. Forster, P., V. Ramaswamy, P. Artaxo, T. Berntsen, R. Betts, D.W. Fahey, J. Haywood, J. Lean, D.C. Lowe, G. Myhre, J. Nganga, R. Prinn, G. Raga, M. Schulz and R. Van Dorland, 2007: Changes in Atmospheric Constituents and in Radiative Forcing. In: Climate Change 2007: The Physical Science Basis. Contribution of Working Group I to the Fourth Assessment Report of the Intergovernmental Panel on Climate Change [Solomon, S., D. Qin, M. Manning, Z. Chen, M. Marquis, K.B. Averyt, M.Tignor and H.L. Miller (eds.)]. Cambridge University Press, Cambridge, United Kingdom and New York, NY, USA. Retrieved from https://hero.epa.gov/hero/index.cfm/reference/details/reference_id/92936

178. French, J. R., & Burningham, H. (2013). Coasts and climate: Insights from geomorphology. Progress in Physical Geography, 37(4), 550-561. DOI: https://doi.org/10.1177/03091333134949
179. Füssel, H. M., & Klein, R. J. (2006). Climate change vulnerability assessments: an evolution of conceptual thinking. Climatic change, 75(3), 301-329. DOI: https://doi.org/10.1007/s10584-006-0329-3
180. Gabriele C Hegerl, Stefan Brönniman, Tim Cowan, Andrew R Friedman, Ed Hawkins, Carley Iles, Wolfgang Müller, Andrew Schurer and Sabine Undorf. (2019). Environmental Research Letters, Volume 14, Number 12. **DOI** 10.1088/1748-9326/ab4557
181. Gadgil, A., and A. Dhorde (2005), Temperature trends in twentieth century at Pune, India, Atmos. Environ., 39(35), 6550–6556. DOI: 10.1016/j.atmosenv.2005.07.032.
182. Gallo, F., Fossi, C., Weber, R., Santillo, D., Sousa, J., Ingram, I., Nadal, A., Romano, D. (2018). Marine litter plastics and microplastics and their toxic chemicals components: the need for urgent preventive measures. Environ. Sci. Eur. 30, 1-14. https://doi.org/10.1186/s12302-018-0139-z.
183. Gálos M, Kertész P. (1997) Mérnökgeológia (Engineering geology). University Notes, M ˝uegyetemi Kiadó, Budapest
184. Ganesh, Vivek. (2015). SHORELINE CHANGE ANALYSIS FOR NORTH EAST COAST OF ANDHRA PRADESH, INDIA. ISPRS WG VIII/1 Workshop on Geospatial Technology for Disaster Risk Reduction. DOI: 10.13140/RG.2.2.19763.73767.
185. Garg, Shivani. (2017). Impact of Overpopulation on Land Use Pattern. DOI: 10.4018/978-1-5225-1683-5.ch008.
186. Garner, A. J., Weiss, J. L., Parris, A., Kopp, R. E., Horton, R. M., Overpeck, J. T., & Horton, B. P. (2018). Evolution of 21st century sea level rise projections. Earth's Future, 6(11), 1603-1615. DOI:
187. Gayathri, R., & Bhaskaran, P.K., & Jose, F., (2017). Coastal inundation research: An overview of the process. Current science, vol. 112, no. 2, 25 January 2017. Retrieved from https://www.currentscience.ac.in/Volumes/112/02/0267.pdf
188. GBD MAPS (2018) Burden of disease attributable to major air pollution sources in India. Working Group, Special Report 21. Boston: Health Effects Institute. Retrieved from https://www.healtheffects.org/publication/gbd-air-pollution-india
189. Gibson, R., Atkinson, R., & Gordon, J. (2007). Loss, status and trends for coastal marine habitats of Europe. Oceanography and Marine Biology: an annual review, 45, 345-405. eBook ISBN 9780429144905. Accessed from https://www.taylorfrancis.com/chapters/mono/10.1201/9781420050943-9/loss-status-trends-coastal-marine-habitats-europe-gibson-atkinson-gordon

190. Gilbert, R., O. (1987). *Statistical Methods for Environmental Pollution Monitoring. Wiley*. ISBN: 978-0-471-28878-7. Retrieved from https://www.osti.gov/servlets/purl/7037501

191. Ginis, I. (2021). Tropical Cyclones. In: Conrad, K. (eds) From Hurricanes to Epidemics. Global Perspectives on Health Geography. Springer, Cham. DOI: https://doi.org/10.1007/978-3-030-55012-7_10

192. Goa Holiday Homes (2018). Siridao Beach. Information, Beaches in Goa. Retrieved on July 13, 2021 from https://www.goaholidayhomes.com/information/siridao-beach.html

193. Goa State Action Plan on Climate Change. (2020. Goa State Biodiversity Board prepared through NABARD Consultancy Services (NABCONS). Retrieved on March 12, 2021 from https://gsbb.goa.gov.in/wp-content/uploads/2020/12/Draft-Goa%20SAPCC-for-public-inputs.pdf

194. Gohain, K. J., Mohammad, P., & Goswami, A. (2020). Assessing the impact of land use land cover changes on land surface temperature over Pune city, India. Quaternary International. DOI: https://doi.org/10.1016/j.quaint.2020.04.052

195. Gong, D.-Y., Wang, W., Qian, Y., Bai, W., Guo, Y., Mao, R., 2014. Observed holiday aerosol reduction and temperature cooling over East Asia. J. Geophys. Res.: Atmosphere 119 (11), 6306–6324. DOI: https://doi.org/10.1002/2014JD021464.

196. Goossens, J., Jonckheere, A. C., Dupont, L. J., & Bullens, D. M. (2021). Air pollution and the airways: lessons from a century of human urbanization. Atmosphere, 12(7), 898. DOI: https://doi.org/10.3390/atmos12070898

197. Gornitz, V. (1990). Vulnerability of the East coast, U.S.A. to future sea level rise. Journal of Coastal Research, Special Issue No. 9, pp. 201-237. Retrieved from https://pubs.usgs.gov/dds/dds68/reports/eastrep.pdf

198. Gornitz, V. M., Beaty, T. W. & Daniels, R. C. (1997). A Coastal Hazard Data Base For The U.S. West Coast. Oak Ridge, Tennessee: Oak Ridge National Laboratory. DOI: https://doi.org/10.3334/CDIAC/SSR.NDP043C

199. Gornitz, V. M., Daniels, R. C., White, T. W. & Birdwell, K. R. (1994). The Development Of A Coastal Risk Assessment Database: Vulnerability To Sea-Level Rise In The U.S. Southeast. Journal Of Coastal Research, Special Issue No. 12, 327-338. https://pubs.usgs.gov/dds/dds68/reports/eastrep.pdf

200. Gornitz, V., Daniels, R. C., White, T. W., and Birdwell, K., R. (1994). The Development of a Coastal Risk Assessment Database for the U.S. Southeast. Journal of Coastal Research 12(SI), 327-338. Retrieved from https://pubs.usgs.gov/dds/dds68/reports/eastrep.pdf

201. Gornitz, V.M., Daniels, R.C., White, T.W., Birdwell, K.R., 1994. The development of a coastal risk assessment database: Vulnerability to sea-level rise in the U.S. southeast.

Journal of Coastal Research Special Issue No. 12, 327-338. Accessed from https://pubs.usgs.gov/dds/dds68/reports/eastrep.pdf
202. Gorokhovich, Y., Leiserowitz, A., and Dugan, D. (2014). Integrating Coastal Vulnerability and Community-Based Subsistence Resource Mapping in Northwest Alaska. Journal of Coastal Research, Vol:30, No:1, pp: 158-169. Coconut Creek (Florida), ISSN 0749-0208. Retrieved from: https://environment.yale.edu/climate-communication OFF/files/Gorokovich_and_Leiserowitz_(2014)_Integrating_coastal_vulnerability_and_subistence_resource_mapping_in_NW_AK.pdf.
203. Goudarzi, Sara (July 18, 2006). "Flocking to the Coast: World's Population Migrating into Danger". Live Science. http://www.livescience.com/environment/060718_map_settle.html
204. Goudie, A. (2020). The human impact in geomorphology–50 years of change. Geomorphology, 366, 106601. DOI: https://doi.org/10.1016/j.geomorph.2018.12.002
205. GoudIe, A. and VIles, H. A. (2016): Geomorphology in the Anthropocene. Cambridge. DOI: https://doi.org/10.1017/CBO9781316498910
206. Government of Goa. (2015). *Economic Survey 2014-15*. Directorate of Planning Statistics and Evaluation, Panaji-Goa. Retrieved from https://www.goa.gov.in/wp-content/uploads/2020/02/Economic-Survey-2017-18-Part-1.pdf
207. Government of Goa. (2021). *Economic Survey 2020-21*. Directorate of Planning Statistics and Evaluation, Panaji-Goa. Retrieved from https://goabudget.gov.in/assets/documents/economicsurvey/Economic%20Survey%202020 20-21.pdf
208. Grases, A., Gracia, V., García-Leon, ´ M., Lin-Ye, J., Pau Sierra, J. (2020). Coastal flooding and erosion under a changing climate: implications at a low-lying coast (Ebro Delta). Water 12, 346. DOI: https://doi.org/10.3390/w12020346
209. Griggs, G., 2020. Coastal Airports and Rising Sea Levels. J. Coast. Res. 36, 1079-1092. https://doi.org/10.2112/JCOASTRES-D-20A-00004.1.
210. Grinsted, A., Jevrejeva, S., Riva, R. E., & Dahl-Jensen, D. (2015). Sea level rise projections for northern Europe under RCP8. 5. Climate Research, 64(1), 15-23. DOI:10.3354/cr01309
211. Güneralp, B., Güneralp, İ., Castillo, C. R., & Filippi, A. M. (2013). Land change in the mission-aransas coastal region, texas: Implications for coastal vulnerability and protected areas. Sustainability, 5(10), 4247-4267. DOI: https://doi.org/10.3390/su5104247
212. Guo, J., Su, T., Chen, D., Wang, J., Li, Z., Lv, Y. (2019). Declining summertime localscale precipitation frequency over China and the United States, 1981–2012: the disparate roles of aerosols. Geophys. Res. Lett. 46 (22), 13281–13289. DOI: https://doi.org/10.1029/2019GL085442.

213. Gupta, A.B. (1999). Vehicular air pollution and asthma. Asthma Sanjeevani 5 (2), 3–5. Henley, S., 1981. Nonparametric Geostatistics. Applied Science Publishers Ltd., London

214. Guttikunda, S. K, Nishadh, K. A., Jawahar, P. (2019). Air pollution knowledge assessments (APnA) for 20 Indian cities. Urban Clim 27:124–141. DOI: https://doi.org/10.1016/j.uclim.2018.11.005

215. Habel, S., Fletcher, C. H., Anderson, T. R., & Thompson, P. R. (2020). Sea-level rise induced multi-mechanism flooding and contribution to urban infrastructure failure. Scientific reports, 10(1), 3796. DOI: https://doi.org/10.1038/s41598-020-60762-4

216. Haff P.K. (2003) - *Neogeomorphology, Prediction, And The Anthropic Landscapes*. In: Wilcock P.R. & Iverson R.M. (Eds.), «Prediction In Geomorphology». AGU, Geophys. Monograph Series. 135, 15-26. DOI:10.1029/135GM02

217. Haigh, J. D. (1999). A GCM study of climate change in response to the 11-year solar cycle. Quarterly Journal of the Royal Meteorological Society, 125(555), 871-892. DOI 10.1002/qj.49712555506

218. Hallegatte, S., Green, C., Nicholls, R. J., & Corfee-Morlot, J. (2013). Future flood losses in major coastal cities. *Nature Climate Change*, *3*(9), 802–806. DOI: https://doi.org/10.1038/nclimate1979

219. Halls, J. N., & Magolan, J. L. (2019). A methodology to assess land use development, flooding, and wetland change as indicators of coastal vulnerability. Remote Sensing, 11(19), 2260. DOI: https://doi.org/10.3390/rs11192260

220. Haque, S., Singh, R. B. (2017). Air Pollution and Human Health in Kolkata, India: A Case Study. Climate, 5(4):77. DOI: 10.3390/ cli5040077.

221. Harley, C. D., Randall Hughes, A., Hultgren, K. M., Miner, B. G., Sorte, C. J., Thornber, C. S., & Williams, S. L. (2006). The impacts of climate change in coastal marine systems. Ecology letters, 9(2), 228-241. DOI: 10.1111/j.1461-0248.2005.00871.x

222. HarnIschMacher, s. and zePP, h. (2014): Mining and its impact on the earth surface in the Ruhr District (Germany). In: Zeitschrift für Geomorphologie, Supplementary Issues 58 (3), 3–22. https://doi.org/10.1127/0372-8854/2013/S-00131

223. HarnIschMacher, s. and zePP, h. (2014): Mining and its impact on the earth surface in the Ruhr District (Germany). In: Zeitschrift für Geomorphologie, Supplementary Issues 58 (3), 3–22. DOI: https://doi.org/10.1127/0372-8854/2013/S-00131

224. Haruyama, S. (2016). Landform and Vulnerability for Disaster in Land Use Changing. Natural Disaster and Coastal Geomorphology, 113-131. DOI:10.1007/978-3-319-33814-9_6

225. Hassan, Z., Shabbir, R., Ahmad, S.S., Malik, A.H., Aziz, N., Butt, A. and Erum, S., 2016. Dynamics of land use and land cover change (LULCC) using geospatial techniques: a case study of Islamabad Pakistan. SpringerPlus, 5, pp.1-11. https://doi.org/10.1186/s40064-016-2414-z

226. Hassan, Z., Shabbir, R., Ahmad, S.S., Malik, A.H., Aziz, N., Butt, A. and Erum, S. (2016). Dynamics of land use and land cover change (LULCC) using geospatial techniques: a case study of Islamabad Pakistan. SpringerPlus, 5, pp.1-11. https://doi.org/10.1186/s40064-016-2414-z
227. Hauer, M. E., Hardy, D., Kulp, S. A., Mueller, V., Wrathall, D. J., & Clark, P. U. (2021). Assessing population exposure to coastal flooding due to sea level rise. Nature communications, 12(1), 6900. doi: 10.1038/s41467-021-27260-1
228. He, B. J. (2018). Potentials of meteorological characteristics and synoptic conditions to mitigate urban heat island effects. *Urban climate*, *24*, 26-33. DOI:10.1016/j.uclim.2018.01.004
229. Health Effects Institute (HEI). (2019). State of Global Air Report 2019 India-Specific Findings Isaksson, C. 2010. Pollution and its impact on wild animals: a meta-analysis on oxidative stress. EcoHealth 7 (3): 342–50. Retrieved from https://www.stateofglobalair.org/sites/default/files/soga_2019_report.pdf
230. Hegde, A. V., and Reju, V.R. (2007). Development of Coastal Vulnerability Index for Mangalore Coast, India. Journal of Coastal Research 23, 1106. Retrieved from https://idr.l4.nitk.ac.in/jspui/handle/123456789/10554
231. Hegde, A.V, & Reju, V.R. (2007). Development Of Coastal Vulnerability Index For Mangalore Coast, India. Journal Of Coastal Research, Vol. 23, No. 5, Pp. 1106-1111. Retrieved From Https://www.Jstor.Org/Stable/4496125
232. Hegde, V. A.; Radhakrishnan Reju, V. (2007). Development of coastal vulnerability index for Mangalore coast, India. J. Coast. Res., 23, 1106–1111. Retrieved from https://idr.nitk.ac.in/jspui/handle/123456789/10554
233. Helderop, E., & Grubesic, T. H. (2019). Social, geomorphic, and climatic factors driving US coastal city vulnerability to storm surge flooding. Ocean & coastal management, 181, 104902. DOI: https://doi.org/10.1016/j.ocecoaman.2019.104902
234. Henzlar, M. P., 2019. Approaches to tackle marine litter in India. Adelphi, Projects, Project Database. Retrieved on March 7, 2021 from https://www.adelphi.de/en/project/approaches-tackle-marine-litter-india.
235. Herald. (March 29, 2019). Pollution in Vasco 'many times better' than other towns: IIT-B. Team Herald. Retrieved from https://www.heraldgoa.in/Goa/Pollution-in-Vasco-%E2%80%98many-times-better%E2%80%99-than-other-towns-IITB/144451

236. Hertig E, Seubert, S., and Jacobeit, J. (2010) Temperature extremes in the Mediterranean area: Trends in the past and assessments for the future; Nat. Hazard Earth Syst. 10(10) 2039–2050. DOI: trends in the past and assessments for the future, Nat. Hazards Earth Syst. Sci., 10, 2039–2050, https://doi.org/10.5194/nhess-10-2039-2010, 2010.

237. Hobohm, C., Schaminée, J., & van Rooijen, N. (2021). Coastal habitats, shallow seas and inland saline steppes: ecology, distribution, threats and challenges. *Perspectives for Biodiversity and Ecosystems*, 279-310. ISBN: 9783030577124
238. Holland, T. L., Mariscal Romero, J., Davidson-Arnott, R., & Cardille, J. (2011). Landscape changes in a coastal system undergoing tourism development: implications for Barra de Navidad Lagoon, Jalisco, Mexico. Investigaciones geográficas, (74), 7-18. Retrieved from https://www.scielo.org.mx/scielo.php?script=sci_arttext&pid=S0188-46112011000100002
239. Hooke R.L. (1994) - On The Efficacy Of Humans As Geomorphic Agents. GSA Today. 4/9, 217, 224-225. DOI:10.1130/0091-7613(2000)28<843:OTHOHA>2.0.CO;2
240. HOOKE R.L. (1994) - *On the Efficacy of Humans as Geomorphic Agents*. GSA Today. 4/9, 217, 224-225. Retrieved from https://rock.geosociety.org/net/gsatoday/archive/4/9/pdf/i1052-5173-4-9-sci.pdf
241. Hooke, R., L. (2000) - *On the history of humans as geomorphic agents*. Geology. 28/9, 843-846. https://www.exploreiowageology.org/assets/text/Gemorph/UNI_Geomorph_papers/hooke_2000.pdf
242. Horton, B. P., Rahmstorf, S., Engelhart, S. E., & Kemp, A. C. (2014). Expert assessment of sea-level rise by AD 2100 and AD 2300. Quaternary Science Reviews, 84, 1-6. DOI: https://doi.org/10.1016/j.quascirev.2013.11.002
243. Houben, P.; Hoffmann, T.; Zimmermann, A. and Dikau, R. (2006): Land use and climatic impacts on the Rhine system (RheinLUCIFS): quantifying sediment fluxes and human impact with available data. In: Catena 66, 42–52. https://doi.org/10.1016/j.catena.2005.07.009
244. Houben, P.; Hoffmann, T.; Zimmermann, A. and Dikau, R. (2006): Land use and climatic impacts on the Rhine system (RheinLUCIFS): quantifying sediment fluxes and human impact with available data. In: Catena 66, 42–52. https://doi.org/10.1016/j.catena.2005.07.009
245. Howe, P. D., Markowitz, E. M., Lee, T. M., Ko, C. Y., & Leiserowitz, A. (2013). Global perceptions of local temperature change. Nature climate change, 3(4), 352-356. DOI: 10.1038/nclimate1768
246. https://books.google.co.in/books?hl=en&lr=&id=ZtGoDwAAQBAJ&oi=fnd&pg=PR11&dq=a+submergent+coastline+is+one+where+the+sea+level+has+risen+due+to+a+global+sea-level+change,+local+subsidence,+or+isostatic+rebound,+with+submerged+or+%22drowned%22+landforms+such+as+rias+(drowned+valleys)+and+fjords+&ots=LQreHp8rFQ&sig=2S49rmy6mVgb2-EXUb3BvyChIaY&redir_esc=y#v=onepage&q&f=false
247. https://doi.org/10.1029/2018EF000991
248. https://doi.org/10.48550/arXiv.1110.3257

249. Huang, Y., Dickinson, R.E., Chameides, W.L. (2006). Impact of aerosol indirect effect on surface temperature over East Asia. In: Proceedings of the National Academy of Sciences of the United States of America, vol. 103, pp. 4371–4376. DOI: https://doi.org/10.1073/pnas.0504428103, 12.
250. Iglesias-Campos, A., Meiner, A., Bowen, K., & Ansong, J. O. (2015). Coastal population and land use changes in Europe, challenges for a sustainable future. Coastal zones: Solutions for the 21st century, 29-49. DOI:10.1016/B978-0-12-802748-6.00003-6
251. Illés L, Konecsny K (2000) Az erdo hidrológiai hatása az árvizek kialakulására a fels ″ o-Tisza víz- ″ gy ″ujtoben (Hydrologic impact of forests on flood formation in the catchment area of the upper ″ Tisza). Vízügyi Közl 82 (2): 167–197
252. INCOIS (2009). Report on use of satellite data for detection of violation of land use along the coastal regulation zone and impact of port structures on shoreline changes. Retrieved o from https://www.icsf.net/wp-content/uploads/2021/02/215_report_on_use_of_satellite_data_for_detection.pdf
253. INCOIS (2012). Coastal Vulnerability Atlas Of India. Coastal Geospatial Application Mission (CGAM), Advisory Services And Satellite Oceanography Group (Asg), INCOIS. https://incois.gov.in/documents/ITCOocean/Coastal_Vulnerability_Mapping.pdf
254. INCOIS. (2015). Coastal vulnerability of Goa. Ministry of Earth Sciences (MoES), Government of India. Retrieved from: https://incois.gov.in/Incois/cvi/pdfs/Karnataka/48ESE.pdf.
255. Incredible Goa Staff (July 30, 2018). Conservation of Turtle Nests at the Goan Beaches – Awareness and Protection. Incredible Goa, Cover story. Retrieved on July 13, 2021 from https://www.incrediblegoa.org/cover-story/conservation-of-turtle-nests-at-the-goan-beaches-awareness-and-protection/#
256. India: Air Quality Profile (2010). Clean Air Initiative for Asian Cities (CAI-Asia) Center, Pasig City, Philippines. Retrieved from https://www.indiaenvironmentportal.org.in/files/India_Air_Quality_Profile_-_2010_Edition.pdf
257. India.com (2020). Colva Beach. Home, Travel, Destinations, Beaches in Goa. Retrieved on July 13, 2021 from https://www.india.com/travel/goa/things-to-do/beaches-colva/
258. International Union for Conservation of Nature, 2020. Marine Plastics. IUCN.org, Resources, Issues Briefs. Retrieved on March 7, 2021 from https://www.iucn.org/resources/issues-briefs/marine-plastics.
259. IPCC (2001) Climate change 2001: Impacts, Adaptation and Vulnerability, Summary for Policymakers, WMO. Working Group II to the Third Assessment Report of the Intergovernmental Panel on Climate Change. Cambridge University Press, ISBN 0 521 80768 9. Accessed from https://www.ipcc.ch/site/assets/uploads/2018/03/WGII_TAR_full_report-2.pdf

260. IPCC (2007): Climate Change 2007: Synthesis Report. Contribution of Working Groups I, II and III to the Fourth Assessment Report of the Intergovernmental Panel on Climate Change [Core Writing Team, Pachauri, R.K and Reisinger, A. (eds.)]. IPCC, Geneva, Switzerland, 104 pp. Retrieved from https://www.ipcc.ch/report/ar4/syr/

261. IPCC (2007). Climate Change 2007: Synthesis Report. Contribution of Working Groups I, II and III to the Fourth Assessment Report of the Intergovernmental Panel on Climate Change [Core Writing Team, Pachauri, R.K and Reisinger, A. (eds.)]. IPCC, Geneva, Switzerland, 104 pp. Retrieved from https://www.ipcc.ch/report/ar4/syr/

262. IPCC (2013) *Climate Change 2013: The Physical Science Basis. Contribution of Working Group I to the Fifth Assessment Report of the Intergovernmental Panel on Climate Change* [Stocker, T.F., D. Qin, G.-K. Plattner, M. Tignor, S.K. Allen, J. Boschung, A. Nauels, Y. Xia, V. Bex and P.M. Midgley (eds.)]. Cambridge University Press, Cambridge, United Kingdom and New York, NY, USA, 1535 pp. Retrieved from https://www.ipcc.ch/report/ar5/wg1/

263. IPCC, 2007: Climate Change 2007: The Physical Science Basis. Contribution of Working Group I to the Fourth Assessment Report of the Intergovernmental Panel on Climate Change [Solomon, S., D. Qin, M. Manning, Z. Chen, M. Marquis, K.B. Averyt, M.Tignor and H.L. Miller (eds.)]. Cambridge University Press, Cambridge, United Kingdom and New York, NY, USA. Accessed from https://www.ipcc.ch/report/ar4/wg1/

264. IPCC, 2007: Climate Change 2007: The Physical Science Basis. Contribution of Working Group I to the Fourth Assessment Report of the Intergovernmental Panel on Climate Change [Solomon, S., D. Qin, M. Manning, Z. Chen, M. Marquis, K.B. Averyt, M.Tignor and H.L. Miller (eds.)]. Cambridge University Press, Cambridge, United Kingdom and New York, NY, USA. Retrieved from https://www.ipcc.ch/report/ar4/wg1/

265. IPCC, 2014: *Climate Change 2014: Synthesis Report. Contribution of Working Groups I, II and III to the Fifth Assessment Report of the Intergovernmental Panel on Climate Change* [Core Writing Team, R.K. Pachauri and L.A. Meyer (eds.)]. IPCC, Geneva, Switzerland, 151 pp. Accessed from https://www.ipcc.ch/report/ar5/syr/

266. IPCC, 2014: *Climate Change 2014: Synthesis Report. Contribution of Working Groups I, II and III to the Fifth Assessment Report of the Intergovernmental Panel on Climate Change* [Core Writing Team, R.K. Pachauri and L.A. Meyer (eds.)]. IPCC, Geneva, Switzerland, 151 pp. https://www.ipcc.ch/report/ar5/syr/

267. IPCC, 2022: Summary for Policymakers [H.-O. Pörtner, D.C. Roberts, E.S. Poloczanska, K. Mintenbeck, M. Tignor, A. Alegría, M. Craig, S. Langsdorf, S. Löschke, V. Möller, A. Okem (eds.)]. In: Climate Change 2022: Impacts, Adaptation, and Vulnerability. Contribution of Working Group II to the Sixth Assessment Report of the Intergovernmental Panel on Climate Change [H.-O. Pörtner, D.C. Roberts, M. Tignor, E.S. Poloczanska, K. Mintenbeck, A. Alegría, M. Craig, S. Langsdorf, S. Löschke, V. Möller,

A. Okem, B. Rama (eds.)]. Cambridge University Press, Cambridge, UK and New York, NY, USA, pp. 3-33, doi:10.1017/9781009325844.001.

268. IPCC: Intergovernmental Panel on Climate Change (2014), Graphics, https://www.ipcc.ch/report/ar5/wg1/summary-for-policymakers/ (retrieved on 2019-10-28)

269. IPCC. (2013). Climate change 2013: The physical science basis. Working Group, I contribution to the IPCC Fifth Assessment Report. Cambridge, United Kingdom: Cambridge University Press. www.ipcc.ch/report/ar5/wg1.https://www.epa.gov/climate-indicators/climate-change-indicators-climate-forcing

270. Islam, M. A., Mitra, D., Dewan, A., & Akhter, S. H. (2016). Coastal multi-hazard vulnerability assessment along the Ganges deltaic coast of Bangladesh–A geospatial approach. Ocean & Coastal Management, 127, 1-15. DOI:10.1016/j.ocecoaman.2016.03.012

271. *Jackson, Julia A.; James P. Mehl; Klaus K. E. Neuendorf (2005). Glossary of geology (5, illustrated ed.). American Geological Institute, Springer Science & Business. p. 134. Accessed from https://www.americangeosciences.org/sites/default/files/pressreleases/Glossary5th_final.pdf*

272. Jackson, N. L., & Nordstrom, K. F. (2011). Aeolian sediment transport and landforms in managed coastal systems: a review. *Aeolian research*, *3*(2), 181-196. DOI: https://doi.org/10.1016/j.aeolia.2011.03.011

273. Jain, S. (2014). Weathering and Mass Wasting. In: Fundamentals of Physical Geology. Springer Geology. Springer, New Delhi. https://doi.org/10.1007/978-81-322-1539-4_7

274. Jain, S.K., Kumar, V., Saharia, M., 2013. Analysis of rainfall and temperature trends in northeast India. Int. J. Climatol. 33 (4), 968–978. DOI: https://doi.org/10.1002/joc.3483.

275. Jambeck, J.R., Geyer, R., Wilcox, C., Siegler, T.R., Perryman, M., Andrady, A., Narayan, R., Law, K.L., 2015. Plastic waste inputs from land into the ocean. Science, 347, 768-771. https://doi.org/10.1126/science.1260352.

276. James, K., Vasant, K., Batcha S.M., Padua, S., Jeyabaskaran, R., Thirumalaiselvan, S., Vineetha G., Benjamin. L, V. Seasonal variability in the distribution of microplastics in the coastal ecosystems and in some commercially important fishes of the Gulf of Mannar and Palk Bay, Southeast coast of India, Regional Studies in Marine Science, Volume 41, 2021, 101558, ISSN 2352-4855, https://doi.org/10.1016/j.rsma.2020.101558

277. James, L.A. (2013). Impacts of early agriculture and deforestation on geomorphic systems. In: Shroder, J. (Editor in Chief), James, L.A., Harden, C.P., Clague, J.J. (Eds.), Treatise on Geomorphology. Academic Press, San Diego, CA, vol. 13, Geomorphology of

Human Disturbances, Climate Change, and Natural Hazards. DOI:10.1016/B978-0-12-374739-6.00342-0

278. Jamir, T., & Krishna Kumar, G. (2015). Assessment of climatic extremes over Northeast and West Coast regions of India. Geoadria, 20(1), 1-11. DOI: DOI:10.15291/geoadria.13

279. Jana, A. & Bhattacharya, A. K. (2013). Assessment Of Coastal Erosion Vulnerability Around Midnapur-Balasore Coast, Eastern India Using Integrated Remote Sensing And Gis Techniques. Journal Of The Indian Society Of Remote Sensing, 41, 675-686. DOI:10.1007/s12524-012-0251-2

280. Jana, A., Bhattacharya, A.K. Assessment of coastal erosion vulnerability around Midnapur-Balasore Coast, Eastern India using integrated remote sensing and GIS techniques. J. Indian Soc. Remote Sens. 2013, 41, 675–686. DOI: 10.1007/s12524-012-0251-2

281. Jaswal, A. K. (2010). Changes in total cloud cover over India based upon 1961-2007 surface observations. Mausam, 61(4), 455-468. DOI: https://doi.org/10.54302/mausam.v61i4.882

282. Jayasiri, H.B., Purushothaman, C.S., Vennila, A., 2013. Plastic litter accumulation on high-water strandline of urban beaches in Mumbai, India. Environ. Monit. Assess. 185, 7709-7719. https://doi.org/10.1007/s10661-013-3129-z.

283. Jayasiri, H.B., Purushothaman, C.S., Vennila, A., 2013. Quantitative analysis of plastic debris on recreational beaches in Mumbai, India. Mar. Pollut. Bull. 77, 107–112. https://doi.org/10.1016/j.marpolbul.2013.10.024

284. Jefferson, A. J., Wegmann, K. W., & Chin, A. (2013). Geomorphology of the Anthropocene: Understanding the surficial legacy of past and present human activities. Anthropocene, 2, 1-3. DOI: 10.1016/j.ancene.2013.10.005

285. Jefferson, M. (1934). The Problem of the Ecumene. The Case of Canada. *Geografiska Annaler*, *16*, 146–158. https://doi.org/10.2307/520101

286. Jelil, S.N., Jain, N., 2014. A rapid assessment of beach litter in Mumbai beaches. Technical Report: Reef Watch Marine Conservation, 25. https://doi.org/10.13140/RG.2.1.4760.3449.

287. Jenerette, G. D., & Wu, J. (2001). Analysis And simulation of land-use change in the Central Arizona: Phoenix region, USA. Landscape Ecology, 16(7), 611–626. DOI: https://doi.org/10.1023/A:1013170528551

288. Jeyasanta, K. I., Sathish, N., Patterson, J., Edward, J. K. P., 2020. Macro-, meso- and microplastic debris in the beaches of Tuticorin district, Southeast coast of India. Mar. Pollut. Bull. 154, 111055. https://doi.org/10.1016/j.marpolbul.2020.111055.

289. Jianya, G., Haigang, S., Guorui, M. and Qiming, Z. (2008). A review of multi-temporal remote sensing data change detection algorithms. The International Archives of the Photogrammetry, Remote Sensing and Spatial Information Sciences, 37(B7), pp.757-762.

290. Jianya, G., Haigang, S., Guorui, M. and Qiming, Z., 2008. A review of multi-temporal remote sensing data change detection algorithms. The International Archives of the Photogrammetry, Remote Sensing and Spatial Information Sciences, 37(B7), pp.757-762. Retrieved from https://www.scirp.org/reference/referencespapers?referenceid=837627

291. Jindal, P., Thapliyal, P. K., Shukla, M. V., Sharma, S. K., & Mitra, D. (2019). Satellite based trend analysis of few atmospheric parameters over the Indian region. Advances in Space Research, 64(11), 2245-2268. DOI: 10.1016/j.asr.2019.09.008

292. Jones, B. (2017). Natural disasters: Cities build their vulnerability. *Nature Climate Change*, *7*(4), 237–238. DOI: https://doi.org/10.1038/nclimate3261

293. Jones, P., D. and Moberg, A. (2003) Hemispheric and large-scale surface air temperature variations: An extensive revision and an update to 2001; J. Climate 16(2) 206–223. DOI: https://doi.org/10.1175/1520-0442(2003)016<0206:HALSSA>2.0.CO;2

294. Joshi, R.R., Warthe, M., Dwivedi, S., Vijay, R., Chakrabarti, T., (2011). Monitoring changes in land use land cover of Yamuna riverbed in Delhi: a multitemporal analysis. Int. J. Remote Sens. 32 (24), 9547–9558. DOI: https://doi.org/10.1080/01431161.2011.565377

295. Kabanda, T. (2018). Long-term rainfall trends over the Tanzania coast. Atmosphere, 9(4), 155. DOI: https://doi.org/10.3390/atmos9040155

296. Kabir, R., Ritchie, E. A., and Stark, C. (2022). Tropical Cyclone Exposure in the North Indian Ocean", Atmosphere, vol. 13, no. 9, p. 1421. 2022. DOI: 10.3390/atmos13091421.

297. Kaladharan, P., Singh, V. V., Asha, P. S., Loveson E., Sukhadane, K. S., 2020. Marine plastic litter in certain trawl grounds along the peninsular coasts of India. Mar. Pollut. Bull. 157, 111299. https://doi.org/10.1016/j.marpolbul.2020.111299.

298. Kaladharan, P., Vijayakumaran, K., Singh, V.V., Prema, D., Asha, P.S., Sulochanan, B., Hemasankari, P., Edward, L., Padua, S., Veena, S., Anasu Koya, A., 2017. Prevalence of marine litter along the Indian beaches: A preliminary account on its status and composition. J. Mar. Biol. Assoc. India 59, 19-24. https://doi.org/10.6024/jmbai.2017.59.1.1953-03.

299. Kaladharan, P., Vijayakumaran, K., Singh, V.V., Prema, D., Asha, P.S., Sulochanan, B., Hemasankari, P., Edward, L., Padua, S., Veena, S., Anasu Koya, A., 2017. Prevalence of marine litter along the Indian beaches: A preliminary account on its status and composition. J. Mar. Biol. Assoc. India 59, 19-24. https://doi.org/10.6024/jmbai.2017.59.1.1953-03.

300. Kalensky, Z.D., Latham, J.S., Van, R., Claasen, D. (2003). Land cover mapping at global and regional levels. J. Cartograp. Geoinform. 5 (1), 3–54.

301. Kaliraj, S. N., Chandrasekar, K. K., Ramachandran, Srinivas, Y., & Saravanan, S. (2017). Coastal land use and land cover change and transformations of Kanyakumari coast,

India using remote sensing and GIS. The Egypthian Journal of Remote Sensing and Space Science. DOI:10.1016/j.ejrs.2017.04.003

302. Kaliraj, S., Chandrasekar, N. (2012). Spectral recognition techniques and MLC of IRS P6 LISS III image for coastal landforms extraction along South West Coast of Tamilnadu, India. Bonfring Int. J. Adv. Image Process. 2 (3), 01–07. DOI: DOI:10.9756/BIJAIP.10028

303. Kaliraj, S., Chandrasekar, N., Ramachandran, K. K., Srinivas, Y., & Saravanan, S. (2017). Coastal landuse and land cover change and transformations of Kanyakumari coast, India using remote sensing and GIS. The Egyptian Journal of Remote Sensing and Space Science, 20(2), 169-185. DOI: https://doi.org/10.1016/j.ejrs.2017.04.003

304. Kaliraj, S., Chandrasekar, N., Simon Peter, T., Selvakumar, S., Magesh, N.S. (2014). Mapping of Coastal Aquifer Vulnerable Zone in the South West Coast of Kanyakumari, South India, Using GIS-Based DRASTIC Model. Monit. Assess, Environ. DOI: 10.1007/s10661-014-4073-2

305. Kalsi S.R., Gupta M. (2003) Success and Failure of Early Warning Systems: A Case Study of the Gujarat Cyclone of June, 1998. In: Zschau J., Küppers A. (eds) Early Warning Systems for Natural Disaster Reduction (pp.199-202). Springer, Berlin, Heidelberg. DOI:10.1007/978-3-642-55903-7_26

306. Kamat, M. (November 1, 2018). Goa's growing urbanisation. Economania, Business Goa. Retrieved on November 17, 2022 from http://businessgoa.in/goas-growing-urbanisation/

307. Kamat, N. (2003). *Preparing for the pending water crisis* [Online]. http://www.goacom.com/news/news2003/mar/ msg000021.html

308. KAMEI, Yasuo & MIYAZAKI, Tomio & YAMAOKA, Hideyuki. (1993). Scrapmelting Using a Shaft Type Furnace with Coke Packed Bed Injected with Highly Oxygen Enriched Air and a Large Quantity of Pulverized Coal. Tetsu-to-Hagane. 79. 139-146. 10.2355/tetsutohagane1955.79.2_139. Singh G, Perwez A. Depreciation in Ambient Air Quality in Iron Ore Mining Region of Goa. Curr World Environ 2015;10(1) DOI: http://dx.doi.org/10.12944/CWE.10.1.17

309. Kan, H., London, S.J., Chen, H., Song, G., Chen, G., Jiang, L., et al., 2007. Diurnal temperature range and daily mortality in Shanghai, China. Environ. Res. 103 (3), 424–431. DOI: https://doi.org/10.1016/j.envres.2006.11.009.

310. Kanakara, R.; Subramanian, B. Oil spill sensitivity analysis and risk assessment for Gulf of Kachchh, India, using integrated modeling. J. Coast. Res. 2007, 14, 1251–1258. DOI:10.2112/04-0362.1

311. Kannan, R., & Kanungo, A., & Ramanamurthy, M.V., (2016). Shoreline Change Monitoring in Nellore Coast at East Coast Andhra Pradesh District using Remote Sensing and GIS. IJIRST –International Journal for Innovative Research in Science & Technology, Volume 2, Issue 10, March 2016.

312. Kantamaneni, K. (2016). Coastal infrastructure vulnerability: an integrated assessment model. Nat Hazards 84, 139–154. https://doi.org/10.1007/s11069-016-2413-y

313. Kantamaneni, Komali & N N V, Sudha & Rice, Louis & sur, Koyel & Thayaparan, Menaha & Kulatunga, Udayangani & Rege, Rajshree & Yenneti, Komalirani & Campos, Luiza. (2019). A Systematic Review of Coastal Vulnerability Assessment Studies along Andhra Pradesh, India: A Critical Evaluation of Data Gathering, Risk Levels and Mitigation Strategies. Water. DOI: 11. 1-25. 10.3390/w11020393.

314. Karancsi Z (2000) A kobányászat során kialakult felszínformák tipizálása (Classification of″ Landforms Resultant from Quarrying). In: A táj és az ember – geográfus szemmel (Geográfus doktoranduszok IV. országos konferenciája, 22nd–23rd October 1999). Szeged. http://phd.ini.hu

315. Karim, M. F., & Mimura, N. (2008). Impacts of climate change and sea-level rise on cyclonic storm surge floods in Bangladesh. *Global environmental change*, *18*(3), 490-500. DOI:10.1016/j.gloenvcha.2008.05.002

316. Karl, T. R., & Trenberth, K. E. (2003). Modern global climate change. science, 302(5651), 1719-1723. DOI: 10.1126/science.1090228

317. Karl, T. R., Nicholls, N., & Gregory, J. (1997). The coming climate. *Scientific American*, *276*(5), 78-83. Retrieved from https://research.monash.edu/en/publications/the-coming-climate

318. Karl, T., Knight, R., Gallo, K., Peterson, T., Jones, P., Kukla, G., Plummer, N., Razuvayev, V., Lindseay, J., and Charson, R. (1993). A new perspective on recent global warming: asymmetric trends of daily maximum and minimum temperature, B. Am. Meteorol. Soc., 74, 1007–1023. DOI: https://doi.org/10.1175/1520-0477(1993)074<1007:ANPORG>2.0.CO;2

319. Karthik, R., Robin, R.S., Ramakrishna, A., Ramesh, R., 2018. Microplastics along the beaches of southeast coast of India. Sci. Total Environ. 645, 1388–1399. https://doi.org/10.1016/j.scitotenv.2018.07.242

320. Karuppusamy, B., Leo George, S., Anusuya, K., Venkatesh, R., Thilagaraj, P., Gnanappazham, L., ... & Balabaskaran Nina, P. (2021). Revealing the socio-economic vulnerability and multi-hazard risks at micro-administrative units in the coastal plains of Tamil Nadu, India. Geomatics, Natural Hazards and Risk, 12(1), 605-630. DOI: https://doi.org/10.1080/19475705.2021.1886183

321. Kaviarasan, T., Naik, S., Sivadas, S. K., Dhineka, K., Sambandam, M., Sivyer, D., Mishra, P., Ramanamurthy, M. V., 2020. Assessment of litter in the remote beaches of Lakshadweep Islands, Arabian Sea. Mar. Pollut. Bull. 161, 111760. https://doi.org/10.1016/j.marpolbul.2020.111760.

322. Keelary, S. (2022). Foreign and domestic tourist arrivals across Goa in India between 2012 and 2021. Travel, Tourism & Hospitality, Statista. Retrieved on April 15, 2023 from https://www.statista.com/statistics/1027205/india-tourist-arrivals-in-goa-by-type/

323. Keelery, S., (2022). Tourist arrivals to Goa India 2012-2021, by type. Statistica, Travel, Tourism & Hospitality, Statista. Retrieved on January 2, 2023 from https://www.statista.com/statistics/1027205/india-tourist-arrivals-in-goa-by-type/
324. Kekeh, M., Akpinar-Elci, M., & Allen, M. J. (2020). Sea level rise and coastal communities. Extreme weather events and human health: International case studies, 171-184. DOI:10.1007/978-3-030-23773-8_12
325. Kendall, M. G,(1948). Rank Correlation Methods. **Open Journal of Statistics**, 4th Edition,Vol.3 No.5 Griffin, London. https://www.scirp.org/(S(351jmbntvnsjt1aadkposzje))/reference/ReferencesPapers.aspx?ReferenceID=957397
326. Khan, A. S., Ramachandran, A., Usha, N., Punitha, P., Selvam, V. (2012). Predicted impact of sea-level rise at Vellar-Coleroon estuarine region of Tamil Nadu Coast, in India: Mainstreaming adaptation as a coastal zone management option. Ocean and Coastal Management; 69:327-339. DOI: 10.1016/j.ocecoaman.2012.08.005
327. Khan, H., Vasilescu, L. G., & Khan, A. (2008). Disaster management cycle-a theoretical approach. *Journal of Management and Marketing*, *6*(1), 43-50. Retrieved from https://EconPapers.repec.org/RePEc:aio:manmar:v:6:y:2008:i:1:p:43-50
328. Khan, M. J. U., Durand, F., Testut, L., Krien, Y., & Islam, A. S. (2020). Sea level rise inducing tidal modulation along the coasts of Bengal delta. Continental Shelf Research, 211, 104289. Retrieved from https://hal.science/hal-03128984v1/file/S0278434320302442.pdf
329. Khan, M. M. H., Bryceson, I., Kolivras, K. N., Faruque, F., Rahman, M. M., & Haque, U. (2015). Natural disasters and land-use/land-cover change in the southwest coastal areas of Bangladesh. Regional environmental change, 15, 241-250. DOI:10.1007/s10113-014-0642-8
330. Khan, S., Yahong, W., & Zeeshan, A. (2022). Impact of poverty and income inequality on the ecological footprint in Asian developing economies: Assessment of Sustainable Development Goals, Energy Reports, Volume 8, P: 670-679, ISSN 2352-4847, https://doi.org/10.1016/j.egyr.2021.12.001.
331. Khojasteh, D., Glamore, W., Heimhuber, V., & Felder, S. (2021). Sea level rise impacts on estuarine dynamics: A review. Science of The Total Environment, 780, 146470. DOI: https://doi.org/10.1016/j.scitotenv.2021.146470
332. Kiefer, R.W., Lillesand, T.M. and Chipman, J.W. (1994). Remote sensing and image interpretation (p. 499). New York: Wiley & Sons. Retrieved from https://www.geokniga.org/bookfiles/geokniga-remote-sensing-and-image-interpretation.pdf
333. Kiefer, R.W., Lillesand, T.M. and Chipman, J.W., 1994. Remote sensing and image interpretation (p. 499). New York: Wiley & Sons. https://www.scirp.org/(S(i43dyn45teexjx455qlt3d2q))/reference/ReferencesPapers.aspx?ReferenceID=2031386

334. Kim K-H, Kabir E, Kabir S (2015) A review on the human health impact of airborne particulate matter. Environ Int 74:136–143. DOI: https://doi.org/10.1016/j.envint.2014.10.005
335. Kim, T. Y., & Cho, K. W. (2013). Forecasting of sea-level rise using a semi-empirical method. Journal of the Korean Society of Marine Environment & Safety, 19(1), 1-8. DOI:10.7837/KOSOMES.2013.19.1.001
336. Kisi, O., and Ay, M. (2014) Comparison of Mann–Kendall and innovative trend method for water quality parameters of the Kizilirmak River, Turkey. *Journal of Hydrology*, 513(NA): 362-375. doi:10.1016/j.jhydrol.2014.03.005.
337. Kjellstrom, T., & McMichael, A. J. (2013). Climate change threats to population health and well-being: the imperative of protective solutions that will last. *Global health action*, *6*(1), 20816. DOI: 10.3402/gha.v6i0.20816
338. Kotha, M. (2013). Land-cover change in Goa– An Integrated RS – GIS Approach. International Journal of Geoinformatics. 9. Retrieved from http://drs.nio.org/drs/handle/2264/4436
339. Kothawale, D. R., and K. Rupa Kumar (2005), On the recent changes in surface temperature trends over India, Geophys. Res. Lett., 32, L18714. DOI:10.1029/2005GL023528.
340. Kotsoni, A., Dimelli, D., & Ragia, L. (2017, April). Land use planning for sustainable development of coastal regions. In International Conference on Geographical Information Systems Theory, Applications and Management (Vol. 2, pp. 290-294). SciTePress. DOI: 10.5220/0006370802900294
341. Kotu, & Deshpande. (2019, January 11). Classification. In *Classification - ScienceDirect* (pp. 65–163). Morgan Kaufmann. https://doi.org/10.1016/B978-0-12-814761-0.00004-6
342. Krelling, A. P., Williams, A. T., & Turra, A. (2017). Differences in perception and reaction of tourist groups to beach marine debris that can influence a loss of tourism revenue in coastal areas. Marine Policy, 85, 87-99. DOI: https://doi.org/10.1016/j.marpol.2017.08.021
343. Krishnakumar, S., Anbalagan, S., Kasilingam, P., Smrithi, P., Anbazhagi, S., Srinivasalu, S., 2020. Assessment of plastic debris in remote islands of Andaman and Nicobar Archipelago, India. Mar. Pollut. Bull. 151, 110841. https://doi.org/10.1016/j.marpolbul.2019.110841.
344. Krishnamurthy, R. R., DasGupta, R., Chatterjee, R., & Shaw, R. (2014). Managing the Indian coast in the face of disasters & climate change: a review and analysis of India's coastal zone management policies. Journal of Coastal Conservation, 18(6), 657–672. Retrieved from http://www.jstor.org/stable/24760673
345. Kulimushi, L.C., Bashagaluke, J.B., Prasad, P., Heri-Kazi, A.B., Kushwaha, N.L., Masroor, M., Choudhari, P., Elbeltagi, A., Sajjad, H. and Mohammed, S., 2023. Soil erosion

susceptibility mapping using ensemble machine learning models: A case study of upper Congo river sub-basin. *Catena*, *222*, p.106858. https://doi.org/10.1016/j.catena.2022.106858
346.

347. Kumar, A. (2014). Delhi Disaster Management Plan, Vol-1. Delhi Disaster Management Authority (Ddma), Revenue Department, Government Of Nct Of Delhi. Retrieved From Http://Ddma.Delhigovt.Nic.In/Wps/Wcm/Connect/8d935d004829d5ec8becebae1ccb7dea/Delhi+Draft+State+Plan+09042015+Part+I.Pdf?Mod=Ajperes&Lmod=-1591939727
348. Kumar, A. A. & Kunte, P. D. (2012). Coastal Vulnerability Assessment For Chennai, East Coast Of India Using Geospatial Techniques. Natural Hazards, 64, 853-872. DOI: 10.1007/s11069-012-0276-4
349. Kumar, A. A., Sivakumar, R., Reddy, Y. S. R., Raja, M. V. B., Nishanth, T., Revanth, V., (2016). Preliminary study on marine debris pollution along Marina beach, Chennai, India. Reg. Stud. Mar. Sci. 5, 35-40. http://dx.doi.org/10.1016/j.rsma.2016.01.002.
350. Kumar, A., & Jayappa, K., S. (2008). Long and Short-Term Shoreline Changes Along Mangalore Coast, India. Int. J. Environ. Res., 3(2):177-188. Retrieved from https://api.semanticscholar.org/CorpusID:97207070.
351. Kumar, A.A., Kunte, P.D., (2012). Coastal vulnerability assessment for Chennai, east coast of India using geospatial techniques. Natural Hazards 64, 853-872. DOI: 10.1007/s11069-012-0276-4
352. Kumar, C. P., Sowmya, K., & Jayappa, K. S. (2018). The probabilistic tsunami hazard assessment along Karnataka Coast from Makran Subduction Zone, west coast of India. Environmental monitoring and assessment, 190(11), 1-13. DOI: DOI: 10.1007/s10661-018-7048-x
353. Kumar, M. S., Kolluru, V., Gowthami, S. B., Anjita, N. A., Nayana, N., Regi, L., & Dwarakish, G. S. (2021). Monitoring land use and land cover changes in coastal karnataka. Trends in Civil Engineering and Challenges for Sustainability: Select Proceedings of CTCS 2019, 785-795. DOI:10.1007/978-981-15-6828-2_57
354. Kumar, P., & Sardana, D. (2021). Regional sea level changes in the Indian shelf sea and its association with SST anomalies. Regional Studies in Marine Science, 47, 101992. DOI: https://doi.org/10.1016/j.rsma.2021.101992
355. Kumar, R., Rani, S., & Maharana, P. (2021). Assessing the impacts of Amphan cyclone over West Bengal, India: a multi-sensor approach. Environmental monitoring and assessment, 193, 1-21. doi: 10.1007/s10661-021-09071-5.
356. Kumar, T. S., Mahendra, R. S., Nayak, S., Radhakrishnan, K., & Sahu, K. C. (2010). Coastal vulnerability assessment for Orissa State, east coast of India. Journal of Coastal research, 26(3), 523-534. DOI: https://doi.org/10.2112/09-1186.1

357. Kumar, T.S.; Mahendra, R.S.; Nayak, S.; Radhakrishnan, K., And Sahu, K.C. (2010). Coastal Vulnerability Assessment for Orissa State, East Coast of India. Journal of Coastal Research, 26(3), 523–534. West Palm Beach (Florida), ISSN 0749-0208. DOI: DOI:10.2307/40605480

358. Kunte, P. D., & Wagle, B. G. (2005). The Beach Ridges of India: A Review. *Journal of Coastal Research*, 174–183. Retrieved from http://www.jstor.org/stable/25736982

359. Kunte, P. D., Jauhari, N., Mehrotra, U., Kotha, M., Hursthouse, A. S. & Gagnon, A. S. (2014). Multi-hazards coastal vulnerability assessment of Goa, India, using geospatial techniques. Ocean & Coastal Management, 95, 264-281. DOI: DOI:10.1016/j.ocecoaman.2014.04.024

360. LaDochy, S., Medina, R., & Patzert, W. (2007). Recent California climate variability: spatial and temporal patterns in temperature trends. Climate research, 33(2), 159-169. DOI:10.3354/cr033159

361. Lakhraj-Govender, R., & Grab, S. W. (2019). Temperature trends for coastal and adjacent higher lying interior regions of KwaZulu-Natal, South Africa. Theoretical and Applied Climatology, 137(1-2), 373-381. DOI:10.1007/s00704-018-2602-6

362. Lakshmi, S. R., & Shaji, T. L. (2016). Transformation of coastal settlements due to tourism. Procedia Technology, 24, 1668-1680. DOI: https://doi.org/10.1016/j.protcy.2016.05.188

363. Lausch, A. and Herzog, F. (2002): Applicability of landscape metrics for the monitoring of landscape change issues of scale, resolution and interpretability. In: Ecological Indicators 2, 3-15. DOI: https://doi.org/10.1016/ S1470-160X(02)00053-5

364. Lazaridis, M., & Lazaridis, M. (2011). Human exposure and health risk from air pollutants. First principles of meteorology and air pollution, 305-354. ISBN: 978-94-007-0161-8. DOI:10.1007/978-94-007-0162-5

365. Leal Filho, W. (2018). Impacts of climate change in coastal areas: lessons learned and experiences. Climate Change Impacts and Adaptation Strategies for Coastal Communities, 471-478. DOI:10.1007/978-3-319-70703-7_25

366. Leuliette, E. W., & Nerem, R. S. (2016). Contributions of Greenland and Antarctica to Global and Regional Sea Level Change. *Oceanography*, *29*(4), 154–159. Retrieved from http://www.jstor.org/stable/24862290

367. Lewsey, C., Cid, G., & Kruse, E. (2004). Assessing climate change impacts on coastal infrastructure in the Eastern Caribbean. *Marine Policy*, *28*(5), 393-409. DOI:10.1016/j.marpol.2003.10.016

368. Li X, Rowley RJ, Kostelnick JC, Braaten D, Miesel J, Hulbutta K. (2009), GIS analysis of global impact from sea level rise. Photogrammetric Engineering and Remote Sensing. 75(7): 807-818. DOI:10.14358/PERS.75.7.807

369. Li, Y., Sun, X., Zhu, X., & Cao, H. (2010). An early warning method of landscape ecological security in rapid urbanizing coastal areas and its application in Xiamen,

China. Ecological Modelling, 221(19), 2251-2260. DOI: https://doi.org/10.1016/j.ecolmodel.2010.04.016
370. Li, Z., Wang, Y., Guo, J., Zhao, C., Cribb, M.C., Dong, X. (2019). East Asian study of tropospheric aerosols and their impact on regional clouds, precipitation, and climate (EAST-AIRCPC). J. Geophys. Res.: Atmosphere 124 (23), 13026–13054. DOI: https://doi.org/10.1029/2019JD030758.
371. Liang, L., & Gong, P. (2020). Urban and air pollution: a multi-city study of long-term effects of urban landscape patterns on air quality trends. Scientific reports, 10(1), 18618. DOI: https://doi.org/10.1038/s41598-020-74524-9
372. Lim, S.S., Vos, T., Flaxman, A.D., Danaei, G., Shibuya, K., Adair-Rohani, H., AlMazroa, M.A., Amann, M., Anderson, H.R., Andrews, K.G., *et al.* (2012). A comparative risk assessment of burden of disease and injury attributable to 67 risk factors and risk factor clusters in 21 regions, 1990–2010: A systematic analysis for the Global Burden of Disease Study 2010. *The Lancet* 380: 2224–2260. DOI: 10.1016/S0140-6736(12)61766-8.
373. Limaye, S., & Salvi, S. (2010) Ambient air pollution and the lungs: what do clinicians need to know? Breathe 2010 6: 234-244; DOI: 10.1183/18106838.0603.234
374. Lin, I. I., Goni, G. J., Knaff, J. A., Forbes, C., & Ali, M. M. (2013). Ocean heat content for tropical cyclone intensity forecasting and its impact on storm surge. Natural Hazards, 66, 1481-1500. DOI: 10.1007/s11069-012-0214-5
375. Linkov, I., & Trump, B. D. (2019). *The science and practice of resilience*. Cham: Springer International Publishing. DOI:10.1007/978-3-030-04565-4
376. Liu-Helmersson, J., Stenlund, H., Wilder-Smith, A., Rocklov, ¨ J. (2014). Vectorial capacity of Aedes aegypti: effects of temperature and implications for global dengue epidemic potential. PLoS One 9 (3), e89783. DOI: https://doi.org/10.1371/journal.pone.0089783.
377. Liu, L., Guo, J., Chen, W., Wu, R., Wang, L., Gong, H.2(018). Large-scale pattern of the diurnal temperature range changes over East Asia and Australia in Boreal winter: a perspective of atmospheric circulation. J. Clim. 31 (7), 2715–2728. DOI: https://doi.org/10.1175/jcli-d-17-0608.1.
378. Lizarazo, I., Angulo, V., Rodriguez, J., 2017. Automatic mapping of land surface elevation changes from UAV-based imagery. Int. J. Remote Sens. 38, 2603–2622. https://doi.org/10.1080/01431161.2016.1278313.
379. Lobell, D.B. (2007). Changes in diurnal temperature range and national cereal yields. Agric. For. Meteorol. 145 (3), 229–238. DOI: https://doi.org/10.1016/j.agrformet.2007.05.002.
380. Loczy, D. (2010). Anthropogenic Geomorphology in Environmental Management. (eds), Anthropogenic Geomorphology- A Guide to Man-Made Landforms. ISBN 978-90-481-3057-3. e-ISBN 978-90-481-3058-. 0. Springer Dordrecht Heidelberg London New York. DOI 10.1007/978-90-481-3058-0

381. Loczy, D. (2010). Human Impact in a system approach. (Eds.) Anthropogenic Geomorphology, A Guide to Man-Made Landforms, pp. 13-24. Springer, ISBN 978-90-481-3057-3. DOI: 10.1007/978-90-481-3058-0.
382. Loh, J. & Wackernagel, M. (2004) - *Living Planet Report 2004*. World Wilde Fund for Nature, Gland, Switzerland, 44 pp. Retrieved from https://wwflpr.awsassets.panda.org/downloads/lpr2004.pdf
383. Loki, J. (2010). Agriculture: Crop cultivation and Horticulture. (Eds.) Anthropogenic Geomorphology, A Guide to Man-Made Landforms, pp. 55-68. Springer, ISBN 978-90-481-3057-3. DOI: 10.1007/978-90-481-3058-0.
384. Longmore, S.N., Collins, R.P., Pfeifer, S., Fox, S.E., Mulero-Pazmany, M., Bezombes, F., Goodwin, A., De Juan Ovelar, M., Knapen, J.H., Wich, S.A., 2017. Adapting astronomical source detection software to help detect animals in thermal images obtained by unmanned aerial systems. Int. J. Remote Sens. 38, 2623–2638. https://doi.org/10.1080/01431161.2017.1280639.
385. Lopes, N. D. R., Li, T., Qian, D., Matomela, N., & Sá, R. M. (2022). Factors influencing coastal land cover change and corresponding impact on habitat quality in the North-western Coastline of Guinea-Bissau (NC-GB). *Ocean & Coastal Management*, *224*, 106181. DOI: 10.1016/j.ocecoaman.2022.106181
386. Louati A, Son LH, Chabchoub H (2018) Smart routing for municipal solid waste collection: a heuristic approach. J Ambient Intell Humaniz Comput 10:1865–1884. DOI: https://doi.org/10.1007/s12652- 018-0778-3
387. Lubis, J. P. G., & Nakagoshi, N. (2011). Land Use and Land Cover change detection using remote sensing and geographic information system in Bodri Watershed, Central Java, Indonesia. Journal of International Development and Cooperation, 18(1), 139-151. Retrieved from https://www.scirp.org/reference/referencespapers?referenceid=1881391
388. Lucas, Robert, E Jr. 2003. "Macroeconomic Priorities". *American Economic Review*, 93 (1): 1-14. DOI: 10.1257/000282803321455133
389. Ludeno, G., & Postacchini, M. (2021). A methodology based on the coupling of marine radar and numerical modeling for beach-inundation prediction (No. EGU21-10930). Copernicus Meetings. DOI: 10.5194/egusphere-egu21-10930
390. Luijendijk, A., Hagenaars, G., Ranasinghe, R., Baart, F., Donchyts, G. and Aarninkhof, S. 2018. The State of the World's Beaches. Scientific reports 8:6641 DOI:10.1038/s41598-018-24630-6
391. M., Mugilarasan., R., Karthik., R., Purvaja., R.S., Robin., B., Subbareddy., G., Hariharan., S., Rohan., T.P.S., Jinoj., I., Anandavelu., P., Pugalenthi., Ramachandran, Ramesh. (2021). Spatiotemporal variations in anthropogenic marine litter pollution along the northeast beaches of India.. Environmental Pollution, 280:116954-116954. doi: 10.1016/J.ENVPOL.2021.116954

392. Macarehanas, A. (1999). The coastal regulation zone of Goa: Oceanographic, environmental and societal perspectives. Current Science, vol.77(12), 1598 1605p. http://drs.nio.org/drs/handle/2264/497

393. Macintosh, A. (2013). Coastal climate hazards and urban planning: how planning responses can lead to maladaptation. Mitigation and Adaptation Strategies for Global Change, 18, 1035-1055. DOI: 10.1007/s11027-012-9406-2

394. Mackay, A., Battarbee, R., Birks, J., & Oldfield, F. (2003). Global change in the Holocene. Arnold, Hodder Headline Group. DOI: https://doi.org/10.4324/9780203785027

395. Magarotto, M., FARIA-DE-DEUS, R. A. Q. U. E. L., Costa, M. F., & Masanet, É. (2017). Green Areas in Coastal Cities–Conflict of Interests or Stakeholders ’Perspectives?. International Journal of Sustainable Development and Planning, 12(8), 1260-1271. DOI: 10.2495/SDP-V12-N8-1260-1271

396. Mahapatra, M., Ramakrishnan, R. & Rajawat, A. S. (2015). Coastal Vulnerability Assessment Using Analytical Hierarchical Process For South Gujarat Coast, India. Natural Hazards, 76, 139-159. DOI:10.1007/s11069-014-1491-y

397. Mahapatra, M., Ramakrishnan, R., & Rajawat, A. (2015). "Coastal vulnerability assessment using analytical hierarchical process for South Gujarat coast, India," Natural Hazards: Journal of the International Society for the Prevention and Mitigation of Natural Hazards, Springer; International Society for the Prevention and Mitigation of Natural Hazards, vol. 76(1), pages 139-159, March. DOI: 10.1007/s11069-014-1491-y

398. Mahapatra, M., Ramakrishnan, R., & Rajawat, A. (2016). Storm surge vulnerability assessment of Saurashtra coast, Gujarat, using GIS techniques. Natural Hazards. 86. 10.1007/s11069-016-2718-x.

399. Mahapatra, Manik & Ramakrishnan, Ratheesh & S. Rajawat, A. (2015). Coastal vulnerability assessment of Gujarat coast to sea level rise using GIS techniques: a preliminary study. Journal of Coastal Conservation. 19. 10.1007/s11852-015-0384-x.

400. Mahendra, R., Mohanty, P., Bisoyi, H., Kumar, T.S., Nayak, S. (2011). Assessment and management of coastal multi-hazard vulnerability along the Cuddalore–Villupuram, east coast of India using geospatial techniques. Ocean Coast. Manag, 54, 302–311. DOI:10.1016/j.ocecoaman.2010.12.008

401. Malik, S., Pal, S. C., Sattar, A., Singh, S. K., Das, B., Chakrabortty, R., & Mohammad, P. (2020). Trendof extreme rainfall events using suitable global circulation model to combat the water logging condition in Kolkata metropolitan Area. Urban Climate, 32, 100599. DOI: https://doi.org/10.1016/j.uclim.2020.100599

402. Maliva, R., & Maliva, R. (2021). Sea Level Rise and Groundwater. Climate Change and Groundwater: Planning and Adaptations for a Changing and Uncertain Future: WSP Methods in Water Resources Evaluation Series No. 6, 113-153.

403. Mann, H., B. (1945) NONPARAMETRIC TESTS AGAINST TREND. *Econometrica*, 13(3): 245-259. doi:10.2307/1907187.

404. Mangotra, K., Chandrashekhar, K., 2020. Are we at sea on marine plastic pollution? Financial Express, Opinion. Retrieved on March 6, 2021 from https://www.financialexpress.com/opinion/are-we-at-sea-on-marine-plastic-pollution/2125852/.

405. Mani Murali, R., Ankita, M., Amrita, S. & Vethamony, P. 2013. Coastal Vulnerability Assessment Of Puducherry Coast, India, Using The Analytical Hierarchical Process. Natural Hazards And Earth System Sciences, 13, 3291-3311. DOI:10.5194/nhessd-1-509-2013

406. Manickavasagam, S., Kumar, S., Kumar, K., Bhuvneshwari, G. R., Paul, T., and Shukla, S. P., 2020. Quantitative assessment of influx and efflux of marine debris in a water channel of South Juhu creek, Mumbai, India. Reg. Stud. Mar. Sci. 34, 101095. https://doi.org/10.1016/j.rsma.2020.101095.

407. Manickavasagam, S., Kumar, S., Kumar, K., Bhuvneshwari, G. R., Paul, T., and Shukla, S. P., 2020. Quantitative assessment of influx and efflux of marine debris in a water channel of South Juhu creek, Mumbai, India. Reg. Stud. Mar. Sci. 34, 101095. https://doi.org/10.1016/j.rsma.2020.101095.

408. Manickavasagam, S., Shukla, S. P., Kumar, S., Kumar, K., Bhuvneshwari, G. R., 2021. Assessment of marine microplastics in floating plastic debris using a fixed sampling device: the example of South Juhu creek, Mumbai coast, India. J. Coast. Conserv. 25: 20. https://doi.org/10.1007/s11852-021-00810-x.

409. Manickavasagam, S., Shukla, S. P., Kumar, S., Kumar, K., Bhuvneshwari, G. R., 2021. Assessment of marine microplastics in floating plastic debris using a fixed sampling device: the example of South Juhu creek, Mumbai coast, India. J. Coast. Conserv. 25: 20. https://doi.org/10.1007/s11852-021-00810-x.

410. Mansui J., Darmon G., Ballerini T., van Canneyt O., Ourmieres Y., Miaud C., Predicting marine litter accumulation patterns in the Mediterranean basin: Spatio-temporal variability and comparison with empirical data. Progress in Oceanography, 182, 2020, 102268, ISSN 0079-6611, https://doi.org/10.1016/j.pocean.2020.102268 .

411. Marope, P.T.M. Literacy: A foundation for achieving the Sustainable Development Goals. *Prospects* 47, 163–165 (2017). https://doi.org/10.1007/s11125-018-9436-y

412. Martin, C., Parkes, S., Zhang, Q., Zhang, X., McCabe, M.F., Duarte, C.M. (2018). Use of unmanned aerial vehicles for efficient beach litter monitoring. Mar. Pollut. Bull. 131, 662–673. https://doi.org/10.1016/j.marpolbul.2018.04.045.

413. MartInez-casasnovas, J. a. (2003): A spatial information technology approach for the mapping and quantification of gully erosion. In: Catena 50, 293–308. https://doi.org/10.1016/S0341-8162(02)00134-0

414. MartInez-casasnovas, J. a. (2003): A spatial information technology approach for the mapping and quantification of gully erosion. In: Catena 50, 293–308. https://doi.org/10.1016/S0341-8162(02)00134-0

415. Martyr-Koller, R., Thomas, A., Schleussner, C. F., Nauels, A., & Lissner, T. (2021). Loss and damage implications of sea-level rise on Small Island Developing States. Current Opinion in Environmental Sustainability, 50, 245-259. Retrieved from https://link.springer.com/book/10.1007/978-3-030-66813-6
416. Mascareanhas, A. (2002). Tourism and Coastal Zone. The Goa Foundation; Mapusa, Goa, India. http://drs.nio.org/drs/handle/2264/1417
417. Mascarenhas, A., 1999. Human interference along the coast of Goa, western India. In: Environmental Problems of Coastal Areas in India, V. K. Sharma (editor), Bookwell Publishers, New Delhi. https://drs.nio.res.in/drs/bitstream/handle/2264/1319/Proc_Workshop_ICMAM_Plan_Goa_1999_204.pdf?sequence=3
418. Mascarenhas, A., 2000, SOME OBSERVATIONS ON THE STATE OF THE COASTAL ENVIRONMENT OF GOA, WEST COAST OF INDIA. Retrieved from https://pdfs.semanticscholar.org/c64f/91da023c764adc48caddef46d41488f53aa2.pdf.
419. Masroor, H., Dongmei, C., Angela, C., Hui, W., David, S. (2013). Change detection from remotely sensed images: From pixel-based to object-based approaches, Journal of Photogrammetry and Remote Sensing, 80, 91–106. DOI: 10.1016/j.isprsjprs.2013.03.006
420. Massoud, S. A., and Wollenberg, B. F. (2005). Toward a smart grid: power delivery for the 21st century, in IEEE Power and Energy Magazine, vol. 3, no. 5, pp. 34-41, DOI: 10.1109/MPAE.2005.1507024.
421. Mathur D.K. (2018). Flood Vulnerability Analysis using Remote Sensing and GIS A Case Study of Olpad Taluka of Surat. Retrieved from http://hdl.handle.net/10603/219624
422. McCloskey, J., Nalbant, S. S., Steacy, S., Nostro, C., Scotti, O., and Baumont, D. (2003), Structural constraints on the spatial distribution of aftershocks, *Geophys. Res. Lett.*, 30, 1610, doi:10.1029/2003GL017225, 12.
423. Mcdonald, K. (2012). Air pollution in the urban atmosphere: Sources and consequences. In Metropolitan Sustainability (pp. 231-259). Woodhead Publishing. DOI: https://doi.org/10.1533/9780857096463.3.231
424. McEvoy, D. (2015). Coastal zones and urbanization. The Summary for Decision-Makers: Coastal Zones and Urbanization. IHDP. https://ugec.org/2015/06/29/summary-for-decision-makers-coastal-zones-and-urbanization/
425. McLachlan, A., Defeo, O., Jaramillo, E., Short, A.D. (2013). Sandy beach conservation and recreation: guidelines for optimizing management strategies for multi-purpose use. Ocean Coast. Manag. 71, 256–268.
426. McMichael, A. J., Campbell-Lendrum, D. H., Corvalán, C. F., Ebi, K. L., Githeko, A. K., Scheraga, J. D., & Woodward, A. (2005). Climate change and human health: Risks and responses, Geneva (Switzerland): World health organization. The Quarterly Review of Biology, 80(2), 260–260. DOI: https://doi.org/10.1086/433125

427. Meadows, M. E. (2016). Geomorphology in the Anthropocene: Perspectives from the Past, Pointers for the Future? Geomorphology and Society, 7-22. DOI:10.1007/978-4-431-56000-5_2
428. Meadows, M. E., & Lin, J. C. (Eds.). (2016). Geomorphology and Society. Advances in Geographical and Environmental sciences. Berlin: Springer. DOI: 10.1007/978-4-431-56000-5
429. Meo, M. (1991). Sea level rise and policy change: Land use management in the Sacramento-San Joaquin and Mississippi River Deltas. Policy Studies Journal, 19(2), 83. DOI:10.1111/j.1541-0072.1991.tb01884.x
430. Merriam-Webster Collegiate Dictionary (10th ed). Coastline definition. Merriam-Webster Incorporated. Retrieved on April 6, 2021 from https://www.merriam-webster.com/dictionary/coastline
431. Michener, W. K., Blood, E. R., Bildstein, K. L., Brinson, M. M., & Gardner, L. R. (1997). Climate change, hurricanes and tropical storms, and rising sea level in coastal wetlands. *Ecological applications*, *7*(3), 770-801. DOI: 10.1890/1051-0761(1997)007[0770:CCHATS]2.0.CO;2
432. Migoń, P., & Latocha, A. (2018). Human impact and geomorphic change through time in the Sudetes, Central Europe. Quaternary International, 470, 194-206. DOI: https://doi.org/10.1016/j.quaint.2018.01.038
433. Mimura N. (2013). Sea-level rise caused by climate change and its implications for society. *Proceedings of the Japan Academy. Series B, Physical and biological sciences*, *89*(7), 281–301. DOI: https://doi.org/10.2183/pjab.89.281
434. Ministry of Earth Science (MoES), Government of India. (2014). Mapping and demarcating of multi-hazard coastal vulnerability for the states. Retrieved from: http://pib.nic.in/newsite/PrintRelease.aspx?relid=108606
435. Mishra. A & Balaji. R., (2015). A Study on the Shoreline Changes and LAND-use/ Land-cover along the South Gujarat Coastline. Procedia Engineering Volume 116, 2015, Pages 381-389. DOI:10.1016/j.proeng.2015.08.311
436. Misra, A., Murali, R.M., Vethamony, P. (2013). Assessment of the land use/land cover (LU/LC) and mangrove changes along the Mandovi-Zuari estuarine complex of Goa. India. Arab. J. Geosci. 8 (1), 267–279. DOI: DOI:10.1007/s12517-013-1220-y
437. Mitra, A. (1984). Rising population and environmental degradation. *Yojana, 1-15;28(18):4-8.* PMID: 12280104. Retrieved from https://pubmed.ncbi.nlm.nih.gov/12280104/
438. Mohammad, P., & Goswami, A. (2019). Temperature and precipitation trend over 139 major Indian cities: An assessment over a century. Modeling Earth Systems and Environment, 5(4), 1481–1493. DOI: https://doi.org/10.1007/s40808-019-00642-7
439. Mohammad, P., Goswami, A., & Bonafoni, S. (2019). The Impact of the land cover dynamics on surface urban heat Island variations in Semi-arid cities: A case study in

Ahmedabad City, India. Using MultiSensor/Source Data. Sensors, 19(17), 3701. DOI: https://doi.org/10.3390/s19173701

440. Mohan, S.G., & Jairaj, P.G., (2014). Coastal Vulnerability Assessment along Kerala Coast using Remote Sensing and GIS. International Journal of Scientific & Engineering Research, Volume 5, Issue 7. ISSN 2229-5518. Retrieved from https://www.ijser.org/researchpaper/Coastal-Vulnerability-Assessment-along-Kerala-Coast-using-Remote-Sensing-and-GIS.pdf

441. Monalisha M, Panda GK (2018) Coastal Erosion and Shoreline Change in Ganjam Coast along East Coast of India . J Earth Sci Clim Change 9: 467. doi: 10.4172/2157-7617.1000467

442. Mondal, M., Haldar, S., Biswas, A., Mandal, S., Bhattacharya, S., & Paul, S. (2021). Modeling cyclone-induced multi-hazard risk assessment using analytical hierarchical processing and GIS for coastal West Bengal, India. Regional Studies in Marine Science, 44, 101779. DOI: https://doi.org/10.1016/j.rsma.2021.101779

443. Monteiro, A. L., Sentelhas, P.C., Pedra, G., U. (2018). Assessment of NASA/POWER satellite-based weather system for Brazilian conditions and its impact on sugarcane yield simulation. *Int. J. Climatol*, *38*, 1571–1581. DOI: 10.1002/joc.5282

444. Moomaw, W. R., Chmura, G. L., Davies, G. T., Finlayson, C. M., Middleton, B. A., Natali, S. M., ... & Sutton-Grier, A. E. (2018). Wetlands in a changing climate: science, policy and management. *Wetlands*, *38*(2), 183-205. DOI: 10.1007/s13157-018-1023-8

445. Morales-Caselles, C., Viejo, J., Martí, E. (2021). An inshore–offshore sorting system revealed from global classification of ocean litter. Nat Sustain 4, 484–493. DOI: https://doi.org/10.1038/s41893-021-00720-8

446. Morner, N.-A., 2017. Coastal morphology and sea-level changes in Goa, India during the last 500 years. Journal of Coastal Research, 33(2), 421–434. Coconut Creek (Florida), ISSN 0749-0208. DOI:10.2112/JCOASTRES-D-16A-00015.1

447. Mugilarasan, M., Karthik, R, Purvaja, , Robin, R.S, Subbareddy, B., Hariharan, G., Rohan, S., Jinoj, T.P.S., Anandavelu, I., Pugalenthi, P., Ramesh, R. (2021). Spatiotemporal variations in anthropogenic marine litter pollution along the northeast beaches of India, Environmental Pollution, 280, 116954, ISSN 0269-7491. DOI: https://doi.org/10.1016/j.envpol.2021.116954.

448. Mujabar, P.S., Chandrasekar, N. (2013). Shoreline change analysis along the coast between Kanyakumari and Tuticorin of India using remote sensing and GIS. Arab. J. Geosci. 6, 647–664. DOI: DOI:10.1007/s12517-011-0394-4

449. Mujabar, P.S.; Chandrasekar, N. (2013). Coastal erosion hazard and vulnerability assessment for southern coastal Tamil Nadu of India by using remote sensing and GIS. Nat. Hazards, 69, 1295–1314. DOI: 10.1007/s11069-011-9962-x

450. Munthali, M. G., Botai, J. O., Davis, N., & Adeola, A. M. (2019). Multi-temporal analysis of land use and land cover change detection for dedza district of Malawi using geospatial techniques. Environmental Science. Retrieved

https://www.semanticscholar.org/paper/Multi-temporal-analysis-of-land-use-and-land-cover-Munthali-Botai/a8e0adba0a0e67a05da210a8a31021919729d282

451. Murakami, H., Vecchi, G.A. & Underwood, S. (2017). Increasing frequency of extremely severe cyclonic storms over the Arabian Sea. *Nature Clim Change* 7, 885–889. https://doi.org/10.1038/s41558-017-0008-6

452. Muthusamy, S., Arunkumar, R. X., Raj, N. T., Lakshumanan, C., & Jayaprakash, M. (2010). Land Use and Land Cover Changes Detection Using Multitemporal Satellite Data, Cuddalore Coastal Zone, Se-Coast of India. International Journal of Geomatics and Geosciences, 1(3), 610. https://www.semanticscholar.org/paper/Land-Use-and-Land-Cover-Changes-Detection-Using-of-Muthusamy-Arunkumar/7b0b88be8065287822e472f9b15fa950c509791f

453. Myhre, G., D. Shindell, F.-M. Bréon, W. Collins, J. Fuglestvedt, J. Huang, D. Koch, J.-F. Lamarque, D. Lee, B. Mendoza, T. Nakajima, A. Robock, G. Stephens, T. Takemura & H. Zhang. (2013). *Anthropogenic and natural radiative forcing*. In: Climate change 2013: The physical science basis. *Working Group I contribution to the fifth assessment report of the Intergovernmental Panel on Climate Change* [Stocker, T.F., D. Qin, G.-K. Plattner, M. Tignor, S.K. Allen, J. Boschung, A. Nauels, Y. Xia, V. Bex and P.M. Midgley (eds.)]. Cambridge University Press, Cambridge, United Kingdom, and New York, NY, p. 685. Retrieved from https://www.ipcc.ch/site/assets/uploads/2018/02/WG1AR5_Chapter08_FINAL.pdf

454. Nadeau, K. C., Agache, I., Jutel, M., Annesi Maesano, I., Akdis, M., Sampath, V., D'Amato, G., Cecchi, L., Traidl-Hoffmann, C., & Akdis, C. A. (2022). Climate change: A call to action for the United Nations. Allergy, 77(4), 1087–1090. https://doi.org/10.1111/all.15079

455. Nadeau, K. C., Agache, I., Jutel, M., Annesi Maesano, I., Akdis, M., Sampath, V., ... & Akdis, C. A. (2022). Climate change: A call to action for the united nations. Allergy, 77(4), 1087-1090. DOI: 10.1111/all.15079

456. Naik, S., Bhat, H, G., and Shreedhara, T, N. (2018). Impact of Land Use Land Cover Change on Coastal Tourism in Kundapura, Karnataka, Using Multi-Temporal Remotely Sensed Data and GIS Techniques. Atna Journal of Tourism Studies 2018, Vol. 13, No. 1, 1-17 ISSN 0975 328. DOI: https://doi.org/10.12727/ajts.19.1

457. NASA (2022). Global Climate Change: Vital Signs. Global Warming vs. Climate Change. Retrieved November 12, 2022 from https://climate.nasa.gov/global-warming-vs-climate
change/#:~:text=Global%20warming%20is%20the%20long,the%20term%20%22climate%20change.%22

458. Natesan U, Parthasarathy A. (2010). The Potential impact of sea level rise along the coastal zone of Kanyakumari District in Tamil Nadu, India. Journal of Coastal Conservator. 14(3): 207-214. DOI:10.1007/s11852-010-0103-6

459. National Disaster management authority (NDMA). Vulnerability profile of India. Retrieved from: https://ndma.gov.in/en/vulnerability-profile.html.

460. Naylor, L. A., Spencer, T., Lane, S. N., Darby, S. E., Magilligan, F. J., Macklin, M. G., & Möller, I. (2017). Stormy geomorphology: geomorphic contributions in an age of climate extremes. *Earth Surface Processes and Landforms*, *42*(1), 166-190. DOI: https://doi.org/10.1002/esp.4062

461. NCSCM. (2010). Coastal Issues and Concerns: Challenges for the Research Community. Ministry of Environment and Forests Government of India. Retrieved from:http://ncscm.res.in/cms/more/pdf/download/Coastal%20Issues%20and%20Concerns%20-%20Challenges%20for%20the%20Research%20Community.pdf.

462. Negm, A.; Jabro, J.; Provenzano, G. (2017). Assessing the suitability of American National Aeronautics and Space Administration (NASA) agro-climatology archive to predict daily meteorological variables and reference evapotranspiration in Sicily, Italy. *Agric. For. Meteorol*, *244–245*, 111–121. DOI: https://doi.org/10.1016/j.agrformet.2017.05.022

463. Neumann B, Vafeidis AT, Zimmermann J, Nicholls RJ (2015), Future Coastal Population Growth and Exposure to Sea-Level Rise and Coastal Flooding - A Global Assessment. PLOS ONE 10(3): e0118571. DOI: https://doi.org/10.1371/journal.pone.0118571

464. Neumann, B., Vafeidis, A.T., Zimmermann, J., Nicholls, R.J. (2015). Future coastal population growth and exposure to sea-level rise and coastal flooding-a global assessment. PloS one, 10, P.E 0118571. DOI: https://doi.org/10.1371/journal.pone.0118571.

465. Newton, A., Carruthers, T. J., & Icely, J. (2012). The coastal syndromes and hotspots on the coast. Estuarine, Coastal and Shelf Science, 96, 39-47. DOI: https://doi.org/10.1016/j.ecss.2011.07.012

466. Ngare, I. O., Koske, J. K., Muriuki, J. N., Chitechi, E. W., & Gathuku, G. N. (2020). Urban climate variability trend in the coastal region of Mombasa Kenya. African Journal of Environmental Science and Technology, 14(8), 214-221. DOI:10.5897/AJEST2020.2837

467. Ngondya, I. B., Ibrahim, R. I. H., & Choo, G. C. (2011). Are Poverty and Illiteracy to Blame for Forests Degradation? A Case Study of Mbeya Range Forest Reserve. Mbaya-Tanzania. Journal of Forest and Environmental Science, 23(2), 93-99. https://doi.org/10.7747/JFS.2011.27.2.4

468. Nicholls, R. J., & Cazenave, A. (2010). Sea-level rise and its impact on coastal zones. *Science*, *328*(5985), 1517–1520. DOI: https://doi.org/10.1126/science.1185782

469. Nicholls, R. J., Hoozemans, F. M. J. and Marchand, M. (1999) Increasing flood risk and wetland losses due to global sea-level rise: regional and global analyses, Global Environmental Change, 9, S69-S87. DOI: https://doi.org/10.1016/S0959-3780(99)00019-9

470. Nicholls, R. J., Wong, P. P., Burkett, V., Codignotto, J., Hay, J., McLean, R., Saito, Y. (2007). Coastal systems and low-lying areas. Retrieved from https://www.ipcc.ch/site/assets/uploads/2018/02/ar4-wg2-chapter6-1.pdf

471. Nicholls, R. J., Wong, P. P., Burkett, V., Woodroffe, C. D., & Hay, J. (2008). Climate change and coastal vulnerability assessment: scenarios for integrated assessment. Sustainability Science, 3, 89-102. DOI:10.1007/s11625-008-0050-4

472. Nicholls, R.J., Wong, P.P., Burkett, V.R., Codignotto, J.O., Hay, J.E., McLean, R.F., Ragoonaden, S., Woodroffe, C.D. (2007). Coastal systems and low-lying areas. Climate Change 2007: Impacts, Adaptation and Vulnerability. Contribution of Working Group II to the Fourth Assessment Report of the Intergovernmental Panel on Climate Change, M.L. Parry, O.F. Canziani, J.P. Palutikof, P.J. van der Linden and C.E. Hanson, Eds., Cambridge University Press, Cambridge, UK, 315-356. Retrieved from https://www.ipcc.ch/site/assets/uploads/2018/02/ar4-wg2-chapter6-1.pdf

473. Nigam, R., Luis, A. J., Gagnon, A. S., Vaz, E., Damásio, B., & Kotha, M. (2024). Assessing coastal vulnerability at the village level using a robust framework, the example of Canacona in South Goa, India. *ISCIENCE*, Article 109129. Advance online publication. https://doi.org/10.1016/j.isci.2024.109129

474. Nigam, R., Ghadamode, V., Luis, A, J., Prasad, P., Vaz, E., Damasio, B., Kotha, M. (2024). Decadal Land Use Land Cover Assessment of the Coastal Tracts of South Goa, India. School of Earth, Ocean and Atmospheric Sciences, Goa University (Under review)

475. Nigam, R., Luis, A. & Kotha, M. (2023) Evaluation of efficiency of the index of potential anthropic geomorphology at meso level: a case study of Goa State, India. The Geographical Journal, 00, 1–12. DOI: https://doi.org/10.1111/geoj.12540

476. Nigam, R., Luis, A. J., Prasad, P., Kuttikar, S., Yadav, R., Vaz, E., & Kotha, M. (2022). Spatio-temporal assessment of COVID-19 lockdown impact on beach litter status and composition in Goa, India. *Marine pollution bulletin*, *174*, 113293. DOI: https://doi.org/10.1016/j.marpolbul.2021.113293

477. Nigam, R., Luis, A., & Kotha, M. (2020). Significance of Local Coastal Geomorphology in Defining Coastal Vulnerability -A Village Level Study of Canacona, Goa. Eds. Applications of Geospatial technologies in Geomorphology and Environment (pp.161), University of North Bengal. *ISBN:978-81-925799-3-1*.

478. Nigam, R., Pandya, K., Luis, A.J. *et al.* (2021). Positive effects of COVID-19 lockdown on air quality of industrial cities (Ankleshwar and Vapi) of Western India. *Sci Rep* 11, 4285 (2021). DOI: https://doi.org/10.1038/s41598-021-83393-9

479. Nikesh Sharma. (2022). Climate Change and Incidences Of Tropical Cyclones In Coastal Areas Of India. *Central Asian Journal of Theoretical and Applied Science*, *3*(6), 98-109. Retrieved from https://cajotas.centralasianstudies.org/index.php/CAJOTAS/article/view/619

480. Nir, D. (1983). Man, a Geomorphological Agent. An Introduction to Anthropic Geomorphology. Reidel, Dordrecht-Boston-London, 165 pp. ISBN 90-1401-0. Retrieved

from
https://webapps.unitn.it/Biblioteca/it/Web/EngibankFile/Man,%20a%20geomorphological%20agent.pdf
481. Nir, D. (1983). Man, a Geomorphological Agent. An Introduction to Anthropic Geomorphology. Reidel, Dordrecht-Boston-London, 165 pp. ISBN 90-1401-0. Retrieved from
https://webapps.unitn.it/Biblioteca/it/Web/EngibankFile/Man,%20a%20geomorphological%20agent.pdf
482. Noelia Ríos, João P.G.L. Frias, Yasmina Rodríguez, Rita Carriço, Sofia M. Garcia, Manuela Juliano, Christopher K. P. (2018). Spatio-temporal variability of beached macro-litter on remote islands of the North Atlantic, Marine Pollution Bulletin, Volume 133, 2018 Pages 304-311, ISSN 0025-326X, https://doi.org/10.1016/j.marpolbul.2018.05.038.
483. North Goa. (2011). Census of India. Registrar General and Census Commissioner of India. Retrieved on May 12, 2020 from https://censusindia.gov.in/nada/index.php/catalog/368
484. NRSC (2014), Land Use / Land Cover database on 1:50,000 scale, Natural Resources Census Project, National Remote Sensing Centre, Department of Space, Hyderabad. Retrieved from https://bhuvan-app1.nrsc.gov.in/2dresources/thematic/LULC503/lulc.pdf
485. NRSC (2018). Land Degradation Database on 1:50,000 scale, Natural Resources Census Project, National Remote Sensing Centre, ISRO, Hyderabad. DOI: https://www.nrsc.gov.in/readmore_land_degradation?language_content_entity=en
486. Obi Reddy, G.P., & Kurothe, R.S., & Sena, D.R., & Harindranath, C.S., & Naidu, L.G.K., & Sarkar, D., & Sharda, V.N., (2013). Soil Erosion in Goa. NBSS Publ. 155. NBSS&LUP (ICAR), Nagpur, p 34. DOI: https://www.currentscience.ac.in/Volumes/115/01/0108.pdf
487. Oliver Wakefield (2018). Palolem Beach Travel Guide. All About India.com, Home, Travel, Travel articles. Retrieved on July 13, 2021 from https://www.all-about-india.com/Palolem.html
488. Oppenheimer, M., B.C. Glavovic , J. Hinkel, R. van de Wal, A.K. Magnan, A. Abd-Elgawad, R. Cai, M. Cifuentes-Jara, R.M. DeConto, T. Ghosh, J. Hay, F. Isla, B. Marzeion, B. Meyssignac, and Z. Sebesvari (2019). Sea Level Rise and Implications for Low-Lying Islands, Coasts and Communities. In: IPCC Special Report on the Ocean and Cryosphere in a Changing Climate [H.-O. Pörtner, D.C. Roberts, V. Masson-Delmotte, P. Zhai, M. Tignor, E. Poloczanska, K. Mintenbeck, A. Alegría, M. Nicolai, A. Okem, J. Petzold, B. Rama, N.M. Weyer (eds.)]. In press.
489. Oppenheimer, M., B.C. Glavovic, J. Hinkel, R. van de Wal, A.K. Magnan, A. Abd-Elgawad, R. Cai, M. Cifuentes-Jara, R.M. DeConto, T. Ghosh, J. Hay, F. Isla, B. Marzeion, B. Meyssignac, and Z. Sebesvari, 2019: Sea Level Rise and Implications for Low-Lying Islands, Coasts and Communities. In: IPCC Special Report on the Ocean and

Cryosphere in a Changing Climate [H.-O. Pörtner, D.C. Roberts, V. Masson-Delmotte, P. Zhai, M. Tignor, E. Poloczanska, K. Mintenbeck, A. Alegría, M. Nicolai, A. Okem, J. Petzold, B. Rama, N.M. Weyer (eds.)]. In press.

490. Ostling, J. L., Butler, D. R., & Dixon, R. W. (2009). The biogeomorphology of mangroves and their role in natural hazards mitigation. *Geography Compass*, *3*(5), 1607-1624. DOI:10.1111/j.1749-8198.2009.00265.x

491. Özyurt, G., & Ergin, A. (2012). Spatial and Time Balancing Act: Coastal Geomorphology in View of Integrated Coastal Zone Management (ICZM). In Studies on Environmental and Applied Geomorphology. IntechOpen. DOI: 10.5772/27340

492. Palmer, B. J., & van der Elst, R. (2012). Trends in coastal development and land cover change: The case of KwaZulu-Natal, South Africa. Western Indian Ocean Journal of Marine Science, 11(2), 193-204. Retrieved from https://www.ajol.info/index.php/wiojms/article/view/69534

493. Panandikar, A.P. (2016). Decoding Goa's vulnerabilities to climate change. The Goan. Retrieved from: https://www.teriin.org/opinion/decoding-goas-vulnerabilities-climate-change.

494. Parry, M., Arnell, N., and McMichael, T. (2001) Millions at risk: defining critical climate change threats and targets, Global Environmental Change, 11 (3), 181-183. doi:10.1016/S0959-3780(01)00011-5.

495. Parsons, A. J., & Abrahams, A. D. (2009). Geomorphology of desert environments. In *Geomorphology of desert environments* (pp. 3-7). Springer, Dordrecht. DOI: https://doi.org/10.1007/978-1-4020-5719-9_1

496. Parthasarathy, A. & Natesan, U. (2015). Coastal Vulnerability Assessment: A Case Study On Erosion And Coastal Change Along Tuticorin, Gulf Of Mannar. Natural Hazards, 75, 1713-1729. DOI:10.1007/s11069-014-1394-y

497. Patankar. A. & Patwardhan. A. & Andharia. J. & Lakhani.V. (2010). Mumbai City Report. International Workshop on Climate Change Vulnerability Assessment and Urban Development Planning for Asian Coastal Cities Bangkok, Thailand, August, 2010. Retrieved on May 17, 2022 from http://startcc.iwlearn.org/doc/Doc_eng16.pdf

498. Patel. V.M. & Dholakia. M.B. & Singh. A.P. (2013). Tsunami Risk 3D Visualizations of Okha Coast, Gujarat (India). International Journal of Engineering Science and Innovative Technology (IJESIT) Volume 2, Issue 2. Retrieved from https://www.researchgate.net/publication/292239377_Tsunami_risk_3D_visualizations_of_Okha_coast_Gujarat_India

499. Paul, S., & Das, C. S. (2021). Delineating the coastal vulnerability using Coastal Hazard Wheel: A study of West Bengal coast, India. Regional Studies in Marine Science, 44, 101794. DOI:

500. Pavri, F. (2010). Urban Expansion and Sea-Level Rise Related Flood Vulnerability for Mumbai (Bombay), India Using Remotely Sensed Data. 10.1007/978-90-481-2238-7_3.

501. Pednekar, G., & Siva Raju, S. (2020). Sea level rise and its socio-economic impacts: a case study in Mumbai, India. Extreme Weather Events and Human Health: International Case Studies, 155-169. DOI:10.1007/978-3-030-23773-8_11

502. Pelling, M., & Uitto, J. I. (2001). Small island developing states: natural disaster vulnerability and global change. *Global Environmental Change Part B: Environmental Hazards*, *3*(2), 49-62. DOI:10.1016/S1464-2867(01)00018-3

503. Perkins, S. (2022). How much of the Earth's ice is melting? New and old techniques combine to paint a sobering picture. *Proceedings of the National Academy of Sciences of the United States of America*, *119*(37), e2213762119. DOI: https://doi.org/10.1073/pnas.2213762119

504. Pervez, R., & Lai, Z. (2022). Spatio-temporal variations of litter on Qingdao tourist beaches in China. *Environmental pollution (Barking, Essex : 1987)*, *303*, 119060. https://doi.org/10.1016/j.envpol.2022.119060

505. Pervez, R., Wang, Y., Mahmood, Q., Zahir, M., & Jattak, Z. (2020). Abundance, type, and origin of litter on No. 1 Bathing Beach of Qingdao, China. Journal of Coastal Conservation, 24, 1-10. DOI:10.1007/s11852-020-00751-x

506. Pethick, J. S. and Crooks, S. (2000). Development of a coastal vulnerability index: a geomorphological perspective. Environmental Conservation 27, 359–367. DOI:10.1017/S0376892900000412

507. Phaldesai, P. R. (2001). *A Cultural History of the Canacona taluka of Goa*. Doctoral Thesis. Retrieved from https://irgu.unigoa.ac.in/drs/handle/unigoa/3898

508. Pikelj, Kristina & Juračić, Mladen. (2013). Eastern Adriatic Coast (EAC): Geomorphology and Coastal Vulnerability of a Karstic Coast. Journal of Coastal Research. 29. 944-957. DOI: 10.2307/23486562.

509. Pirkhoffer, E., Czigány, S., & Geresdi, I. (2009). Impact of rainfall pattern on the occurrence of flash floods in Hungary. Zeitschrift für Geomorphologie. Supplementband, 53(2), 139. DOI:10.1127/0372-8854/2009/0053S3-0139

510. Pirkhoffer, E., Czigány, S., & Geresdi, I. (2009). Impact of rainfall pattern on the occurrence of flash floods in Hungary. *Zeitschrift für Geomorphologie. Supplementband*, *53*(2), 139. DOI: 10.1127/0372-8854/2009/0053S3-0139

511. Planning Commission. (2012). Report of the steering committee on urbanisation (p. 232). New Delhi: Planning Commission, Government of India. Retrieved from http://planningcommission.gov.in/aboutus/committee/strgrp12/strrep_urban0401.pdf.

512. Poeta, G., Conti, L., Malavasi, M., Battisti, C., & Acosta, A. T. R. (2016). Beach litter occurrence in sandy littorals: The potential role of urban areas, rivers and beach users in central Italy. Estuarine, coastal and shelf science, 181, 231-237. DOI:

513. Poompavai, V., Ramalingam, M. (2013). Geospatial analysis for coastal risk assessment to cyclones. J. Indian Soc. Remote Sens. 41, 157–176. DOI10.1007/s12524-011-0198-8

514. Pradeep Kumar, A. and Thakur, N. K. (2007). Role of bathymetry in Tsunami devastation along the East coast of India. Current Science 92(4), 432-434. Retrieve from https://www.researchgate.net/publication/315668249_Role_of_bathymetry_in_tsunami_devastation_along_the_East_Coast_of_India
515. Prakash, S. (2021). Impact of Climate change on Aquatic Ecosystem and its Biodiversity: An overview. International Journal of Biological Innovations, 3(2). DOI:10.46505/ijbi.2021.3210
516. Pramanik MK, Biswas SS, Mukherjee T, Roy AK, Pal R. (2015) Sea Level Rise and Coastal Vulnerability along the Eastern Coast of India through Geo-spatial Technologies. J Geophys Remote Sensing 4:145. doi:10.4172/2469-4134.1000145
517. Pramova, E., Locatelli, B., Djoudi, H., Somorin, O.A. (2012). Forests and trees for social adaptation to climate variability and change Wiley Interdisciplinary Reviews: Climate Change, 3 (6) : 581–596. http://dx.doi.org/10.1002/wcc.195
518. Prasad, G., & Ramesh, M. V. (2019). Spatio-temporal analysis of land use/land cover changes in an ecologically fragile area—Alappuzha District, Southern Kerala, India. Natural Resources Research, 28, 31-42. DOI:10.1007/s11053-018-9419-y
519. Prasad, P., Loveson, V.J., Chandra, P. and Kotha, M. (2022). Evaluation and comparison of the earth observing sensors in land cover/land use studies using machine learning algorithms. Ecological Informatics, 68, p.101522. https://doi.org/10.1016/j.ecoinf.2021.101522
520. Prasad, P., Loveson, V.J., and Kotha, M. (2023a). Probabilistic wetland mapping with integration of optical, SAR and hydro-geomorphic data through stacking ensemble machine learning model. Ecological Informatics. https://doi.org/10.1016/j.ecoinf.2023.102273
521. Prasad, P., Loveson, V.J., Das, B., and Kotha, M 2021. Novel Ensemble Machine Learning Models in Flood Susceptibility Mapping. Geocarto International, 37:16, 4571-4593 https://doi.org/10.1080/10106049.2021.1892209
522. Prasad, P., Loveson, V.J., Kumar, V., Shukla, A.D., Chandra, P., Verma, S., Yadav, R., Magotra, R. and Tirodkar, G.M. (2023c). Reconstruction of Holocene relative sea-level from beach ridges of the central west coast of India using GPR and OSL dating. *Geomorphology* 442: 108914.
523. Prasad, P., Loveson, V.J., Mondal, S., and Chandra, P (2023b). Multi-resource potentiality and multi-hazard susceptibility assessments of the central west coast of India applying machine learning and geospatial techniques. Environmental Earth Sciences, 82, 226. https://doi.org/10.1007/s12665-023-10901-7

524. Prasad, Y. D. (2016). Statistical Handbook of Goa. Publication division, Directorate of Planning, Statistics and Evaluation, Government of Goa. Retrieved from http://goadpse.gov.in/Statistical%20Hand%20Book%20of%20Goa%202016-17.pdf.
525. Prasanna, S., K., Raj, P., R., Narvekar, J., Kumar, P., K., & Vivekanandan, E. (2009). Response of the Arabian Sea to global warming and associated regional climate shift, Marine Environmental Research, Volume 68, Issue 5, Pages 217-222, ISSN 0141-1136. DOI: https://doi.org/10.1016/j.marenvres.2009.06.010.

526. Praveen, D., & Ramchandran, A., & Palanivelu, K., (2018). Constructing Local Sea Level Rise Scenarios for Assessing Possible Impacts and Adaptation Needs: Insights. http://dx.doi.org/10.5772/intechopen.74325

527. Price, S. J.; Ford, J. R.; Cooper, A. H. And Neal, C. (2011): Humans as major geological and geomorphological agents in the Anthropocene: the significance of artificial ground in Great Britain. In: Philosophical Transactions of the Royal Society A 369, 1056–1084. https://doi.org/10.1098/rsta.2010.0296

528. Pye, k. and blott, s. J. (2014): The geomorphology of UK estuaries: the role of geological controls, antecedent conditions and human activities. In: Estuarine, Coastal and Shelf Science 150, 196-214. https://doi.org/10.1016/j.ecss.2014.05.014

529. Pye, k. and blott, s. J. (2014): The geomorphology of UK estuaries: the role of geological controls, antecedent conditions and human activities. In: Estuarine, Coastal and Shelf Science 150, 196-214. https://doi.org/10.1016/j.ecss.2014.05.014

530. Qiu, Haijun & Cui, Peng & Regmi, Amar & Hua, Sheng & Wang, Xiangang & Zhang, Yuzhu. (2018). The effects of slope length and slope gradient on the size distributions of loess slides: Field observations and simulations. Geomorphology. 300. 69-76. DOI: 10.1016/j.geomorph.2017.10.020.

531. Radhakrishnan, K., Sivaraman, I., Jena, S. K., Sarkar, S., & Adhikari, S. (2017). A climate trend analysis of temperature and rainfall in India. Climate Change and Environmental Sustainability, 5(2), 146-153. DOI:10.5958/2320-642X.2017.00014.X

532. Rahman, M. A., Hartmann, C., Moser-Reischl, A., von Strachwitz, M. F., Paeth, H., Pretzsch, H., ... & Rötzer, T. (2020). Tree cooling effects and human thermal comfort under contrasting species and sites. *Agricultural and Forest Meteorology*, *287*, 107947. DOI: 10.1016/j.agrformet.2020.107947

533. Rahmstorf S., (2007), A Semi-Empirical Approach to Projecting Future Sea-Level Rise, Vol. 315, Issue 5810, pp. 368-370. DOI: 10.1126/science.1135456,

534. Rai, A., Joshi, M.K., Pandey, A.C. (2012). Variations in diurnal temperature range over India: under global warming scenario. J. Geophys. Res.: Atmosphere 117 (D2). DOI: https://doi.org/10.1029/2011jd016697.

535. Ramakritinan, C. M., Ramkumar, B., Kumaraguru, A. M. (2015). Growth of sponges around nylon rope and E-waste in the coastal water of Veedhalai, Gulf of Mannar, India. Int. J. Curr. Microbiol. Appl. Sci. 4, 61-65. Retrieved from https://www.ijcmas.com/vol-4-8/C.M.%20Ramakritinan,%20et%20al.pdf

536. Ramamurthy, P., & Sangobanwo, M. (2016). Inter-annual variability in urban heat island intensity over 10 major cities in the United States. *Sustainable Cities and Society*, *26*, 65-75. DOI:10.1016/j.scs.2016.05.012

537. Ramm, T. D., Watson, C. S., & White, C. J. (2018). Strategic adaptation pathway planning to manage sea-level rise and changing coastal flood risk. Environmental Science & Policy, 87, 92-101. DOI:10.1016/j.envsci.2018.06.001

538. Rao K. N., Subraelu, P., Rao T. V., Hema Malini, B., Ratheesh, R., Bhattacharya, S., Rajawat, A. S., and Ajai. (2008). Sea-level rise and coastal vulnerability: an assessment of Andhra Pradesh coast, India through remote sensing and GIS. Journal of Coastal Conservation 12, 195–207. DOI:10.1007/s11852-009-0042-2

539. Rao, A. D., Upadhaya, P., Pandey, S., & Poulose, J. (2020). Simulation of extreme water levels in response to tropical cyclones along the Indian coast: a climate change perspective. Natural Hazards, 100, 151-172. DOI: 10.1007/s11069-019-03804-z

540. Rao, P. (2013). Building climate resilience in coastal ecosystems in India: cases and trends in adaptation practices. Climate change and disaster risk management, 335-349. DOI:10.1007/978-3-642-31110-9_21

541. Rao, Y. R., Chittibabu, P., Dube, S. K., Rao, A. D., & Sinha, P. C. (1997). Storm surge prediction and frequency analysis for Andhra coast of India. Mausam, 48(4), 555-566. DOI: https://doi.org/10.54302/mausam.v48i4.4322

542. Rawat, J.S., Biswas, V., Kumar, M. (2013). Changes in land use/cover using geospatial techniques: a case study of Ramnagar town area, district Nainital, Uttarakhand, India. Egypt. J. Rem. Sens. Space Sci. 16, 111–117. DOI: https://doi.org/10.1016/j.ejrs.2013.04.002

543. Reckermann, M., Omstedt, A., Soomere, T., Aigars, J., Akhtar, N., Bełdowska, M., Bełdowski, J., Cronin, T., Czub, M., Eero, M., Hyytiäinen, K. P., Jalkanen, J.-P., Kiessling, A., Kjellström, E., Kuliński, K., Larsén, X. G., McCrackin, M., Meier, H. E. M., Oberbeckmann, S., Parnell, K., Pons-Seres de Brauwer, C., Poska, A., Saarinen, J., Szymczycha, B., Undeman, E., Wörman, A., and Zorita, E.: Human impacts and their interactions in the Baltic Sea region, Earth Syst. Dynam., 13, 1–80, https://doi.org/10.5194/esd-13-1-2022, 2022.

544. Reed, A. J., Mann, M. E., Emanuel, K. A., Lin, N., Horton, B. P., Kemp, A. C., & Donnelly, J. P. (2015). Increased threat of tropical cyclones and coastal flooding to New York City during the anthropogenic era. *Proceedings of the National Academy of Sciences of the United States of America*, *112*(41), 12610–12615. DOI: https://doi.org/10.1073/pnas.1513127112

545. Reed, D. J., Davidson-Arnott, R., & Perillo, G. M. (2009). Estuaries, coastal marshes, tidal flats and coastal dunes. *Geomorphology and global environmental change*, *30*(3), 130-157. Retrieved from https://www.researchgate.net/publication/233986211_Estuaries_coastal_marshes_tidal_flats_and_coastal_dunes

546. Ribeiro, V. V., Pinto, M. A., Mesquita, R. K., Moreira, L. B., Costa, M. F., & Castro, Í. B. (2021). Marine litter on a highly urbanized beach at Southeast Brazil: a contribution to the development of litter monitoring programs. Marine Pollution Bulletin, 163, 111978. DOI: 10.1016/j.marpolbul.2021.111978

547. RISHI, P., & MUDALIAR, R. (2014). Climate Stress, Behavioral Adaptation and Subjective Well Being in Coastal Cities of India. American Journal of Applied Psychology,

(1), pp 13-21. DOI: 10.12691/ajap-2-1-3

548. Rizvi, S. H., Fatima, H., Iqbal, M. J., & Alam, K. (2020). The effect of urbanization on the intensification of SUHIs: Analysis by LULC on Karachi. Journal of Atmospheric and Solar-Terrestrial Physics, 207, 105374. DOI: 10.1016/j.jastp.2020.105374

549. Rodrigues, G. C., & Braga, R. P. (2021). Evaluation of NASA POWER Reanalysis Products to Estimate Daily Weather Variables in a Hot Summer Mediterranean Climate. *Agronomy*, *11*(6), 1207. DOI: https://doi.org/10.3390/agronomy11061207

550. Rosendahl A, L. (2013). Generic framework for meso-scale assessment of climate change hazards in coastal environments, Journal of Coastal Conservation 17, 1, 59–74. https://doi.org/10.1007/s11852-012-0218-z

551. Rosendahl A, L., Balstrøm T., Halsnæs K. (2016): Managing climate change hazards in coastal areas - The Coastal Hazard Wheel decision-support system, UNEP. ISBN 978-92-807-3593-2

552. Rosza, P. (2007). Attempts at qualitative and quantitative assessment of human impact on the landscape. Geogr. Fis. Dinam. Quat. 30, 233-238, IT ISSN 1724-4757. Retrieved fromhttp://www.glaciologia.it/wp content/uploads/Abstracts/Abstract_30_2/15_Rozsa_233_238_abst.pdf

553. Rosza, P. (2007). Attempts at qualitative and quantitative assessment of human impact on the landscape. Geogr. Fis. Dinam. Quat. 30, 233-238, IT ISSN 1724-4757. Retrieved from http://www.glaciologia.it/wp content/uploads/Abstracts/Abstract_30_2/15_Rozsa_233_238_abst.pdf

554. Roy, A. (2019). Making India's Coastal Infrastructure Climate-Resilient: Challenges and Opportunities. *Occasional Paper No. 207*, Observer Research Foundation Retrieved on November 14, 2022 from https://www.orfonline.org/research/making-indias-coastal-infrastructure-climate-resilient-challenges-and-opportunities-54330/

555. Rózsa, P. (2010). Nature and extent of human geomorphological impact–a review. Anthropogenic Geomorphology: A Guide to Man-Made Landforms, 273-291. DOI: DOI:10.1007/978-90-481-3058-0_17

556. RS, Mahendra & Mohanty, Prakash & Kumar, T & Shenoi, Satheesh & Nayak, Shailesh. (2010). Coastal Multi-Hazard Vulnerability Mapping: A Case Study Along The Coast of Nellore District, East Coast of India. Italian Journal of Remote Sensing. 42. 67-76. 10.5721/ItJRS20104235.

557. SAATY, T., L. (1977) A scaling method for priorities in hierarchical structures. Journal of Mathematical Psychology 15(3), 234–281. DOI: https://doi.org/10.1016/0022-2496(77)90033-5

558. SAATY, T., L. (1980) The Analytic Hierarchy Process. McGraw-Hill, New York. Retrieved from https://www.scirp.org/reference/ReferencesPapers?ReferenceID=1895817

559. SAATY, T., L. (1993) The analytic hierarchy process: a 1993 overview. Central European Journal of Operation Research and Economics 2(2), 119–137. Retrieved from https://core.ac.uk/download/pdf/82000104.pdf
560. Sahoo, B., & Bhaskaran, P. K. (2018). Multi-hazard risk assessment of coastal vulnerability from tropical cyclones–A GIS based approach for the Odisha coast. Journal of environmental management, 206, 1166-1178. DOI: https://doi.org/10.1016/j.jenvman.2017.10.075
561. Sahoo, M., & Sethi, N. (2022). The dynamic impact of urbanization, structural transformation, and technological innovation on ecological footprint and PM2. 5: evidence from newly industrialized countries. Environment, Development and Sustainability, 24(3), 4244-4277. DOI:10.1007/s10668-021-01614-7
562. Salahodjaev, R. (2014). Over-urbanization and air pollution: a cross-country analysis. International Economics Letters, 3(2), 69-75. Retrieved from https://www.semanticscholar.org/paper/Over-urbanization-and-air-pollution%3A-a-analysis-Salahodajev/0ba0aac760a2d27836b5841905466dc6c648f945
563. Salgado, K., & Martinez, M. L. (2017). Is ecosystem-based coastal defense a realistic alternative? Exploring the evidence. Journal of Coastal Conservation, 21, 837-848. DOI:10.1007/s11852-017-0545-1
564. Sankari, T. S., Chandramouli, A. R., Gokul, K., Surya, S. S. M. & Saravanavel, J. (2015). Coastal Vulnerability Mapping Using Geospatial Technologies In Cuddalore-Pichavaram Coastal Tract, Tamil Nadu, India. Aquatic Procedia, 4, 412-418. DOI:10.1016/j.aqpro.2015.02.055
565. Santos, I. R., Friedrich, A. C., Wallner-Kersanach, M., & Fillmann, G. (2005). Influence of socio-economic characteristics of beach users on litter generation. Ocean & Coastal Management, 48(9-10), 742-752. DOI:10.1016/j.ocecoaman.2005.08.006
566. Sarewitz, D., Pielke, R., Jr, & Keykhah, M. (2003). Vulnerability and risk: some thoughts from a political and policy perspective. Risk analysis : an official publication of the Society for Risk Analysis, 23(4), 805–810. https://doi.org/10.1111/1539-6924.00357
567. Sarkar, Md. Sujahangir Kabir & Begum, Rawshan & Pereira, Joy & Jaafar, Abdul & Saari, Mohd Yusof. (2014). Impacts of and Adaptations to Sea Level Rise in Malaysia. Asian Journal of Water, Environment and Pollution. 11. 29-36. DOI:10.1007/s11356-020-07601-1
568. Sarzynski, A. (2012). Bigger is not always better: a comparative analysis of cities and their air pollution impact. Urban Studies, 49(14), 3121-3138. DOI: 10.1177/0042098011432557
569. Sathish, N., Jeyasanta, K. I., Patterson, J. (2019). Abundance, characteristics and surface degradation features of microplastics in beach sediments of five coastal areas in Tamil Nadu, India. Mar. Pollut. Bull. 142, 112-118. https://doi.org/10.1016/j.marpolbul.2019.03.037.

570. Sathiya Bama, V. P., Rajakumari, S., & Ramesh, R. (2020). Coastal vulnerability assessment of Vedaranyam swamp coast based on land use and shoreline dynamics. Natural Hazards, 100, 829-842. DOI: 10.1007/s11069-019-03844-5

571. Saunders, I. and Young, A. (1983), Rates of surface processes on slopes, slope retreat and denudation. Earth Surf. Process. Landforms, 8: 473-501. https://doi.org/10.1002/esp.3290080508

572. Sawkar, K. (1998). Tourism and the environment: Case Studies on Goa, India and Maldives. International Bank for Reconstruction and Development. Retrieved from https://www.indiaenvironmentportal.org.in/files/wbi37134.pdf

573. Sawkar, K.; Noronha, L.; Masraenhas, A.; Chauhan, O.S.; Saeed, S. (YEAR).Tourism and the environment: Case studies on Goa, India, and the Maldives. Eds. by: 1-19p. http://drs.nio.org/drs/handle/2264/1322

574. Schnurr, R.E.J., Alboiu, V., & Chaudhary, M., et al. (2018). Reducing marine pollution from single-use plastics (SUPs): A review. Marine Pollution Bulletin 137: 157-171. DOI: 10.1016/j.marpolbul.2018.10.001

575. Schultz, B. (2018). Impacts of man-induced changes in land use and climate change on living in coastal and deltaic areas. Irrigation and Drainage, 67, 6-18. DOI: https://doi.org/10.1002/ird.1969

576. Schulz, M., Neumann, D., Fleet, D. M., & Matthies, M. (2013). A multi-criteria evaluation system for marine litter pollution based on statistical analyses of OSPAR beach litter monitoring time series. Marine Environmental Research, 92, 61–70. DOI: 10.1016/j.marenvres.2013.08.013

577. Sear, C., Hulme, M., Adger, N. and Brown, K. (2001) The Impacts of Global Climate Change on the UK Overseas Territories: Issues and Recommendations - A Summary Report, Natural. Retrieved on June 23, 2022 from http://www.seaturtle.org/PDF/SearC_2001_TechReportClim.pdf

578. Sen, P., K. (1968) Estimates of the Regression Coefficient Based on Kendall's Tau. *Journal of the American Statistical Association*, 63(324): 1379-1389 (doi:10.1080/01621459.1968.10480934)

579. Seneviratne, S.I., X. Zhang, M. Adnan, W. Badi, C. Dereczynski, A. Di Luca, S. Ghosh, I. Iskandar, J. Kossin, S. Lewis, F. Otto, I. Pinto, M. Satoh, S.M. Vicente-Serrano, M. Wehner, and B. Zhou. (2021). Weather and Climate Extreme Events in a Changing Climate. In Climate Change 2021: The Physical Science Basis. Contribution of Working Group I to the Sixth Assessment Report of the Intergovernmental Panel on Climate Change [Masson-Delmotte, V., P. Zhai, A. Pirani, S.L. Connors, C. Péan, S. Berger, N. Caud, Y. Chen, L. Goldfarb, M.I. Gomis, M. Huang, K. Leitzell, E. Lonnoy, J.B.R. Matthews, T.K. Maycock, T. Waterfield, O. Yelekçi, R. Yu, and B. Zhou (eds.)]. Cambridge University Press, Cambridge, United Kingdom and New York, NY, USA, pp. 1513–1766, doi:10.1017/9781009157896.013

580. Shaddick, G., Yan, H., & Vienneau, D. (2011). Modelling the impact of human activity on nitrogen dioxide concentrations in Europe. arXiv preprint arXiv:1110.3257. DOI:
581. Shalaby, A. and Tateishi, R. (2007). Remote sensing and GIS for mapping and monitoring land cover and land-use changes in the Northwestern coastal zone of Egypt. Applied geography, 27(1), pp.28-41. https://doi.org/10.1016/j.apgeog.2006.09.004
582. Shalaby, A. and Tateishi, R., 2007. Remote sensing and GIS for mapping and monitoring land cover and land-use changes in the Northwestern coastal zone of Egypt. Applied geography, 27(1), pp.28-41. https://doi.org/10.1016/j.apgeog.2006.09.004
583. Sharma, D., Pandey, N., 2020. Community Driven Beach Management Practices: Case Study Velas, Kelshi, Anjarla Villages of India. Int. J. Inf. Manage. 6, 1-12. https://doi.org/10.11648/j.ijsmit.20200601.11.
584. Sharma, S., & Patil, K, V. (2016). Emission scenario and health impacts of air pollutants in Goa. *Aerosol and Air Quality Research*, 16: 2474–2487. ISSN: 1680-8584 print / 2071-1409 online. DOI: 10.4209/aaqr.2015.12.0664
585. Sharp, T., 2017. How Big is Earth? Space.com, Reference, Science and Astronomy. Retrieved on March 3, 2021 from https://www.space.com/17638-how-big-is-earth.html.
586. Shi P, Yang, X., Fang, J., Xu, W., and Han, G. (2016). Mapping and ranking global mortality, affected population and GDP loss risks for multiple climatic hazards; J. Geogr. Sci. 26(7) 878–888. DOI: https://doi.org/10.1007/s11442-016-1304-1
587. Shin, E. C., Kim, S. H., Hakam, A., & Istijono, B. (2019). Erosion problems of shore line and counter measurement by various geomaterials. In MATEC Web of Conferences (Vol. 265, p. 01010). EDP Sciences. DOI:10.1051/matecconf/201926501010
588. Shital V., L. (2012) "Risk and management of climate induced disasters in coastal Gujarat in India", Management of Environmental Quality, Vol. 23 No. 1, pp. 82-100. DOI:10.1108/14777831211191610
589. Shivakrishna, A., Ramteke, K.K., Kesavan, S.,Prasad, P., Naidu, B.C., Dhanya, M. and Abidi, Z.J., 2021. Monitoring of current land use pattern of Ramsar designated Kolleru Wetland, India using geospatial technologies. Journal of Environmental Biology, 42(1106-111). http://doi.org/10.22438/jeb/42/1/MRN-1404
590. Short, A.D., Trembanis, A.C. (2004). Decadal scale patterns in beach oscillation and rotation Narrabeen beach, Australia-Time series, PCA and Wavelet analysis. J. Coastal Res. 20 (2), 523–532. DOI:10.2112/1551-5036(2004)020[0523:DSPIBO]2.0.CO;2
591. Shrivastava, R. (July 24, 2020). Golden Sand, Stunning sunsets and not a soul in sight, Goa's Velsao beach is our fave secret spot. Home, Things To Do. Retrieved on July 13, 2021 from https://www.whatshot.in/goa/golden-sand-stunning-sunsets-goas-velsao-beach-c-23859
592. Shukla. P.R., (2003). Climate Change and India: Vulnerability Assessment and Adaptation. Universities Press, 2003. ISBN: 8173714711. Retrieved from https://www.researchgate.net/publication/312164636_Climate_Change_and_India_Vulnerability_Assessment_and_Adaptation

593. Shukla., S. (2015). Vulnerability and risk measurement of climate change induced disasters in Gujarat. Retrieved from: http://academicfoundation.org/index.php?route=product/product&product_id=213
594. Šilc, U., Küzmič, F., Caković, D., & Stešević, D. (2018). Beach litter along various sand dune habitats in the southern Adriatic (E Mediterranean). Marine pollution bulletin, 128, 353-360. DOI: https://doi.org/10.1016/j.marpolbul.2018.01.045
595. Silva, J. S., da Silva, R. M., & Santos, C. A. G. (2018). Spatiotemporal impact of land use/land cover changes on urban heat islands: A case study of Paço do Lumiar, Brazil. *Building and Environment*, *136*, 279-292. DOI:10.1016/j.buildenv.2018.03.041
596. Simolo, C., Brunetti, M., Maugeri, M., and Nanni, T. (2014). Increasingly warm summers in the Euro–Mediterranean zone: Mean temperatures and extremes; Reg. Environ. Change 14(5) 1825–1832. DOI: 10.1007/s10113-012-0373-7
597. Singh P.D., Kambekar A.R. (2017) Assessing Impact of Sea Level Rise Along the Coastline of Mumbai City Using Geographic Information System. (Eds). Understanding Built Environment. Springer Transactions in Civil and Environmental Engineering. Springer, Singapore. DOI: 10.1007/978-981-10-2138-1_9
598. Singh, K. (June 13, 2020) National Marine Litter Policy: Government Begins Work On An Action Plan To Check Plastic Waste Flowing Into Oceans. https://swachhindia.ndtv.com/national-marine-litter-policy-government-begins-work-action-plan-check-plastic-waste-flowing-oceans-21330/
599. Singh, S, (2002). "Contracting Out Solutions: Political Economy of Contract Farming in the Indian Punjab," World Development, Elsevier, vol. 30(9), pages 1621-1638, September. Accessed from RePEc:eee:wdevel:v:30:y:2002:i:9:p:1621-1638
600. Singh, V. K., & Roxy, M. K. (2022). A review of ocean-atmosphere interactions during tropical cyclones in the north Indian Ocean. Earth-Science Reviews, 226, 103967. DOI:10.1016/j.earscirev.2022.103967
601. Sirianni, H., Fletcher, C., Chen, Q., & Barbee, M. (2013). Sea-level rise vulnerability mapping for adaptation decisions using LiDAR DEMs. Progress in Physical Geography. 10.1177/0309133313496835.
602. Slabá, E.; JakubínSký, J.; báčová, R.; HERbER, v. and kubíčEk, P. (2015): Inventory of anthropogenic landforms for flood management in small catchments of the Czech Republic. In: Zeitschrift für Geomorphologie, Supplementary Issues 59 (2), 75–93. https://doi.org/10.1127/zfg_suppl/2015/S-59205
603. Slabá, E.; JakubínSký, J.; báčová, R.; HERbER, v. and kubíčEk, P. (2015): Inventory of anthropogenic landforms for flood management in small catchments of the Czech Republic. In: Zeitschrift für Geomorphologie, Supplementary Issues 59 (2), 75–93. https://doi.org/10.1127/zfg_suppl/2015/S-59205
604. Slavin, C., 2016. 4 Countries generate about half the plastic marine debris. Packaging Digest, Trends and Issues, Sustainability. Retrieved on March 6, 2021 from https://www.packagingdigest.com/sustainability/4-countries-generate-about-half-plastic-

marine-debris.
605. Smith, K. (2011). We are seven billion. *Nature Climate Change*, *1*(7), 331–335. DOI: https://doi.org/10.1038/nclimate1235

606. Soeder, D. J., & Soeder, D. J. (2021). Fossil fuels and climate change. Fracking and the Environment: A scientific assessment of the environmental risks from hydraulic fracturing and fossil fuels, 155-185. DOI:10.1007/978-3-030-59121-2_9
607. Sofia, G.; Marinello, F. And Tarolli, P. (2016): Metrics For Quantifying Anthropogenic Impacts On Geomorphology: Road Networks. In: Earth Surface Processes And Landforms 41 (2), 240–255. Https://Doi.Org/10.1002/Esp.3842
608. Sofia, G.; Marinello, F. And Tarolli, P. (2016): Metrics for Quantifying Anthropogenic Impacts On Geomorphology: Road Networks. In: Earth Surface Processes And Landforms 41 (2), 240–255.DOI: https://Doi.Org/10.1002/Esp.3842
609. Son LH, Louati A (2016) Modeling municipal solid waste collection: a generalized vehicle routing model with multiple transfer stations, gather sites and inhomogeneous vehicles in time windows. Waste Manag 52:34–49. DOI: https://doi.org/10.1016/j.wasman.2016.03.041
610. South Goa. (2011). Census of India. Registrar General and Census Commissioner of India. Retrieved on May 17, 2020 from https://censusindia.gov.in/nada/index.php/catalog/371
611. South Goa. (2011). Census of India. Registrar General and Census Commissioner of India. Retrieved on May 17, 2020 from https://censusindia.gov.in/nada/index.php/catalog/371
612. South Goa. (2011). Census of India. Registrar General and Census Commissioner of India. Retrieved on May 17, 2020 from https://censusindia.gov.in/nada/index.php/catalog/371
613. Sridhar, K. R., Deviprasad, B., Karamchand, K. S., Bhat, R., 2007. Plastic litter along the beaches of Karnataka, southwest coast of India. Asian J. Water, Environ. Pollut.6, 87-93. Retrieved from https://www.researchgate.net/publication/267449826.
614. Srivastava, A., Yetemen, O., Saco, P.M., Rodriguez, J.F., Kumari, N. & Chun, K.P. (2022) Influence of orographic precipitation on coevolving landforms and vegetation in semi-arid ecosystems. *Earth Surface Processes and Landforms*, 47 (12), 2846– 2862. Available from: https://doi.org/10.1002/esp.5427

615. Steffen, W., Crutzen, P. J., & McNeill, J. R. (2007). The Anthropocene: are humans now overwhelming the great forces of nature. Ambio-Journal of Human Environment Research and Management, 36(8), 614-621. Accessed from http://www.jstor.org/stable/25547826
616. Su, Q., Chen, K., & Liao, L. (2021). The impact of land use change on disaster risk from the perspective of efficiency. Sustainability, 13(6), 3151. DOI: https://doi.org/10.3390/su13063151

617. Subash, N., Singh, S., and Priya, N. (2011) Variability of rainfall and effective onset and length of the monsoon season over a sub-humid climatic environment. *Atmospheric Research*, 99(3): 479-487 doi:10.1016/j.atmosres.2010.11.020

618. Sudha Rani, N.N.V., Satyanarayana, A.N.V. & Bhaskaran, P.K. Nat Hazards (2015) "Coastal vulnerability assessment studies over India: a review," Natural Hazards: Journal of the International Society for the Prevention and Mitigation of Natural Hazards, Springer;International Society for the Prevention and Mitigation of Natural Hazards, vol. 77(1), pages 405-425. https://doi.org/10.1007/s11069-015-1597-x.

619. Sudha Rani, N.N.V., Satyanarayana, A.N.V. & Bhaskaran, P.K. Nat Hazards (2015) 77: 405. https://doi.org/10.1007/s11069-015-1597-x.

620. Sulochanan, B., Veena, S., Ratheesh, L., Padua, S., Rohit, P., Kaladharan, P., Kripa, V., 2019. Temporal and spatial variability of beach litter in Mangaluru, India. Marine Pollution Bulletin, 149, 110541. https://doi.org/10.1016/j.marpolbul.2019.110541.

621. Sulochanan, B., Veena, S., Ratheesh, L., Padua, S., Rohit, P., Kaladharan, P., Kripa, V., 2019. Temporal and spatial variability of beach litter in Mangaluru, India. Marine Pollution Bulletin, 149, 110541.DOI: https://doi.org/10.1016/j.marpolbul.2019.110541.

622. Sun, C., Wu, Z., Lv, Z., Yao, N., & Wei, J. (2013). Quantifying different types of urban growth and the change dynamic in Guangzhou using multi-temporal remote sensing data. International Journal of Applied Earth Observation and Geoinformation, 21, 409–417. https://doi.org/10.1016/j.jag.2011. 12.012

623. Sun, X., Ren, G., You, Q., Ren, Y., Xu, W., Xue, X. (2019). Global diurnal temperature range (DTR) changes since 1901. Clim. Dynam. 52 (5), 3343–3356. https://doi.org/10.1007/s00382-018-4329-6.

624. Suto, L. (2010). Mining: Extraction of fossil fuels. (Eds.) Anthropogenic Geomorphology, A Guide to Man-Made Landforms, pp. 131-154. Springer, ISBN 978-90-481-3057-3. DOI: 10.1007/978-90-481-3058-0.

625. Szabó, J. (1993) A társadalom hatása a földfelszínre (The impact of society on the surface). In: Borsy Z (ed.), Általános természeti földrajz. Egyetemi tankönyv, Budapest

626. Szabo, J. (2010). Anthropogenic Geomorphology: Subject and System. (eds), Anthropogenic Geomorphology- A Guide to Man-Made Landforms. ISBN 978-90-481-3057-3. e-ISBN 978-90-481-3058-. 0. Springer Dordrecht Heidelberg London New York. DOI: 10.1007/978-90-481-3058-0

627. Szabó, J. (2010). Anthropogenic geomorphology: subject and system. Anthropogenic geomorphology: A guide to man-made landforms, 3-10. DOI:10.1007/978-90-481-3058-0

628. Tabari, H., and Marofi, S. (2010) Changes of Pan Evaporation in the West of Iran. *Water Resources Management*, 25(1): 97-111. doi:10.1007/s11269-010-9689-6.

629. Tandon, A., Yadav, S., Attri, A.K. (2008). City-wide sweeping a source for respirable particulate matter in the atmosphere. Atmos. Environ. 42, 1064–1069. DOI: 10.1016/j.atmosenv.2007.12.006
630. TarollI, P. (2014): High-resolution topography for understanding earth surface processes: opportunities and challenges. In: Geomorphology 216, 295–312. https://doi.org/10.1016/j.geomorph.2014.03.008
631. TarollI, P. (2014): High-resolution topography for understanding earth surface processes: opportunities and challenges. In: Geomorphology 216, 295–312. https://doi.org/10.1016/j.geomorph.2014.03.008
632. Tarolli, P.; Sofia, G. And Ellis, E. (2017): Mapping the topographic fingerprints of humanity across Earth, In: Eos 98. https://doi.org/10.1029/2017EO069637
633. Tarolli, P.; Sofia, G. And Ellis, E. (2017): Mapping the topographic fingerprints of humanity across Earth, In: Eos 98. DOI: https://doi.org/10.1029/2017EO069637
634. TERI. 1996, The economic impact of a one-metre sea level rise on the Indian coastline: method and case studies, New Delhi: Tata Energy Research Institute. [Report No 93/GW/52, submitted to the Ford Foundation], www.envfor.nic.in accessed on 1st Nov, 2007.
635. The Energy and Resources Institute. (2014). Study #2: Assessment of the knowledge and data gaps to deliver SAPCCs, and a strategy to address needs of six States – Assam, Bihar, Chhattisgarh, Kerala, Maharashtra & Orissa. Climate Change Innovation Programme (CCIP). Retrieved on May 17, 2019 from http://www.climatechange.mp.gov.in/sites/default/files/resources/Scoping%20study%20on%20Data%20%26%20Knowledge%20Gap%20Assessment%20of%206%20states.pdf
636. The Ocean Conference, 2017. Factsheet: People and Oceans. United Nations, New York, USA. 5-9 June, 2017. Retrieved from https://www.un.org/sustainabledevelopment/wp-content/uploads/2017/05/Ocean-fact-sheet-package.pdf.
637. Thiel, M., Bravo, M., Hinojosa, I. A., Luna, G., Miranda, L., Núñez, P., ... & Vásquez, N. (2011). Anthropogenic litter in the SE Pacific: an overview of the problem and possible solutions. Revista de Gestão Costeira Integrada-Journal of Integrated Coastal Zone Management, 11(1), 115-134. DOI:10.5894/rgci207
638. THIELER, E. R. & HAMMER-KLOSE, E. S. 1999. National Assessment of Coastal Vulnerability to Sea-Level Rise: Preliminary Results for the U.S. Atlantic Coast. Woods Hole, Massachusetts: United States Geological Survey (USGS). https://pubs.usgs.gov/of/1999/of99-593/
639. Thieler, E. R. & Hammer-Klose, E., S. (2000a). National Assessment of Coastal Vulnerability to Sea-Level Rise: Preliminary Results for the U.S. Gulf of Mexico Coast. Woods Hole, Massachusetts: United States Geological Survey (USGS). https://pubs.usgs.gov/dds/dds68/reports/gulfrep.pdf

640. Thieler, E., R. & Hammer-Klose, E., S. (2000b). National Assessment of Coastal Vulnerability to Sea-Level Rise: Preliminary Results for the U.S. Pacific Coast. Woods Hole, Massachusetts: United States Geological Survey (USGS). https://pubs.usgs.gov/dds/dds68/reports/westrep.pdfo

641. Thompson R. C., Moore C. J., Vom F. S., & Swan S. H., 2009. Plastics, the environment and human health: current consensus and future trends. Phil. Trans. R. Soc. B 364, 2153–2166. DOI: https://doi.org/10.1098/rstb.2009.0053.

642. Thorat, B.R., Prasad, P. and Ram, A., 2023. Heavy metal accumulation in a moderately polluted Ulhas estuary, Western India. *Regional Studies in Marine Science*, 60, 102818. https://doi.org/10.1016/j.rsma.2023.102818

643. Thushari, G.G.N., Senevirathna, J.D.M. (2020). Plastic pollution in the marine environment. Heliyon, 6, P.E 04709. https://doi.org/10.1016/j.heliyon.2020.e04709.

644. Tirabassi, T, F. Fortezza, F., and Vandini, W (1990). Wind circulation and air pollutant concentration in the coastal city of Ravenna, Energy Build., 15-16, 699-704. DOI: 10.1016/0378-7788(91)90040-A

645. Titus, J.G. and Richman, C. (2001) Maps of Lands Vulnerable to Sea Level Rise: Modeled Elevations along the US Atlantic and Gulf Coasts. Climate Research, 18, 205-228. DOI: http://dx.doi.org/10.3354/cr018205

646. Tiwari, G., Kumar, P., & Tiwari, P. (2022). The appraisal of tropical cyclones in the North Indian Ocean: An overview of different approaches and the involvement of Earth's components. Frontiers in Earth Science, 10, 823090. DOI: 10.3389/feart.2022.823090

647. Tiwari, S., Thomas, A., Rao, P., Chate, D., Soni, V., Singh, S., & Hopke, P. K. (2018). Pollution concentrations in Delhi India during winter 2015–16: A case study of an odd-even vehicle strategy. Atmospheric Pollution Research, 9(6), 1137–1145. https://doi.org/10.1016/j.apr.2018.04.008.

648. Torresan, S., Critto, A., Rizzi, J., and Marcomini, A.: Assessment of coastal vulnerability to climate change hazards at the regional scale: the case study of the North Adriatic Sea, Nat. Hazards Earth Syst. Sci., 12, 2347–2368, https://doi.org/10.5194/nhess-12-2347-2012, 2012.

649. Toth, C. (2010). Agriculture: Grazing land and other grasslands. (Eds.) Anthropogenic Geomorphology, A Guide to Man-Made Landforms, pp. 69-82. Springer, ISBN 978-90-481-3057-3. DOI: 10.1007/978-90-481-3058-0.

650. Tour my India (2020). Miramar Beach Goa. Home, States, Goa, Beaches in Goa, Miramar beach. Retrieved on July, 13, 2021 from https://www.tourmyindia.com/states/goa/miramar-beach.html

651. Trenberth, K. E., Dai, A., Rasmussen, R. M., & Parsons, D. B. (2003). The changing character of precipitation. *Bulletin of the American Meteorological Society*, *84*(9), 1205-1218. DOI: https://doi.org/10.1175/BAMS-84-9-1205

652. U.S. Federal Government (2023). U.S. Climate Resilience Toolkit Climate Explorer. Accessed from https://crt-climate-explorer.nemac.org/

653. UN DHA (1992). Internationally Agreed Glossary of Basic Terms Related to Disaster Management, United Nations Department of Humanitarian Affairs, Geneva. Retrieved on Aug 17, 2022 from https://reliefweb.int/report/world/internationally-agreed-glossary-basic-terms-related-disaster-management
654. UN ESCAP-INCOIS. (2016). Multi hazard Vulnerability Mapping. Regional Training for capacity Building in Multi-Hazard Early Warning Systems. ESSO-Indian National Centre for Ocean Information Services (ESSO-INCOIS) Ministry of Earth Sciences, Hyderabad-90. Retrieved from https://incois.gov.in/ITCOocean/rtcd.jsp
655. United Nations (2002) Risk awareness and assessment, in Living with Risk, ISDR, UN, WMO and Asian Disaster Reduction Centre, Geneva, 39-78. Accessed from https://www.unisdr.org/files/657_lwr1.pdf
656. United Nations (2015). Framework Convention on Climate Change. UNFCCC, Cge Training Materials On Vulnerability And Adaptation Assessment, Coastal resources. Retrieved from: file:///Users/md101/Downloads/IMP%20UNFCCC%20SLR%20tutorial.pdf
657. United Nations (2017). Resolution adopted by the General Assembly on 6 July 2017, Work of the Statistical Commission pertaining to the 2030 Agenda for Sustainable Development (A/RES/71/313). Accessed from https://ggim.un.org/documents/a_res_71_313.pdf
658. United Nations (2017). The Ocean Conference, Save Our Oceans, 5-9 June, 2017. Accessed on November, 10, 2023 from https://www.un.org/sustainabledevelopment/wp-content/uploads/2017/05/Ocean-fact-sheet-package.pdf
659. United Nations Environmental Programme. (2021). Marine Litter. Explore topics, Ocean and Seas, what we do, Regional Seas Programme. Retrieved from https://www.unep.org/explore-topics/oceans-seas/what-we-do/working-regional-seas/marine-litter.
660. United Nations, “The Ocean conference” (New York, 5-9 June 2017), https://www.un.org/sustainabledevelopment/wp-content/uploads/2017/05/Ocean-fact-sheet-package.pdf
661. United Nations, Asia Development Bank, The World Bank and European Union, “Kerala Post Disaster Needs Assessment Floods and Landslides - August 2018,” United Nations Development Programme, October 2018. https://www.undp.org/content/undp/en/home/ librarypage/crisis-prevention-and-recovery/post-disaster-needsassessment—kerala.html.
662. US Climate Toolkit. (2015). Components of Vulnerability. Retrieved from https://toolkit.climate.gov/image/985
663. Vágvölgyi, R., Coldea, A., Dresler, T., Schrader, J., & Nuerk, H. C. (2016). A Review about Functional Illiteracy: Definition, Cognitive, Linguistic, and Numerical Aspects. *Frontiers in psychology*, *7*, 1617. DOI: https://doi.org/10.3389/fpsyg.2016.01617

664. Vanwalleghem, T.; Gómez, J. A.; Infante Amate, J.; Gonzalez De Molina, M.; Vanderlinden, K.; Guzmán, G.; Laguna, A. And Giráldez, J. V. (2017): Impact Of Historical Land Use And Soil Management Change On Soil Erosion And Agricultural Sustainability During The Anthropocene. In: Anthropocene 17, 13-19. DOI: https:/Doi.Org/10.1016/J.Ancene.2017.01.002

665. Vaz, E. (2014). Managing urban coastal areas through landscape metrics: An assessment of Mumbai's mangrove system. Ocean & coastal management, 98, 27-37. DOI:10.1016/j.ocecoaman.2014.05.020

666. Vaz, E., Taubenböck, H., Kotha, M., & Arsanjani, J. J. (2017). Urban change in Goa, India. Habitat International, 68, 24-29. DOI: https://doi.org/10.1016/j.habitatint.2017.07.010

667. Veerasingam, S., Mugilarasan, M., Venkatachalapathy, M., Vethamony, P., 2016. Influence of 2015 flood on the distribution and occurrence of microplastic pellets along the Chennai coast, India. Mar. Poll. Bull. 109, 196-204. http://dx.doi.org/10.1016/j.marpolbul.2016.05.082.

668. Vega, A., J., and Rohli, R., V. (2012). Climatology, Burlington, M A: Jones and Bartlett Learning L L C, ISBN 978-0-7637-9101-8.

669. Venkateshwaralu, B., Singh, A.K., Prasad, Y.G., Ravindrachary, G., Srinivasa Rao, C.H., Ramana, D.B.V. and Rao, V.U.M. (2011) 'District level contingency plans for weather aberrations in India', Central Research Institution for Dry Land Agriculture and IndianCouncil Agricultural Research Publication. Retrieved from https://www.icar-crida.res.in/assets/img/Books/2011-12/contingency%20plans%20book.pdf

670. Verdecchia, M., Visconti, F., Giorgi, M.R., Marinucci, H. (1994). Diurnal temperature range for a doubled carbon dioxide concentration experiment: analysis of possible physical mechanisms, Geophys. Res. Lett., 21, 1527-1530. DOI: https://doi.org/10.1029/94GL00188

671. Vethamony, P., Mani Murali, R., Ankita, M., & Amrita, S. (2013). Coastal vulnerability assessment of Puducherry coast, India using analytical hierarchical process. Natural Hazards Earth System Sciences,1, 509-559. DOI: https://doi.org/10.5194/nhess-13-3291-2013, 2013.

672. Vidyasakar, A., Krishnakumar, S., Kasilingam, K., Neelavannan, K., Bharathi, V. A., Godson, P. A., Prabha, K., Magesh, N. S., 2020. Characterization and distribution of microplastics and plastic debris along Silver Beach, Southern India. Mar. Poll. Bull. 158, 111421. https://doi.org/10.1016/j.marpolbul.2020.111421.

673. Vijayan, P. (2019). Resilient Rebuilding – Lessons from the Kerala Floods. The Hindu, May 15, 2019. Accessed November 13, 2022 from https://www.thehindu.com/news/national/kerala/resilientrebuilding-lessons-from-the-kerala-floods/article27134928.ece.

674. Viles, H., & Spencer, T. (2014). *Coastal problems: geomorphology, ecology and society at the coast*. Routledge. DOI: https://doi.org/10.4324/9781315832586

675. Vincent, A. E., & Hoellein, T. J. (2017). Anthropogenic litter abundance and accumulation rates point to seasonal litter sources on a Great Lakes Beach. Journal of Contemporary Water Research & Education, 160(1), 72-84. DOI:10.1111/j.1936-704X.2017.03241.x
676. Vivek, G. and Grinivasa Kumar, T. (2016). “Multi-Hazard Vulnerability Assessment Along the Coast of Visakhapatnam, North-East Coast of India”. Living Planet Symposium, Proceedings of the conference held 9-13 May 2016 in Prague, Czech Republic. Edited by L. Ouwehand. ESA-SP Volume 740, ISBN: 978-92-9221-305-3, p.53
677. Vollstedt, B., Koerth, J., Tsakiris, M., Nieskens, N., & Vafeidis, A. T. (2021). Co-production of climate services: A story map for future coastal flooding for the city of Flensburg. Climate Services, 22, 100225. DOI: https://doi.org/10.1016/j.cliser.2021.100225
678. Wahl, T. (2017). Sea-level rise and storm surges, relationship status: complicated!. Environmental Research Letters, Volume 12, Number 11. DOI 10.1088/1748-9326/aa8eba
679. *Waltham, Nathan J.; Elliott, Michael; Lee, Shing Yip; Lovelock, Catherine; Duarte, Carlos M.; Buelow, Christina; Simenstad, Charles; Nagelkerken, Ivan; Claassens, Louw; Wen, Colin K-C; Barletta, Mario (2020).* "UN Decade on Ecosystem Restoration 2021–2030—What Chance for Success in Restoring Coastal Ecosystems?". *Frontiers in Marine Science. 7: 71.* doi:10.3389/fmars.2020.00071. hdl:2440/123896. ISSN 2296-7745.
680. Wang, H., Easter, R.C., Rasch, P.J., Wang, M., Liu, X., Ghan, S.J. (2013). Sensitivity of remote aerosol distributions to representation of cloud–aerosol interactions in a global climate model. Geosci. Model Dev. (GMD) 6 (3), 765–782. DOI: https://doi.org/10.5194/gmd-6-765-2013.
681. Wang, X., & Zhou, D. (2021). Exploring the nonlinear impact of urbanization on pollutant emissions: a spatial approach. Atmospheric Pollution Research, 12(11), 101220. DOI:10.1016/j.apr.2021.101220
682. Wang, X., Hou, X., & Wang, Y. (2017). Spatiotemporal variations and regional differences of extreme precipitation events in the Coastal area of China from 1961 to 2014. Atmospheric Research, 197, 94-104. DOI: https://doi.org/10.1016/j.atmosres.2017.06.022
683. Wang, Y., Jiang, J.H., Su, H. (2015). Atmospheric responses to the redistribution of anthropogenic aerosols. J. Geophys. Res.: Atmosphere 120 (18), 9625–9641. DOI: https://doi.org/10.1002/2015JD023665.
684. Ward, R. D., Friess, D. A., Day, R. H., & Mackenzie, R. A. (2016). Impacts of climate change on mangrove ecosystems: a region by region overview. *Ecosystem Health and sustainability*, *2*(4), e01211. DOI: https://doi.org/10.1002/ehs2.1211
685. Watkinson, A. R. (2009). Climate change at the coast: from global to local. Houille Blanche, 38-44. DOI: https://doi.org/10.1051/lhb:2009012

686. Weber, H., Sciubba, J., D. (2018). The Effect of Population Growth on the Environment: Evidence from European Regions. Eur J Popul. 2018 Apr 9;35(2):379-402. doi: 10.1007/s10680-018-9486-0. PMID: 31105504; PMCID: PMC6497702. DOI: 10.1007/s10680-018-9486-0
687. Wei, G., Zhang, Z., Ouyang, X., Shen, Y., Jiang, S., Liu, B., & He, B. J. (2021). Delineating the spatial-temporal variation of air pollution with urbanization in the Belt and Road Initiative area. Environmental Impact Assessment Review, 91, 106646. DOI:10.1016/j.eiar.2021.106646
688. Weisse, R., von Storch, H., Niemeyer, H. D., & Knaack, H. (2012). Changing North Sea storm surge climate: An increasing hazard? Ocean & Coastal Management, 68, 58-68. doi:10.1016/j.ocecoaman.2011.09.005.
689. White, J.W., Hoogenboom, G., Stackhouse, P.W., Hoell, J., M. (2008). Evaluation of NASA satellite- and assimilation model-derived longterm daily temperature data over the continental US. *Agric. For. Meteorol*, *148*, 1574–1584. DOI: https://doi.org/10.1016/j.agrformet.2008.05.017
690. Whittow, John (1984). Dictionary of Physical Geography. London: Penguin, 1984, p. 97. ISBN 0-14-051094-X.
691. WHO (2018) WHO global ambient air quality database (update 2018). World Health Organization, Geneva. Retrieved from https://www.who.int/data/gho/data/themes/air-pollution/who-air-quality-database/2018
692. Wickramaarachchi, W. W. U. I., Peiris, T. U. S., & Samita, S. (2020). Rainfall trends in the North-Western and Eastern coastal lines of Sri Lanka using non–parametric analysis. DOI: 10.4038/tar.v31i2.8366
693. Williams, A.T., Rangel-Buitrago, N., 2019. Marine litter: Solutions for a major environmental problem. J. Coast. Res. 35, 648-663. https://doi.org/10.2112/JCOASTRES-D-18-00096.1.
694. Williams, L. L., & Lück-Vogel, M. (2020). Comparative assessment of the GIS based bathtub model and an enhanced bathtub model for coastal inundation. Journal of Coastal Conservation, 24(2), 23. DOI: https://doi.org/10.1007/s11852-020-00735-x
695. Wood, N. J., Jones, J., Spielman, S., & Schmidtlein, M. C. (2015). Community clusters of tsunami vulnerability in the US Pacific Northwest. *Proceedings of the National Academy of Sciences of the United States of America*, *112*(17), 5354–5359. DOI: https://doi.org/10.1073/pnas.1420309112
696. Woodruff, J. D., Irish, J. L., & Camargo, S. J. (2013). Coastal flooding by tropical cyclones and sea-level rise. *Nature*, *504*(7478), 44–52. DOI: https://doi.org/10.1038/nature12855
697. World Meteorological Organization. (December 2, 2020). 2020 on track to be one of three warmest years on record. Press Release Number: 02122020. Retrieve on Dec 15, 2022 from https://public.wmo.int/en/media/press-release/2020-track-be-one-of-three-warmest-years-

record#:~:text=2011%2D2020%20will%20be%20the,to%20the%20World%20Meteorological%20Organization.

698. Wu, S. Y., Yarnal, B., & Fisher, A. (2002). Vulnerability of coastal communities to sea-level rise: a case study of Cape May County, New Jersey, USA. Climate research, 22(3), 255-270. DOI:10.3354/cr022255

699. Wu, S.Y., Yarnal, B., Fisher, A. (2002). Vulnerability of coastal communities to sea level rise: a case study of Cape May County, New Jersey, USA. Climate Res. 22, 255–270. DOI: DOI:10.3354/cr022255

700. Wuebbles, D. J., & Jain, A. K. (2001). Concerns about climate change and the role of fossil fuel use. Fuel processing technology, 71(1-3), 99-119. DOI: https://doi.org/10.1016/S0378-3820(01)00139-4

701. Wuebbles, D.J., D.R. Easterling, K. Hayhoe, T. Knutson, R.E. Kopp, J.P. Kossin, K.E. Kunkel, A.N. LeGrande, C. Mears, W.V. Sweet, P.C. Taylor, R.S. Vose & M.F. Wehner. (2017). *Our globally changing climate*. In: *Climate science special report: Fourth national climate assessment, volume I* [Wuebbles, D.J., D.W. Fahey, K.A. Hibbard, D.J. Dokken, B.C. Stewart, and T.K. Maycock (eds.)]. U.S. Global Change Research Program, Washington, DC, pp. 35-72. doi: 10.7930/J08S4N35

702. WWF. (2020). Living Planet Report 2020 - Bending the curve of biodiversity loss. Almond, R.E.A., Grooten M. and Petersen, T. (Eds). WWF, Gland, Switzerland. Retrieved from https://wwfin.awsassets.panda.org/downloads/lpr_2020_full_report.pdf

703. Xanthos, D., & Walker, T.R. (2017). International policies to reduce plastic marine pollution from single-use plastics (plastic bags and microbeads): a review. Marine Pollution Bulletin 118(1-2): 17-26. http://doi.org/10.1016/j.marpolbul.2017.02.048

704. Xiuwan, C. (2002). Using remote sensing and GIS to analyse land cover change and its impacts on regional sustainable development. Int. J. Remote Sens. 23 (1), 107– 124. DOI:10.1080/01431160010007051

705. Xu, B., Feng, G., Li, Z., Wang, Q., Wang, C., & Xie, R. (2016a). Coastal subsidence monitoring associated with land reclamation using the point target based SBAS-InSAR method: A case study of Shenzhen, China. *Remote Sensing*, *8*(8), 652. https://doi.org/10.3390/rs8080652

706. Xu, L., He, Y., Huang, W., & Cui, S. (2016b). A multi-dimensional integrated approach to assess flood risks on a coastal city, induced by sea-level rise and storm tides. *Environmental Research Letters*, *11*(1), 014001. DOI: 10.1088/1748-9326/11/1/014001

707. Xue, W., Guo, J., Zhang, Y., Zhou, S., Wang, Y., Miao, Y., et al., 2019. Declining diurnal temperature range in the North China Plain related to environmental changes. Clim. Dynam. DOI: https://doi.org/10.1007/s00382-018-4505-8.

708. Yadav, D. & Barve, A. (2017). Analysis Of Socioeconomic Vulnerability For Cyclone-Affected Communities In Coastal Odisha, India. International Journal Of Disaster Risk Reduction, 22, 387-396. DOI: https://doi.org/10.1016/j.ijdrr.2017.02.003

709. Yang, X., Hou, Y., & Chen, B. (2011). Observed surface warming induced by urbanization in east China. Journal of Geophysical Research. DOI: https://doi.org/10.1029/2010jd015452

710. Yaranal, N.A., Subbiah, S., Mohanty, K., 2021. Identification, extraction of microplastics from edible salts and its removal from contaminated seawater. Environ. Technol. Innov. 21 https://doi.org/10.1016/j.eti.2020.101253

711. Yaw, A. B., Alex, B. A., Kwasi, A. A., Kwabena, E. A., & John, B. D. (2014). Assessing Land Cover Changes from Coastal Tourism Development in Ghana: Evidence from the Kokrobite-Bortianor Coastline, Accra. Civil and Environmental Research, 6 (6). Retrieved from https://core.ac.uk/download/pdf/234677788.pdf

712. Yuan, F., Sawaya, K.E., Loeffelholz, B.C., Bauer, M.E. (2005). Land cover classification and change analysis of the twin cities (Minnesota) metropolitan area by multitemporal Landsat remote sensing. Remote Sens. Environ. 98, 317–328. DOI: https://doi.org/10.1016/j.rse.2005.08.006

713. Yuda, M. (2019). Asian countries rush to fight toxic air pollution. Accessed from https://asia.nikkei.com/Economy/Asian-countries-rush-to- fight-toxic-air-pollution.

714. Yue, S., Pilon, P., Phinney, B., and Cavadias, G. (2002) The influence of autocorrelation on the ability to detect trend in hydrological series. *Hydrological Processes*, 16(9): 1807-1829. doi:10.1002/hyp.1095

715. Yunus, A. P., Avtar, R., Kraines, S., Yamamuro, M., Lindberg, F., & Grimmond, C. S. B. (2016). Uncertainties in tidally adjusted estimates of sea level rise flooding (bathtub model) for the greater London. Remote Sensing, 8(5), 366. DOI: https://doi.org/10.3390/rs8050366

716. Zhang, H., Wang, Y., Park, T., W., and Deng, Y. (2017). Quantifying the relationship between extreme air pollution events and extreme weather events; Atmos. Res. 188 64–79. DOI:10.1016/j.annosres.2016.11.010

717. Zhang, Keqi & Gann, Daniel & Ross, Mike & Robertson, Quin & Sarmiento, Juan & Santana, Sheyla & Rhome, Jamie & Fritz, Cody. (2019). Accuracy assessment of ASTER, SRTM, ALOS, and TDX DEMs for Hispaniola and implications for mapping vulnerability to coastal flooding. Remote Sensing of Environment. 225. 290-306. DOI: 10.1016/j.rse.2019.02.028.

718. Zhang, L., Wu, B., Yin, K., Li, X., Kia, K., & Zhu, L. (2015). Impacts of human activities on the evolution of estuarine wetland in the Yangtze Delta from 2000 to 2010. *Environmental Earth Sciences*, *73*, 435-447. DOI: 10.1007/s12665-015-4197-x

719. Zhang, R., Zhu, D. (2011). Study of land cover classification based on knowledge rules using high-resolution remote sensing images. Expert Syst. Appl. 38 (4), 3647– 3652. DOI:10.1016/j.eswa.2010.09.019

720. Zhang, X., Alexander, L., Hegerl, G. C., Jones, P., Tank, A. K., Peterson, T. C., & Zwiers, F. W. (2011). Indices for monitoring changes in extremes based on daily

temperature and precipitation data. Wiley Interdisciplinary Reviews: Climate Change, 2(6), 851-870. DOI: https://doi.org/10.1002/wcc.147

721. Zhou, L., Dai, A., Dai, Y., Vose, R., Zou, C., Tian, Y., and Chen, H. (2004). Spatial dependence of diurnal temperature range trends on precipitation from 1950 to 2004, Clim. Dynam., 32, 429–440, DOI:10.1007/s00382-008-0387-5.

722. Zhou, L., Dickinson, R., Dai, A., and Dirmeyer, P. (2010). Detection and attribution of anthropogenic forcing to diurnal temperature range changes from 1950 to 1999: comparing multi-model simulations with observations, Clim. Dynam., 35, 1289–1307. DOI:10.1007/s00382-009-0644-2.

723. Zhou, Y., Pu, L., & Zhu, M. (2020). Coastal landscape vulnerability analysis in Eastern China—based on land-use change in Jiangsu Province. International Journal of Environmental Research and Public Health, 17(5), 1702. doi: 10.3390/ijerph17051702

724. Zoran, M.E. (2006). The use of multi-temporal and multispectral satellite data for change detection analysis of Romanian Black Sea Coastal zone. J. Optoelectron. Adv. Mater. 8, 252–256. DOI: https://old.joam.inoe.ro/arhiva/pdf8_1/Zoran1.pdf

Appendices

Supplementary Table-1 Rationale and Concept behind the variables used in the Nigam-Kotha model of AGI@E

Parameters	Concept	Rationale	Source
Ecumene Pressure	The term is derived from an ancient Greek word "oecumene" which referred to the known world or the habitable world. In modern times ecumene refers to any inhabited land or "the area under human influence".	Human influence upon geomorphology starts when an uninhabited land area gets transformed to pursue anthropogenic activities. Hence, the direct impact of anthropogeomorphic process is evident only in the ecumene.	Land Use Land Cover classification mapping
Ecumene population density	Human pressure upon the land increases with the increment in human population because humans require land resources to survive. Therefore, higher the density of the population, greater will be the pressure upon limited terrestrial resources.	Instead of population density of an administrative area, A novel approach of ecumene population density is considered in this study because an administrative unit can have a large part under non-ecumene zone (forest, waste land, water body etc.) which minimizes actual population impact upon the land resources.	Population Census
Illiteracy (in %)	Illiteracy indicates level of education, which is a necessary condition to form a public degree of perception (Nir, 1983) to utilize limited land resources in a sustainable way.	Illiteracy is a major determinant in lowering the impact of AGP in an area. First, an illiterate individual or a society would find it very hard to understand the concept of sustainable development due to lack of knowledge which would increase the AGP impact and second,	Population Census

		they would not try mitigate the negative effects already induced by the AGP due to lack of perception.	
Population Below Poverty Line (in %)	Below poverty line population is generally conceived as the section of society which lacks minimum sufficient resources (financial and materialistic) to maintain a satisfactory lifestyle.	It becomes an important determinant in restricting the AGP impacts because it encourages the over-exploitation of resources (land, water etc.) to fulfil the needs and discourages the sustainable use of resources wherever possible.	Population Census
Rock type	A rock is the parent material which forms a landform. Hence, rock erodability determines how stable or fragile a landform would be when the processes start acting upon it.	Rock type denotes the ability of the rock to resist erosion induced by different geomorphic processes (hard rock and soft rock). The erodability of a rock is determined by the type and material by which it is formed. Higher the erosion rate greater the risk of AGP impact.	Field survey
Slope	Steepness refers to the range between the highest and the lowest point of a landform or a land surface. Lower degree of steepness is favorable for anthropogenic activities because it provides stability while the higher degree of slope is conductive to landslides consequently higher amount of erosion	Slope degree define that the higher the degree of slope of an ecumene, higher would be the AGP pressure thus, greater would be the magnitude of landform modifications.	DEM
Aspect (Rain)	The 'windward side' of a landforms experiences more amount of rainfall	The windward aspect of an ecumene becomes highly prone to chemical weathering and erosion	DEM

	compared to the 'leeward side'.	due to high rainfall penetration which increases the AGP stress many-folds. On the other hand, the intensity of rainfall gets reduced away from the windward side leading to low chemical weathering.	
Aspect (Solar)	The solar insolation increases the rock temperature during the daytime and during the night time, the rock loses heat received during the insolation process. This process goes on diurnal basis and eventually top layers of the rock start experiencing weathering due to continuous fluctuation in the temperature. Consequently, it becomes weaker over a period of time.	Regions (landforms) which directly face sunlight for longer period of the day are more susceptible to exfoliation weathering (onion weathering). because they face larger range of temperature fluctuation during the day and night times than those which do not directly face the sunshine. If AGP is also working in the region where exfoliation weathering is active then increment in the AGP stress is guaranteed because it would increase the weathering rate thus, rapid modification in landforms.	DEM
Climate	Climatic variables such as; precipitation, temperature, wind speed and direction etc. are the sources of different geomorphic processes. These processes further carve the landforms of the region and defines its geomorphology.	Wet tropical climate produces the highest amount of rain hence, higher rate of erosion. On the other hand, hot and dry desert climate have one of the lowest erosion rate amongst all the climate type. Hence, different climate have different intensity of landform erosion.	Meteorological database
Hazard	Natural processes of low frequency and high magnitude generated by	Hazard parameter describes the presence of different natural hazards	Disaster management authority

	endogenetic and exogenetic energy of the earth are nothing but geological and geomorphic processes which negatively impact human lives and assets.	in an area which could strike and act upon a landform as a geomorphic process. However, this impact could get exponentially increased if the AG process is also dominant in the given area. The hazard and AGP would together bring severe modifications in a landform.	

Supplementary Table-2: Different land-use impact on geomorphology

Land-Use/ Anthropogenic activities	Impact on geomorphology
Forest	The rate of forest destruction worldwide, particularly in the tropics, has been unprecedented. The removal of forest cover starts the surface modification process since it reduces the surface's ability to absorb water during rainfall. As a result, severe rain can wash away top soil containing humus, making revegetation virtually impossible. Aside from soil conservation, forest foliage, litter, and roots absorb water, slowing surface runoff and increasing infiltration. On an average, water infiltration is 7-8 times higher and surface runoff is 2-3 times lower in wooded regions than in non-forested areas (Illes and Konecsny, 2000).
Agriculture	Agriculture is the oldest land use activity with geomorphic influence since tillage clears all vegetation and drastically alters surface runoff patterns, resulting in rapid soil erosion and a reduction in water retention capacity (Loczy, 2010). Any landform generated by wind erosion can be modified indirectly by agriculture, but the direct impact on geomorphology is the construction of terraces and levelling of the land (Loki, 2010). Agricultural terraces, in fact, have the greatest impact on landform modification of any human activity since they affect not only landforms but also soil, climatic, fluvial, and biogeographic conditions (Csorba and Zsadányi 2003).
Grassland	Similarly, converting grassland to farmland increases soil erosion and land modification since grassland has a limited surface modification ability in comparison to agriculture and built-up activities where grass growth and consumption are balanced. Thus, grassland only causes geomorphic changes when this balance is disrupted (Toth, 2010).
Mining	Large-scale mining operations have emerged during the nineteenth century. This human activity produces geomorphic landforms through extraction (huge hollow land, valleys etc.) as well as accumulation (plateaux and

	slopes). These landforms are a result of mining operations and have one of the most significant geomorphic effects because they force geomorphic processes to define a new state of equilibrium (Suto, 2010). Different landforms formed during excavation can be classified into three types: macroforms, mesoforms, and microforms (David and Patrick 1998; Karancsi, 2000; David, 2000).
Built-Up	Built-up areas have the smallest land surface area globally, yet their geomorphic impact is the most intense of all anthropic activities. Concretization not only seals the surface but also suspends the functioning of natural processes. Building debris and garbage accumulation lead to landfills, which alters the drainage extent. Excavation and surface planation during construction destroy minor geomorphic features and cause erosion, mass movements along slopes (Szabó 1993), and cave in manmade hollows (Gálos and Kertész 1997).
Terrestrial transportation	Terrestrial transportation lines are built in small strips with a linear design, but they have the greatest impact on geomorphology by creating steep slopes that lead to natural landform instability (David et al., 2010). A four-lane one-kilometer highway stretch with a width of 92 feet consumes approximately 8 hectares of land area during construction. While the development of inland canals necessitates the removal of thousands of millions of cubic meters of dirt, railways have a lower slope grade but require deeper cutting.
Pipeline	Pipelines, which are often thought to have a minor influence on the environment, have the maximum impact on geomorphology of all since they are topographically independent and are planned for the shortest route possible, resulting in the cutting of all landforms that come along the route (David et al., 2010).
Acid rain	Additionally, although minor and difficult to quantify, air pollution contributes to erosion. When air pollutants (so2, no2, ammonia) reach a considerable amount in the atmosphere, they return to the surface in the form of acid rain, which promotes chemical weathering and consequently increases erosion.
Water resource management	Moreover, flood control methods and water resource management directly and indirectly alter local terrain morphology by creating new landforms and processes by preventing and accelerating sedimentation and channel erosion.

Supplementary Table-3 Showing Physical variables significance and source with respect to coastal vulnerability.

S No.	Variable	**Derived by**	Significance	Source	Year	**Ground Truth**
1	Coastal Slope (Degree)	Referred to CVI of Goa coast by	Locations with gentle slope are more prone to flooding as	ETOPO 2 bathymetric	1971-1984	The devastating Indian Ocean tsunami in 2004 had a profound impact on the coastal

		Kunte et al.	gentle slopes retreat faster than steeper slope and wave energy can penetrate far inland due to less frictional force restricting it.	dataset from the NIO, Goa		Indonesia. The coastal areas with gentle slopes were more vulnerable to the powerful tsunami waves that penetrated far inland, causing widespread destruction. The lack of natural barriers and the flat terrain allowed the waves to travel much farther inland, causing more extensive flooding.
2	Coastal regional Elevation (m)	SRTM 30m DEM, using QGIS	Coastal regional elevation is an important parameter as it provides an estimate of the extent of land threatened by projected SLR (Kumar and Kunte, 2012; Kumar et al., 2010), as well as the sensitivity of the coast to flooding during a storm surge (Diez et al., 2007) or tsunami. Hence, areas with high coastal elevation will be considered less vulnerable and vice-versa (Gornitz et al., 1994).	SRTM 30 m DEM	2019	The 2011 Tohoku, Japan earthquake and resultant tsunami highlighted the importance of coastal elevation in tsunami vulnerability. For example, Aonae city suffered less severe impacts due to its elevated location on a hillside.
3	Sandy coast (%)	Total sandy coast length in	Sandy coasts have gentle slope towards inland which makes	Google Earth and	2019	The 2011 Tohoku, Japan earthquake and resultant tsunami highlighted the

		each village / Total coastline length of each village x 100.	their inland areas more vulnerable to coastal flooding. Higher the amount of sandy coast in a given transect higher will be the vulnerability.	Digimizer		importance of coastal elevation in tsunami vulnerability. For example, Aonae city suffered less severe impacts due to its elevated location on a hillside.
4	Sand dune density	Dune areas from NCSCM study were digitized and measured using Digimizer software	Sand dunes protect the inland area from seawater intrusion during high tides. Sand dunes also act as a reservoir for future supply to maintain the beach. Sparse sand dune areas are more vulnerable as there is no restriction in between the sandy beach and inland areas.	NCSCM 2017, Field Study	Oct, 2019	The Dutch coast along the North Sea have significant amount of sand dunes which critically protects low-lying coastal areas from flooding.
5	Vegetation behind the beach	Vegetation areas in the imageries were measured using DIgimizer software.	Casaurina and coconut plantation help to decrease cyclonic winds and storm waves energy which reduces risk of inland damages. Dense vegetation could lessen the vulnerability	Field survey, Google Earth Imageries and Digimizer	Sept 2019	The Tamil Nadu Forest Department established casuarina plantations along vulnerable stretches of the coastline. These casuarina plantations act as windbreaks and help protect coastal communities from the destructive forces of cyclonic winds and storm waves.
6	Rate of relative SLR (m)	Referred to CVI of Goa	Higher SLR increment rate will increase the	Annual mean relative	1969-2017	The combination of susceptible coastal flooding and the flat

		coast by Kunte et al.	vulnerability as it denotes increasing the risk of inundation in low lying coastal areas.	sea level data from Indian Ocean tide gauge stations 1969-2017.		topography makes any area highly vulnerable to coastal inundation. For ex. Bangladesh's significant human population lives in the low-lying coastal plains
7	Shoreline erosion rate (m)	Referred to Indian shoreline atlas, 2018	Shoreline erosion rate over a period of time indicates the sensitivity of the coast thus, increased vulnerability.	NCCR, MoES 2018	2018	Erosion along the coastlines has led to the loss of valuable land, including r infrastructure. For ex. the Chesapeake Bay region in Canada is experiencing high erosion due to SLR and anthropogenic activities.
8	Mean tidal range (m)	Referred to National Institute of Oceanography, Goa data	Coastal areas with high tidal range and low coastal regional elevation are highly vulnerable.	NIO, Goa India, 2011	2011	Low-lying coastal areas such as in West Bengal, Odisha states in India are particularly vulnerable to cyclones and storm surges, which periodically lead to flood, erosion and damage to infrastructure.
9	Significant wave height (m)	Referred to National Institute of Oceanography, Goa data	The average height (trough to crest) of one-third of the waves in a wave spectrum for a given period of time (Kumar et al., 2010). Dwarakish et al. (2009) considered	NIO, Goa, India using studies on directional waves off Mormugao	2009	The Bay of Bengal coastal area is exposed to both high significant wave heights and storm surges during cyclones. The combination of these factors leads to coastal flooding, erosion and eventually damage to infrastructure and human lives.

			significant wave heights range from 1.6 to 2.8 m as moderately vulnerable.	Port, 2009		
10	Plausible storm surge height (m)	Derived from Vulnerability Atlas of India, 2019	Storm surge can destroy low lying coastal areas due to its high-intensity waves. Thus, Surge height in any region is an important criteria.	BMTPC, Ministry of Home and Urban Affairs (MoHUA)	2019	The surge height was the major factor in the unprecedented devastation during Hurricane Katrina which reached about 28 feet in some areas along the Gulf Coast. The storm surge inundated low-lying coastal regions in Louisiana, Mississippi, and Alabama states, caused major flooding.

Supplementary Table-4 Showing socio-economic variables significance and source with respect to coastal vulnerability.

S No.	Variable	Derived using	Significance	Source	Year	Ground Truth
1	Village Population Density	Total population/ Total village area (Sq. Km) x 100	High population density in a region will lead to higher vulnerability due to high pressure on available resources	Census of India	2011	Tokyo is the most populous cities in the world. The combination of high population density and the city's coastal location makes it vulnerable to coastal hazards. The Fukushima nuclear disaster in 2011, highlighted the risks posed by coastal hazards to densely populated coastal areas.
2	Road Density	Measured road length from	Low road density will	Regional planning	2019	The Andaman and Nicobar Islands were

		regional planning map using Digimizer and calculated Total road length/ 100 Sq. Km for each village	lead to high vulnerability as evacuation and assistance will be more difficult during an emergency.	map of Canacona, 2021 and Digimizer		severely affected when the Indian Ocean tsunami in 2004 had hit the islands. But more damages to life occurred due to the low road density on some of these islands, which had hampered the medical aid and evacuation efforts.
3	Total settlement area under village (%)	Digitized and measured regional planning map of Canacona taluka using Digimizer software.	Higher the settlement area under a coastal village, higher will be the exposure to coastal hazard thus, higher vulnerability.	Regional planning map of Canacona, 2021 and Digimizer	2019	Palu, Indonesia experienced a devastating tsunami in 2018. The extensive settlement area along the coast increased exposure to the tsunami hazard. The high population density and significant infrastructure within the settlement area exacerbated the impacts, leading to widespread destruction and loss of life.
4	Water supply through Pipeline (%)	No. of metered connection/ Total village population x 100	Households without metered water connection extract groundwater, could become vulnerable during salt water intrusion due to a coastal hazard	Statistical handbook of Goa	2016 -17	Cyclone Sidr in 2007, in Bangladesh had caused widespread devastation. Many households relied on shallow tube wells for freshwater, as they lacked metered water connections. The cyclone's storm surge led to saltwater intrusion into groundwater sources, rendering the well water undrinkable. This left households without access to safe

						drinking water, exacerbating the already dire situation after the disaster.
5	Literacy Rate	Total literate population/ Total population x 100	Higher % of literacy suggests better decision making capacity during a hazard, hence low vulnerability	Census of India	2011	Cyclone Phailin had struck Odisha, India in 2013. The Indian government's efforts to promote literacy and disaster preparedness played a crucial role in reducing vulnerability. As a result, despite the cyclone's intensity, a large number of people were successfully evacuated, which significantly reduced casualties and mitigated the impact on coastal communities.
6	Dependent Population (%)	Total village population - Total working population (14-45 yrs.) = non- working population Then, Total non-working population/Total village population x 100 = Dependent population in %	Dependent population is always at highest risk as well as it can decrease the efficiency of a non-dependent person during an emergency	Census of India	2011	The aftermath of Hurricane Katrina highlighted the vulnerabilities of dependent populations. Many elderly residents and those with limited mobility were unable to evacuate before the storm hit. The lack of accessible transportation, shelters, and proper support networks led to these outcomes.
7	Female Population (%)	Total female population/ Total village population x 100	Generally, low literacy rate along with high malnutrition	Census of India	2011	The Indian Ocean tsunami in 2004 disproportionately affected

			rate make them dependent population during the time of an emergency.			women in vulnerable coastal communities. Low literacy rates and cultural norms restricted their ability to seek safety and access information. Especially, pregnant women or caring for young children, faced challenges in evacuating and accessing resources.
8	Population between (0-6) years (%)	Under 6 years population/ Total village population x 100	Illiteracy and lack of physical efficiency makes population under 6 years dependent population and highly vulnerable.	Census of India	2011	The aftermath of Hurricane Katrina highlighted the vulnerabilities of children. The evacuation process was complicated by ensuring care and safety of children, and overcrowded shelters further increased the difficulties faced by families
9	Tourist Density (Person/Sq. Km)	Total tourist visited/ Total village population x 100	High tourist population in a coastal village will increase their exposure and add	Field observation and Directorate of tourism, Goa data	2016-17	The presence of tourists on the island added complexity to emergency response and recovery efforts when the Hurricane Maria struck in Puerto Rico in 2017. Tourists

			pressure on available resources during a coastal hazard.			faced challenges in accessing timely information and evacuating. Also, the stress on resources and infrastructure impacted the overall ability to respond effectively to the disaster.
10	Settlements between 200m to 500m from HTL	Settlement areas under 500m HTL shown in regional planning map of Canacona were digitized and measured using Digimizer.	Due to high exposure to coastal hazard, this zone cannot have high concentration of settlement areas.	Regional plan of Canacona, Goa, T And CP, Goa		The Indian Coastal Regulation Zone (CRZ) framework specifies zones along the coast with varying degrees of restrictions on development activities, within certain distances from the high tide line, to protect the coastal environment and reducing vulnerability to hazards.
11	Settlements under 200m HTL	Settlement areas under 200m HTL shown in regional planning map of Canacona were digitized and measured using Digimizer.	According to CZMP 2019, CRZ-3B zone cannot have any permanent settlement development under 200m from High tide line. They	Regional plan of Canacona, Goa, Town and country planning, Panaji, Goa		The Indian Coastal Regulation Zone (CRZ) framework specifies zones along the coast with varying degrees of restrictions on development activities, within certain

			are most exposed and vulnerable.			distances from the high tide line, to protect the coastal environment and reducing vulnerability to hazards.

Supplementary Table-5 Land Use Land Cover statistics of the four taluka(s) located in coastal South Goa during 2000 and 2020

Taluka	Year	Built-Up	Agriculture	Barren land	Forest	Wetland	Water body
Marmugao	2000	16.02	11.12	30.44	23.99	6.92	2.39
Marmugao	2020	29.49	26.35	11.11	29.49	5.89	1.61
Salcete	2000	44.70	98.24	68.19	77.85	11.97	5.88
Salcete	2020	74.44	91.84	56.50	64.31	14.32	5.38
Quepem	2000	11.63	42.45	64.66	202.24	1.16	1.90
Quepem	2020	15.79	43.88	62.57	198.68	2.97	1.04
Canacona	2000	10.78	49.11	40.95	285.64	1.81	1.97
Canacona	2020	13.50	55.06	38.24	277.90	4.70	0.80

Supplementary Table-6 Showing the amount of soil erosion (Tons/ht./yr.), proportion of the amount among the total erosion (in %) and the growth rate (between 2000 & 2020) under different levels of erosion during 2000 and 2020 in the study area.

Taluka	Soil Erosion (%)				
	Slight	Moderate	High	Very High	Severe
Marmugao 2000	27 (27)	2 (2)	2 (2)	12 (12)	57 (57)
Marmugao 2020	28 (28)	3 (3)	6 (6)	10 (10)	53 (53)
Growth Rate	3.70	50.00	200.00	-16.67	-7.02
Salcete	34 (11)	26 (8.4)	39 (12.7)	66 (21.4)	143 (46.4)

2000					
Salcete 2020	17 (5.5)	5 (1.5)	28 (9.1)	108 (35.2)	149 (48.5)
Growth Rate	-50.00	-80.77	-28.21	63.64	4.20
Quepem 2000	13 (4)	13 (4)	30 (9.3)	63 (19.4)	205 (63.3)
Quepem 2020	31 (9.6)	31 (9.6)	70 (21.6)	70 (21.6)	122 (37.7)
Growth Rate	138.46	138.46	133.33	11.11	-40.49
Canacona 2000	19 (4.9)	12 (3.1)	31 (7.9)	49 (12.6)	279 (71.5)
Canacona 2020	74 (19)	32 (8.2)	64 (16.4)	83 (21.3)	137 (31.5)
Growth Rate	289.47	166.67	106.45	69.39	-50.90

List of publications of Ritwik Nigam

1. **Nigam, R.,** Luis, A., & Kotha, M. (2020). Significance of Local Coastal Geomorphology in Defining Coastal Vulnerability -A Village Level Study of Canacona, Goa. Applications of Geospatial technologies in Geomorphology and Environment (pp.161), ISSN: 9788192579931, University of North Bengal**. (Published as Book chapter)**

2. **Nigam, R.,** Luis, A., Prasad, P., Kuttikar, S., Yadav, R., Vaz, E., & Kotha, M. (2021). Spatio-temporal assessment of COVID-19 lockdown impact on beach litter status and composition in Goa, India. Marine Pollution Bulletin. 113293. 10.1016/j.marpolbul.2021.113293. **(Published - IF: 7.001)**

3. **Nigam, R.,** Pandya, K., Luis, A., Sengupta, R., Kotha, M. (2021). Positive effects of COVID-19 lockdown on air quality of industrial cities (Ankleshwar and Vapi) of Western India. Scientific Reports. 11. 10.1038/s41598-021-83393-9. **(Published - IF: 4.996)**

4. **Nigam, R.,** Tripathi, G., Priya, T., Luis, A., Vaz, E., Kumar, S., Shakya, A., Damásio, B., & Kotha, M. (2022). Did Covid-19 lockdown positively affect the urban environment and UN- Sustainable Development Goals? PLOS ONE. 17. e0274621. 10.1371/journal.pone.0274621.
(Published - IF: 3.752)

5. **Nigam, R.,** Pandya, K., Luis, A., & Kotha, M. (2023). Multi-temporal Impact Analysis of Covid-19 Lockdown and Unlock Measures on Major Air Pollutants in Guwahati City, India. 10.1007/978-3-031-13119-6_23. **(Published as Book chapter)**

6. Shakya, A., Tripathi, G., **Nigam, R.,** & Chakraverti, A. (2022). Quantifying Spatio Temporal Changes in Coastal Built-up area of South Goa based on Landsat Imageries using Google Earth Engine. ADBU Journal of Engineering Technology (AJET). 11. 1. **(Published)**

7. Kotecha, M., Kanga, S., Singh, S., **Nigam, R.,** Nagarajan, K., & Shakya, A. (2022). Analysis of Urban Heat Island Effect in Rajkot City Using Geospatial Techniques. 10.1007/978-981-16-7373-3_18. **(Published as Book chapter)**

8. **Nigam, R.,** Luis, A. & Kotha, M. (2023) Evaluation of efficiency of the index of potential anthropic geomorphology at meso level: a case study of Goa State, India. *The Geographical Journal*, 00, 1–12. Available from: https://doi.org/10.1111/geoj.12540. **(Published - IF: 3.0)**

9. **Nigam, R.,** Luis, A., J., Gagnon, A, S., Vaz, E., Damasio, B., & Kotha, M. (2024)

Assessing coastal vulnerability at the village level using a robust framework, the example of Canacona in South Goa, India. iScience. 109129. 10.1016/j.isci.2024.109129. **(Published – IF: 5.8)**

10. **Nigam, R.,** Luis, A., J., & Kotha, M. (2024) Recent Trends of Air Pollution and Its Implication on Human Health: A Spatio-Temporal Study of Two Coastal Cities of Goa. Air Quality and Human Health (eds.) ISBN: 978-9819713622, Springer; 1st ed. 2024 edition. **(Published as Book Chapter)**

11. Luis, A., J., Nigam, R., Pandya, K. & Kotha, M. (2023) Environmental Assessment of Air Pollution Scenario (2014-2020) in the Tourist state of Goa, India **(Second Revision Completed)**

12. **Nigam, R.,** Dey R., Daphale, R., Luis, A., J., Vaz, E., Damasio, B., & Kotha, M. (2023) Multi Temporal Climate Trend Analysis of the Coastal State of Goa, India, Using Mann-Kendall Test. **(Under Review)**

13. **Nigam, R.,** Ghadamode, V., Luis, A, J., Prasad, P., Kotha, M. (2024) Decadal Land Use Land Cover Assessment of the Coastal Tracts of South Goa, India. **(Under Review)**

14. **Nigam, R.,** Ghadamode, V., Yovan, L., Luis, A., J., Kotha, M. (2024) Identification of future hazard zones creating due to compounded coastal flooding in the low-lying coastal tracts of South Goa, India. **(Under Review)**

15. **Nigam, R.,** and Kotha, M. (2024) A Novel Model to Quantify Anthropogeomorphic Process at an Ecumene. **(Under Review)**

16. Tripathi, G., **Nigam, R.,** Prasad, P. et al (2024) Morphometric and Morpho-tectonic Assessment of Jimma Watershed, Southwest Ethiopia, Using GIS Based Approach. **(Manuscript Completed, to be Submitted)**